PROBING LYMPHOCYTE RESPONSES TO MODULATION OF THE F_0F_1-ATPASE BY BZ-423

by

Li Wang

A dissertation submitted in partial fulfillment
of the requirements for the degree of
Doctor of Philosophy
(Chemistry)
in the University of Michigan
2009

Doctoral Committee:

Professor Gary D. Glick, Chair
Professor Dennis Keith Bishop
Professor Robert T. Kennedy
Associate Professor Philip D. King
Associate Professor Anna K. Mapp

This dissertation is dedicated to my loving husband Dr. Jun Cheng

ACKNOWLEDGEMENTS

This thesis could not have been finished without the help and support from everyone I have worked with over the past six years. First, I am really thankful to my advisor Prof. Gary Glick for supporting me in all aspects of my graduate career. His guidance, intellect and expertise on my thesis projects as well as providing a world-class scientific training environment are priceless. I would also like to thank Dr. Tony Opipari for his countless in-depth discussions regarding my research data, which have greatly enhanced my intellectual development.

In addition, I would like to thank all members of my dissertation committee: Dennis K Bishop, Robert T Kennedy, Philip D King, and Anna K Mapp. I appreciate their time taken out of busy schedules to serve on my committee as well as provide constructive feedback through the dissertation process.

I would like to thank all current and former Glick lab members for their friendships and contributions: Lara Swenson, Tom Sundberg, Joanne Cleary, Neal Blatt, Tony Boitano, Katie Groendyke, Gina Ney, Shawn Stevens, Richard Frazee, Xueni Chen, Tasha Francis, Dan Wahl, Melissa Bobeck, Ben Farrar, Jenny Rush and Costas Lyssiotis.

I am also grateful for the Jim Mobley, Lara Swanson, and Rod Morgan to isolate splenic lymphocytes from mice for me. I also would like to thank Chitra for the protocol of nucleus isolation.

Special thanks go to Gary, Lara, and Amberlyn Wands for their time and effort to read and critique my thesis.

Finally, I would thank my friends and family. I must also thank my parents Xianqin and Jinsheng, parents-in-law Fulan and Xianlin, my brothers Changqing and Changhong and my sister Xiufang for their love, encouragements and understandings. But most of all, it would have been impossible to complete this thesis without the tremendous love and support from my husband Jun throughout the whole graduate school.

TABLE OF CONTENTS

CHAPTER 3

LIST OF TABLES

Table

LIST OF FIGURES

Figure

LIST OF ABBREVIATIONS

AA	Antimycin A
Act D	Actinomycin D
ADP	Adenosine-5′-diphosphate
AICD	Activation induced cell death
AIF	Apoptosis inducing factor
ANT	Adenine nucleotide translocator
Apaf-1	Apoptosis protease activating factor-1
APC	Antigen-presenting cell
As_2O_3	Arsenic trioxide
ASO	Anti-sense oligonucleotide
ASK1	Apoptosis signal-regulated kinase-1
ATP	Adenosine-5′-triphosphate
BA	Bongkrekic acid
BAFF	B cell activating factor
BAFF-R	BAFF receptor
Bad	Bcl-2 agonist of cell death
Bak	Bcl-2 antagonist killer1
Bax	Bcl-2-associated X protein

Bcl-2	B cell CLL/lymphoma 2
BCR	B cell receptor
bHLHzip	basic Helix/Loop/Helix-Leucine Zipper
BH	Bcl-2 homology
t-BHP	*tert*-Butyl hydroperoxide
Bid	BH3-interacting death domain agonist
Bik	Bcl-2-interacting killer
Bim	Bcl-2-interacting protein
BL	Burkitt's Lymphoma
BLK	B-lymphocyte specific tyrosine kinase
Bmf	Bcl-2 modifying factor
BSA	Bovine serum albumin
BSO	L-buthionine sulfoximine
BTK	Bruton's tyrosine kinase
CBR	Central benzodiazepine receptor
CD	Cluster of differentiation
CD40L	CD40 Ligand
CDK	Cyclin-dependent kinase
CDDP	Cis-diamineplatinum(II)dichloride
CHX	Cycloheximide
CICD	Caspase-independent cell death
CK	Creatine kinase
CLAMI	Cell lysis and mitochondrial isolation

4-Cl-Dz	4′-Chlorodiazepam
CRAC	Ca^{2+}-release activated Ca^{2+} channel
CsA	Cyclosporine A
CTLA-4	Cytotoxic T lymphocyte antigen-4
CTLA-4Ig	Cytotoxic T lymphocyte antigen-4•Immunoglobin fusion protein
CuZnSOD	Copper and zinc superoxide dismutases
CypD	Cyclophillin D
Cyt. *c*	Cytochrome *c*
Cz	Clonazepam
DCFH-DA	Dichlorofluorescin diacetate
DFMO	Difluoromethylornithine
DHE	Dihydroethidium
DIM	Diindolylmethane
DISC	Death inducing signaling complex
DKO	Double knockout
DLC	Dynein light chain
DMSO	Dimethylsulfoxide
DNase	Deoxyribonuclease
Drp-1	dynamin-related protein-1
dsDNA	Double-stranded DNA
Dz	Diazepam
EAE	Experimental autoimmune encephalitis

EC_{50}	Effective concentration that produces a response in 50% of the cells
EndoG	Endonuclease G
ER	Endoplasmic reticulum
ERK	Extracellular signal-regulated kinase
ETC	Electron transport chain
FBS	Fetal bovine serum
FADD	Fas-associated death domain
FasL	Fas ligand
FCCP	Carbonyl cyanide-4 (trfluoromethoxy) phenylhydrazone
FDC	Follicular dendritic cell
Fe-S	Iron-sulfur cluster
FITC	Fluorescein-isothiocyanate-conjugated
FKBP	FK506 binding protein
FOXO3a	Forkhead box O3a
GABA	γ-aminobutyric acid
GC	Germinal center
GF	Growth factor
GFP	Green fluorescent protein
GI_{50}	Effective concentration that inhibits 50% growth
GPX	Glutathione peroxidase
GSIS	Glucose-stimulated insulin secretion
GSH	Glutathione
GSK-3β	Glycogen synthase kinase-3β

GSSG	Glutathione disulfide
GST	Glutathione *S*-transferase
H_2O_2	Hydrogen peroxide
HCK	Hemopoietic cell kinase
HDAC	Histone deacetylase
HEK 293	Human embryonic kidney 293
HIF-1α	Hypoxia inducible factor-1α
HK	Hexokinase
HPLC	High pressure liquid chromatography
Hrk	Harakiri
HSP	Heat shock proteins
HSV	Herpes simplex virus
HUVAC	Human umbilical vein endothelial cell
IAP	Inhibitor of apoptosis
ICAD	Inhibitor of caspase activated DNase
IFN-γ	Interferon-γ
Ig	Immunoglobulin
InsP3	Inositol-1,4,5-trisphosphate
IL-2	Interleukin-2
IMM	Inner mitochondrial membrane
IMS	Intermembrane space
ITAM	Immunoreceptor tyrosine-based activation motif
ITIM	Immunoreceptor tyrosine-based inhibition motif

JNK	c-Jun N-teminal kinase
K_d	Equilibrium dissociation constant
K_i	Equilibrium dissociation constant for binding of an inhibitor to an enzyme
LC_{50}	Lethal concentration that kills 50% of the cells
LUV	Large unilamellar vesicle
lpr	lymphoproliferative
MAPK	Mitogen-activated protein kinases
MAPKK	Mitogen-activated protein kinase kinase
MAPKKK	Mitogen-activated protein kinase kinase kinase
MB1	Myc box I
Mcl-1	Myeloid cell leukemia 1
2-ME	2-methoxyesteradiol
MEF	Mouse embryonic fibroblasts
mGSH	Mitochondrial glutathione
MHC	Major histocompatability complex
Mfn2	Mitofusion 2
MIS	Mitochondrial intermembrane space
MnSOD	Manganese superoxide dismutase
MnTBAP	Manganese(III)*meso*-tetrakis(4-benzoic acid)porphyrin
MOMP	Mitochondrial outer membrane permeabilization
mRNA	messenger RNA
MPT	Mitochondrial permeability transition
MS	Multiple sclerosis

mTOR	Mammalin target of rapamycin
MX	Myxothiazole A
MRC	Mitochondrial respiratory chain
mtDNA	Mitochondrial DNA
NFAT	Nuclear factor of activated T cells
NPA	3-nitropropionic acid
NZB/W	F_1 offspring of NZB x NZW mice
$O_2^{\bullet -}$	Superoxide
OAZ1	Ornithine decarboxylase antizyme-1
ODC	Ornithine decarboxylase
OMM	Outer mitochondrial membrane
OPA1	Optic atrophy type 1 protein
OSCP	Oligomycin sensitive conferring protein
$p56^{Lck}$	Lymphocyte-specific kinase
PARP-1	Poly (ADP-ribose) polymerase-1
PCD	Programmed cell death
PBR	Peripheral benzodiazepine receptor
PBS	Phosphate buffered saline
PCC	Pigeon cytochrome *c*
PD-1	Programmed death-1
PD-1L	Programmed death-1 ligand
PI	Propidium iodide
P_i	Inorganic phosphate

PI3K	Phosphatidylinositol 3-kinase
PKA	Protein kinase A
PK 11195	1-(2-chlorophenyl)-N-methyl-N-(1-methylpropyl)-3-Isoquinoline carboxamide
PLA2	Phospholipase A2
PMA	Phorphol 12-myristate 13-acetate
pRb	Retinoblastoma protein
PT	Permeability transition
PTEN	Phosphatase and tensin homolog
PTP	Protein tyrsonine phosphatase
PUMA	p53-upregulated modulator of apoptosis
Q	Ubiquinone
$QH^{\bullet -}$	Ubisemiquinone anion
QH_2	Ubiquinol
RA	Rheumatoid arthritis
RAG1	Recombination activating gene 1
RNAi	RNA interference
ROS	Reactive oxygen species
RSK	p90 ribosoml S6 kinase
SAHA	Suberoylanilide hydroxamic acid
SAPK	Stress-activated protein kinase
SAR	Structure activity relationship
SERCA	sarcoplasmid-endoplasmic reticulum calcium adenosine
SfA	Sangliferin A

SHIP	SH2 containing inositol phosphate phosphatase
Skp2	S-phase kinase-associated protein 2
siRNA	Small inhibitory RNA
SLE	Systemic lupus erythematosus
Sm	Small nuclear ribonucleoprotein
SMPs	Submitochondrial particles
Smac/DIABLO	Second mitochondrial-derived activator of caspase/direct IAP-associated binding protein with low PI
SRB	Sulforhodamine B
SSc	Systemic sclerosis
STS	Staurosporine
SYK	Spleen tyrosine kinase
TCA	Trichloroacetic acid
TCR	T cell antigen receptor
TEM	Transmission electron microscopy
TNF	Tumor necrosis factor
TLR	Toll-like receptor
TRAIL	TNF-related apoptosis inducing ligand
TRAF2	TNF receptor–associated factor 2
Trx	Thioredoxin
β-TRCP	β-Transducin repeating containing protein
TSK	Tight skin
TTFA	Thenoyltrifluoroacetone
UV	Ultraviolet

VDAC	Voltage-dependant anion channel
Vpr	Viral protein of regulation
Yaa	Y-linked autoimmune acceleration
zVAD	Benzyloxycarbonyl-valine-alanine-aspartic acid fluoromethyl ketone
$\Delta\psi_m$	Mitochondrial transmembrane potential

ABSTRACT

Bz-423 is an immunomodulatory 1,4-benzodiazepine that binds to the oligomycin sensitivity conferring protein (OSCP) of the mitochondrial F_0F_1-ATPase and modulates its activity. Inhibition of the F_0F_1-ATPase by Bz-423 causes mitochondrial membrane hyperpolarization and superoxide production by the mitochondrial electron transport chain (ETC). Bz-423 ameliorates diseases in mouse models of lupus, arthritis and psoriasis. Unlike conventional immunosuppressants, Bz-423 does not interfere with normal immune function. Concomitant with its specific therapeutic effects, Bz-423 selectively induces apoptosis in pathogenic lymphocytes. As pathogenic lymphocytes are abnormally activated by chronic receptor stimulation, it was hypothesized that activation sensitizes cells to Bz-423.

The overall goal of experiments reported in this dissertation was to identify factors that underlie the selectivity of Bz-423 on pathogenic lymphocytes observed *in vivo*. Towards this goal, anti-IgM and Bz-423 co-treatment in Ramos B cells was established as an *in vitro* model, and the apoptotic signaling pathways were explored. These experiments found that superoxide and calcium are critical second messengers that increase levels of BH3-only proteins Bim, Bmf, tBid, which in turns activates Bax and Bak. Activated Bax and Bak induce the release of mitochondrial pro-apoptotic factors and subsequent cell death.

Bz-423 also activates NFAT. Mechanistic studies using Ramos B cells demonstrate superoxide induced by Bz-423 triggers the opening of CRAC channel, which leads to calcium influx, calcineurin activation, and NFAT activation. NFAT activation leads to transcription of NFAT-dependent genes including IRF4, which may play an important role in receptor editing. Bz-423 also renders cells resistant to subsequent activation, downregulates surface IgM expression, and activates NFAT but not NFκB or AP-1. As these changes induced by Bz-423 are characteristics of anergic B cells, Bz-423 may also promote anergy.

Anergy, apoptosis, and receptor editing are three main mechanisms to maintain peripheral tolerance and to repress autoimmunity. These effects may underlie efficacy and specificity of Bz-423 *in vivo*.

CHAPTER 1

INTRODUCTION

Autoimmune disease results from loss of peripheral tolerance to self-antigens: A critical feature of the immune system is its ability to differentiate between self and non-self [1]. When the immune system fails to recognize foreign pathogens, infection occurs. When the immune system fails to identify the body's own tissue as self antigen (loss of self-tolerance), an inappropriate inflammatory response is generated, which leads to autoimmune disease such as systemic lupus erythematosus (SLE) [2].

SLE is a heterogeneous autoimmune disease characterized by non-specific inflammation and multiple-systems damage. The hallmark of SLE is the production of a range of autoantibodies against self antigens such as double-stranded DNA (dsDNA) and small nuclear ribonucleoprotein (Sm) [3]. These autoantibodies, as well as abnormal lymphocytes and cytokines, lead to damage in multiple systems including skin, joints, brain, heart, lungs, and kidneys membranes [4, 5]. The presence of autoantibodies indicates the breakdown of self-tolerance, which is the initial and critical abnormality observed in SLE [6]. Once self-tolerance is broken, binding of self antigens to the self-reactive lymphocytes leads to their abnormal proliferation and secretion of autoantibodies and cytokines [6]. However, the mechanism leading to

loss of tolerance is still elusive [7]. It is thought to be a result of a complex interaction between genetic predisposition and non-genetic factors such as sex hormones and viral infection [8]. Genetic studies of various lupus-prone mouse models have identified lupus susceptibility genes, some of which have been shown to be involved in regulating tolerance [7, 9-11]. For instance, Ly108.1, a member of the signaling lymphocytic activating molecule (SLAM) co-stimulatory molecule family, is shown to regulate B cell tolerance [11]. 90% of the SLE cases occur in females between the ages of 20 to 40 years, suggesting sex hormones also play a role in the disease onset and progression [12]. Other autoimmune diseases, such as rheumatoid arthritis (RA), multiple sclerosis (MS) and type I diabetes, are also known to be the results of the interaction between genetic and environmental risk factors [7]. Therefore, studying SLE may also help to understand other autoimmune diseases.

***Immunological tolerance is critical for maintaining normal immune function*:** Immunological tolerance is the phenomenon in which self-reactive lymphocytes are repressed by an active and dynamic process [13]. Based on where the tolerance occurs, tolerance is divided into central tolerance and peripheral tolerance. Central tolerance occurs in the primary lymphoid organs such as bone marrow and thymus where immature lymphocytes bind to self-antigens with high avidity and affinity undergo clonal deletion, receptor editing and clonal anergy to reduce their self-reactivity [14]. This elimination process is incomplete as some tissue antigens are not present within primary lymphoid organs [14]. Moreover, during further differentiation in the secondary lymphoid organs such as spleen and lymph nodes, B

cells could regain self-reactivity [15]. Because central tolerance is not complete, in the secondary lymphoid organs peripheral tolerance has also been evolved to remove self-reactive lymphocytes [14]. There are three common mechanisms to maintain B-cell peripheral tolerance (Figure 1.1). Apoptosis is a critical form of cell death that occurs physiologically [16], and it is a default mechanism to eliminate autoreactive B cells [16]. Apoptosis is induced when high-avidity forms of self antigen bind to B cell receptor (BCR) in autoreactive B cells [17]. Receptor editing (revision) is a process during which BCR is arranged to change the specificity from self to non-self [18]. Binding of BCR with self-antigen activates RAG gene, initiates V(D)J recombination and results in altered BCR specificity [19, 20]. Anergy is a state of unresponsiveness to antigen stimulation. It occurs when self-antigen binds to BCR, which induces expression of anergy-associated genes for anergy induction and maintenance [21]. Constant antigen receptor occupancy and signaling are required to maintain B cell anergy [22]. Among these three mechanisms, apoptosis is triggered only if receptor editing fails to eliminate high affinity for self antigens [23], and anergy presumably silences cells with low-affinity for self antigens [24]. Therefore, which tolerance mechanism is used depends on the nature of B cell receptor and autoantigens. Higher avidity favors receptor editing and apoptosis deletion, and low avidity invokes anergy [25]. Apoptosis and anergy are two major forms to maintain peripheral T-cell tolerance [26]. In anergy induction, regulatory T cells (Tregs, $Foxp3^{+}CD4^{+}CD25^{+}$) are identified to actively suppress autoreactive T cells, which contributes to the hyporesponsiveness in the lymphocytes [27, 28].

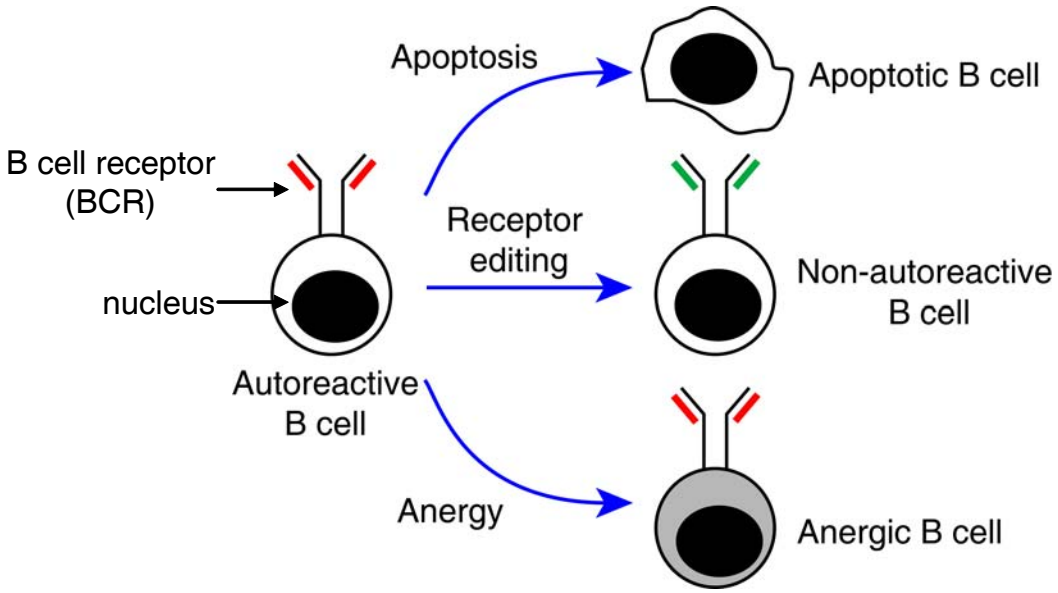

Figure 1.1: Peripheral tolerance mechanisms for B cells. In response to BCR binding by self-antigen, self-reactive B cells are deleted by apoptosis, or self-reactive BCR is replaced by non-self-reactive BCR (receptor editing), or the cells are functionally inactivated (anergy).

Pathogenic lymphocytes derived from defective peripheral tolerance are critical for SLE pathogenesis. Although the exact cause for SLE is not clear, it is well-established that self-reactive lymphocytes play a critical role in the onset and progression of SLE [6]. In SLE patients or lupus mice, there are increased percentage of several subsets of lupus B cells [29-33]. Further studies of their BCRs identified these lupus B cells are self-reactive [29-33]. As tolerance is broken down, the binding of self-antigen to self-reactive B cells will activate these self-reactive B cells [34]. Thus it is not surprising to observe that lupus B cells exhibit "generalized B cell hyperactivation", including spontaneous proliferation, autoantibody anti-dsDNA production and cytokine IL-10 secretion [34, 35]. In response to BCR stimulation, enhanced $[Ca^{2+}]_i$ increase is observed in B cells isolated from SLE patients [34, 36].

Although there is no success in identifying self-reactive T cells in the SLE patients, lupus T cells display a variety of abnormalities [37]. They exhibit a persistent mitochondrial hyperpolarization, increased ROS production and ATP depletion [37]. In response to TCR stimulation, the proximal signaling is enhanced [38], such as calcium mobilization and protein tyrosine phosphorylation, which results in altered cytokines production, including increased IL-6 and IL-10 production but decreased IL-2 and IFN-γ production [38]. IL-2 reduction is associated with defective activation induced apoptosis [37, 38]. These abnormal T cells provide help to autoreactive B cells, resulting in even greater activation of auto-reactive B cells [37].

Further studies of self-reactive B cells from SLE patients demonstrate intact central tolerance and defective peripheral tolerance [39-41]. Loss of B cell tolerance will increase the frequency of autoreactive B cells. As the percentage of self-reactive immature B cells generated in the bone marrow from SLE patients is similar to that in normal individuals, central tolerance is intact [41]. In contrast, the percentage of self-reactive mature B cells is higher in SLE patients (35 - 50%) than in controls (5 – 20%) [41], suggesting a defective peripheral tolerance. This finding suggests autoimmune disease arises from the failure to maintain peripheral tolerance. Actually, in response to BCR stimulation, defective apoptosis [42, 43], receptor editing [44, 45] and anergy induction [46, 47] are reported in both SLE patients and lupus mice. The defective peripheral tolerance detected in lupus mice and SLE patients further suggest that breakdown of peripheral tolerance may be involved in the disease development. In lupus-prone B6.Sleb1 mice, the expression of Ly108.1 impaired B cell anergy,

receptor editing, and deletion, which results in disease development [11]. Defective T cell tolerance is also reported in SLE patients and lupus-prone mice [48, 49]. Defective antigen-stimulated apoptosis was observed in mature T cells in MRL-*lpr* mice [48]. Regulatory T cells (Tregs, $Foxp3^{+}CD4^{+}CD25^{+}$), which participate in anergy by actively suppressing effector T cells, were reduced in SLE patients, suggesting defective anergy in lupus T cells [49].

Co-stimulatory signaling molecules and inhibitory signaling molecules work together and tightly regulate the threshold of BCR signaling [34, 50, 51]. Studies of lupus susceptibility loci suggest these signaling molecules are involved in regulating tolerance [11, 52-55]. For example, decreased expression levels of inhibitory signaling molecule FcγRIIB are observed in autoimmune diseases [56-58]. Partial restoration of FcγRIIB levels on B cells from lupus-prone mouse strains is sufficient to restore B cell tolerance and prevent autoimmunity [54]. The 2- to 4-fold increase in CD19, a co-receptor that positively regulates BCR signaling, was reported in a subset of memory B cells from SLE patients [59]. Moreover, these $CD19^{hi}$ memory B cells are autoreactive as they exhibit high levels of antibodies to Sm and low levels of anti-glomerular autoantibodies. This observation suggests CD19 increase might be associated with presence of autoreactive B cells [59].

Mechanisms of deletion, anergy and receptor editing in maintaining peripheral tolerance: The current understandings of how apoptosis, anergy, and receptor editing contribute to tolerance are discussed below.

Apoptosis: Apoptosis is an important mechanism for lymphocyte

homeostasis. Defective apoptosis therefore leads to abnormal survivals of potentially harmful lymphocytes [42]. In this sense, self-antigen-mediated apoptosis in autoreactive lymphocytes plays a central role [42], and defective self-antigen-mediated apoptosis was observed in numerous lupus-prone mouse models [34, 60, 61]. Among these defects, both enhanced survival signals [42] and impaired death pathways were identified [34, 60, 61].

Genetic studies performed on spontaneous lupus models have identified several SLE susceptibility genes in apoptotic signaling pathway, which suggests the possible participation of apoptosis in initiating and perpetuating the autoimmunity process [60, 61]. Mice deficient in Fas (CD95) or Fas ligand (FasL, CD95L) develop lupus-like diseases [62, 63], as Fas-FasL signaling pathway plays a critical role in the lupus development. Death ligand FasL binds to death receptor Fas and triggers apoptosis, deficiency in Fas or FasL therefore results in defective cell death, which leads to the abnormal survival and activation of self-reactive lymphocytes [63, 64]. Concomitant to the role of Fas-FasL signaling in apoptosis, self-reactive T cells are actually observed in Fas-deficient mice [64]. Defective apoptosis mediated by BCR are also detected in the lupus B cells from lupus-prone mice such as New Zealand Black (NZB) mice, F1 hybrid offspring of NZB mothers and New Zealand White fathers (NZB/NZW F1) mice, MRL-*lpr* mice, further supporting the idea that apoptosis plays a critical role in lupus development [33, 43]. Transgenic mice overexpressing anti-apoptotic factors or deficient in pro-apoptotic factors develop lupus-like diseases, confirming the role of apoptosis in lupus [65, 66]. For example,

transgenic mice overexpressing anti-apoptotic Bcl-2 spontaneously produce anti-DNA and anti-Sm autoantibodies and developed glomeronephritis [65]. Indeed, Bcl-2 expression is abnormal in T cells from SLE patients and may prolong the survival of autoreactive T cells [67, 68]. Pro-apoptotic BH3-only protein Bim knockout ($Bim^{-/-}$) mice develop an autoimmune kidney disorder [66]. Bim is involved in apoptosis induced by cell receptor as apoptosis mediated by both BCR and TCR are defective in Bim-deficient mice [66].

Factors that promote survival, including CD40 Ligand (CD40L) and B cell activating factor (BAFF), also participate in autoimmune disease [69]. They promote cell survival by upregulating anti-apoptotic Bcl-2-like family proteins [70], by enhancing pro-survival signaling pathways such as protein kinase B (Atk) and protein kinase C-β (PKC-β) [71], or by inhibiting apoptotic signaling such as PKC-δ [72]. The level of BAFF is elevated in the sera of patients with autoimmune disorders such as SLE [73], RA [74] and Sjogren's syndrome [75], indicating BAFF in the development of autoimmune diseases. Moreover, transgenic mice with overexpressed BAFF exhibit SLE-like symptoms [76, 77], confirming its role in autoimmune diseases. Its involvement might be due to that the increased BAFF provides B-cells with extra survival signaling and prevents apoptosis [78]. As TACI is a receptor for BAFF, soluble TACI-Ig fusion proteins is developed to block BAFF signaling. Treatment of NZB/NZW F1 mice with this TACI-Ig fusion proteins improve renal function and prolongs survival [79]. The efficacy further supports the abnormal survival of autoreactive lymphocyte is involved in autoimmune diseases.

Anergy: Similar to T cell anergy induction, whether B cell tolerance is induced was determined by whether or not two signals occurred. Signal 1 is induced through BCR, and signal 2 is induced by a co-stimulatory molecules such as CD19, CD21, CD40, toll-like receptor (TLR), and BAFF receptors (BAFF-R, TACI and BCMA) [25]. Engagement of cell receptor in the absence of co-stimulation leads to anergy [80]. For example, similar to T cell anergy induction by partial TCR stimulation such as anti-CD3, anergy is induced by binding autoantigen to BCR [80, 81]. Continuous BCR signaling is required for B cell anergy [25]. As signal 1 from receptor stimulation predominantly triggers Ca^{2+} signaling, the role of Ca^{2+} increase in anergy induction was studied [82]. Ionomycin, an ionophore that induces sustained $[Ca^{2+}]_i$ increase, induces anergy in T cells *in vitro* [82], confirming the critical role of calcium in establishing anergy. Anergy is inhibited by calcineurin inhibitor cyclosporine A, indicating that calcium-calcineurin pathway is important for anergy [83].

Anergy is a physiologically important mechanism for peripheral tolerance. In immunoglobulin (Ig) transgenic mice, the existence of self-antigen does not eliminate all the autoreactive B cells that express BCR for self-antigen [46]. The lack of autoantibodies product indicates they are functionally inactive [84]. *In vitro* characterization of these anergic autoreactive B cells indicates they display reduced immune response in response to stimulation [85], partially due to reduced BCR proximal signaling. Further characterization indicates that they have reduced half-life (4-5 days) when compared to 40 days of resting lymphocytes. The expression levels

of receptor (IgM or/and IgD) are also decreased. Based on these characteristics of anergic B cells from Ig transgenic mice, naturally occurring anergic B cells An1 are detected among normal lymphocytes [86]. Moreover, anergic B cells (naïve $IgD^{+}IgM^{-}$ B cells) are also identified in normal human individuals [87]. The detection of naturally anergic B cells in normal mice clearly indicates that anergy is a physiologically important mechanism for tolerance [86]. Defective anergy leads to lupus development, as abnormal anergy is observed in both human SLE and lupus mice [46, 88, 89].

Mechanism of anergy: Studies of Ig transgenic mice have shown that at least three partially distinct mechanisms contribute to reduced immune response in anergic cells: attenuated cell receptor signaling, reduced membrane Ig expression, and reduced lifespan [25]. Their relative contribution is dependent on transgenic mice models [25]. On the transcription level, anergy-associated genes were identified by studying the gene expression in anergic lymphocytes [90, 91]. They are either upregulated or downregulated in response to anergy stimuli [90, 91]. A majority of anergy-associated genes are induced by activated NFAT alone [90, 91]. For instance, E3 ubiquitin ligases such as Cbl-b and GRAIL are upregulated in a NFAT-dependent manner. They are both necessary and sufficient to induce anergy in both T cells and B cells [90, 92, 93]. These anergy-associated genes are involved in anergy by affecting the three mechanism listed [90, 92, 93]. For example, E3 ubiquitin ligases induce anergy by promoting the degradation of PKC-θ and PLC-γ, two critical mediators in TCR signaling, which attenuates TCR signaling [93].

Receptor editing: Receptor editing is the process of cell receptor rearrangement, which results in the change of its specificity to be less self-reactive [18]. The binding of autoantigen to the BCR triggers receptor editing, which is mediated by the recombination activating gene RAG1 and RAG2 through V(D)J recombination (Figure 1.2; [94]). V(D)J recombination is a mechanism of genetic recombination to generate diverse immunoglobulin (Ig) by recombining various V, D and J genes [95]. Studies of autoreactive B cells from transgenic mice indicate both membrane and soluble self-antigens can induce receptor editing [96, 97]. In periphery, receptor editing mainly occurs during GC reactions [98]. During receptor editing, Jκ distal Vκ genes are recombined to Jκ to replace a proximal Vκ1-Jκ segment; therefore this usage of distal Vκ genes can be an indicator of receptor editing (Figure1.2; [99]). The overusage of distal Vκ genes indicates that BCR editing occurs frequently and is therefore the most important mechanism of B cell tolerance [99]. Deficiency in receptor editing is observed in autoimmune diseases and is proposed to play a role in maintaining peripheral B-cell tolerance [100, 101]. In SLE patients an overusage of Jκ proximal Vκ1 genes, instead of an overusage of Jκ distal Vκ genes, suggests a defective receptor editing [44]. Genetic studies identified lupus susceptibility genes SLE2 and SLE3/5 are associated with impaired receptor editing observed in SLE patients, although the mechanism is not clear [9, 102]. This finding indicates that impaired receptor editing may lead to the development of lupus.

The role of B cells in autoimmunity: It is widely accepted that B cells play a critical role in the onset of autoimmune disease [103]. Primarily, B cells are thought

to mediate lupus via autoantibodies, which form immunocomplexes with self-antigen, deposit in renal membrane, and result in renal damage [104]. Old MRL mice develop severe nephritis, and B cell deficiency results in the attenuation of symptoms, thus indicating B cells play a critical role in lupus nephritis in old MRL mice [105]. This B cell-mediated lupus nephritis is not caused by autoantibodies, as B cells that can not

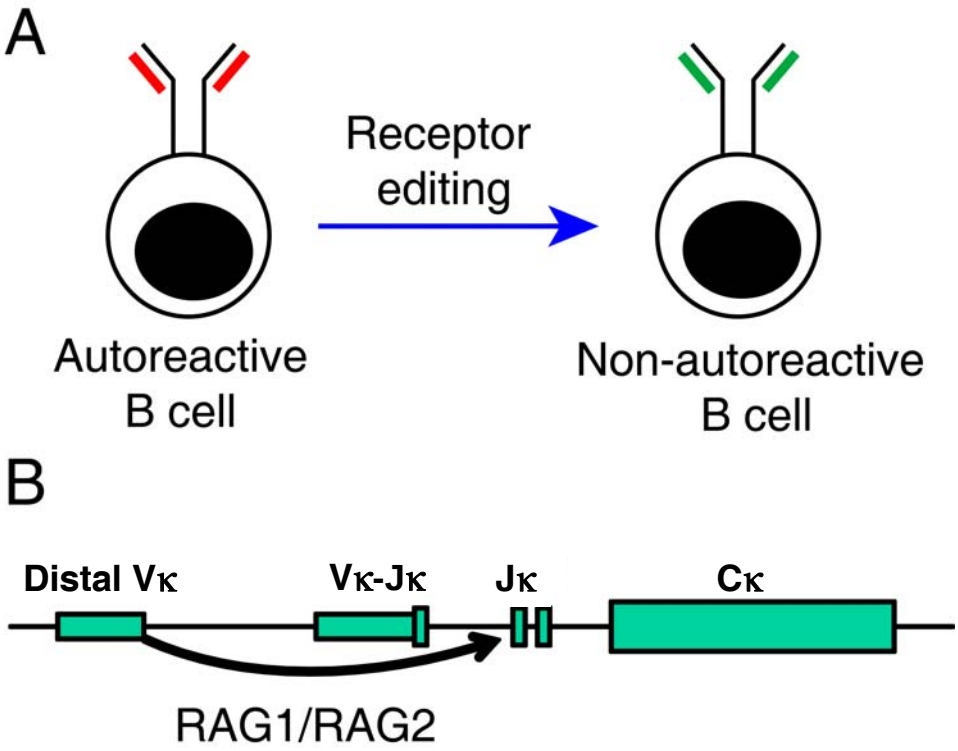

Figure 1.2: Receptor editing: (A) Receptor editing generates a new non-autoreactive BCR and replaces the autoreactive BCR. (B) The distal various region of κ light chain (Vκ) can rearrange to downstream J gene segment of κ light chain (Jκ) to generate a new immunoglobulin chain for BCR. This process is mediated by recombination activating gene 1 (RAG1) and RAG2. Panel B is adopted from [106].

secrete circulating immunoglobulin can still induce glomerulonephritis in MRL mice [107]. Based on these observations, B cells are proposed to mediate glomerulonephritis in an autoantibody-independent manner. In addition to antibody production, B cells can also function as antigen presenting cells (APCs) and secrete

cytokines, which activate T cells, improving the effectiveness of the immune response [108]. Therefore B cells abnormally activate and mediate glomerulonephritis by secreting cytokines or acting as APCs. Actually, expansion of activated T cells is impaired in B cell-deficient MRL mice [109]. On the other hand, the activated T cells assist the immune response of B cells. This interplay between self-reactive T cells and B cells has an essential role in the development of autoimmune diseases [110]. Therefore, breaking this cycle is critical for effective treatment of autoimmune disease. In summary, Autoreactive B cells are involved in the onset and pathogenesis of autoimmune disease in an autoantibody-dependent and an autoantibody-independent manner.

During development, B cells are regulated to maintain tolerance for self-antigens. Bone marrow B cells undergo pro-B and Pre-B stages, and develop into immature B cells (Figure 1,3; [111]). Because the recombination is random, autoreactive B cells will be inevitably generated. There are around 75% immature B cells generated in the bone marrow that express self-reactive BCRs [112]. After central B cell tolerance, the self-reactivity is reduced to ~40% [111]. These immature B cells then migrate into the periphery for further maturation (Figure 1.3; [113, 114]). In periphery, immature B cells evolve into mature (naïve) B cells with IgM and IgD expression (Figure1.3; [113, 114]). They undergo further peripheral tolerance checkpoints and their self-reactivity is reduced to 20% [111].

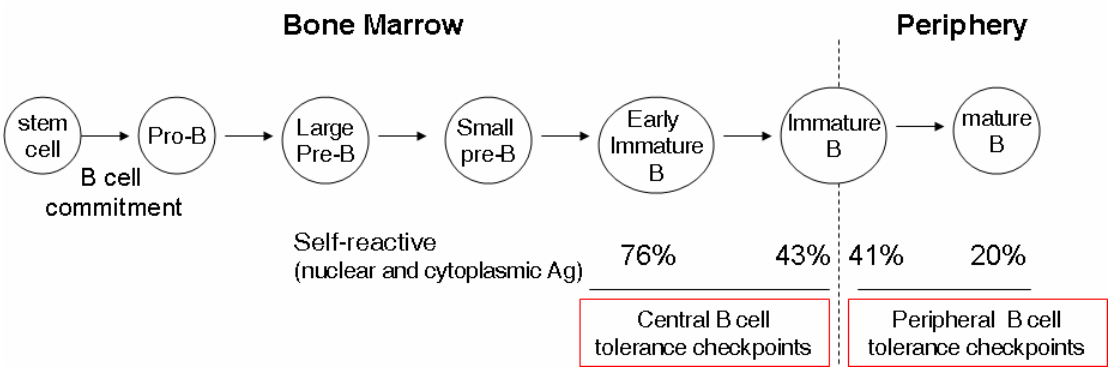

Figure 1.3: B cell development and checkpoints. Immature B cells and mature B cells are tightly regulated. Series of checkpoints decrease the self-reactivity and poly-reactivity of BCR along with development. This picture is adapted from [111].

Resting mature B cells translocate to the primary follicles, where they bind to specific antigens and undergo antigen-induced activation [113, 114]. Activated B cells then migrate towards the interface between the primary follicles and T cells zone, where activated B cells present antigen to antigen-specific T cells [113, 114]. These activated T cells secrete lymphokines and support B cell proliferation to form germinal centers (GCs) (Figure 1.4; [113, 114]). In the dark region of the GC, proliferating centroblasts undergo extensive somatic hypermutation, including random substitutions, deletions and insertions to generate a diversity of BCR clones [113, 114]. These BCR clones migrate to the light zone of the GC and differentiate into non-proliferating centrocytes [113, 114], which then undergo clonal selection (Figure1.4; [113, 114]). Centrocytes with high affinity for the antigen presented by the follicular dendritic cell network (FDC) will be positively selected [113, 114]. They further undergo isotype switching and differentiate into either memory or plasma cells [113, 114]. Centrocytes with low affinity for the antigen in FDC and self-reactive

centrocytes undergo negative selection [113, 114]. Centrocytes that bind to self-antigen with high affinity or high avidity undergo apoptosis or receptor editing to reduce autoimmunity [115], while cells that bind to self-antigen with low affinity or avidity exit the GC and render anergic in the periphery [115].

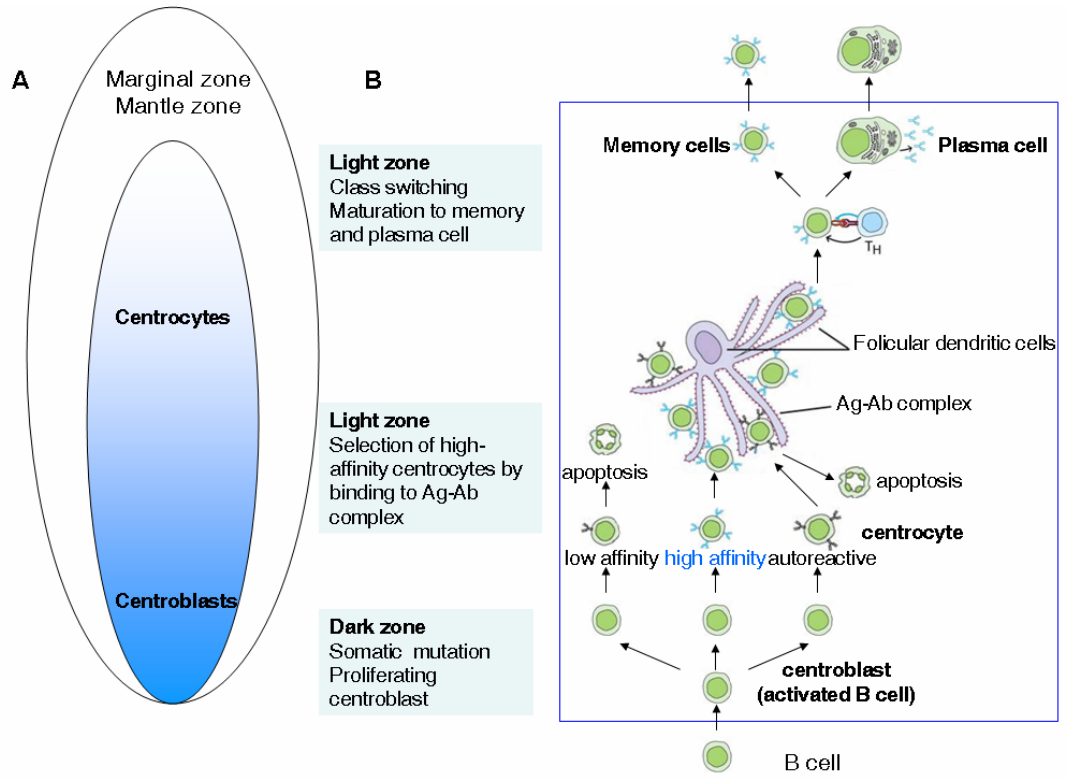

Figure 1.4: Germinal center reaction: Activated B cells form GCs. During GCs reactions, affinity maturation and class switching to generate B cells with various high affinity. Then the cells with high affinity undergo positive cells and differentiate into memory and plasma cells. The cells with low affinity and self-reactive B cells undergo negative selection, including extensive apoptosis, receptor editing. This picture is adapted from [116].

BCR signaling in peripheral tolerance: BCR signaling is involved in peripheral tolerance by inducing apoptosis, anergy or receptor editing [14, 16, 17, 19-21]. Altered BCR signaling has been demonstrated in human SLE [117]. In response to BCR stimulation by anti-IgM or IgD antibodies, elevated calcium influx and enhanced tyrosine phosphorylation are observed, indicating abnormal regulation of the BCR signaling pathway [36]. This abnormal BCR signaling could be due to enhanced activity of a positive co-receptor or reduced activity of a negative co-receptor [117]. CD19 is a positive co-receptor that increases the BCR-mediated survival signaling [50]. Abnormal CD19 activation enhances recruitment of several pro-survival mediators, which override the inhibitory mediators. Therefore, CD19 signaling lowers the threshold for BCR activation and participates in autoimmune diseases [118]. CD19 overexpression leads to the breakdown of peripheral tolerance and autoantibody production [119], and is closely associated with autoimmune diseases such as systemic sclerosis (SSc). Human SSc B cells have constitutively higher CD19 surface expression level [120], and in the tight skin mouse (TSK/+) model of SSc, CD19 is constitutively phosphorylated [121]. Crossing of TSK/+ mice to a $CD19^{-/-}$ mice reduces CD19 expression, abolishes the autoantibody production, and improves the symptoms [121], indicating the critical role of CD19 in the development of this autoimmune phenotype.

Deficiency of negative co-receptor also plays a critical role in autoimmune disease development [122, 123]. FcγRIIB is an inhibitory immunoglobulin G Fc receptor which contains an immunoreceptor tyrosine-based inhibition motif (ITIM)

[122]. Upon phosphorylation by Lyn, ITIM recruits SH2 containing inositol phosphate phosphatase (SHIP), which downregulates BCR signaling [123]. Impaired FcγRIIB signaling is observed in autoimmune diseases such as SLE [117]. A FcγRIIB mutant that is unable to localize to lipid rafts is found in SLE patients in Asian and African populations [124-126]. In addition, decreased FcγRIIB expression is associated with SLE in European-Americans [127]. Spontaneous autoimmunity develops in FcγRIIB-deficient mice [128].

Lyn is a tyrosine protein kinase that can phosphorylate tyrosine in both ITIM and the immunoreceptor tyrosine-based activation motif (ITAM) [129]. Thus Lyn initiates both negative and positive signaling for BCR signaling pathway. Decreases in mRNA and protein level are detected in B cells from SLE patients [130, 131]. This Lyn decrease is correlated with decreased phosphorylation of FcγRIIB and CD22, resulting in decreased SHP-1/SHIP-1 recruitment. Mice with both constitutively active Lyn and Lyn deficiency develop autoimmune disease [132, 133]. The possible explanation to this confusing observation is that the positive signaling pathway for survival and proliferation is dominant in both Lyn-deficient and Lyn-constitutive active lymphocyte.

Other factors that contribute to abnormal activation of self-reactive B cells: TLRs are found on the surface of B cells, and recognize a variety of microbial components and potential host-derived agonists [134]. The signaling pathways mediated by several TLR receptors play a critical role in induction and progression of autoimmune diseases such as RA, experimental autoimmune encephalitis (EAE),

myocarditics, and SLE [134]. TLR-7 and TLR-9 are of significant interest because they may contribute to the immunological response to well-known self-antigens such as single-stranded RNA (TLR-7) and DNA (TLR-9) in SLE [135, 136]. Co-activation of BCR and TLR signaling induces proliferation, differentiation and isotype switching [137]. Removal of TLR9 prevents isotype switching of pathogenic antibodies from IgM to more responsive IgG2a and IgG2b in the lupus-prone mouse models [138], which may contribute to attenuation of autoimmunity by TLR9 deletion. Duplication of TLR-7 in Y-linked autoimmune acceleration (*Yaa*) locus is associated with accelerated lupus development [139], which is attenuated by its null mutation [140].

Although defective apoptosis results in the appearance of self-reactive lymphocytes and lupus development, there are several pieces of evidence that defective clearance of potential autoantigens may also be involved in lupus development. The increased spontaneous cell death releases nuclear proteins and chromatin, which is an important source of autoantigens for the activation of self-reactive lymphocytes. Defective clearance of autoantigens is observed in SLE patients [141, 142]. Low expression or activity of deoxyribonuclease I-like 3 (DNase I-like 3) is also detected in lupus-prone mice including NZB/NZW F1 mice [143, 144]. The serum level of DNA is increased, possibly due to defective DNA clearance [143, 144]. Moreover, DNase $I^{-/-}$ mice produce anti-nuclear antibodies, which form immune complexes and deposit in the kidneys, causing glomerulonephritis [145]. However, the efficacy of Bz-423 and other apoptotic-inducing reagents argue against the actual role of the defective clearance system in the disease development.

SLE treatment:

The challenge of SLE treatment and potential novel lupus treatments: Because the cause is unknown, current treatment for SLE is non-specific, which including cytotoxic drugs and general immunosuppressants [146]. These non-specific treatments increase serious side effects such as osteoporosis, skin atrophy, cushingoid appearance, diabetes and glaucoma [147]. Therefore the need for safer, more selective therapies has been recognized. However, it becomes a challenge to improve the selectivity while maintaining efficacy. With better understanding of the immunopathogenesis of SLE, more potential targets can be discovered for potential SLE treatment. There is the large body of evidence implicating the abnormalities in the B cell compartment in the SLE [148]. The important role of B cells in the pathogenesis of autoimmune disorders has therefore provided a rationale to target B cells with SLE (Figure 1.5). This approach has been validated by the observed beneficial effect of B-cell depletion therapies in autoimmune diseases mediated by autoreactive B cells [149-152].

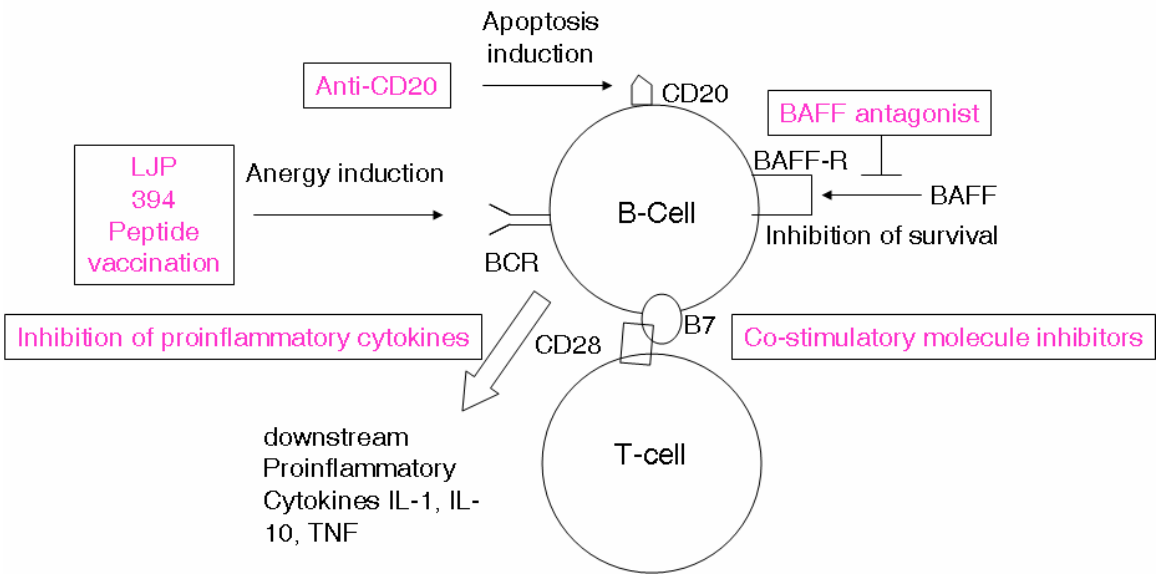

Figure 1.5: Proposed B-cell targeted SLE treatment. This picture is adapted from [153].

B cell targeted SLE treatment

B cell depletion: autoreactive B cells can be depleted by promoting the apoptotic signaling pathway (anti-CD20, anti-CD22 and anti-CD72) and blocking the survival signaling pathway (anti-BAFF). CD20 is expressed during all stages of B cell development except on pro-B and plasma B cells. Rituximab, a chimeric murine-human monoclonal antibody, binds to the CD20 receptor and results in the depletion of CD20-positive B cells [154]. However, clinical trials demonstrate that only a fraction of SLE patients respond to rituximab [155], demonstrating the heterogeneity of lupus diseases.

The receptors for BAFF, TACI, BCMA, BAFF-R are largely restricted to immature and mature B cells [156]. Overexpression of BAFF leads to the lupus-like disease development [77], while BAFF knockout ameliorates the disease [79].

Moreover, in human SLE, BAFF overexpression is observed [157]. The newly developed drug belimumab is a human monoclonal antibody that specifically binds and neutralizes the soluble BAFF, therefore blocking BAFF, and is shown to significantly decrease B cells [158].

Anergy induction: As tolerance is lost in autoimmune diseases, it will be an effective way to restore peripheral tolerance, which can be achieved by promoting apoptosis, anergy and receptor editing. LJP 394 is this kind of reagent developed, since it induces either anergy or apoptosis by crosslinking with anti-dsDNA antibodies on the surface of B cells [159]. Administration of LJP 394 significantly delays the time and incidence of renal flares, as well as reduces the anti-dsDNA Ab levels [159]. Anergy is promoted by peptide specific tolerance and can be used for autoimmune diseases. ELDI-peptide-coupled cells with specific peptides was developed to bind to TCR and promote T cell tolerance, which was used to treat MS [160]. Administration of specific antigen (myelin basic protein or type II collagen) is shown to suppress experimental autoimmune encephalomyelitis (EAE) and collagen-induced arthritis respectively [161], proving the potential application of anergy induction for autoimmune disease treatment.

Bz-423, a pro-apoptotic benzodiazepine, improves lupus disease. Pathogenic lymphocytes play a critical role in onset and progress of autoimmune diseases; they are therefore a logical target for therapeutic strategies. This strategy aims to specifically delete or to functionally inhibit pathogenic autoreactive lymphocytes without altering the normal immune system, therefore, providing both efficacy and specificity [162].

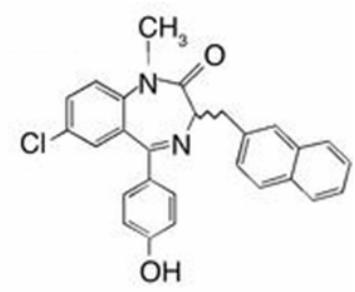

Figure 1.6: The structure of Bz-423

Bz-423 is a novel chemical for lupus treatment with efficacy and specificity: Bz-423 is a pro-apoptotic immunomodulatory benzodiazepine (Figure 1.6). Administration of Bz-423 to two lupus-prone mouse models (NZB/NEW F1 mice and MRL-*lpr* mice) ameliorates disease and improves renal function [163, 164]. This attenuation of lupus disease is associated with reduction in pathogenic lymphocytes (B cells in NZB/NZW F1 mice and T cells in MRL-*lpr* mice) [163, 164]. The reduction of lymphocytes suggests the possible induction of cell death or growth arrest. This hypothesis is supported by the observation that Bz-423 inhibits cell proliferation at low [Bz-423] (≤ 5μM in 2% FBS media or ≤ 20 μM in 10% FBS media) in Ramos B cell line and it induces cell death in several B cell and T cell lines high [Bz-423] [164, 165]. Both cell death and growth arrest are dependent on ROS, as

anti-oxidants inhibit Bz-423 induced cell death and growth arrest [164, 165].

Although the cytotoxic and growth inhibitory effects induced by Bz-423 can explain the efficacy of Bz-423 treatment, it does not explain how Bz-423 selectively reduces pathogenic lymphocytes. Moreover, Bz-423 does not affect the number and the normal immune response of normal lymphocytes [163]. Exaggerated GC expansion is observed in the spleen of NZB/NZW F1 mice. Bz-423 reduces both the size and number of GCs. This reduction is due to apoptosis as the increased apoptosis activity is observed in the Bz-423 treated spleen. Moreover, expanded GC indicates abnormal B cell activation. It was therefore hypothesized that activation sensitizes cells to Bz-423. This hypothesis was tested by study of cell death induced by co-treatment of anti-IgM and Bz-423 in Ramos B cells. Co-treatment of anti-IgM and Bz-423 induces a synergistic cell death, indicating anti-IgM stimulation sensitizes Ramos B cells to Bz-423 [166]. Selectivity happens as low [Bz-423] (<5 μM in 2% FBS) induces cell death in anti-IgM-stimulated B cells but not in resting B cells. Because anti-oxidant, extracellular calcium chelator and protein synthesis inhibitor protects cells from synergistic cell death, it is concluded that ROS, calcium and protein synthesis are required for synergistic cell death induction [166].

Bz-423 induces superoxide as a result of inhibiting mitochondrial F_0F_1-ATPase. Protons are pumped from the matrix into the mitochondrial intermembrane space (IMS) by the electron transport chain (ETC) complexes, and then return to the matrix by passing through the mitochondrial F_0F_1-ATPase during ATP synthesis [167, 168]. The balance between ETC and F_0F_1-ATPase activity leads

to a steady state of mitochondrial membrane potential ($\Delta\psi_m$) at ~ 150 mV. Mitochondrial hyperpolarization (more ETC activity and/or less ATPase activity) slows electron transport, which forces the ETC into a reduced state that favors production of superoxide [167]. Therefore, mitochondrial F_0F_1-ATPase inhibitors induce superoxide production by increasing $\Delta\psi_m$ (Figure 1.7). In isolated mitochondria, mitochondrial F_0F_1-ATPase inhibitors oligomycin and diindolylmethane (DIM) are shown to induce superoxide [169-171]. Bz-423 treatment also induces superoxide in isolated mitochondria, indicating the possible inhibition of mitochondrial F_0F_1-ATPase [164]. Bz-423 inhibits both the synthesis and hydrolysis activity of mitochondrial F_0F_1-ATPase *in vitro* [172], confirming that Bz-423 is a mitochondrial F_0F_1-ATPase inhibitor. Phage display showed that Bz-423 binds to the oligomycin sensitivity conferring protein (OSCP), a peripheral stalk protein linking the membrane F_0 and catalytic F_1 component [172]. Binding of Bz-423 to OSCP binding leads to inhibition of the F_0F_1-ATPase synthesis and hydrolysis activity *in vivo* and *in vitro* [172]. Inhibition of mitochondria F_0F_1-ATPase by Bz-423 induces mitochondria hyperpolarization, which results in superoxide production [172]. RNAi knockdown of OSCP in HEK cells render cells resistant to ROS production and cell death induced by Bz-423 [172], confirming the critical role of OSCP in Bz-423 induced superoxide production and subsequent cell death.

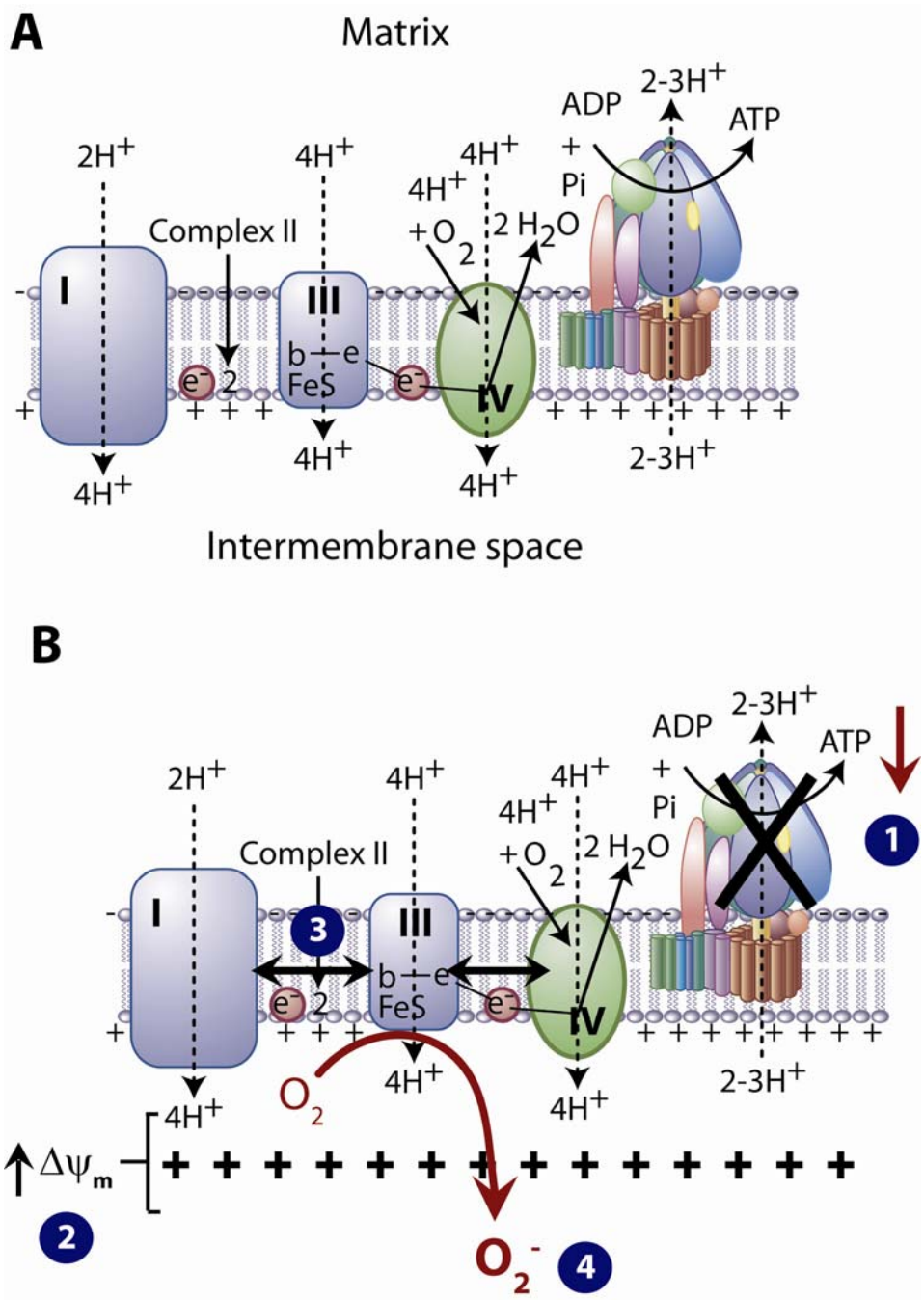

Figure 1.7: Inhibition of the mitochondrial F_0F_1-ATPase induces superoxide production. (A) Mitochondrial membrane potential ($\Delta\psi_m$) is achieved by the balance between the activity of electron transport chain (ETC) and mitochondrial F_0F_1-ATPase activity. The increased activity of ETC will increase proton pumping from matrix to mitochondrial intermembrane space (IMS), therefore, increasing $\Delta\psi_m$. The increase in mitochondrial F_0F_1-ATPase activity will allow the passage of proton from IMS to matrix, lowering $\Delta\psi_m$. (B) mitochondrial F_0F_1-ATPase induces superoxide by increasing $\Delta\psi_m$. Inhibition of mitochondrial F_0F_1-ATPase activity (step 1) results in increase in $\Delta\psi_m$ (step 2). The increase in proton motive force slows electron transport by ETC (step 3), which eventually leads to superoxide production (step 4). Figures are adopted from [173]

Statement of Goals: Administration of Bz-423 to two lupus-prone mouse models, NZB/NZW F1 and MRL-*lpr* mice, improves disease with few side effects [163, 164]. Enlarged and increased GCs are observed in the spleen of NZB/NZW F1 mice, which was reduced by 40% by Bz-423 [164]. GC is formed by a rapid clonal division of activated B cells [174]. The reduction in GCs by Bz-423, together with increased apoptotic activity in the remaining GCs, suggests Bz-423 may selectively reduce GC B cells via apoptosis [174]. As GC B cells are activated [174], it was hypothesized that activation sensitizes cells to Bz-423 [166]. To test this hypothesis, Ramos B cells were co-treated with Bz-423 and anti-IgM, and the cell death induced by co-treatments was determined. Compared with the cell death induced by anti-IgM and Bz-423 alone, co-treatment induced a supra-additive effect on cell death, indicating anti-IgM sensitizes Ramos B cells to Bz-423 [166]. The protection of antioxidant, extracellular calcium chelator, new protein synthesis inhibitor against cell death by anti-IgM and Bz-423 co-treatment indicates ROS, calcium, and new protein synthesis are required for synergistic cell death [166].

The goal of my research is to understand the selectivity of Bz-423 observed *in vivo*. In Chapter 2, the apoptotic signaling pathway induced by anti-IgM and Bz-423 co-treatment in Ramos B cell *in vitro* model was studied. This *in vitro* model was first verified to be appropriate for studying the selectivity of Bz-423 observed *in vivo*. As calcium and superoxide are critical mediators, their involvement was studied in detail. Then the apoptotic signaling downstream of calcium and superoxide were explored. During these Chapter 2 studies, Bz-423 was first observed to activate NFAT.

As NFAT plays a critical role in modulating the immune function such as anergy, Bz-423 induced NFAT activation was further studied in Chapter 3. Bz-423 induced NFAT dephosphorylation, nuclear translocation, and NFAT-dependent gene expression were first studied. How Bz-423 activates NFAT by inhibitors was then studied. Lastly, the possible consequences of Bz-423 induced NFAT activation were explored.

Bibliography

1. Keir, M.E., Sharpe, A.H. (2005). The B7/CD28 costimulatory family in autoimmunity. Immunol Rev *204*, 128-43.

2. Carpenter, A.B., Rabin, B.S. (1983). Autoimmunity in immunopathology. Clin Lab Med *3*, 745-62.

3. Demas, K.L., Costenbader, K.H. (2009). Disparities in lupus care and outcomes. Curr Opin Rheumatol *21*, 102-9.

4. Hauff, K., Zamzow, C., Law, W.J., De Melo, J., Kennedy, K., Los, M. (2005). Peptide-based approaches to treat asthma, arthritis, other autoimmune diseases and pathologies of the central nervous system. Arch Immunol Ther Exp (Warsz) *53*, 308-20.

5. Maddison, P.J. (1999). Autoantibodies in SLE. Disease associations. Adv Exp Med Biol *455*, 141-5.

6. Kanta, H., Mohan, C. (2009). Three checkpoints in lupus development: central tolerance in adaptive immunity, peripheral amplification by innate immunity and end-organ inflammation. Genes Immun

7. Hewagama, A., Richardson, B. (2009). The genetics and epigenetics of autoimmune diseases. J Autoimmun

8. Munz, C., Lunemann, J.D., Getts, M.T., Miller, S.D. (2009). Antiviral immune responses: triggers of or triggered by autoimmunity? Nat Rev Immunol *9*, 246-58.

9. Liu, Y., Li, L., Kumar, K.R., Xie, C., Lightfoot, S., Zhou, X.J., Kearney, J.F., Weigert, M., Mohan, C. (2007). Lupus susceptibility genes may breach tolerance to DNA by impairing receptor editing of nuclear antigen-reactive B cells. J Immunol *179*, 1340-52.

10. Wither, J.E., Lajoie, G., Heinrichs, S., Cai, Y.C., Chang, N., Ciofani, A.,

Cheung, Y.H., MacLeod, R. (2003). Functional dissection of lupus susceptibility loci on the New Zealand black mouse chromosome 1: evidence for independent genetic loci affecting T and B cell activation. J Immunol *171*, 1697-706.

11. Kumar, K.R., Li, L., Yan, M., Bhaskarabhatla, M., Mobley, A.B., Nguyen, C., Mooney, J.M., Schatzle, J.D., Wakeland, E.K., Mohan, C. (2006). Regulation of B cell tolerance by the lupus susceptibility gene Ly108. Science *312*, 1665-9.

12. Hochberg, M.C. (1990). Systemic lupus erythematosus. Rheum Dis Clin North Am *16*, 617-39.

13. Romagnani, S. (2006). Immunological tolerance and autoimmunity. Intern Emerg Med *1*, 187-96.

14. Ring, G.H., Lakkis, F.G. (1999). Breakdown of self-tolerance and the pathogenesis of autoimmunity. Semin Nephrol *19*, 25-33.

15. Nossal, G.J. (1997). B lymphocyte physiology: the beginning and the end. Ciba Found Symp *204*, 220-30; discussion 30-1.

16. Edinger, A.L., Thompson, C.B. (2004). Death by design: apoptosis, necrosis and autophagy. Curr Opin Cell Biol *16*, 663-9.

17. Nemazee, D., Russell, D., Arnold, B., Haemmerling, G., Allison, J., Miller, J.F., Morahan, G., Buerki, K. (1991). Clonal deletion of autospecific B lymphocytes. Immunol Rev *122*, 117-32.

18. Gay, D., Saunders, T., Camper, S., Weigert, M. (1993). Receptor editing: an approach by autoreactive B cells to escape tolerance. J Exp Med *177*, 999-1008.

19. Jankovic, M., Casellas, R., Yannoutsos, N., Wardemann, H., Nussenzweig, M.C. (2004). RAGs and regulation of autoantibodies. Annu Rev Immunol *22*, 485-501.

20. Nemazee, D., Weigert, M. (2000). Revising B cell receptors. J Exp Med *191*, 1813-7.

21. Fathman, C.G., Lineberry, N.B. (2007). Molecular mechanisms of CD4+ T-cell anergy. Nat Rev Immunol *7*, 599-609.

22. Gauld, S.B., Benschop, R.J., Merrell, K.T., Cambier, J.C. (2005). Maintenance of B cell anergy requires constant antigen receptor occupancy and signaling. Nat Immunol *6*, 1160-7.

23. Halverson, R., Torres, R.M., Pelanda, R. (2004). Receptor editing is the main mechanism of B cell tolerance toward membrane antigens. Nat Immunol *5*, 645-50.

24. Hippen, K.L., Schram, B.R., Tze, L.E., Pape, K.A., Jenkins, M.K., Behrens, T.W. (2005). In vivo assessment of the relative contributions of deletion, anergy, and editing to B cell self-tolerance. J Immunol *175*, 909-16.

25. Gauld, S.B., Merrell, K.T., Cambier, J.C. (2006). Silencing of autoreactive B cells by anergy: a fresh perspective. Curr Opin Immunol *18*, 292-7.

26. Srinivasan, M., Frauwirth, K.A. (2009). Peripheral tolerance in CD8(+) T cells. Cytokine

27. Verhagen, J., Blaser, K., Akdis, C.A., Akdis, M. (2006). Mechanisms of allergen-specific immunotherapy: T-regulatory cells and more. Immunol Allergy Clin North Am *26*, 207-31, vi.

28. Yi, H., Zhen, Y., Jiang, L., Zheng, J., Zhao, Y. (2006). The phenotypic characterization of naturally occurring regulatory CD4+CD25+ T cells. Cell Mol Immunol *3*, 189-95.

29. Zhang, J., Jacobi, A.M., Wang, T., Diamond, B. (2008). Pathogenic autoantibodies in systemic lupus erythematosus are derived from both self-reactive and non-self-reactive B cells. Mol Med *14*, 675-81.

30. Chang, N.H., MacLeod, R., Wither, J.E. (2004). Autoreactive B cells in lupus-prone New Zealand black mice exhibit aberrant survival and proliferation in the presence of self-antigen in vivo. J Immunol *172*, 1553-60.

31. Fraser, N.L., Rowley, G., Field, M., Stott, D.I. (2003). The VH gene repertoire of splenic B cells and somatic hypermutation in systemic lupus erythematosus. Arthritis Res Ther *5*, R114-21.

32. Erikson, J., Mandik, L., Bui, A., Eaton, A., Noorchashm, H., Nguyen, K.A., Roark, J.H. (1998). Self-reactive B cells in nonautoimmune and autoimmune mice. Immunol Res *17*, 49-61.

33. Tsubata, T. (2005). B cell abnormality and autoimmune disorders.

Autoimmunity *38*, 331-7.

34. Peng, S.L. (2009). Altered T and B lymphocyte signaling pathways in lupus. Autoimmun Rev *8*, 179-83.

35. Flores-Borja, F., Kabouridis, P.S., Jury, E.C., Isenberg, D.A., Mageed, R.A. (2005). Decreased Lyn expression and translocation to lipid raft signaling domains in B lymphocytes from patients with systemic lupus erythematosus. Arthritis Rheum *52*, 3955-65.

36. Liossis, S.N., Kovacs, B., Dennis, G., Kammer, G.M., Tsokos, G.C. (1996). B cells from patients with systemic lupus erythematosus display abnormal antigen receptor-mediated early signal transduction events. J Clin Invest *98*, 2549-57.

37. Nagy, G., Koncz, A., Perl, A. (2005). T- and B-cell abnormalities in systemic lupus erythematosus. Crit Rev Immunol *25*, 123-40.

38. Tenbrock, K., Juang, Y.T., Kyttaris, V.C., Tsokos, G.C. (2007). Altered signal transduction in SLE T cells. Rheumatology (Oxford) *46*, 1525-30.

39. Hillion, S., Rochas, C., Devauchelle, V., Youinou, P., Jamin, C. (2006). Central and peripheral RAG protein re-expression: underestimate mechanisms of tolerance? Scand J Immunol *64*, 185-9.

40. Wellmann, U., Werner, A., Winkler, T.H. (2001). Altered selection processes of B lymphocytes in autoimmune NZB/W mice, despite intact central tolerance against DNA. Eur J Immunol *31*, 2800-10.

41. Yurasov, S., Wardemann, H., Hammersen, J., Tsuiji, M., Meffre, E., Pascual, V., Nussenzweig, M.C. (2005). Defective B cell tolerance checkpoints in systemic lupus erythematosus. J Exp Med *201*, 703-11.

42. Kuhtreiber, W.M., Hayashi, T., Dale, E.A., Faustman, D.L. (2003). Central role of defective apoptosis in autoimmunity. J Mol Endocrinol *31*, 373-99.

43. Kozono, Y., Kotzin, B.L., Holers, V.M. (1996). Resting B cells from New Zealand Black mice demonstrate a defect in apoptosis induction following surface IgM ligation. J Immunol *156*, 4498-503.

44. Dorner, T., Lipsky, P.E. (2005). Molecular basis of immunoglobulin variable region gene usage in systemic autoimmunity. Clin Exp Med *4*, 159-69.

45. Suzuki, N., Mihara, S., Sakane, T. (1997). Development of pathogenic anti-DNA antibodies in patients with systemic lupus erythematosus. Faseb J *11*, 1033-8.

46. Cambier, J.C., Gauld, S.B., Merrell, K.T., Vilen, B.J. (2007). B-cell anergy: from transgenic models to naturally occurring anergic B cells? Nat Rev Immunol *7*, 633-43.

47. Seo, S.J., Mandik-Nayak, L., Erikson, J. (2003). B cell anergy and systemic lupus erythematosus. Curr Dir Autoimmun *6*, 1-20.

48. Russell, J.H., Rush, B., Weaver, C., Wang, R. (1993). Mature T cells of autoimmune lpr/lpr mice have a defect in antigen-stimulated suicide. Proc Natl Acad Sci U S A *90*, 4409-13.

49. Venigalla, R.K., Tretter, T., Krienke, S., Max, R., Eckstein, V., Blank, N., Fiehn, C., Ho, A.D., Lorenz, H.M. (2008). Reduced CD4+,CD25- T cell sensitivity to the suppressive function of CD4+,CD25high,CD127 -/low regulatory T cells in patients with active systemic lupus erythematosus. Arthritis Rheum *58*, 2120-30.

50. Buhl, A.M., Cambier, J.C. (1997). Co-receptor and accessory regulation of B-cell antigen receptor signal transduction. Immunol Rev *160*, 127-38.

51. Pugh-Bernard, A.E., Cambier, J.C. (2006). B cell receptor signaling in human systemic lupus erythematosus. Curr Opin Rheumatol *18*, 451-5.

52. Gutierrez-Roelens, I., Lauwerys, B.R. (2008). Genetic susceptibility to autoimmune disorders: clues from gene association and gene expression studies. Curr Mol Med *8*, 551-61.

53. Criswell, L.A. (2008). The genetic contribution to systemic lupus erythematosus. Bull NYU Hosp Jt Dis *66*, 176-83.

54. McGaha, T.L., Sorrentino, B., Ravetch, J.V. (2005). Restoration of tolerance in lupus by targeted inhibitory receptor expression. Science *307*, 590-3.

55. Pisitkun, P., Deane, J.A., Difilippantonio, M.J., Tarasenko, T., Satterthwaite, A.B., Bolland, S. (2006). Autoreactive B cell responses to RNA-related antigens due to TLR7 gene duplication. Science *312*, 1669-72.

56. Jiang, Y., Hirose, S., Sanokawa-Akakura, R., Abe, M., Mi, X., Li, N., Miura, Y., Shirai, J., Zhang, D., Hamano, Y., Shirai, T. (1999). Genetically determined

aberrant down-regulation of FcgammaRIIB1 in germinal center B cells associated with hyper-IgG and IgG autoantibodies in murine systemic lupus erythematosus. Int Immunol *11*, 1685-91.

57. Siriboonrit, U., Tsuchiya, N., Sirikong, M., Kyogoku, C., Bejrachandra, S., Suthipinittharm, P., Luangtrakool, K., Srinak, D., Thongpradit, R., Fujiwara, K., Chandanayingyong, D., Tokunaga, K. (2003). Association of Fcgamma receptor IIb and IIIb polymorphisms with susceptibility to systemic lupus erythematosus in Thais. Tissue Antigens *61*, 374-83.

58. Pan, F., Zhang, K., Li, X., Xu, J., Hao, J., Ye, D. (2006). Association of Fcgamma receptor IIB gene polymorphism with genetic susceptibility to systemic lupus erythematosus in Chinese populations--a family-based association study. J Dermatol Sci *43*, 35-41.

59. Culton, D.A., Nicholas, M.W., Bunch, D.O., Zhen, Q.L., Kepler, T.B., Dooley, M.A., Mohan, C., Nachman, P.H., Clarke, S.H. (2007). Similar CD19 dysregulation in two autoantibody-associated autoimmune diseases suggests a shared mechanism of B-cell tolerance loss. J Clin Immunol *27*, 53-68.

60. Krammer, P.H. (2000). CD95's deadly mission in the immune system. Nature *407*, 789-95.

61. Los, M., Wesselborg, S., Schulze-Osthoff, K. (1999). The role of caspases in development, immunity, and apoptotic signal transduction: lessons from knockout mice. Immunity *10*, 629-39.

62. Fisher, G.H., Rosenberg, F.J., Straus, S.E., Dale, J.K., Middleton, L.A., Lin, A.Y., Strober, W., Lenardo, M.J., Puck, J.M. (1995). Dominant interfering Fas gene mutations impair apoptosis in a human autoimmune lymphoproliferative syndrome. Cell *81*, 935-46.

63. Takeoka, Y., Taguchi, N., Shultz, L., Boyd, R.L., Naiki, M., Ansari, A.A., Gershwin, M.E. (1999). Apoptosis and the thymic microenvironment in murine lupus. J Autoimmun *13*, 325-34.

64. Zhou, T., Song, L., Yang, P., Wang, Z., Lui, D., Jope, R.S. (1999). Bisindolylmaleimide VIII facilitates Fas-mediated apoptosis and inhibits T cell-mediated autoimmune diseases. Nat Med *5*, 42-8.

65. Strasser, A., Harris, A.W., Huang, D.C., Krammer, P.H., Cory, S. (1995). Bcl-2 and Fas/APO-1 regulate distinct pathways to lymphocyte apoptosis. Embo J *14*, 6136-47.

66. Bouillet, P., Metcalf, D., Huang, D.C., Tarlinton, D.M., Kay, T.W., Kontgen, F., Adams, J.M., Strasser, A. (1999). Proapoptotic Bcl-2 relative Bim required for certain apoptotic responses, leukocyte homeostasis, and to preclude autoimmunity. Science *286*, 1735-8.

67. Ohsako, S., Hara, M., Harigai, M., Fukasawa, C., Kashiwazaki, S. (1994). Expression and function of Fas antigen and bcl-2 in human systemic lupus erythematosus lymphocytes. Clin Immunol Immunopathol *73*, 109-14.

68. Aringer, M., Wintersberger, W., Steiner, C.W., Kiener, H., Presterl, E., Jaeger, U., Smolen, J.S., Graninger, W.B. (1994). High levels of bcl-2 protein in circulating T lymphocytes, but not B lymphocytes, of patients with systemic lupus erythematosus. Arthritis Rheum *37*, 1423-30.

69. Noelle, R.J., Erickson, L.D. (2005). Determinations of B cell fate in immunity and autoimmunity. Curr Dir Autoimmun *8*, 1-24.

70. Saito, Y., Miyagawa, Y., Onda, K., Nakajima, H., Sato, B., Horiuchi, Y., Okita, H., Katagiri, Y.U., Saito, M., Shimizu, T., Fujimoto, J., Kiyokawa, N. (2008). B-cell-activating factor inhibits CD20-mediated and B-cell receptor-mediated apoptosis in human B cells. Immunology *125*, 570-90.

71. Patke, A., Mecklenbrauker, I., Erdjument-Bromage, H., Tempst, P., Tarakhovsky, A. (2006). BAFF controls B cell metabolic fitness through a PKC beta- and Akt-dependent mechanism. J Exp Med *203*, 2551-62.

72. Mecklenbrauker, I., Kalled, S.L., Leitges, M., Mackay, F., Tarakhovsky, A. (2004). Regulation of B-cell survival by BAFF-dependent PKCdelta-mediated nuclear signalling. Nature *431*, 456-61.

73. Zhang, J., Roschke, V., Baker, K.P., Wang, Z., Alarcon, G.S., Fessler, B.J., Bastian, H., Kimberly, R.P., Zhou, T. (2001). Cutting edge: a role for B lymphocyte stimulator in systemic lupus erythematosus. J Immunol *166*, 6-10.

74. Cheema, G.S., Roschke, V., Hilbert, D.M., Stohl, W. (2001). Elevated serum B lymphocyte stimulator levels in patients with systemic immune-based rheumatic diseases. Arthritis Rheum *44*, 1313-9.

75. Groom, J., Kalled, S.L., Cutler, A.H., Olson, C., Woodcock, S.A., Schneider, P., Tschopp, J., Cachero, T.G., Batten, M., Wheway, J., Mauri, D., Cavill, D., Gordon, T.P., Mackay, C.R., Mackay, F. (2002). Association of BAFF/BLyS overexpression and altered B cell differentiation with Sjogren's syndrome. J Clin Invest *109*, 59-68.

76. Khare, S.D., Sarosi, I., Xia, X.Z., McCabe, S., Miner, K., Solovyev, I., Hawkins, N., Kelley, M., Chang, D., Van, G., Ross, L., Delaney, J., Wang, L., Lacey, D., Boyle, W.J., Hsu, H. (2000). Severe B cell hyperplasia and autoimmune disease in TALL-1 transgenic mice. Proc Natl Acad Sci U S A *97*, 3370-5.

77. Mackay, F., Woodcock, S.A., Lawton, P., Ambrose, C., Baetscher, M., Schneider, P., Tschopp, J., Browning, J.L. (1999). Mice transgenic for BAFF develop lymphocytic disorders along with autoimmune manifestations. J Exp Med *190*, 1697-710.

78. Szodoray, P., Jellestad, S., Teague, M.O., Jonsson, R. (2003). Attenuated apoptosis of B cell activating factor-expressing cells in primary Sjogren's syndrome. Lab Invest *83*, 357-65.

79. Gross, J.A., Johnston, J., Mudri, S., Enselman, R., Dillon, S.R., Madden, K., Xu, W., Parrish-Novak, J., Foster, D., Lofton-Day, C., Moore, M., Littau, A., Grossman, A., Haugen, H., Foley, K., Blumberg, H., Harrison, K., Kindsvogel, W., Clegg, C.H. (2000). TACI and BCMA are receptors for a TNF homologue implicated in B-cell autoimmune disease. Nature *404*, 995-9.

80. Diz, R., McCray, S.K., Clarke, S.H. (2008). B cell receptor affinity and B cell subset identity integrate to define the effectiveness, affinity threshold, and mechanism of anergy. J Immunol *181*, 3834-40.

81. Yamamoto, T., Hattori, M., Yoshida, T. (2007). Induction of T-cell activation or anergy determined by the combination of intensity and duration of T-cell receptor stimulation, and sequential induction in an individual cell. Immunology *121*, 383-91.

82. Gajewski, T.F., Fields, P., Fitch, F.W. (1995). Induction of the increased Fyn kinase activity in anergic T helper type 1 clones requires calcium and protein synthesis and is sensitive to cyclosporin A. Eur J Immunol *25*, 1836-42.

83. Powell, J.D., Zheng, Y. (2006). Dissecting the mechanism of T-cell anergy with immunophilin ligands. Curr Opin Investig Drugs *7*, 1002-7.

84. Nossal, G.J. (1993). Tolerance and ways to break it. Ann N Y Acad Sci *690*, 34-41.

85. Moura, R., Agua-Doce, A., Weinmann, P., Graca, L., Fonseca, J.E. (2008). B cells from the bench to the clinical practice. Acta Reumatol Port *33*, 137-54.

86. Merrell, K.T., Benschop, R.J., Gauld, S.B., Aviszus, K., Decote-Ricardo, D., Wysocki, L.J., Cambier, J.C. (2006). Identification of anergic B cells within a wild-type repertoire. Immunity *25*, 953-62.

87. Duty, J.A., Szodoray, P., Zheng, N.Y., Koelsch, K.A., Zhang, Q., Swiatkowski, M., Mathias, M., Garman, L., Helms, C., Nakken, B., Smith, K., Farris, A.D., Wilson, P.C. (2009). Functional anergy in a subpopulation of naive B cells from healthy humans that express autoreactive immunoglobulin receptors. J Exp Med *206*, 139-51.

88. Ravirajan, C.T., Isenberg, D.A. (2002). Transgenic models of tolerance and autoimmunity: with special reference to systemic lupus erythematosus. Lupus *11*, 843-9.

89. Cappione, A., 3rd, Anolik, J.H., Pugh-Bernard, A., Barnard, J., Dutcher, P., Silverman, G., Sanz, I. (2005). Germinal center exclusion of autoreactive B cells is defective in human systemic lupus erythematosus. J Clin Invest *115*, 3205-16.

90. Soto-Nieves, N., Puga, I., Abe, B.T., Bandyopadhyay, S., Baine, I., Rao, A., Macian, F. (2009). Transcriptional complexes formed by NFAT dimers regulate the induction of T cell tolerance. J Exp Med

91. Bandyopadhyay, S., Soto-Nieves, N., Macian, F. (2007). Transcriptional regulation of T cell tolerance. Semin Immunol *19*, 180-7.

92. Huang, F., Gu, H. (2008). Negative regulation of lymphocyte development and function by the Cbl family of proteins. Immunol Rev *224*, 229-38.

93. Lin, A.E., Mak, T.W. (2007). The role of E3 ligases in autoimmunity and the regulation of autoreactive T cells. Curr Opin Immunol *19*, 665-73.

94. Ding, C., Yan, J. (2007). Regulation of autoreactive B cells: checkpoints and activation. Arch Immunol Ther Exp (Warsz) *55*, 83-9.

95. Yachimovich, N., Mostoslavsky, G., Yarkoni, Y., Verbovetski, I., Eilat, D. (2002). The efficiency of B cell receptor (BCR) editing is dependent on BCR light chain rearrangement status. Eur J Immunol *32*, 1164-74.

96. Shivtiel, S., Leider, N., Melamed, D. (2002). Receptor editing in CD45-deficient immature B cells. Eur J Immunol *32*, 2264-73.

97. Tze, L.E., Hippen, K.L., Behrens, T.W. (2003). Late immature B cells

(IgMhighIgDneg) undergo a light chain receptor editing response to soluble self-antigen. J Immunol *171*, 678-82.

98. Giachino, C., Padovan, E., Lanzavecchia, A. (1998). Re-expression of RAG-1 and RAG-2 genes and evidence for secondary rearrangements in human germinal center B lymphocytes. Eur J Immunol *28*, 3506-13.

99. Radic, M.Z., Erikson, J., Litwin, S., Weigert, M. (1993). B lymphocytes may escape tolerance by revising their antigen receptors. J Exp Med *177*, 1165-73.

100. Panigrahi, A.K., Goodman, N.G., Eisenberg, R.A., Rickels, M.R., Naji, A., Luning Prak, E.T. (2008). RS rearrangement frequency as a marker of receptor editing in lupus and type 1 diabetes. J Exp Med *205*, 2985-94.

101. Hansen, A., Dorner, T., Lipsky, P.E. (2000). Use of immunoglobulin variable-region genes by normal subjects and patients with systemic lupus erythematosus. Int Arch Allergy Immunol *123*, 36-45.

102. Wakui, M., Kim, J., Butfiloski, E.J., Morel, L., Sobel, E.S. (2004). Genetic dissection of lupus pathogenesis: Sle3/5 impacts IgH CDR3 sequences, somatic mutations, and receptor editing. J Immunol *173*, 7368-76.

103. Anolik, J., Sanz, I. (2004). B cells in human and murine systemic lupus erythematosus. Curr Opin Rheumatol *16*, 505-12.

104. Sherer, Y., Gorstein, A., Fritzler, M.J., Shoenfeld, Y. (2004). Autoantibody explosion in systemic lupus erythematosus: more than 100 different antibodies found in SLE patients. Semin Arthritis Rheum *34*, 501-37.

105. Chan, O.T., Madaio, M.P., Shlomchik, M.J. (1999). B cells are required for lupus nephritis in the polygenic, Fas-intact MRL model of systemic autoimmunity. J Immunol *163*, 3592-6.

106. Schlissel, M.S. (2007). The regulation of receptor editing. Adv Exp Med Biol *596*, 173-9.

107. Chan, O.T., Hannum, L.G., Haberman, A.M., Madaio, M.P., Shlomchik, M.J. (1999). A novel mouse with B cells but lacking serum antibody reveals an antibody-independent role for B cells in murine lupus. J Exp Med *189*, 1639-48.

108. Chan, O.T., Madaio, M.P., Shlomchik, M.J. (1999). The central and multiple roles of B cells in lupus pathogenesis. Immunol Rev *169*, 107-21.

109. Takemura, S., Klimiuk, P.A., Braun, A., Goronzy, J.J., Weyand, C.M. (2001). T cell activation in rheumatoid synovium is B cell dependent. J Immunol *167*, 4710-8.

110. Cheung, Y.H., Chang, N.H., Cai, Y.C., Bonventi, G., MacLeod, R., Wither, J.E. (2005). Functional interplay between intrinsic B and T cell defects leads to amplification of autoimmune disease in New Zealand black chromosome 1 congenic mice. J Immunol *175*, 8154-64.

111. Wardemann, H., Yurasov, S., Schaefer, A., Young, J.W., Meffre, E., Nussenzweig, M.C. (2003). Predominant autoantibody production by early human B cell precursors. Science *301*, 1374-7.

112. Nemazee, D. (1996). Antigen receptor 'capacity' and the sensitivity of self-tolerance. Immunol Today *17*, 25-9.

113. Monson, N.L. (2008). The natural history of B cells. Curr Opin Neurol *21 Suppl 1*, S3-8.

114. Dalakas, M.C. (2006). B cells in the pathophysiology of autoimmune neurological disorders: a credible therapeutic target. Pharmacol Ther *112*, 57-70.

115. Allen, C.D., Okada, T., Cyster, J.G. (2007). Germinal-center organization and cellular dynamics. Immunity *27*, 190-202.

116. Kindt, T.J. (2007). *Kuby Immunology*. New York: W.H. Freeman. pp 292-7.

117. Jenks, S.A., Sanz, I. (2009). Altered B cell receptor signaling in human systemic lupus erythematosus. Autoimmun Rev *8*, 209-13.

118. Tedder, T.F., Inaoki, M., Sato, S. (1997). The CD19-CD21 complex regulates signal transduction thresholds governing humoral immunity and autoimmunity. Immunity *6*, 107-18.

119. Taylor, D.K., Ito, E., Thorn, M., Sundar, K., Tedder, T., Spatz, L.A. (2006). Loss of tolerance of anti-dsDNA B cells in mice overexpressing CD19. Mol Immunol *43*, 1776-90.

120. Tsuchiya, N., Kuroki, K., Fujimoto, M., Murakami, Y., Tedder, T.F., Tokunaga, K., Takehara, K., Sato, S. (2004). Association of a functional CD19 polymorphism with susceptibility to systemic sclerosis. Arthritis Rheum *50*, 4002-7.

121. Saito, E., Fujimoto, M., Hasegawa, M., Komura, K., Hamaguchi, Y., Kaburagi, Y., Nagaoka, T., Takehara, K., Tedder, T.F., Sato, S. (2002). CD19-dependent B lymphocyte signaling thresholds influence skin fibrosis and autoimmunity in the tight-skin mouse. J Clin Invest *109*, 1453-62.

122. Isnardi, I., Lesourne, R., Bruhns, P., Fridman, W.H., Cambier, J.C., Daeron, M. (2004). Two distinct tyrosine-based motifs enable the inhibitory receptor FcgammaRIIB to cooperatively recruit the inositol phosphatases SHIP1/2 and the adapters Grb2/Grap. J Biol Chem *279*, 51931-8.

123. Sohn, H.W., Pierce, S.K., Tzeng, S.J. (2008). Live cell imaging reveals that the inhibitory FcgammaRIIB destabilizes B cell receptor membrane-lipid interactions and blocks immune synapse formation. J Immunol *180*, 793-9.

124. Li, X., Wu, J., Carter, R.H., Edberg, J.C., Su, K., Cooper, G.S., Kimberly, R.P. (2003). A novel polymorphism in the Fcgamma receptor IIB (CD32B) transmembrane region alters receptor signaling. Arthritis Rheum *48*, 3242-52.

125. Kyogoku, C., Dijstelbloem, H.M., Tsuchiya, N., Hatta, Y., Kato, H., Yamaguchi, A., Fukazawa, T., Jansen, M.D., Hashimoto, H., van de Winkel, J.G., Kallenberg, C.G., Tokunaga, K. (2002). Fcgamma receptor gene polymorphisms in Japanese patients with systemic lupus erythematosus: contribution of FCGR2B to genetic susceptibility. Arthritis Rheum *46*, 1242-54.

126. Kono, H., Kyogoku, C., Suzuki, T., Tsuchiya, N., Honda, H., Yamamoto, K., Tokunaga, K., Honda, Z. (2005). FcgammaRIIB Ile232Thr transmembrane polymorphism associated with human systemic lupus erythematosus decreases affinity to lipid rafts and attenuates inhibitory effects on B cell receptor signaling. Hum Mol Genet *14*, 2881-92.

127. Blank, M.C., Stefanescu, R.N., Masuda, E., Marti, F., King, P.D., Redecha, P.B., Wurzburger, R.J., Peterson, M.G., Tanaka, S., Pricop, L. (2005). Decreased transcription of the human FCGR2B gene mediated by the -343 G/C promoter polymorphism and association with systemic lupus erythematosus. Hum Genet *117*, 220-7.

128. Bolland, S., Ravetch, J.V. (2000). Spontaneous autoimmune disease in Fc(gamma)RIIB-deficient mice results from strain-specific epistasis. Immunity *13*, 277-85.

129. Hibbs, M.L., Dunn, A.R. (1997). Lyn, a src-like tyrosine kinase. Int J Biochem Cell Biol *29*, 397-400.

130. Huck, S., Le Corre, R., Youinou, P., Zouali, M. (2001). Expression of B cell receptor-associated signaling molecules in human lupus. Autoimmunity *33*, 213-24.

131. Liossis, S.N., Solomou, E.E., Dimopoulos, M.A., Panayiotidis, P., Mavrikakis, M.M., Sfikakis, P.P. (2001). B-cell kinase lyn deficiency in patients with systemic lupus erythematosus. J Investig Med *49*, 157-65.

132. Nishizumi, H., Taniuchi, I., Yamanashi, Y., Kitamura, D., Ilic, D., Mori, S., Watanabe, T., Yamamoto, T. (1995). Impaired proliferation of peripheral B cells and indication of autoimmune disease in lyn-deficient mice. Immunity *3*, 549-60.

133. Hibbs, M.L., Tarlinton, D.M., Armes, J., Grail, D., Hodgson, G., Maglitto, R., Stacker, S.A., Dunn, A.R. (1995). Multiple defects in the immune system of Lyn-deficient mice, culminating in autoimmune disease. Cell *83*, 301-11.

134. Li, M., Zhou, Y., Feng, G., Su, S.B. (2009). The critical role of toll-like receptor signaling pathways in the induction and progression of autoimmune diseases. Curr Mol Med *9*, 365-74.

135. Takeda, K., Kaisho, T., Akira, S. (2003). Toll-like receptors. Annu Rev Immunol *21*, 335-76.

136. Baccala, R., Hoebe, K., Kono, D.H., Beutler, B., Theofilopoulos, A.N. (2007). TLR-dependent and TLR-independent pathways of type I interferon induction in systemic autoimmunity. Nat Med *13*, 543-51.

137. Kim, W.U., Sreih, A., Bucala, R. (2009). Toll-like receptors in systemic lupus erythematosus; prospects for therapeutic intervention. Autoimmun Rev *8*, 204-8.

138. Ehlers, M., Fukuyama, H., McGaha, T.L., Aderem, A., Ravetch, J.V. (2006). TLR9/MyD88 signaling is required for class switching to pathogenic IgG2a and 2b autoantibodies in SLE. J Exp Med *203*, 553-61.

139. Fairhurst, A.M., Hwang, S.H., Wang, A., Tian, X.H., Boudreaux, C., Zhou, X.J., Casco, J., Li, Q.Z., Connolly, J.E., Wakeland, E.K. (2008). Yaa autoimmune phenotypes are conferred by overexpression of TLR7. Eur J Immunol *38*, 1971-8.

140. Santiago-Raber, M.L., Kikuchi, S., Borel, P., Uematsu, S., Akira, S., Kotzin, B.L., Izui, S. (2008). Evidence for genes in addition to Tlr7 in the Yaa

translocation linked with acceleration of systemic lupus erythematosus. J Immunol *181*, 1556-62.

141. Bijl, M., Reefman, E., Horst, G., Limburg, P.C., Kallenberg, C.G. (2006). Reduced uptake of apoptotic cells by macrophages in systemic lupus erythematosus: correlates with decreased serum levels of complement. Ann Rheum Dis *65*, 57-63.

142. Moosig, F., Damm, F., Knorr-Spahr, A., Ritgen, M., Zeuner, R.A., Kneba, M., Ernst, M., Schroder, J.O. (2006). Reduced expression of C1q-mRNA in monocytes from patients with systemic lupus erythematosus. Clin Exp Immunol *146*, 409-16.

143. Pawar, R.D., Patole, P.S., Ellwart, A., Lech, M., Segerer, S., Schlondorff, D., Anders, H.J. (2006). Ligands to nucleic acid-specific toll-like receptors and the onset of lupus nephritis. J Am Soc Nephrol *17*, 3365-73.

144. Wilber, A., O'Connor, T.P., Lu, M.L., Karimi, A., Schneider, M.C. (2003). Dnase1l3 deficiency in lupus-prone MRL and NZB/W F1 mice. Clin Exp Immunol *134*, 46-52.

145. Napirei, M., Karsunky, H., Zevnik, B., Stephan, H., Mannherz, H.G., Moroy, T. (2000). Features of systemic lupus erythematosus in Dnase1-deficient mice. Nat Genet *25*, 177-81.

146. Dooley, M.A., Ginzler, E.M. (2006). Newer therapeutic approaches for systemic lupus erythematosus: immunosuppressive agents. Rheum Dis Clin North Am *32*, 91-102, ix.

147. Lowenberg, M., Stahn, C., Hommes, D.W., Buttgereit, F. (2008). Novel insights into mechanisms of glucocorticoid action and the development of new glucocorticoid receptor ligands. Steroids *73*, 1025-9.

148. Sabahi, R., Anolik, J.H. (2006). B-cell-targeted therapy for systemic lupus erythematosus. Drugs *66*, 1933-48.

149. Edwards, J.C., Szczepanski, L., Szechinski, J., Filipowicz-Sosnowska, A., Emery, P., Close, D.R., Stevens, R.M., Shaw, T. (2004). Efficacy of B-cell-targeted therapy with rituximab in patients with rheumatoid arthritis. N Engl J Med *350*, 2572-81.

150. Hasegawa, M., Hamaguchi, Y., Yanaba, K., Bouaziz, J.D., Uchida, J., Fujimoto, M., Matsushita, T., Matsushita, Y., Horikawa, M., Komura, K.,

Takehara, K., Sato, S., Tedder, T.F. (2006). B-lymphocyte depletion reduces skin fibrosis and autoimmunity in the tight-skin mouse model for systemic sclerosis. Am J Pathol *169*, 954-66.

151. Ahuja, A., Shupe, J., Dunn, R., Kashgarian, M., Kehry, M.R., Shlomchik, M.J. (2007). Depletion of B cells in murine lupus: efficacy and resistance. J Immunol *179*, 3351-61.

152. Hu, C.Y., Rodriguez-Pinto, D., Du, W., Ahuja, A., Henegariu, O., Wong, F.S., Shlomchik, M.J., Wen, L. (2007). Treatment with CD20-specific antibody prevents and reverses autoimmune diabetes in mice. J Clin Invest *117*, 3857-67.

153. Vasoo, S., Hughes, G.R. (2005). Theory, targets and therapy in systemic lupus erythematosus. Lupus *14*, 181-8.

154. Sfikakis, P.P., Boletis, J.N., Tsokos, G.C. (2005). Rituximab anti-B-cell therapy in systemic lupus erythematosus: pointing to the future. Curr Opin Rheumatol *17*, 550-7.

155. Demidem, A., Lam, T., Alas, S., Hariharan, K., Hanna, N., Bonavida, B. (1997). Chimeric anti-CD20 (IDEC-C2B8) monoclonal antibody sensitizes a B cell lymphoma cell line to cell killing by cytotoxic drugs. Cancer Biother Radiopharm *12*, 177-86.

156. Stohl, W. (2004). A therapeutic role for BLyS antagonists. Lupus *13*, 317-22.

157. Stohl, W., Metyas, S., Tan, S.M., Cheema, G.S., Oamar, B., Xu, D., Roschke, V., Wu, Y., Baker, K.P., Hilbert, D.M. (2003). B lymphocyte stimulator overexpression in patients with systemic lupus erythematosus: longitudinal observations. Arthritis Rheum *48*, 3475-86.

158. Halpern, W.G., Lappin, P., Zanardi, T., Cai, W., Corcoran, M., Zhong, J., Baker, K.P. (2006). Chronic administration of belimumab, a BLyS antagonist, decreases tissue and peripheral blood B-lymphocyte populations in cynomolgus monkeys: pharmacokinetic, pharmacodynamic, and toxicologic effects. Toxicol Sci *91*, 586-99.

159. Alarcon-Segovia, D., Tumlin, J.A., Furie, R.A., McKay, J.D., Cardiel, M.H., Strand, V., Bagin, R.G., Linnik, M.D., Hepburn, B. (2003). LJP 394 for the prevention of renal flare in patients with systemic lupus erythematosus: results from a randomized, double-blind, placebo-controlled study. Arthritis Rheum *48*, 442-54.

160. Turley, D.M., Miller, S.D. (2009). Prospects for Antigen-Specific Tolerance Based Therapies for the Treatment of Multiple Sclerosis. Results Probl Cell Differ

161. al-Sabbagh, A., Nelson, P.A., Akselband, Y., Sobel, R.A., Weiner, H.L. (1996). Antigen-driven peripheral immune tolerance: suppression of experimental autoimmmune encephalomyelitis and collagen-induced arthritis by aerosol administration of myelin basic protein or type II collagen. Cell Immunol *171*, 111-9.

162. Lutterotti, A., Sospedra, M., Martin, R. (2008). Antigen-specific therapies in MS - Current concepts and novel approaches. J Neurol Sci *274*, 18-22.

163. Bednarski, J.J., Warner, R.E., Rao, T., Leonetti, F., Yung, R., Richardson, B.C., Johnson, K.J., Ellman, J.A., Opipari, A.W., Jr., Glick, G.D. (2003). Attenuation of autoimmune disease in Fas-deficient mice by treatment with a cytotoxic benzodiazepine. Arthritis Rheum *48*, 757-66.

164. Blatt, N.B., Bednarski, J.J., Warner, R.E., Leonetti, F., Johnson, K.M., Boitano, A., Yung, R., Richardson, B.C., Johnson, K.J., Ellman, J.A., Opipari, A.W., Jr., Glick, G.D. (2002). Benzodiazepine-induced superoxide signals B cell apoptosis: mechanistic insight and potential therapeutic utility. J Clin Invest *110*, 1123-32.

165. Boitano, A., Ellman, J.A., Glick, G.D., Opipari, A.W., Jr. (2003). The proapoptotic benzodiazepine Bz-423 affects the growth and survival of malignant B cells. Cancer Res *63*, 6870-6.

166. Bednarski, J.J., Lyssiotis, C.A., Roush, R., Boitano, A.E., Glick, G.D., Opipari, A.W., Jr. (2004). A novel benzodiazepine increases the sensitivity of B cells to receptor stimulation with synergistic effects on calcium signaling and apoptosis. J Biol Chem *279*, 29615-21.

167. Adam-Vizi, V., Chinopoulos, C. (2006). Bioenergetics and the formation of mitochondrial reactive oxygen species. Trends Pharmacol Sci *27*, 639-45.

168. Perl, A., Gergely, P., Jr., Nagy, G., Koncz, A., Banki, K. (2004). Mitochondrial hyperpolarization: a checkpoint of T-cell life, death and autoimmunity. Trends Immunol *25*, 360-7.

169. Fink, B.D., Reszka, K.J., Herlein, J.A., Mathahs, M.M., Sivitz, W.I. (2005). Respiratory uncoupling by UCP1 and UCP2 and superoxide generation in endothelial cell mitochondria. Am J Physiol Endocrinol Metab *288*, E71-9.

170. Korshunov, S.S., Skulachev, V.P., Starkov, A.A. (1997). High protonic potential actuates a mechanism of production of reactive oxygen species in mitochondria. FEBS Lett *416*, 15-8.

171. Gong, Y., Sohn, H., Xue, L., Firestone, G.L., Bjeldanes, L.F. (2006). 3,3'-Diindolylmethane is a novel mitochondrial H(+)-ATP synthase inhibitor that can induce p21(Cip1/Waf1) expression by induction of oxidative stress in human breast cancer cells. Cancer Res *66*, 4880-7.

172. Johnson, K.M., Chen, X., Boitano, A., Swenson, L., Opipari, A.W., Jr., Glick, G.D. (2005). Identification and validation of the mitochondrial F1F0-ATPase as the molecular target of the immunomodulatory benzodiazepine Bz-423. Chem Biol *12*, 485-96.

173. Sundberg, T.B. (2008). *Elucidation of anti-proliferative and pro-apoptotic signaling induced by the immunomodulatory Benzodiazepine Bz-423*. University of Michigan, Ann Arbor

174. Wolniak, K.L., Shinall, S.M., Waldschmidt, T.J. (2004). The germinal center response. Crit Rev Immunol *24*, 39-65.

CHAPTER 2

MECHANISM OF ANTI-IGM INDUCED SYNERGY WITH BZ-423

Introduction:

Apoptotic signaling pathway: Apoptosis is a form of cell death with specific morphological and biochemical changes, including plasma membrane blebbing, chromatin condensation, and DNA fragmentation [1]. In contrast to necrosis, another form of cell death, apoptosis eliminates unwanted cells without inducing an inflammatory response [2]. Apoptosis is critical for normal lymphocyte development and immune function. Thus, it is a tightly regulated process. Too much apoptosis will lead to immunodeficiency, and too little apoptosis will result in lymphoma or autoimmune diseases [3]. Drugs that promote apoptosis and drugs that inhibit apoptosis have been used to treat various cancers and degenerative diseases, respectively [4, 5].

Apoptosis results from cleaving a variety of subcellular targets by effector caspase proteases [6]. Caspases are a family of cysteine proteases requiring cleavage for activation. There are four ways to activate caspase: self-cleavage; cleavage by other caspases or proteases such as granzyme B [7]; activation by death receptor complexes (Figure 2.1; [8]); or apoptosome activation during mitochondria-dependent cell death (Figure 2.1; [9]). Depending on their roles in apoptosis, caspases are

divided into initiator caspases and effector caspases [10] . Initiator caspases including caspases-8, 9 and 10 are initially activated. They in turn cleave and activate effector caspases such as caspase-3 and caspase-7 [10]. These activated effector caspases then cleave vital structural proteins such as lamins and spectrin, and prototypically active enzyme for cell dismantling such as inhibitor of caspase activated DNase (ICAD) (Figure 2.1; [10]).

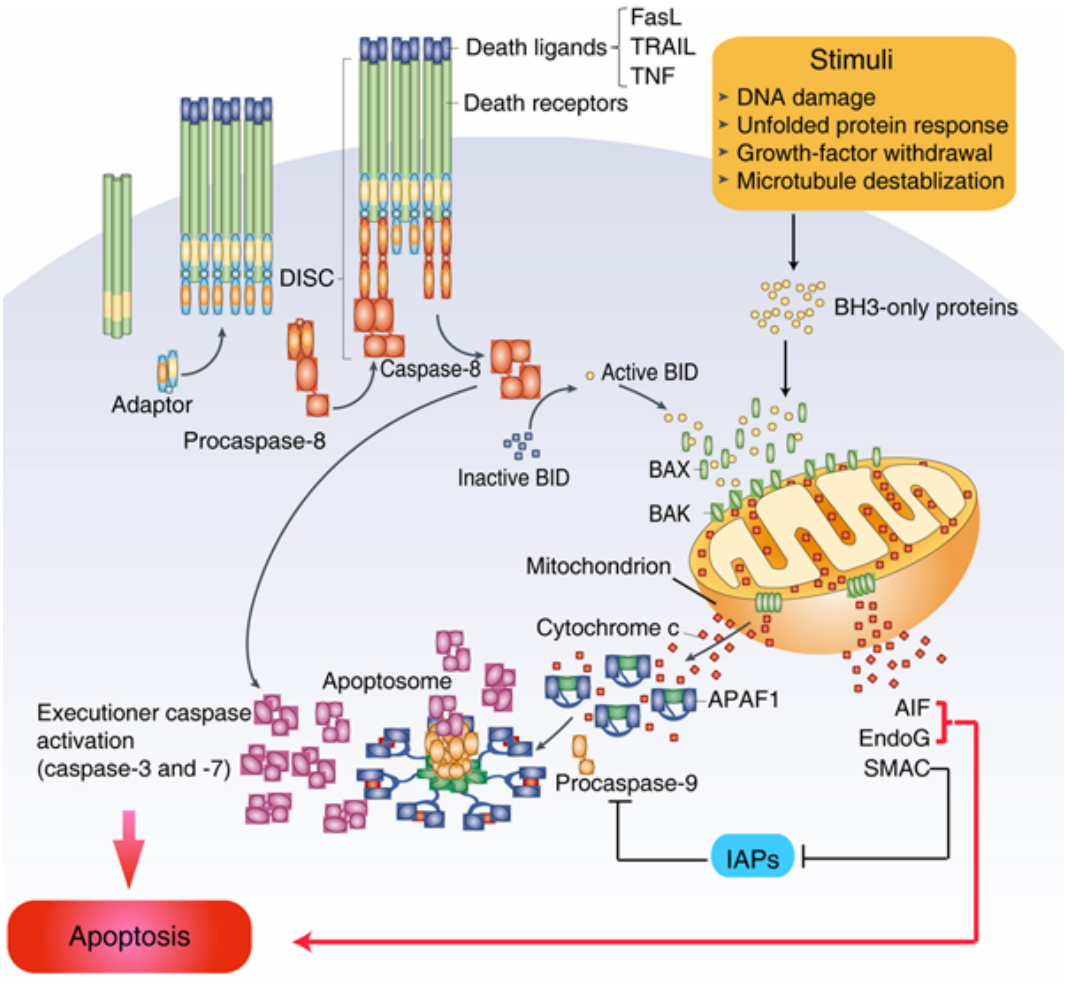

Figure 2.1: Overview of apoptotic signaling pathway. See text for details. This figure is adapted from [11].

Extrinsic and intrinsic pathways are two common apoptotic signaling pathways for caspase activation. The extrinsic apoptotic pathway is initiated by binding of death factors such as Fas ligand (FasL) to death receptors such as Fas, followed by multimerization of receptors, recruitment of adaptor molecules, and formation of a death inducing signaling complex (DISC) to activate caspase-8 (Figure 2.1; [7, 12]). The best studied example of extrinsic apoptotic signaling pathway is the Fas-FasL signaling pathway. Once FasL binds to Fas, the death domain of Fas recruits the adaptor Fas-associated death domain protein (FADD), of which the death effector domain recruits pro-caspase 8 to form DISC. Self-cleavage of pro-caspase 8 is triggered to form activated caspase 8. The activated caspase 8 then cleaves and activates effector caspse-3 and caspase-7, which lead to apoptosis [13].

Mitochondria are important in intrinsic apoptotic signaling pathway. They sense and integrate various intracellular stresses, which triggers signals to permeablize mitochondrial membrane and to release pro-apoptotic factors from intermembrane to cytosol (Figure 2.1; [14]). These pro-apoptotic factors include cytochrome c, second mitochondria-derived activator of caspase/direct IAP-binding protein with low pI (Smac/DIABLO), apoptosis inducing factor (AIF), endonuclease G. (Endo-G) (Figure 2.1). Cytochrome c binds to apoptotic protease activating factor-1 (Apaf-1), dATP, and pro-caspase 9 to form the apoptosome (Figure 2.1; [9]). In the apoptosome, caspase 9 is autocatalytically activated, which activates downstream effector caspases to induce apoptosis (Figure 2.1; [9]). Smac assists in caspase activation by binding to inhibitors of apoptosis protein (IAPs), which releases

caspase from IAPs inhibition (Figure 2.1; [15, 16]). AIF induces nuclear condensation and DNA fragmentation [17], while Endo-G degrades single-strand DNA [18, 19]. Both of them can cause apoptosis independent of caspases (Figure 2.1; [20]). There is cross-talk between intrinsic and extrinsic apoptotic signaling pathway. Caspase 8 activated by death receptor can cleave BH3-only protein Bid. The cleaved form tBid then translocates to the mitochondria to induce release of mitochondrial pro-apoptotic factors (Figure 2.1; [21]).

Mechanisms for mitochondrial pro-apoptotic factors release: Two mechanisms are proposed to release pro-apoptotic factors such as cytochrome c (Figure 2.2). One mechanism is repetitive opening of the mitochondrial membrane transition (MPT) pore [22]; the other is through the pores formed by oligomerization of activated Bax and Bak in the outer mitochondrial membrane [23].

***Involvement of MPT pore in cytochrome c release*:** Existence of the mitochondrial permeability transition (MPT) pore is derived from the observation that several cellular toxins, including ROS (H_2O_2, O_2^{-}, $O_2^{\cdot}$, $^{\cdot}OH$) and calcium, induced cytochrome c release in isolated mitochondria, which was inhibited by cyclosporine A [24, 25]. The MPT pore is located at contact sites between the inner mitochondrial membrane (IMM) and the outer mitochondrial membrane (OMM). IMM is impermeable to all but a few ions and metabolites [26]. Under physiological conditions, physiological factors such as ROS and calcium can induce transient opening of the MPT pore, allowing the exchange of ions and metabolites to maintain normal physiological activity [26]. Under pathological conditions, these factors

induce repetitive opening of MPT pore, which is followed by $\Delta\psi_m$ collapse, mitochondrial Ca^{2+} release, and uncoupling of oxidative phosphorylation [27]. The repetitive MPT opening allows the free diffusion of low molecule solutes across the inner membrane, which leads to the high colloid osmotic pressure in the matrix, water influx into the matrix, and subsequent matrix swelling. Pro-apoptotic factors such as

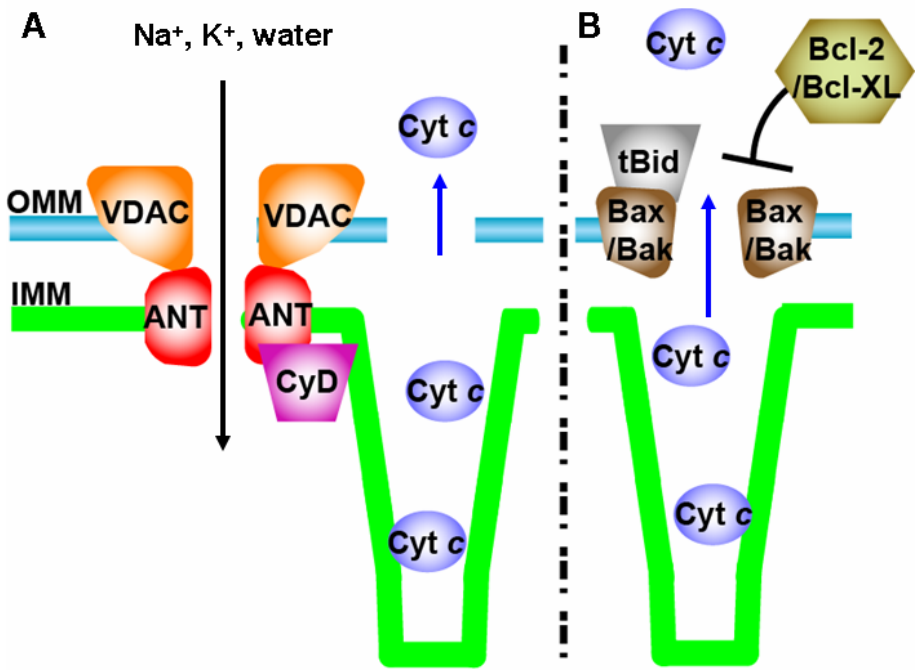

Figure 2.2: Different pathways of mitochondrial cytochrome c release. (A) Mitochondrial permeability transition (MPT) pore-dependent cytochrome c release. Apoptotic stimuli, such as $[Ca^{2+}]_i$ and ROS, trigger MPT pore opening, allowing the free diffusion of low molecule solutes across the inner membrane. The resulting high colloid osmotic pressure in the matrix then causes water influx and subsequent matrix swelling, which results in outer mitochondrial membrane (OMM) rupture and cytochrome c release. (B) Bax and Bak mediated cytochrome c release. Oligomerization of activated Bax or Bak forms pore in the OMM to release cytochrome c. Bax, Bak activation are regulated by BH3-only protein and Bcl-2 subfamily proteins. (C) This picture is adapted from [28]. IMM, Inner mitochondrial membrane; cyto c, cytochrome c; VDAC, voltage-dependent anion channels; adenine nucleotide translocator, ANT; cyclophilins D, CyD.

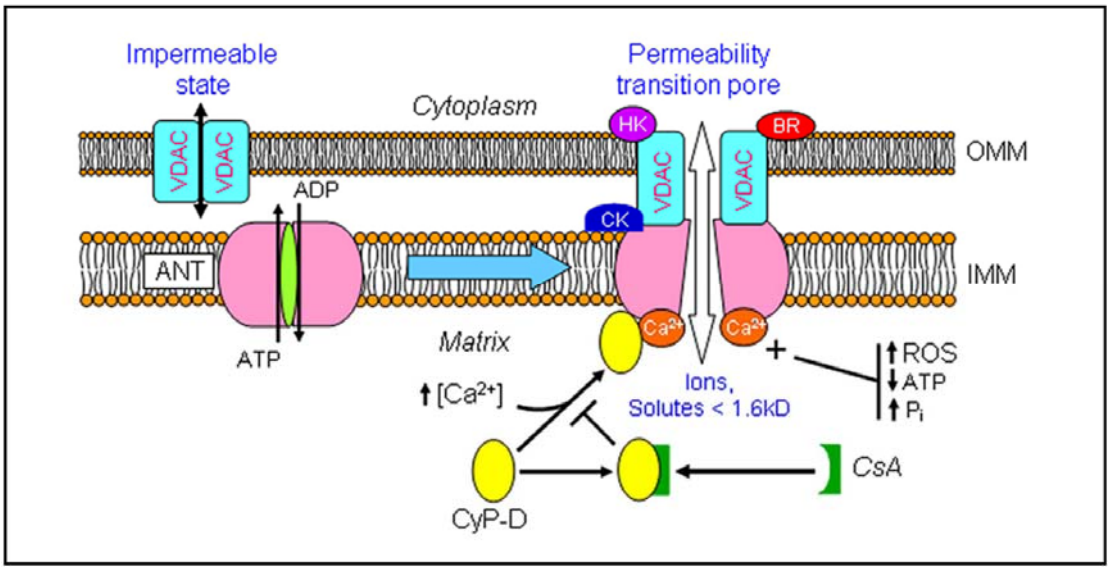

Figure 2.3: Proposed structure of MPT pore and its regulation mechanism. ANT and VDAC form the core elements of MPT pore. HK, PBR, and mtCK are associated with core elements of MPT pore to regulate its activity. Reagents to trigger the MPT pore opening are shown in green and Reagents to close the MPT pore are shown in pink. This picture is adapted from [29]. VDAC, voltage-dependent anion channels; adenine nucleotide translocator, ANT; cyclophilins D, Cyp-D; peripheral benzodiazepine receptor, PBR; creatine kinase, CK; Hexokinase, HK; outer mitochondrial membrane OMM; inner mitochondrial membrane IMM.

cytochrome c are thus released from mitochondria through IMM remodeling and eventually OMM rupture (Figure 2.2A; [30]).

Characterization of MPT pore indicates that it is a voltage-dependent, high-conductance channel that allows passage of molecules up to 1.5 kilodalton (kDa) [27]. The molecular composition of the MPT pore has not been completely resolved. However, the adenine nucleotide translocator (ANT), cyclophilin D (Cyp-D), and the voltage-dependent anion channels (VDACs) are implicated as core elements of the MPT pore. Hexokinase (HK), creatine kinase (CK), and the peripheral benzodiazepine receptor (PBR) are reported to be associated with MPT pore (Figure 2.3; [29, 31]). It is not clear whether these proteins are structural components or rather they play a

regulatory role [32]. The subunits of the MPT pore sense and integrate stress signals from both the matrix and the cytosol, such as mitochondrial membrane potential ($\Delta\psi_m$), adenine nucleotides, pH, ROS, and Ca^{2+} (Figure2.3; [29, 31]). These factors regulate the opening and closure of the MPT pore.

Ca^{2+} is a well-established activator of MPT pore opening. Ca^{2+} opens the MPT pore through increasing Cyp-D binding to ANT (Figure 2.3; [33]). Cyclosporine A binds to Cyp-D, blocks the interaction between Cyp-D and ANT, and thus inhibits calcium-mediated MPT pore opening [34]. Consistent with the inhibitory effect of cyclosporine A, a three-fold excess of calcium is required to trigger the MPT pore opening in liver mitochondria isolated from mice lack of Cyp-D [35]. Glutamate induces cell death in neurons through triggering mitochondrial calcium uptake and the opening of MPT pore in neurons [36]. Neurons from Cyp-D knockout mice were resistant to the MPT pore opening and subsequent cell death induced by low-concentration glutamate. However, at high glutamate concentration, which induce high calcium uptake, this inhibition by cyclosporine A was lost [37], indicating the existence of Cyp-D-independent pathway.

In addition to calcium, ROS is also known to activate MPT pore opening. Thiol oxidants, such as diamide, phenylarsine oxide, stimulate MPT pore opening by crosslinking of cysteine residues (cys56, cys159) in Cyp-D [38-40], which results in the increased binding of CyP-D to ANT [41]. MPT pore opening induced by the thiol oxidants was inhibited by anti-oxidants such as dithiothreitol [42]. Yeast mitochondria lack both cysteine residues in ANT do not possess pore opening activity inhibitable by

cyclosporine A [43, 44]. Oxidative stress also sensitizes the MPT to calcium by increasing CyP-D binding to the ANT, less calcium is thus required for the MPT pore opening [45]. For example, in isolated mitochondria, low concentration of calcium (500 μM) $CaCl_2$ does not induce mitochondrial swelling, one indicator of MPT opening. When co-incubated with t-butyl hydroperoxide and O_2, which produce superoxide, this concentration of $CaCl_2$ significantly induces mitochondrial swelling [45].

MPT pore opening has been implicated in apoptosis induced by a variety of stimuli [22]. N-methy-4-Val-cyclosporine A, a non-immunosuppressive derivative of cyclosporine A which selectively binds to Cyp-D in the mitochondria to block the Cyp-D binding to ANT and MPT opening, inhibits apoptosis induced in vivo by brain trauma [46], by ischemia reperfusion damage [22] and by anti-CD95 in hepatocytes [47]. Bongkrekic acid, which makes ANT adopt a "close" state conformation, inhibits MPT pore opening, and prevents cell death induced by glucocorticoids [48], excitotoxin [49], and tumor necrosis factor (TNF) [50]. Some viral and bacterial proteins modulate apoptosis by interacting with the components of MPT pore [51]. HIV viral protein of regulation (Vpr) binds to ANT, triggers MPT pore opening and induces cell death [51]. While porin B from neisseria meningidis exerts its anti-apoptotic activity by binding to VDAC and inhibiting the opening of MPT pore [52].

Involvement of mitochondrial outer membrane permeablization (MOMP) in mitochondrial pro-apoptotic factors release: MOMP is another mechanism to

release mitochondrial pro-apoptotic factors. The oligomerization of Bcl-2 associated X protein (Bax) and Bcl-2 antagonist/killer (Bak) are proposed to form pores in the mitochondrial outer membrane, which releases pro-apoptotic factors (Figure 2.3B [53]). Bax was known to form channels in artificial membranes [54], resulting in the release of liposome-encapsulated carboxyfluorescein [55], fluorescein-isothiocyanate-conjugated dextran (FITC-dextran) or FITC-cytochrome c [56]. Up to four Bax molecules was shown to form a pore with the capacity to release the molecules up to 22 Å [56]. Bak could form pore in response to activation signals [57]. Addition of tBid to isolated mitochondria induces Bak oligomerization, which results in cytochrome c release. The cytochrome c release is blocked in Bak-deficient mitochondria [57], indicating the critical role of Bak in cytochrome c release.

Since Bax and Bak promote apoptosis through forming pores and trigger pro-apoptotic factor releases from mitochondria, they are tightly regulated. Bax has two stable conformational states: native Bax and activated Bax. Native Bax is a closely packed, globular protein, and located in the cytosol. Bax activation involves a conformational change, which exposes an amino-terminal epitope, which contains a mitochondrial targeting sequence [58]. The activated Bax then translocates into the mitochondria, where it undergoes oligomerization for pore formation [59]. Using green fluorescent protein labeled Bax (GFP-Bax), Bax was shown to be primarily localized in the cytosol and translocated into the mitochondria upon a physiological death stimuli [59]. FK1012 enforced Bax dimerization by binding to FK506 binding protein (FKBP) in FKBP-Bax, which leads to Bax mitochondrial translocation,

cytochrome c release and apoptosis [60], indicating dimerization is involved in apoptosis. Bak is already located in the outer mitochondria membrane [61]. In response to apoptotic signals, it undergoes analogous conformational change and oligomerization to form channels [62]. Apoptosis is induced by Bax overexpression or Bak overexpression [63-65], indicating their critical roles in apoptosis. Either Bax knockout or Bak knockout produced no phenotype, or mild lymphoid hyperplasia in aged mice [66, 67], suggesting Bax and Bak are functionally redundant. Mice with Bax and Bak double knockouts displayed an array of developmental defects [67], which is possibly due to abnormal survivals. The defective cell death induction is confirmed by studying the immortalized embryonic fibroblasts from Bax and Bak deficient mice, since they are resistant to various apoptotic stimuli, such as cytokine withdrawal or certain cytotoxic drugs [68].

Bcl-2 family proteins are shown to participate in apoptosis via other mechanisms. They can regulate cytochrome c release through the MPT pore. Bcl-2 family members (Bcl-2, Bax, Bak) interact subunits of MPT pore (ANT, VDAC) [69, 70]. As ANT2 (amino acid 105-156) is Bcl-2/Bax binding site, ANT2 (1-141) can bind to Bcl-2/Bax while ANT2 (1-101) can not. Bax induces apoptosis in cells expressing ANT2 (1-141). In contrast, Bax does not induce apoptosis in cells expressing ANT2 (1-101) [70]. Bcl-2 family proteins are also shown to regulate apoptosis through modulating the calcium levels in endoplasmic reticulum (ER) [71, 72]. In Bax and Bak double knockout cells, calcium levels in the ER are lower than wild type cells. Overexpression of sarco-endoplasmic reticulum calcium adenosine

triphosphatase (SERCA) corrects ER calcium levels and restores cellular sensitivity to reagents such as arachidonic acid, C2-ceramide [73-75]. Anti-apoptotic Bcl-2 is also shown to exert its protection against cell death by decreasing ROS level [76].

Bcl-2 family proteins regulate MOMP through Bax and Bak: Bcl-2 family proteins are important regulators of mitochondria-mediated apoptosis. All Bcl-2 family proteins contain the Bcl-2 homolog (BH) domain. Based on the Bcl-2 homolog (BH) region they shared, they are divided into three groups, anti-apoptotic Bcl-2 subfamily proteins (Bcl-2 like proteins: Bcl-2, Bcl-xL, A1, Mcl-1) which contain BH1 to BH4 domains, pro-apoptotic Bax subfamily proteins (Bax-like proteins: Bax, Bak) which contain BH1 to BH3 domains, and pro-apoptotic BH3-only proteins [including Bcl-2 antagonist of cell death (Bad), Bcl-2 interacting domain death agonist (Bid), Bcl-2 interacting mediator of cell death (Bim), Bcl-2 interacting killer (Bik), Noxa, p53 up regulated mediator of apoptosis (Puma), Bcl-2 modifying factor (Bmf), and Harakiri (Hrk)] which only contain BH3 domain (Figure 2.4; [77]).

Bcl-2 subfamily proteins exert their anti-apoptotic effect by inhibiting Bax and Bak activation (Figure 2.5). Bcl-2 subfamily protein can bind to Bax and Bak and directly inhibit their activation. They also can indirectly inhibit Bax and Bak activation by binding to BH3-only protein (Figure 2.6). When overexpressed, each of the Bcl-2 subfamily members, such as Bcl-2, Bcl-xL, Mcl-1, A1, protect cells against a variety of apoptotic stimuli [63-65]. Knocking out these Bcl-2-like proteins suggest they regulate cell death of different lymphocytes. The diminished numbers of lymphocytes and shortened life-span of immature lymphocyte in Bcl-X knockout

chimeric mice indicate the critical role of Bcl-X_L in lymphocyte differentiation [78]. In Bcl-2 deficient mice, a massive apoptosis occurs in the spleen and thymus, reflecting that Bcl-2 deficiency predisposes mature B and T cells to apoptosis [79].

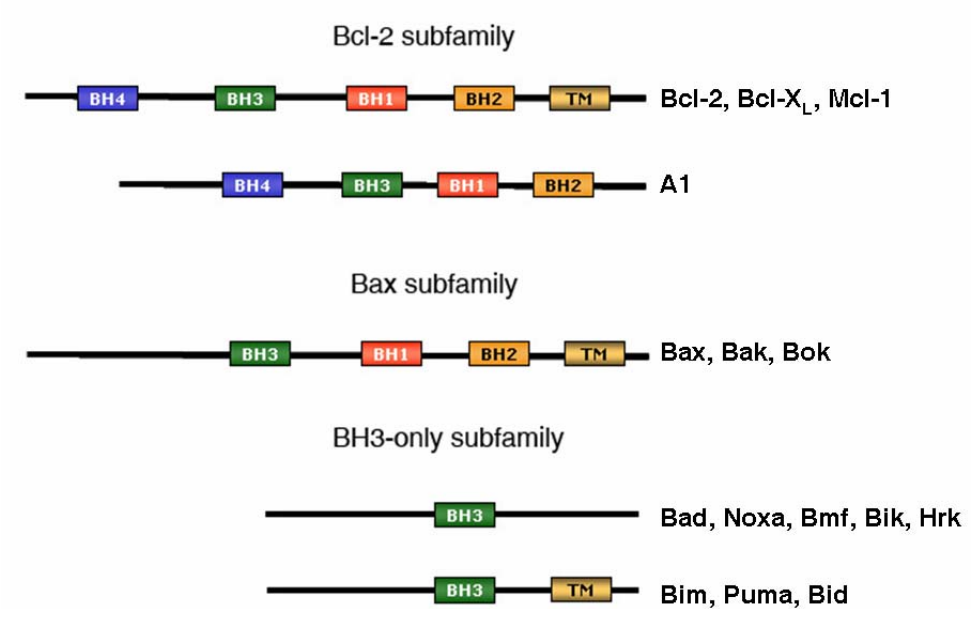

Figure 2.4: Bcl-2 family proteins. Based on the composition of Bcl-2 homolog domains (BHs), Bcl-2 family of protein is divided into three functional groups: anti-apoptotic Bcl-2 subfamily, pro-apoptotic Bax subfamily and pro-apoptotic BH3-only subfamily. The figures are adapted from [77]

Lymphocytes lacking Bcl-2 differentiate into phenotypically mature cells, indicating that Bcl-2 does not affect lymphocyte differentiation. Mcl-1 knockout is lethal [80]. However, conditional removal of Mcl-1 during the early lymphoid development results in increased apoptosis and arrested development at stages of pro-B and double-negative T cell, indicating the involvement of Mcl-1 in lymphoid development [80]. Conditional knockout Mcl-1 in mature B cells and T cells leads to a profound increase in apoptosis and rapid loss in both B and T cells, suggesting its critical role in maintenance of mature lymphocytes [80].

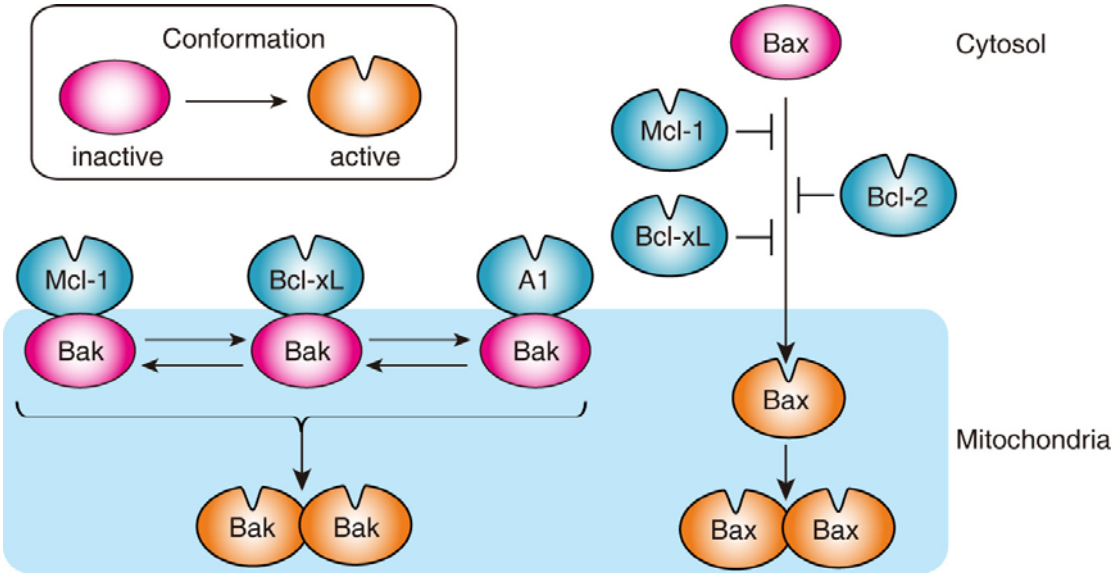

Figure 2.5: The inhibition of Bax and Bak by Bcl-2 subfamily proteins. Bak is sequestered by Mcl-1, Bcl-xL and A1 to maintain its inactive state. Bax is inactive, the Mcl-1, Bcl-2 and Bcl-xL inhibit Bax activation. Once Bak and Bax are activated, they homodimerizes together to release cytochrome c. This picture is adapted from [81].

The overexpression of BH3 only proteins induces apoptosis. In contrast, MEFs lacking Bax and Bak are refractory to the apoptosis induced by overexpression of BH3-only proteins [68]. This observation suggests that BH3-only proteins cause apoptosis by activating Bax and Bak. How BH3-only proteins activate Bax and Bak is still controversial. However, there are two models for Bax and Bak activation. The "direction activation model" was developed based on the studies of the ability of BH3-only proteins to release cytochrome c in a liposome made from artificial membrane of which the lipid content mimics the mitochondrial outer membrane (LUVs) [82]. Dextran was enclosed in LUVs and its release is thus the sign of membrane permeablization. Addition of recombinant Bax does not release dextran from LUVs [82]. Addition BH3-only peptides derived from Bim and Bid could induce

dextran in the presence of Bax, suggesting they can directly activate Bax to release dextran [82]. This BH3-only peptide and Bax mediated dextran release can be inhibited by Bcl-xL [82]. These BH3-only proteins are thus called as direct activator. Other BH3-only proteins could not induce dextran from LUVs when co-treated with recombinant Bax. However, they could potentiate dextran release mediated by director activator and Bax. As a result, these BH3-only proteins are called sensitizers (Figure 2.6A). In the LUVs in presence of recombinant Bax and Bcl-xL, tBid induced less than 20% dextran release. When Bid and Bad were added together, more than 80% dextran release resulted [83]. These findings suggest that Bad can promote Bax activation by displacing Bid from inhibitory Bcl-2 binding. In this "direct activation model", direct activator such as Bim is required for Bax and Bak activation; sensitizer such as Bad assists in Bax and Bak activation through binding to Bcl-2 subfamily (Bcl-2 like) proteins (Figure 2.6A).

Although there is some evidence to support the direct activation model, there are some data against it. For example, Bax and Bak mediate apoptosis without discernable association with Bim and Bid [84], suggesting that Bax and Bak are not activated by BH3-only protein through direct binding. Moreover, Bim mutants with alanine substitution of a conserved BH3 domain residue Gly66 failed to bind to Bax or Bak. However, it induced apoptosis to an equivalent degree as wild-type Bim [84], suggesting direct activator Bim is not essential for Bax and Bak-induced apoptosis.

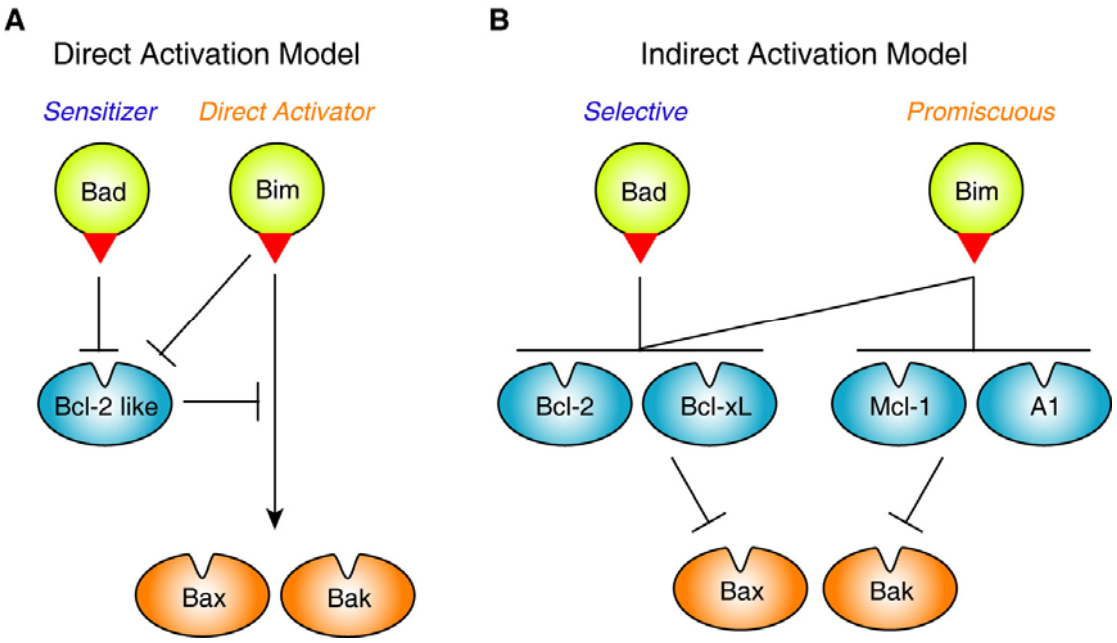

Figure 2.6: The mode of Bax and Bak activation by BH3-only proteins. (A) Direct activation model for Bax and Bak activation. Direct activator such as Bim and tBid is required for Bax and Bak activation. Sensitizer regulates Bax and Bak activation by inhibiting Bcl-2 like proteins. (B). Indirect activation model for Bax and Bak activation. BH3-only protein activates Bax and Bak by inhibiting Bcl-2 like proteins. Dependently on their binding potency for Bcl-2-like family, they are divided as promiscuous BH3-only proteins which can bind to all Bcl-2 like proteins and selective BH3-only proteins which only bind to several Bcl-2 like proteins. The red triangle indicates the BH3 domain. This figure is adapted from [85]

Alternatively, "indirect activation model" has also been proposed. In this model, Bax and Bak can be activated by neutralizing anti-apoptotic Bcl-2 proteins, and BH3-only proteins induce apoptosis by binding to Bcl-2-like proteins (Figure 2.6B). BH3-only proteins have different potencies to activate Bax and Bak and cell death induction, depending on their affinities for Bcl-2-like protein (Figure 2.7). For example, as Bim and Puma can bind to all the Bcl-2 subfamily proteins, they are the most versatile killers. In contrast, Bad only binds to Bcl-2 and Bcl-xL while Noxa only binds to Mcl-1 and A1, making Bad and Noxa weak activator of Bax and Bak. Therefore, activation of potent BH3 only proteins such as Bim or Puma alone is

sufficient to suppress all Bcl-2 like proteins and to activate Bax and Bak. On the other hand, activation of potent BH3 only proteins such as Bad is not sufficient to suppress Bcl-2 like protein and requires additional BH3 only proteins such as Noxa to suppress the Bcl-2 like protein and to activate Bax and Bak. Co-immunoprecipitation result indicates that Bak binds to Bcl-xL and Mcl-1 but not other Bcl-2 subfamily proteins. Neutralization of both Bcl-xL and Mcl-1 is required to activate Bak for apoptosis induction [86], which suggests that Bak is activated through the indirect activation model.

As Bak is already present in the mitochondrial outer membrane, it is appealing that Bak is kept inactive by a Bcl-2 subfamily protein. Bax, however, is largely cytosolic. And a Bax-activating signal is necessary to trigger its mitochondrial translocation [77]. In this sense, both of these models may exist for Bax and Bak activation.

BH3 only proteins activate Bax and Bak in response to various apoptotic stimuli as well as in cell type-specific manner (Figure 2.8). Hrk-deficient mice are viable and exhibited normal postnatal development. Neurons from Hrk-deficient mice were resistant to axotomy, and delayed the cell death induced by NGF removal (Figure 2.8; [87]), which is consistent with the restricted expression of Hrk in the developing nervous system [87]. The activity of BH3-only protein can be BH3 only proteins activate Bax and Bak in response to various apoptotic stimuli as well as in cell type-specific manner (Figure 2.8). Hrk-deficient mice are viable and exhibited normal postnatal development. Neurons from Hrk-deficient mice were resistant to

axotomy, and delayed the cell death induced by NGF removal (Figure 2.8; [87]), which is consistent with the restricted expression of Hrk in the developing nervous system [87]. The activity of BH3-only protein can be transcriptionally regulated and post-translationally regulated, such as phosphorylation, sequestration to cytoskeletal proteins, or inactive zymogens. DNA damage in response to γ-irradiation, cisplatin or etoposide activates transcription factor p53, which leads to Puma and Noxa increase (Figure 2.8; [88, 89]). In response to growth factor withdrawal or B cell receptor

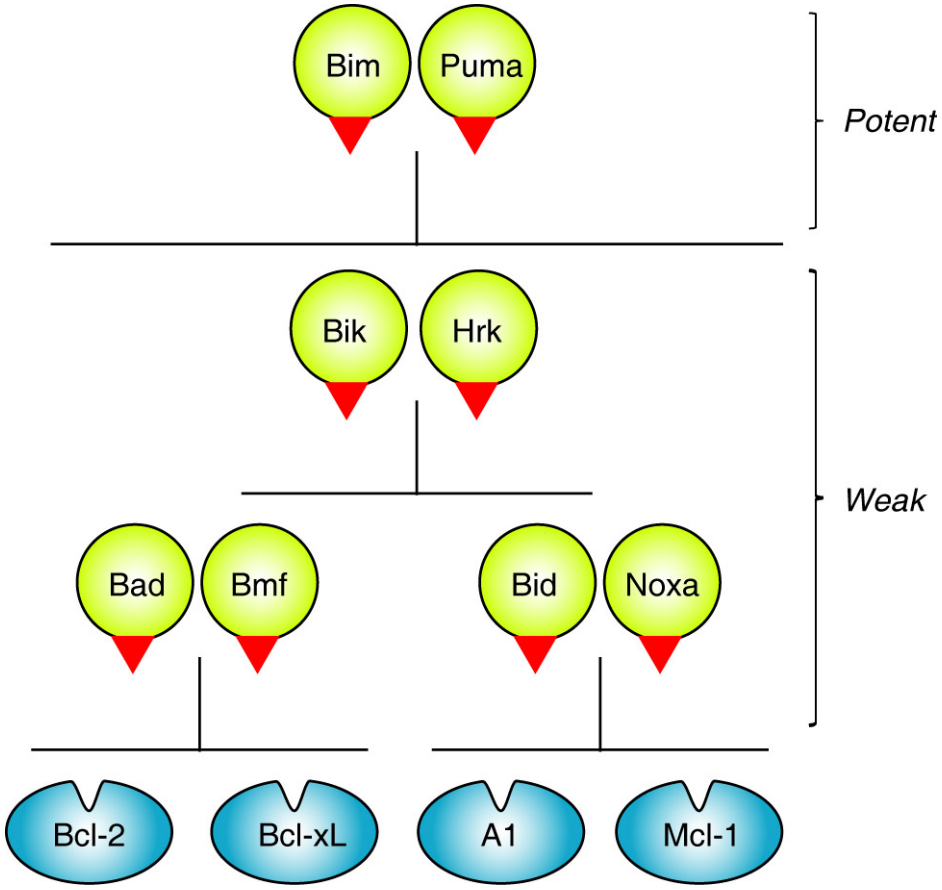

Figure 2.7: BH3-only proteins promiscuously or selectively bind to Bcl-2 like proteins. BH3-only proteins Bim and Puma engage all Bcl-2-like proteins and thus are potent killer. All other BH3-only proteins bind selectively to subsets of Bcl-2-like proteins and hence are weak killer. BH3-only proteins Bad, Bmf only bind to Bcl-2, Bcl-xL; BH3-only proteins Bid and Noxa only bind to MCl-1 and A1; BH3-only protein Bik and Hrk only bind to Bcl-xL and A1.The red triangle indicate the BH3 domain. This figure is adapted from [90]

stimulation, Bim and Bik can be increased by transcription activation (Figure 2.8; [91-93]). Bim and Bmf can bind to dynein light chain (DLC) and be sequestered to inhibit their pro-apoptotic activity. Reagents such as taxol that destabilize microtubules release Bim from DLC and trigger cell death. Bim and Bmf can also be released through phosphorylation by MAPK [94, 95]. Bad, on the other hand, can be dephosphorylated activated by cytokine withdrawal, which results in the dissociation of Bad with 14-3-3 and the released Bad could exert its pro-apoptotic activity by

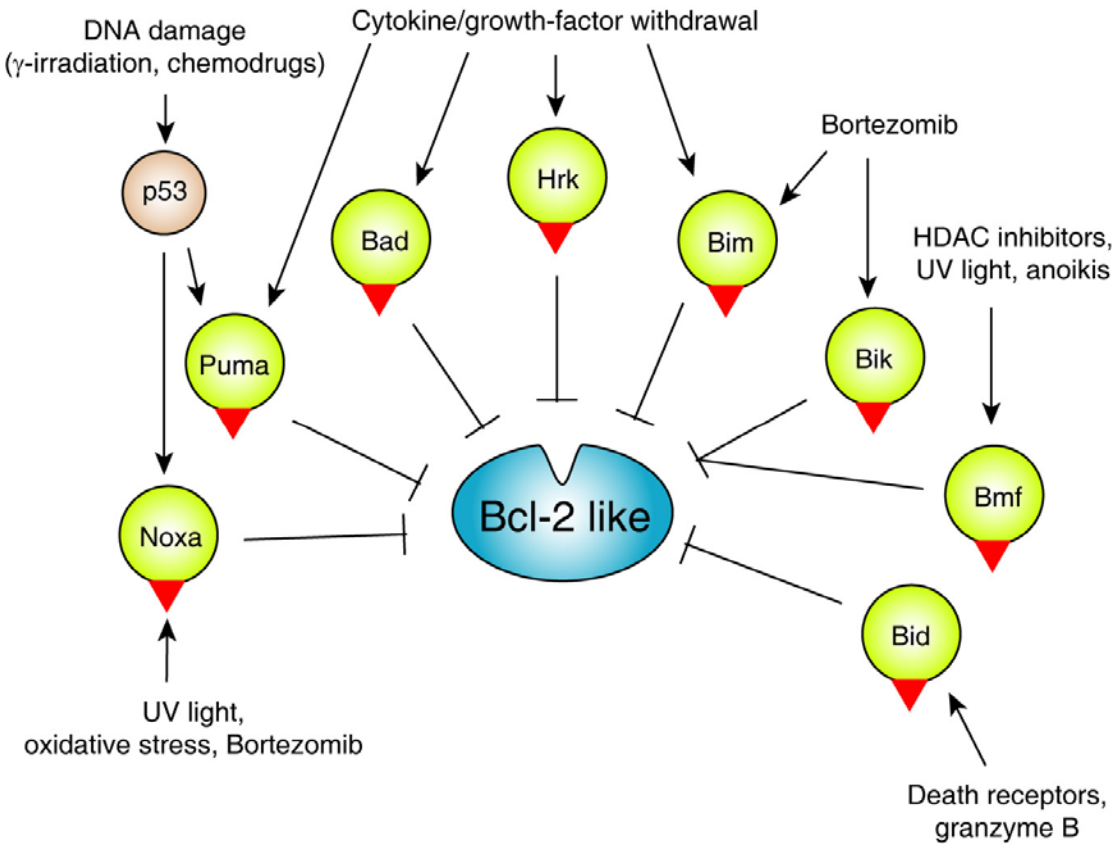

Figure 2.8: BH3-only proteins are activated in response to various activations. BH3 only proteins are activated by a variety of cellular stresses. Once activated, they initiate apoptosis by binding and neutralizing Bcl-2-like proteins via their BH3 domain (red triangle). This picture is adapted from [86].

neutralizing Bcl-2-like proteins (Figure 2.8; [96-98]). Bcl-2 interacting domain death agonist (Bid) is activated through cleavage by calpains, caspases, Granzyme B and cathepsins [99]. The actived tBid therefore activate Bax and Bak and thereafter apoptosis (Figure 2.8; [100]).

B cell receptor mediated signaling pathway: The B cell receptor (BCR) is a multimeric protein complex consisting of antigen binding membrane immunoglobin (mIg) and the Igα and Igβ heterodimer (Figure 2.9; [101]). In the cytoplasmic tail of Igα and Igβ, there is a consensus sequence termed the immunoreceptor tyorosine-based activation motifs (ITAMs) [102]. Binding of antigen to mIg induces tyrosine phosphorylation of the ITAM by Src family protein tyrosine kinases (Src-PTKs), such as Lyn. Phosphorylated tyrosines recruit B cell linker protein (BLNK) and promote its phosphorylation by PTKs, and trigger cascade activation of protein tyrosine kinases (PTKs), including spleen tyrosine kinase (SYK), B-lymphocyte specific tyrosine kinase (BLK), hemopoietic cell kinase (HCK), and Bruton's tyrosine kinase (BTK) (Figure 2.9; [103]). These activated PTKs phosphorylate and activate different substrates to direct NFκB, ERK, PI3K, JNK, calcium mobilization, and PKC activation (Figure 2.9; [103]).

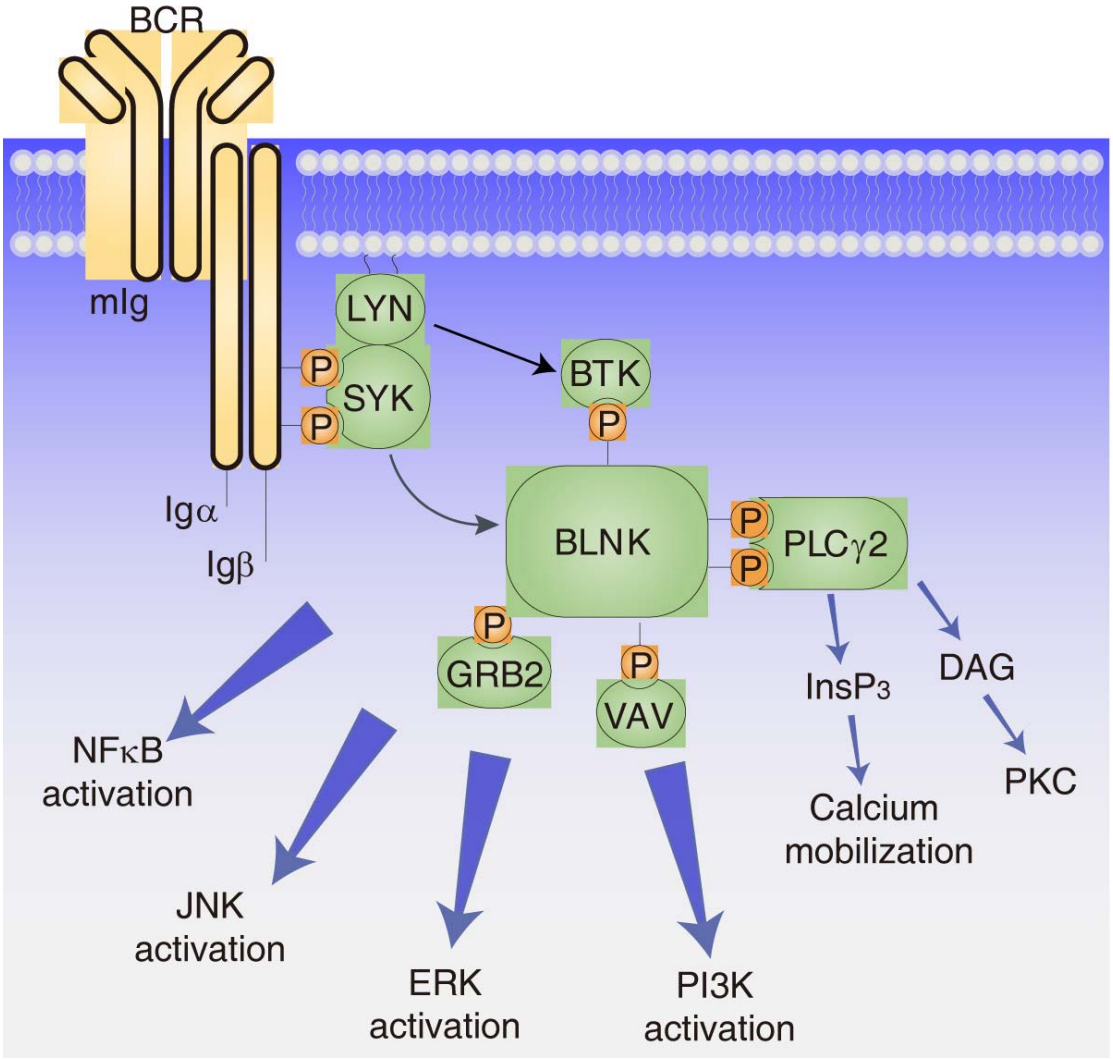

Figure 2.9: Proximal BCR signaling for activation of various downstream signaling pathways. After B antigen ligation, three main protein tyrosine kinases Lyn, Syk and Btk are activated. PI3K, PLCγ2, NFκB, JNK and ERK are important downstream effectors for B cell receptor signaling. B cell adaptor, such as BLNK, fine-tunes B cell signals by efficiently connecting the kinase and effectors. This picture is adapted from [103].DAG, diacylglycerol; InsP3, inositol-1,4,5-triphosphate; BLNK, B cell linker; PI3K, phosphatidylinositol 3-kinase; PLCγ2, phospholipase Cγ2.

BTK, together with SYK, phosphorylates and activates phospholipase γ2 (PLCγ2) [104], which hydrolyzes phosphatidylinositol-4,5-bisphosphate ($PtdInsP_2$) to produce inositol-1,4,5-triphosphate ($InsP_3$) and diacylglycerol (DAG). The increased $InsP_3$ binds to the $InsP_3$ receptor, releasing calcium from the endoplasmic reticulum (ER) [105]. The calcium depletion from ER then signals the opening of calcium

release activated calcium (CRAC) channel for extracellular calcium influx, which is responsible for the sustained $[Ca^{2+}]_i$ increase [105]. The sustained calcium increase activates calcineurin, a serine/threonine phosphatase [106]. One of the substrates of calcineurin is nuclear factor of activated T cells (NFAT) [106]. Transcription factor NFAT is dephosphorylated by calcineurin, which triggers its nuclear translocation for transcription activation [106]. DAG activates PKCδ, which phosphorylates and activates Ras. Activated Ras will phosphorylate and activate ERK, which phosphorylates and activate c-fos, a subunit of transcription factor AP-1. DAG and calcium activate PKCβ, which activate transcription factor NFκB [107-109]. The balance among these transcription factors determines cell fate. Apoptosis is induced when calcium signaling pathway overrides other survival signaling pathways induced by BCR ligation [110].

BCR-induced survival and proliferation

NFκB pathway: NFκB is sequestered in the cytosol by binding to the inhibitory protein IκB. In BCR-stimulated cells, IκB is phosphorylated by IKKα/β and tagged for proteasomal degradation. The released NFκB then translocates into the nucleus and activates transcription [111]. BCR-induced NFκB activation is blocked in BTK-, BLNK-, and PLCγ2-deficient B cells [112-114], indicating the critical role of PLCγ2. PLCγ2-induced Ca^{2+} influx and PKC activation are required as Ca^{2+} chelator and specific PKC inhibitor block BCR-directed NFκB activation [113]. It is thought that PKCβ, which requires both Ca^{2+} and DAG for its activation, is involved in the BCR-induced NFκB activation. This hypothesis is supported by the observation that

PKCβ is required to activate IKKα/β, an upstream kinase of NFκB activation [115, 116].

The NFκB transcription factor complex consists of heterodimers or homodimers of the subunits NF-κB1 (p50), NF-κB2 (p52), c-REL, REL A (p65) and REL B [117]. NFκB induced the expression of Bcl-2 and Bcl-xL to protect cells from BCR-induced cell death [118, 119]. NFκB is also shown to induce cyclin D2 expression, as blockade of calcium entry completely blocks BCR-induced cyclin D2 increase [120].

PI3K pathway: Phosphoinositide-3-kinase (PI3K) is a primary candidate for mediating B cell survival, as treatment of B cells with PI3K inhibitors leads to an increase in BCR-induced cell death [121, 122]. PI3K is a complex with regulatory subunit p85 and catalytic subunit p110. BCR signaling and its co-receptor CD19 play a synergistic way in PI3K activation [123]. The phosphorylation of cytosolic tail of co-receptor CD19, signals the binding of PI3K to the cytosolic tail of CD19 through p85. Its catalytic domain p110 is therefore activated by the activated protein tyrosine kinase such as SYK [122, 123]. PI3K phosphorylates phosphatidylinositol (3,4)-bisphosphate [PI(3,4)P2] to phosphatidylinositol (3,4,5)-trisphosphate [PI(3,4,5)P3], which assists in recruitment of BTK and AKT and their subsequent activation [124]. The activated AKT phosphorylates and inactivates pro-apoptotic BH3 only protein Bad, promoting cell survival [125]. ATK can also phosphorylate and inhibit glycogen synthase kinase 3 (GSK3). GSK3 inhibits cell cycle-progress by phosphorylating and destabilizing MYC and cyclin D [126].

ERK pathway: ERK is shown to be involved in B cell proliferation by upregulating cyclin D2 [127]. Cyclin D2 binds and regulates cyclin-dependent kinase 4 (CDK4) or CDK6 [128]. This complex phosphorylates retinoblastoma protein (Rb) and induces cell cycle G1/S transition [128]. BCR-induced proliferation is blocked by a specific ERK inhibitor [129], confirming the role of ERK in B cell proliferation. There are two pathways for ERK activation: one is through PLCγ2 and the other one is through Ras-Raf-ERK pathway [130, 131]. The activation of extracellular signal-regulated kinase (ERK) was only partially impaired in PLCγ2-deficent B cells [130], indicating that PLCγ2 is only partially responsible for ERK activation. ERK can also be activated by Ras-Raf-ERK pathway [131]. However, Raf is also shown to be involved in cell survival in a ERK-independent pathway, as enhanced cell death but normal ERK activation were detected in Raf1-deficient mice[132, 133].

Co-receptor of BCR signaling pathway: Co-receptors are cell surface receptors that bind to signaling molecules and facilitate BCR responses. There are both negative and positive regulators of BCR signaling that modulate the threshold for BCR activation (Figure 2.11). The positive co-receptors include CD19, CD21 (receptor for C3d), and CD81 (receptor for anti-proliferative antigen-1). CD19, CD21 and CD81 form a complex. Binding of C3d to this complex induces phosphorylation of CD19 cytosolic tail, which recruits PI3K (Figure 2.11; [134, 135]). The negative co-receptors are FcγIIB (low-affinity receptor for the Fc portion of IgG) [136], CD72 [137], CD22 (receptor for sialic acid) [138], CD5 [124, 139]. Binding of immune complexes containing IgG antibodies to B cells leads to co-aggregation of BCR and

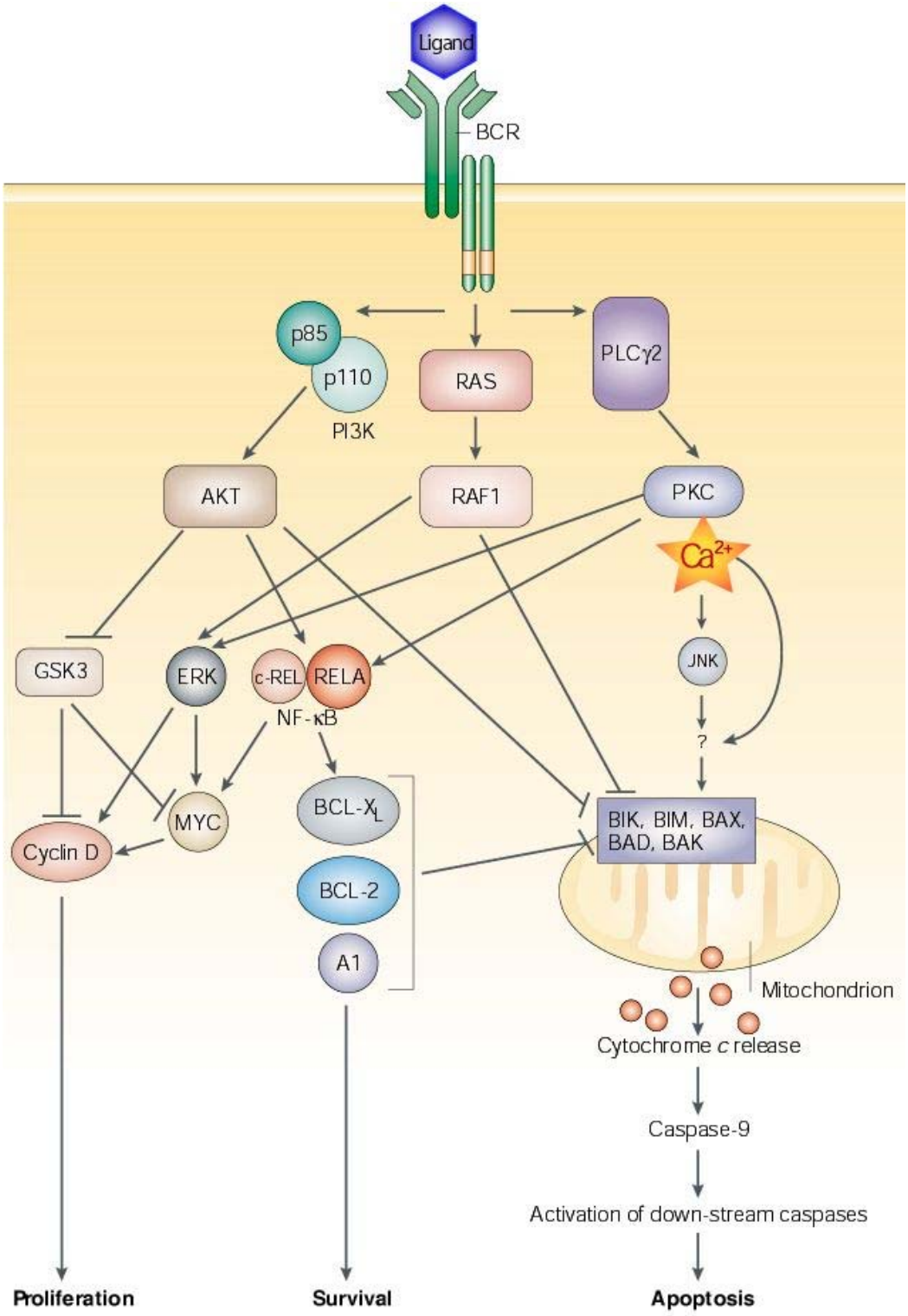

Figure 2.10: B cell receptor induced cell death, survival and proliferation. The upstream BCR signaling activates PI3K, Ras and PLCγ2, which results in AKT, Raf1, protein kinase C (PKC) and calcium activation. Three main pathways (PI3K-ATK, NFκB, and ERK) are involved in BCR-mediated survival and proliferation. In contrast, calcium leads to mitochondria dysfunction and apoptosis. This figure is adapted from [140]

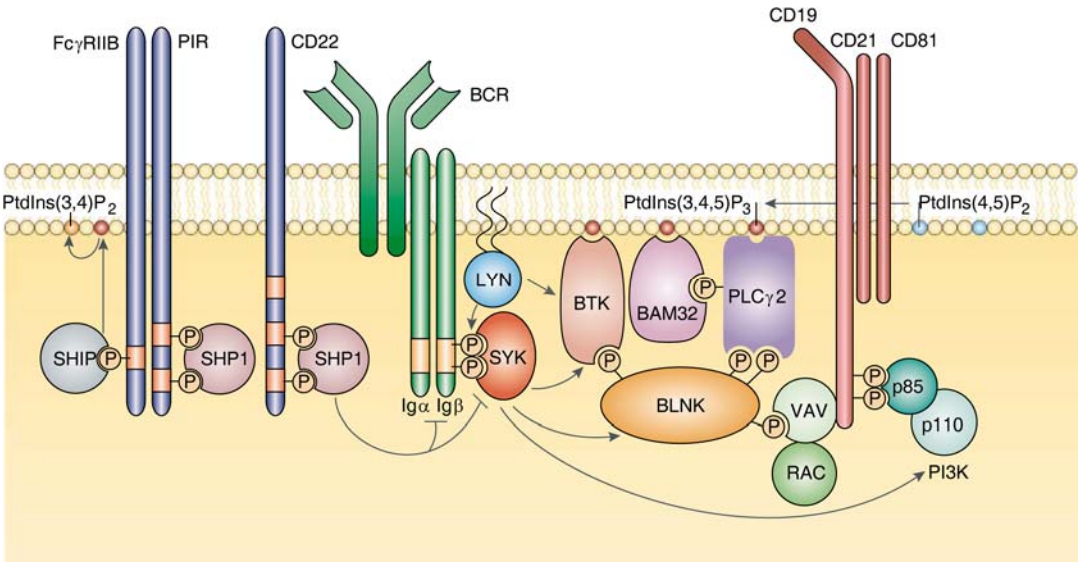

Figure 2.11: Co-receptor for B cell receptor signaling. Negative co-receptor FcγRIIB, PIRB, CD22 contains ITIM in the cytosol tail (show in orange). Phosphorylation of ITIM by src-PTK recruits SHIP or SHP1, which inhibits BCR signaling. Positive co-receptor CD19, CD21 and CD81 form a complex. Once the cytoplasmic tail is phosphorylated, it can help to recruit PI3K and enhance PI3K activation. This figure is adapted from [140]. SH2-domain-containing inositol polyphosphate 5' phosphatase; SHP1, SH2-domain-containing protein tyrosine phosphatase 1; FcγRIIB, low-affinity Fc receptor for IgG; PIRB, paired immunoglobulin-like receptor B.

FcγIIB, which block antigen-induced B cell activation [136]. The inhibition through FcγIIB is mediated primary through SH2-containing inositol 5'-phosphatase (SHIP), which hydrolyzes PI(3,4,5)P3, an essential element for BTK and AKT activation [124]. In the cytoplasmic tail of these negative co-receptors, there is a consensus sequence termed immunoreceptor tyorosine-based inhibition motifs (ITIMs), whose phosphorylation recruits a tyrosine phosphatase [136-139]. The ITIM in the CD22 is phosphorylated by Lyn [138]. This results in recruitment of Src-homology 2 domain containing phosphatase-1 (SHP-1), which limits B cell receptor signaling by dephosphorylating a range of targets, including Igα, Igβ, Syk, Vav, BLNK [138]. Lack of CD22 to suppress the BCR signaling, B cells from CD22-deficient mice

exhibited increased calcium in response to antigen receptor crosslinking [141].

In addition to those co-receptors that directly regulate proximal BCR signaling, there are several cell surface receptors to provide survival signals, such as CD40, B cell-activating factor (BAFF) receptor, and receptors for several cytokines such as Interleukin-4 (IL-4). Ligation of these receptors inhibits B cell receptor-mediated apoptosis [142-144].

***B cell receptor mediated apoptosis*:** In response to BCR stimulation, B cells can undergo proliferation, anergy, or apoptosis [145]. The development state of B cells affects the outcome of BCR signaling. Upon encountering an antigen, mature B cells undergo activation and proliferation, which result in immune response against harmful pathogens. In contrast, antigen stimulation of immature B cells and mature B cells with GC phenotype causes apoptosis in the absence of survival signal. This may serve as an important mechanism to deplete potential self-reactive B cells [146]. Consistent with the *in vivo* observation, apoptosis induced by BCR ligation was first demonstrated in immature B cells but not in mature B cells [147, 148]. However, later studies demonstrated that mature B cells could also undergo apoptosis when BCR was ligated by membrane-bound antigens or immobilized anti-Ig antibodies [149-151]. As membrane-bound antigen or BCR crosslinking induced stronger signal than soluble antigen binding or BCR ligation, it is suggested that there is certain threshold for BCR-mediated apoptosis [152]. Once above this threshold, BCR ligation will result in apoptosis. Therefore, BCR-induced apoptosis can be regulated by either modulating BCR-induced signaling strength or regulating threshold.

BCR-induced apoptosis adopts intrinsic apoptotic signaling pathway: In anti-IgM induced apoptosis, mitochondrial membrane potential ($\Delta\psi_m$) disruption and caspase activation are observed, which suggests the involvement of mitochondria (Figure 2.12; [153]). Cells expressing FADD dominant negative mutant are resistant to death receptor-mediated apoptosis. However, this mutation does not block BCR-mediated apoptosis. This result thus excludes the involvement of extrinsic signaling pathway in BCR-mediated apoptosis [154]. In addition, the specific caspase 8 inhibitor z-IETD-fmk did not protect against anti-IgM induced apoptosis [153, 155]. In contrast, the general caspase inhibitor z-VAD-fmk and the caspase 9-specific inhibitor z-LEHD-fmk inhibited apoptosis but not $\Delta\psi_m$ disruption, indicating caspase activation is downstream of mitochondria [153, 155]. This post-mitochondria caspase activation was also confirmed by overexpression of catalytically inactive caspase-9, which interfered anti-IgM induced DNA fragmentation [156]. Mitochondrial pro-apoptotic factor cytochrome c release was induced by anti-IgM stimulation [155, 157]. Moreover, the overexpression of Bcl-2 or Bcl-X_L, important regulators for the intrinsic pathway, blocked BCR-mediated apoptosis in both B cell lines and mouse B cells [158-160]. These results suggest that anti-IgM induced apoptosis occurs via the intrinsic pathway. Cycloheximide interferes with translation step in protein synthesis thus blocking translation elongation. Pre-incubation with cycloheximide blocked anti-IgM induced $\Delta\psi_m$ disruption and apoptosis, suggesting the requirement of new protein synthesis [161, 162].

Calcineurin is involved in BCR-mediated apoptosis: Several studies have

shown the involvement of calcium in B cell death and specifically BCR-mediated apoptosis. Calcium ionophores induce cell death, indicating calcium increase can cause B cell apoptosis [163]. Disruption of $InsP_3$ receptors in DT40 B cells blocked BCR-induced calcium release and prevented subsequent cell death [164], indicating calcium plays a role in mediating BCR-induced cell death (Figure 2.12). Pretreatment with calcineurin inhibitor cyclosporine A or FK506 protects human B cells MBC-1 against anti-IgM induced apoptosis [165], revealing the critical role of calcineurin (Figure 2.12). NFATc2, a transcription factor that can be activated by calcineurin, is shown to increase Nur77 expression, which translocated into the mitochondria, triggered mitochondrial pro-apoptotic factors release [166]. The VIVIT peptide, a specific NFAT inhibitor, blocked anti-IgM induced Nur77 expression and subsequent cell death, indicating the critical role of NFATc2 [166].

Calcineurin could be involved in anti-IgM induced cell death through modulating BH3-only proteins. Calcineurin is known to be involved in Bim expression as calcineurin inhibitor cyclosporine A or FK506 inhibited T cell receptor induced Bim expression increase [167]. BCR crosslinking induced Bim increase [168], and Bim deficient cells are resistant to BCR-mediated cell death [169]. Calcineurin could also dephosphorylate and activate Bad dephosphorylation during BCR-induced apoptosis [170]. Bik expression level was also increased by BCR ligation by anti-IgM, and this Bik increase is calcineurin-dependent as cyclosporine A pre-treatment inhibited anti-IgM induced increase [91].

MAPK pathway is involved in BCR-mediated apoptosis: Mitogen-activated

protein kinase (MAPK) is a group of serine/threonine-specific protein kinases. Anti-IgM stimulation activates three main forms of MAPK: JNK, p38 and ERK. Although JNK and p38 activation were not observed in anti-IgM stimulated WEHI-231 cells [171], a delayed and sustained activation of JNK and p38 kinases was observed during BCR-mediated apoptosis in B104 cells (Figure 2.12; [172]). A selective p38 inhibitor, SB203580, suppressed BCR-mediated caspase activity and apoptosis [173]. Extracellular signal regulated kinases (ERK), another MAPK, which has previously been connected to survival signaling, was shown to mediate BCR-mediated apoptosis (Figure 2.12; [174]).

Survival signaling is suppressed in BCR-mediated apoptosis: In addition to promotion of apoptotic signaling, suppression of survival signaling was observed during BCR-mediated apoptosis (Figure 2.12; [175]) . In WHEI-231 cells stimulated with anti-IgM, PI3K activity was suppressed, which leaded to increased p27kip activity and decreased c-myc activity (Figure 2.12; [176]).The increase in p27kip and decrease in c-myc was responsible for the observed growth arrest by anti-IgM stimulation. In WHEI-231 cells, BCR stimulation also leads to stimulation and accumulation of IκBα (Figure 2.12; [177]). As IκBα binds to NFκB and inhibit the activity of NFκB, IκBα increase is predicted to suppress the survival signaling pathway activated by NFκB (Figure 2.12).

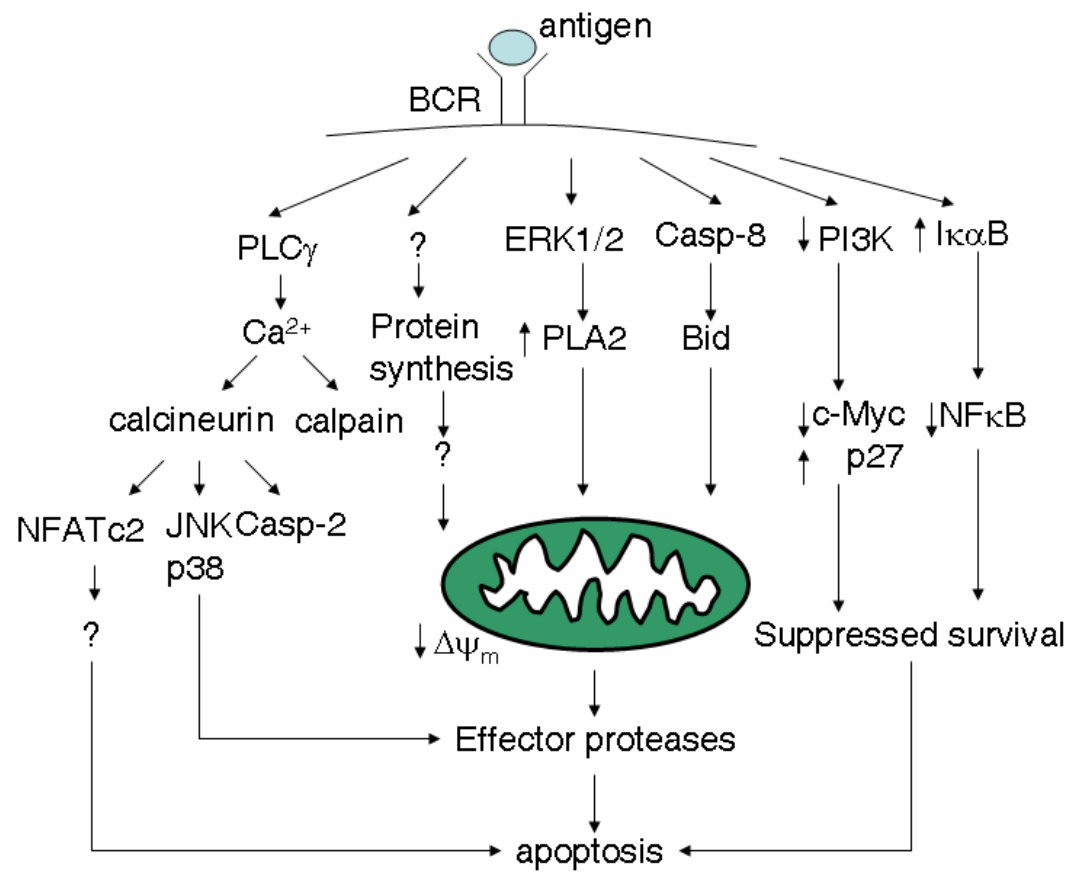

Figure 2.12: BCR-mediated apoptotic signaling pathway. See texts for detailed description. This picture is adapted from [175]**.**

Defective B cell receptor signaling and apoptosis in SLE: One of the hallmarks of SLE patients is the autoantibodies. They form immune complex with self-antigens, deposit in a variety of organs such as kidney and skin, and cause organ damage. Therefore, autoantibodies titers can be used to diagnose SLE and evaluate disease activity [178]. Autoantibody production is the result of dysregulated B cells. These dysregulated B cells may participate in SLE in autoantibody-independent manner, such as presenting autoantigen to T cells, secreting cytokines to regulate other immune cells. It is not surprising to find that B cells unable to secrete

autoantibodies are still critical to the development of disease [179]. Moreover, genetically knockout these cells in the MRL/lpr lupus-prone mice have attenuate disease [179]. In a word, dysregulated B cells play a critical role in the disease development.

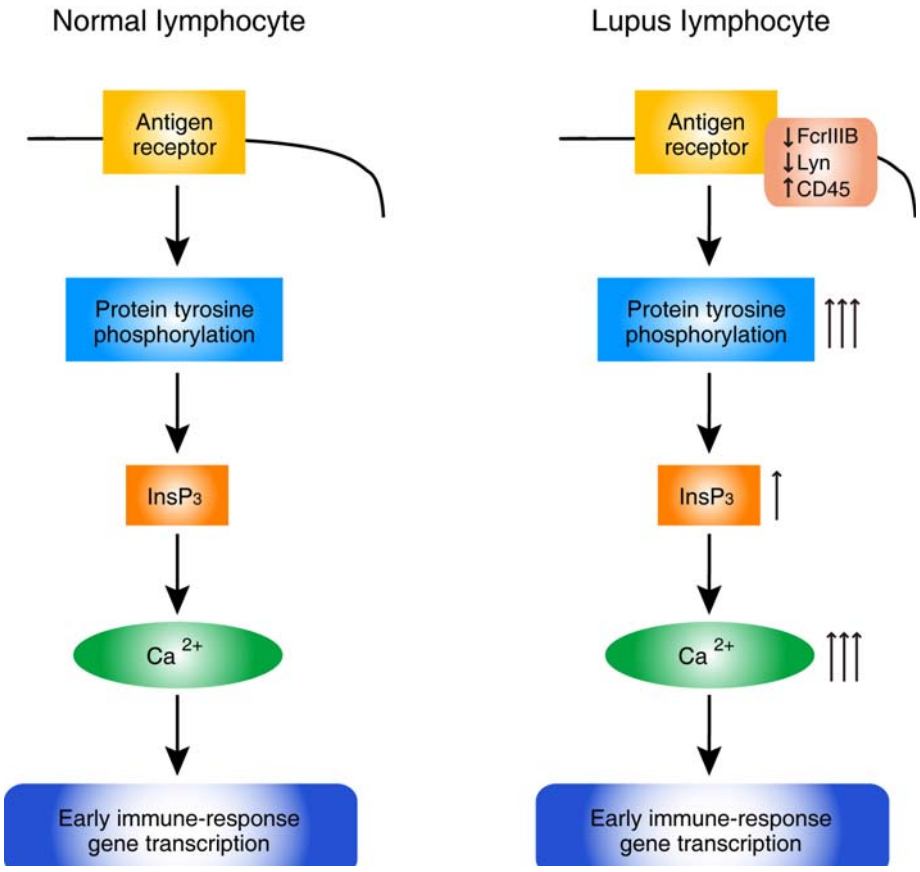

Figure 2.13: Defective BCR signaling in the SLE patients. In response to antigen receptor stimulation, there is a cascade of protein tyrosine phosphorylation, which results in the production of InsP3. InsP3 will binds to InsP3 receptor in the ER, lead to calcium release from the ER and subsequent calcium influx. Compared to the normal B cell response, BCR-mediated proximal signaling is significantly increased in B cells from SLE patients. This hyper-responsive BCR signaling may be due to decreased negative regulation from co-receptor, as decreased FcγIIB, Lyn and increased CD45 expressions are observed in B cell of the SLE patients. This picture is adapted in [180].

Defective BCR signaling in SLE: The dysregulated B cell function observed

in SLE patients may be the result of defective BCR signaling. Studies of BCR signaling in SLE patients indicated defects in the proximal events [180], which may be associated with hyperactivity in response to activation signals and increased CD40L expression in lupus B cells [181]. Abnormal BCR signaling is not observed in other autoimmune disease, such as rheumatoid arthritis (RA) [182], indicating it is disease-specific.

Compared with B cells from health individuals, stimulation of surface membrane immunoglobulin in lupus B cells leads to significantly more intracellular Ca^{2+} increase, which is associated with the enhanced proximal BCR signaling, such as increased cytosolic protein tyrosine phosphorylation, inositol triphosphate (IP_3) generation (Figure 2.13; [182]). The expression level of IgM is similar in B cells from SLE patients and normal controls, excluding the possibility of increased IgM for the hyperactivity [182]. Ligation of FcγIIB recruits SHIP, which exerts its tyrosine phosphatase activity and thus negatively regulates BCR signaling [183, 184]. In SLE patients, the suppression of FcγIIB on BCR signaling is attenuated [185]. This decreased FcγIIB signaling is not due to the expression level change of FcγIIB because comparable expression level of FcγIIB is detected [185, 186]. In contrast, reduced SHIP has been observed in SLE patient, which may be responsible for the defective FcγIIB signaling [185]. In SLE B cells, reduced expression level of Lyn and CD45 (SHP-1) have also been observed, indicating their possible involved in the exaggerated calcium response [186, 187]. In response to stimulation Lyn translocates to the lipid raft microdomains for its function, and slower recruitment is observed in

lupus B cells [188], which results in decreased Lyn in the lipid raft [189]. Since Lyn plays a critical role in SHIP recruitment [184], this altered Lyn distribution might be responsible for reduced FcγIIB signaling.

Defective BCR-mediated apoptosis in SLE: Defective BCR-mediated apoptosis was first demonstrated in the lupus-prone New Zealand mouse strains [150, 190, 191]. Peritoneal B cells from NZB/NZW F1 mice are resistant to cell death induced by surface immunoglobulin crosslinking [150]. Splenic transitional T1 B cells from NZB mice are also resistant to IgM crosslinking [190]. The spleen B cells from both NZB and older NZB/NZW F1 mice are resistant to surface-Ig-crosslinking induced apoptosis [191]. These observations indicate negative selection through BCR is a critical mechanism to maintain tolerance.

Lupus genes are associated with defective BCR signaling: Several genes identified to be associated with the SLE are also involved in BCR signaling. The Sle 2 gene is identified in the MZM2410 mice and thought to cause SLE onsets by reducing the B cell signaling threshold, resulting in B cell hyperactivity [192]. The Y-linked autoimmune accelerating (Yaa) locus is a potent autoimmune disease allele [193]. Duplication of Toll-like receptor 7 (TLR7) was detected in this locus and was proposed to increase susceptibility to lupus disease, as the binding of RNA and DNA to TLR7 provides co-stimulatory signal for B cells stimulation [193]. Targeted TLR7 disruption attenuated the lupus-like symptoms [194]. SLAM (Ly108) was identified in Sle 1 susceptibility locus of lupus-prone NZM2410 mice. Lupus-associated Ly108.1 allele was found resistant to anti-IgM induced cell death in immature B cells by

reducing $[Ca^{2+}]_i$ [195].

Modulation of BCR-induced apoptosis leads to autoimmune disease: Lupus-like disease is induced by abnormalities in B cell antigen receptor signaling. Overexpression, knockdown and dominant negative mutants of many BCR signaling proteins have been shown involved in the development of autoimmune diseases (Table 2.1; [196, 197]). Based on their functions in BCR signaling, they are grouped into three groups. CD45, CD22, CD72, SHP-1, and FcγRIIB are negative regulators for BCR signaling. Deficiency in negative regulator results in the lupus-like disease. CD72 is a B cell surface protein which recruits tyrosine phosphatase SHP-1 and negatively regulates B cell receptor signaling pathway. CD72 deficiency lowers the threshold for BCR activation and responsible for B cell hyperactivity (Table 2.1; [137]). Rai (ShcC) belongs to the family of Shc adaptor proteins detected in the lymphocyte. Rai knockout enhanced the cell signaling by T cell receptor (TCR) and BCR, which results in the enhanced proliferative response to antigen receptor engagement *in vitro*, leading to SLE-like disease [198]. CD19 is a positive regulator for BCR signaling. In the TSK/+ mouse model of autoimmune disease systemic sclerosis, CD19 is constitutively activated. This CD19 hyper-phosphorylation leads to autoantibodies production, which can be reversed by crossing of TSK/+ mice to a CD19-/- mice (Table 2.1; [199]). B cell hyper-responsiveness and autoantibodies production are observed in mice with deficient or with overexpressed Lyn, suggesting that Lyn acts as both a negative and a positive regulator. This is consistent with the observation that Lyn can phosphorylate both ITIM and ITAM, which initiate the

inhibitory and stimulatory signaling pathway, respectively. However, as the positive role of Lyn appears to be redundant, its role as a negative regulator of BCR signaling

Signaling molecule	**Cell function**	**method**	**phenotype**	**citation**
CD19	Positive co-receptor	Targeted disruption	Hyporesponsiveness to transmembrane signal	[200, 201]
CD19	Positive co-receptor	Transgenic expression	Tolerance breakdown SLE-like disease	[200, 202]
CD22	Negative co-receptor	Targeted disruption	B cell hyper-responsiveness, B-1 increase, autoantibodies production in aging mice	[141, 203, 204]
CD72	Negative co-receptor	Targeted disruption	SLE-like disease	[137]
Lyn	Protein tyrosine phosphorylation as a positive and negative regulator	Targeted disruption	B cell hyperactivity, autoantibodies production, SLE-like disease	[196, 197, 205]
Lyn	Protein tyrosine phosphorylation as a positive and negative regulator	Constitutive active Lyn	Hyperresponsive BCR signaling, autoantibodies production, glomerulonephritis	[206]
SHP-1	Phosphatase for negative signaling	Targeted disruption and mutation	B-1 expansion, autoantibodies production, SLE-like disease	[207-209]
CD45	Phosphatase as a positive and negative signaling	Targeted disruption	Reduced activation	[210]
FcγRIIB	Negative regulator	Targeted disruption	Spontaneous autoantibodies production and glomerulonephritis	[211, 212]
BAFF	Survival signal	Transgenic expression	Increased peripheral B cells, SLE-like disease	[213]
CD40L	Survival signal	Transgenic expression	Autoantibodies production, glomerulonephritis	[214]

Table 2.1: Molecules that modulate BCR-mediated apoptosis are involved in SLE development.

is indispensable. Therefore, the negative signaling role of Lyn was identified in Lyn-deficient mice.

Beside the molecules directly modulate BCR signaling, overexpression of survival factors such as CD40L or BAFF also induces lupus-like disease. Transgenic mice with CD40L-overexpressing B cells produce autoantibodies and develop lupus-like glomerulonephritis as a result of defective BCR-induced apoptosis is observed (Table 2.1; [214]). Transgenic mice overexpressing BAFF, another co-stimulatory signaling for survival signaling, develops lupus-like autoimmune disease (Table 2.1; [215]).

Bz-423 mediated apoptotic signaling pathway in Ramos B cells. Bz-423 attenuates disease in two lupus-prone NZB/NZW F1 mice and MRL-*lpr* mice, which are driven by abnormal B cells and T cells, respectively [216, 217]. Further studies of Bz-423 on various lymphocyte cell lines indicates it induces cell growth arrest at low concentrations; and induces apoptosis at high concentrations [218]. This growth modulatory and apoptotic-inducing effect is ROS-dependent as antioxidants inhibit the proliferation and apoptosis induced by Bz-423 [217].

As Bz-423 induces superoxide in both isolated mitochondria and cells, Bz-423 potentially targets mitochondria [217]. Phage display screening identified the oligomycin sensitivity conferring protein (OSCP) as a binding partner for Bz-423 [219]. In mitochondrial F_0F_1-ATPase, OSCP is the part of peripheral stalk that links the integral membrane F_0 component with the catalytic F_1 domain. Studies of the effect Bz-423 on the enzymatic activity of isolated mitochondrial F_0F_1-ATPase

indicated that Bz-423 inhibited both the ATP hydrolysis and ATP synthesis function in an OSCP-dependent manner [219]. Moreover, Bz-423 was shown to inhibit mitochondrial F_0F_1-ATPase in cells [219]. Using permeablized Ramos cells, Bz-423 was shown to inhibit ATP synthesis with IC_{50} of approximately 5 μM [219]. This inhibition of mitochondrial F_0F_1-ATPase by Bz-423 results in the mitochondria transition from state 3 to state 4 and superoxide production [219]. Cells with reduced OSCP expression are less sensitive to Bz-423 in superoxide production and cell death induction [219], verifying the critical role of OSCP in mediating Bz-423 induced superoxide (Figure 2.14).

Although Bz-423 targets mitochondria, the apoptotic pathway it adopts requires a specific extra-mitochondrial cascade [220]. Activated Bax induced by Bz-423 translocates to mitochondria, where both activated Bax and activated Bak form channels in the outer mitochondrial membrane (OMM), resulting in pro-apoptotic factors release from mitochondria to cytosol [220]. Single RNA interference (RNAi) knockdown of Bax and Bak partially inhibit Bz-423 induced apoptosis, and double Bax and Bak RNAis knockdown abolished Bz-423 induced apoptosis, suggesting Bax and Bak activation are both involved in Bz-423 induced apoptosis [220]. Ramos B cells with stable overexpression of Bcl-2 and Bcl-xL do not modulate Bz-423 induced superoxide production. However, they inhibit Bax and Bak activation and their downstream signaling [220]. These results exclude the possibility that Bcl-2 like family members modulate Bz-423 induced apoptosis through ROS. These released mitochondrial pro-apoptotic factors trigger both caspase-dependent

and caspase-dependent apoptotic pathways [220]. The apoptotic signaling pathway induced by Bz-423 is summarized in Figure 2.14.

Bz-423 and anti-IgM co-treatment results in synergistic cell death: Administration of Bz-423 to lupus NZB/NZW F1 mice, which is associated with the abnormal expansion of germinal center (GC) B cells [217], greatly attenuates the symptoms with little side effects. Bz-423 treatment greatly reduces both the number and the size of GC in the spleen, along with increased apoptotic activity [217]. This observation suggests that Bz-423 selectively induces apoptosis in GC B cells, which is proposed to account for the efficacy and specificity of Bz-423 treatment.

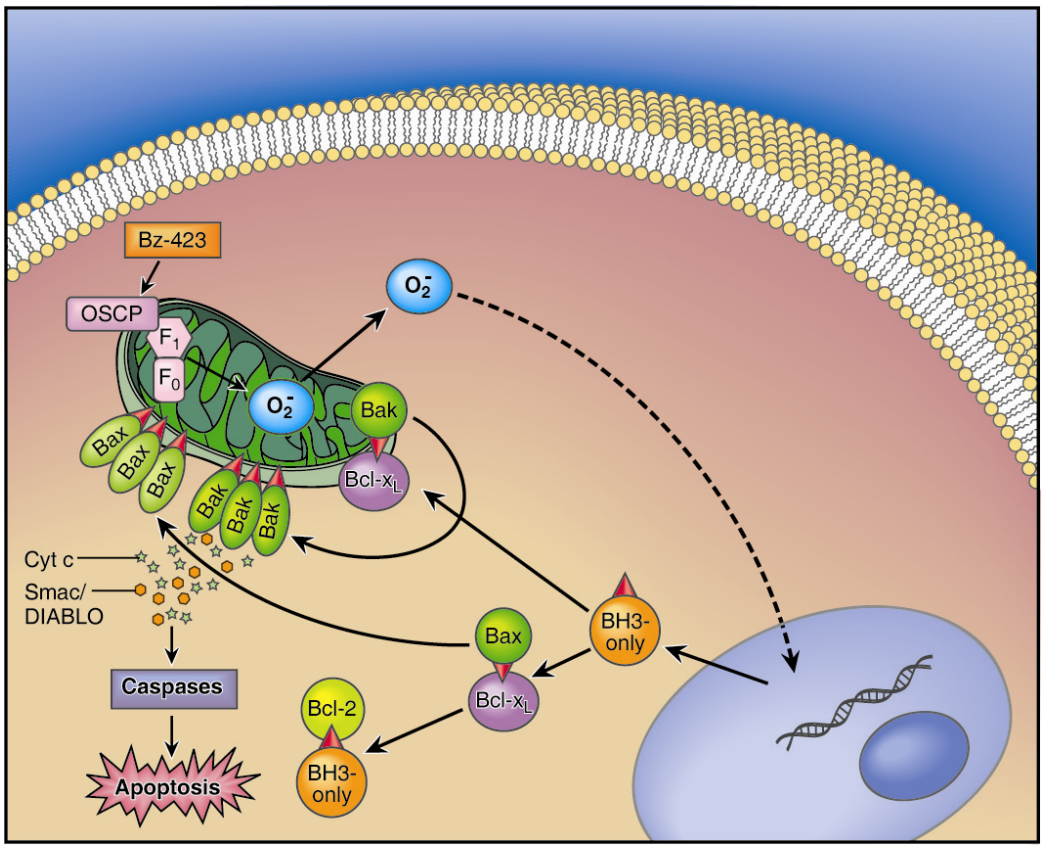

Figure 2.14: Bz-423 induced apoptotic signaling pathway in Ramos B cells. See text for details. Figure adapted from [220].

This observation that Bz-423 selectively kills pathogenic B cells *in vivo* was studied using an *in vitro* cell line model [221]. Ramos B cell line was selected because it displays a GC-phenotype. Since GC B cells are activated, it is then hypothesized that activation sensitizes Ramos B cells to Bz-423 treatment. This hypothesis was tested by studying the effect of Bz-423 on Ramos B cells stimulated by anti-IgM, which binds to the B cell receptor and activates the cells. Co-treatment of sub-apoptotic anti-IgM and non-toxic Bz-423 induced a supra-additive apoptosis[221]. As ROS and calcium are important mediators for cell death induced by Bz-423 alone and anti-IgM, respectively, their involvement in cell death by co-treatment was studied. The cell death by co-treatment is inhibited by anti-oxidants and extracellular calcium chelator, indicating their involvement. Cycloheximide blocks new protein synthesis and inhibits cell death by co-treatment. This result suggests new protein is required for apoptosis induction [221]. Although superoxide was shown to be involved in the cell death by co-treatment, anti-IgM stimulation does not modulate Bz-423-induced superoxide change [221]. Bz-423 pre-treatment augmented and sustained anti-IgM induced calcium change, suggesting this synergistic calcium change is responsible for cell death by co-treatment [221].

Statement of problem: The purpose of this chapter is to elucidate the apoptotic signaling pathway of the cell death by co-treatment induced by anti-IgM and Bz-423 treatment, especially the role of calcium. Toward this goal, the Ramos B cell *in vitro* model was verified as a model to study anti-IgM induced synergy. Second, it is clear from inhibitor experiments that the apoptotic signaling pathway induced by

anti-IgM and Bz-423 co-treatment is distinct from the apoptotic signaling pathway induced by Bz-423. Therefore, the detailed apoptotic signaling pathway under synergistic condition was studied in this chapter. Understanding the cell death by co-treatment will help to design better drug for autoimmune disease development.

Results:

Bz-423 selectively kills activated B cells with either a GC phenotype or immature B characteristics: Administration of Bz-423 to NZB/NZW F1 mice, a lupus-prone murine model, significantly reduces glomerulonephritis, improves renal function, and increases overall survival rate with little side effects [217]. Since aberrant survival and expansion of GC B cells are associated with the disease in NZB/NZW F1 mice [222], the effect of Bz-423 on GC B cells was studied [217]. Bz-423 significantly reduces the size and number of GC B cells, along with increased apoptosis. This result suggests that Bz-423 selectively kills GC B cells. Other studies have shown that Bz-423 does not suppress normal lymphocyte function in normal BALB/c mice [216]. These observations suggest that Bz-423 may selectively kill pathogenic lymphocytes over normal lymphocyte.

To better study the mechanism of Bz-423 specificity observed *in vivo*, an *in vitro* system was developed. Ramos B cells were selected because it displays a GC phenotype ($CD77^+$, $CD22^+$, and surface IgM^+) [223, 224]. During GC reaction, GC B cells are activated [225]. Especially B cell hyperactivation is a distinguishing feature of autoreactive lymphocyte in lupus [226]. It was thus hypothesized that activation

sensitizes Ramos B cells to Bz-423 [221]. This hypothesis was tested by studying the cell death induced by the co-treatment of Bz-423 and anti-IgM in Ramos B cells [221]. Anti-IgM stimulation mimics the BCR signaling events that occur upon exposure to antigen binding [227]. Anti-IgM co-treatment shifted the dose response curve of Bz-423 to the left and up, indicating that anti-IgM co-treatment sensitizes cells to Bz-423 co-treatment (Figure 2.15A; [221]). In particular, at low Bz-423 concentration (≤ 5 μM in 2% FBS media), co-treatment of Bz-423 and anti-IgM induced a supra-additive or cell death by co-treatment (Figure 2.15A; [221]). This increased cellular sensitivity to Bz-423-induced cell death by anti-IgM stimulation is referred as anti-IgM induced synergy. This observation is significant because Bz-423 selectively kills anti-IgM stimulated Ramos cells over non-stimulated Ramos cells, which could mimic the selectivity for the pathogenic cells observed during Bz-423 treatment of lupus mice. Therefore, understanding of cell death by co-treatment may identify mediators for this phenomenon.

As abnormality of other B cell subsets are observed in SLE patients [228], it would be interesting to study whether anti-IgM induced synergy is observed in B cell subsets other than GC B cells. Ramos is a Burkitt's lymphoma (BL) cell line; other BL cell lines were therefore tested. There are two types of BL cell lines and they can be distinguished based on presence of the Epstein-Barr virus (EBV). Ramos, CA46, and ST486 are EBV negative while Daudi, Raji, and Namalwa are EBV positive. Unlike Ramos B cells, anti-IgM stimulation did not shift the dose response of Bz-423 induced cell death in any other BL cell lines, regardless of the EBV infection state

A: Ramos

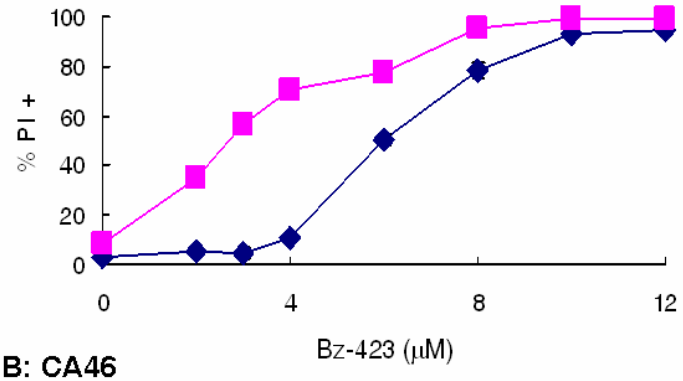

B: CA46

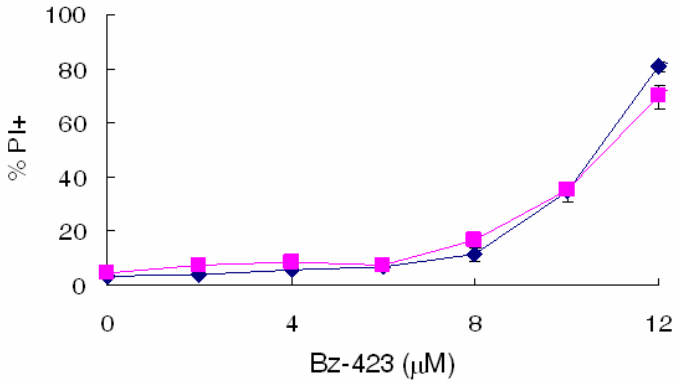

C: Raji

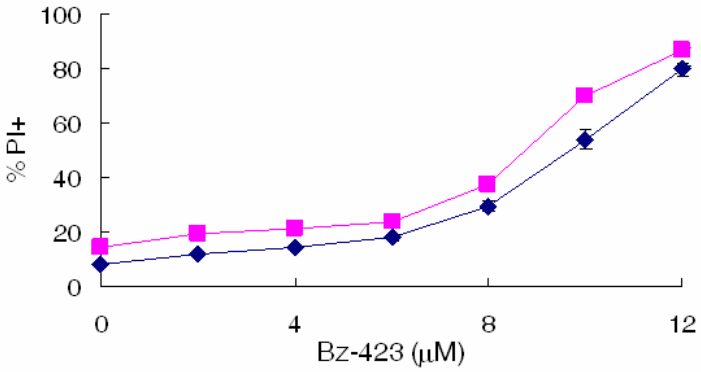

D: summary of anti-IgM induced synergy

	EBV	sIgM expression	Cell death	Synergy with Bz-423
Ramos	—	+	+	+
CA46	—	+	—	—
ST486	—	+	+	—
Daudi	+	+	—	—
Raji	+	+	—	—
Namalwa	+	+	—	—

Figure 2.15: Anti-IgM stimulation does not affect cellular sensitivity to Bz-423 in other human Burkitt's lymphoma cell lines except Ramos B cells. Various cell lines in 2% FBS media were concurrently treated with various concentrations of Bz-423 and stimulating antibody anti-IgM (1 μg/mL; ■), using control Ig (1 μg/mL, ◆) as an isotype control. 24 h later, cell death was determined by PI staining. (A) Anti-IgM induced synergy in Ramos B cells. (B) Anti-IgM does not modulate cellular sensitivity to Bz-423 in EBV-negative BL cell line CA46. (C) Anti-IgM does not modulate cellular sensitivity to Bz-423 in EBV-positive BL cell line Raji. (D) The summary table of human BL cell lines. Both anti-IgM induced cell death by co-treatment and anti-IgM induced cell death are indicated. "+" and "–" indicates positive or negative, respectively. These data were representative of at least three repeated experiments. The absence of an error bar indicates ≤ 1% standard deviation.

(Figure 2.15D). Representative cell death responses for both an EBV negative (CA46) and an EBV positive (Raji) BL cell lines were shown in Figure 2.15. Lack of synergy between anti-IgM and Bz-423 in other BL cell lines suggests that anti-IgM induced synergy only occurs in certain B cell subsets such as GC B cells. This result is consistent with the observation that Bz-423 does not interfere with the activation of normal lymphocytes [216].

Considering Ramos B cells display GC phenotype [223], it was then hypothesized that anti-IgM induced synergy occurs only in cells with GC phenotype. This hypothesis was tested by using GC B-like human diffuse large B-cell lymphoma (DLBCL) line OCI-Ly7 [229]. Anti-IgM stimulation shifted the dose response of Bz-423 to the left. And co-treatment resulted in supraadditve cell death at several subapoptotic Bz-423 concentrations (Figure 2.16A). The observation of anti-IgM induced synergy in the OCI-Ly7 cell line supports the hypothesis that Bz-423 selectively kills activated GC B cells. However, more cell lines with GC phenotype need to be tested to confirm this hypothesis. This is hindered by the limited numbers of GC-like B cell lines available.

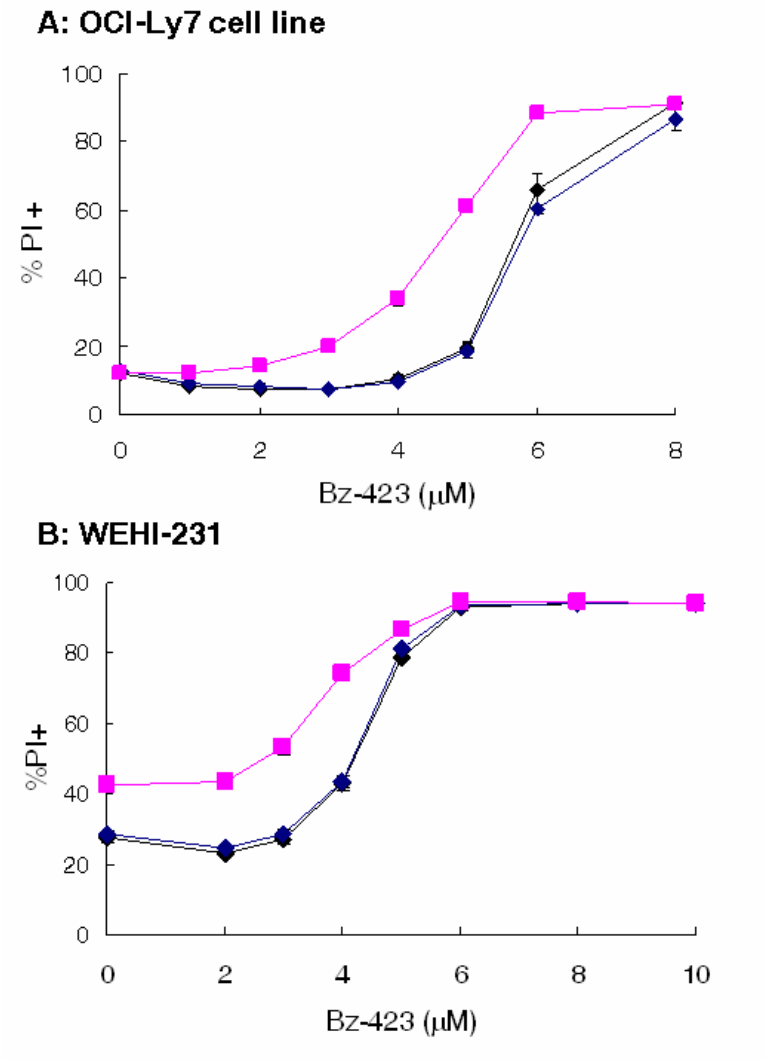

Figure 2.16: Anti-IgM induced synergy in OCI-Ly7 (A) and WEHI-231 cells (B). OCI-Ly7 or WEHI-231 cells were treated with various [Bz-423] alone (◆) or in the presence of anti-IgM (0.5 μg/mL, ■) or control Ig (0.5 μg/mL, ◆). 24 h later, cell death was determined through PI permeability. These experiments were repeated for ≥ two times. The absence of an error bar indicates ≤ 1% standard deviation.

Although Ramos B cells express both IgM and IgD, the cell receptors characteristic of mature B cells [230], they display several characteristics of immature B cells, including that they undergo apoptosis in response to BCR ligation [231-233]. Therefore, they are used to study the negative selection mechanism of deleting autoreactive B cells for self antigen [231-233]. Moreover, abnormal activated

immature B cells are observed in SLE patients [234]. Whether anti-IgM sensitized WEHI-231 cells to Bz-423 in cell death was explored. WEHI-231 was chosen as it is another immature mouse B cell line used for studying the mechanism of negative selection [153]. Anti-IgM stimulation shifted the dose response of Bz-423-induced cell death in WEHI-231 cells. At several sub-apoptotic [Bz-423], co-treatment induced supra-additive cell death (Figure 2.16B). This observation may suggest that Bz-423 may selectively kills immature B cells in presence of anti-IgM stimulation.

The roles of Bz-423 and anti-IgM in cell death induced by co-treatment

Bz-423 is not required for early proximal activation signals to establish synergy: In the *in vitro* experiments described above, B cells are treated concurrently with anti-IgM and Bz-423. However, in lupus mice, B cells are persistently activated [235]. The efficacy of Bz-423 observed in vivo suggests Bz-423 is not required for early proximal activation signals to establish synergy. Therefore, whether Bz-423 must be present during early activation signaling in order to achieve synergy was studied. In those experiments, anti-IgM was added to Ramos cells at various times relative to Bz-423, and cell death was monitored 24 h after Bz-423 addition. Compared to 71.4% cell death induced by simultaneous anti-IgM and Bz-423 co-treatment, 94% cell death was induced when anti-IgM was applied 13.5 h before Bz-423 treatment (Figure 2.17B). A comparable amount of cell death (74%) was induced when anti-IgM was applied 1 h before Bz-423 treatment. These results indicate that the presence of Bz-423 is not necessary during early activation in the cell death induced by anti-IgM and Bz-423 cotreatment. When anti-IgM was applied at 3

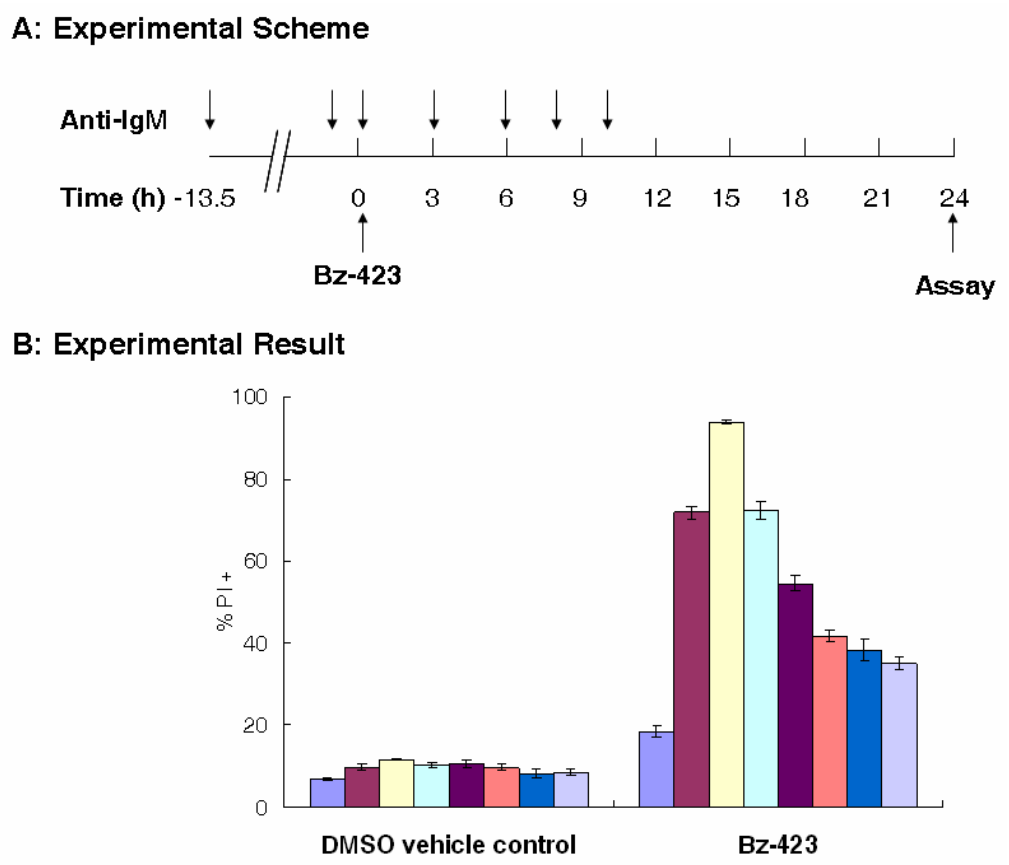

Figure 2.17: The effects of various anti-IgM additions on cell death by co-treatment. (A) The experimental scheme: anti-IgM (1 μg/mL) was added relative to Bz-423 (5 μM), as indicated as arrows. 24 h later, cell death was determined by PI exclusion. (B) The results of 24 h cell death by Bz-423 and anti-IgM treatment were shown. anti-IgM was added at 13.5 h before ( ), 1 h before( ), the same time as ( ), 3 h after ( ), 6 h( ), 8 h( ), and 10 h( ) after Bz-423 treatment. Control Ig (1 μg/mL,) was added at the same time of Bz-423 treatment. This experiment was repeated two times. The absence of an error bar indicates ≤ 1 % standard deviation

and 6 h after Bz-423 treatment, 54% and 42% cell death were induced, which is slightly less than that induced by concurrent treatment. Even applied at 8 and 10 h after Bz-423 treatment, there was still significant cell death compared to Bz-423 alone. These data indicate the existence of persistent signaling induced by Bz-423, which interacts with anti-IgM signaling to produce cell death by co-treatment. It is also very appealing to observe that even more cell death by co-treatment is induced when anti-IgM is applied 13.5 h before Bz-423 treatment because it indicated that Bz-423

kills pre-activated B cells over resting B cells.

Anti-IgM pre-stimulation sensitizes Ramos B cells to Bz-423: Considering that lupus B cells are chronically activated by self-antigen, it is significant that Bz-423 at low concentrations (≤ 5 μM in 2% FBS media) selectively kills Ramos B cells with overnight anti-IgM stimulation over Ramos B cells. To confirm this observation, a full dose response of Bz-423 in Ramos B cells with overnight anti-IgM stimulation was performed. Moreover, to determine whether continuing ligation of BCR is required during Bz-423 treatment to establish cell death by co-treatment, anti-IgM was washed and its effect on cell death by co-treatment was studied. Prior to Bz-423 treatment, Ramos cells were first stimulated with anti-IgM for 14 h in 10% FBS media. The cells were washed and resuspended in 2% FBS media with either anti-IgM (no wash) or without anti-IgM (wash). Cells were then treated with increasing amounts of Bz-423. After 24 h, cell death was measured. Independent of whether anti-IgM is washed out or not, anti-IgM overnight stimulation sensitized Ramos cells to Bz-423 compared to cells treated with isotype-control immunoglobulin (control Ig) (Figure 2.18A). These findings confirm the previous observation. The lack of difference between anti-IgM wash and no anti-IgM wash (Figure 2.18A) supports the possibility ligation of BCR by anti-IgM is no longer required once the cells are stimulated with anti-IgM for 14 h. However, a significant FITC-anti-IgM staining was observed even after extensive washes (Figure 2.18B), indicating anti-IgM binding is not successfully removed and that anti-IgM still binds to BCR. In BCR-mediated cell death in mature B cells, normally anti-IgM ligation is not enough, and crosslinking is required [150]. Different

from other mature B cells, anti-IgM ligation alone is sufficient to induced apoptosis. Therefore, the tight binding of anti-IgM to BCR in Ramos B cells might explain the phenomenon [236].

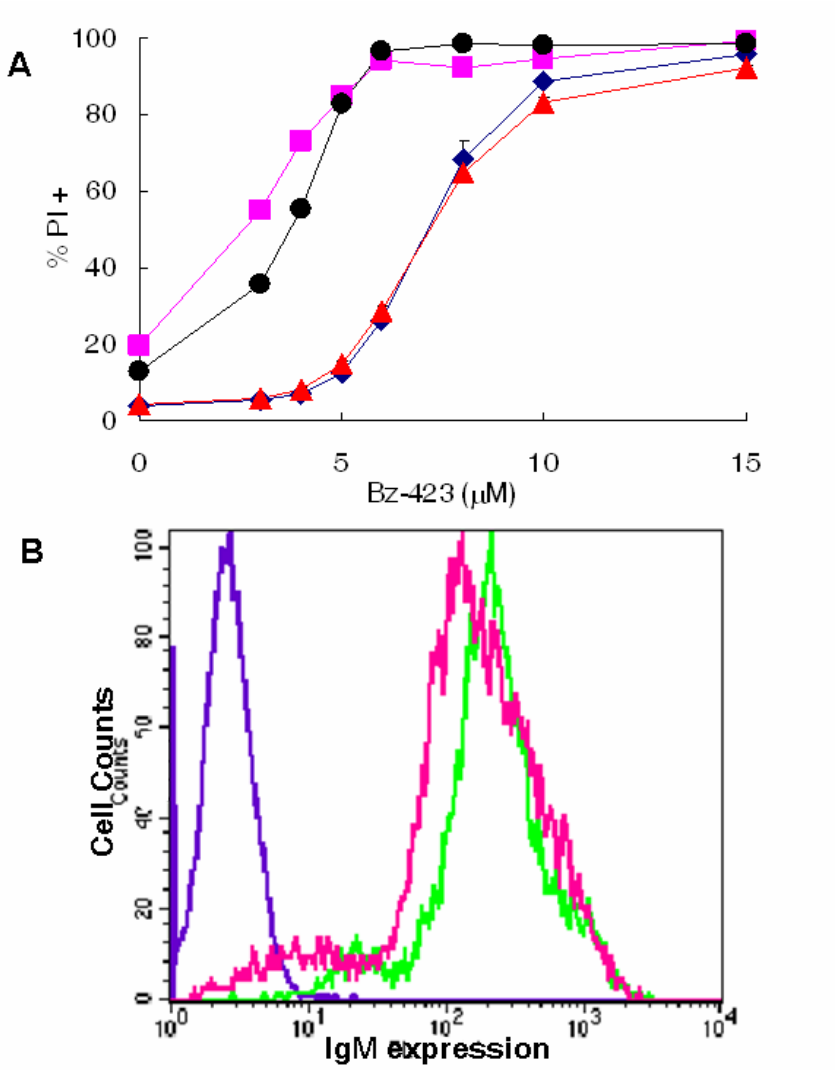

Figure 2.18: Anti-IgM overnight incubation sensitizes Ramos B cells to Bz-423 induced cell death. (A) Ramos B cells were pre-incubated with either anti-IgM (1 μg/mL) or control Ig (1 μg/mL) in media with 10% FBS for 14 h, cells were washed and resuspended in 2% FBS media with control Ig (◆) and anti-IgM (■), or without control Ig (▲) or anti-IgM (●). These cells were treated with increased amounts of Bz-423. 24 h later, the cell death was determined. (B) The effect of anti-IgM wash was evaluated by FITC-anti-IgM staining. Ramos B cells were stained with FITC-anti-IgM, washed 3 times with ice-cold PBS, and were analyzed in the flow cytometry. The histograms of purple, pink and light green are cells without staining, cells with FITC-anti-IgM staining and wash, and cells with FITC-anti-IgM staining but no wash, respectively. These experiments were repeated ≥ 2 times. The absence of an error bar indicates ≤ 1 % standard deviation.

Basic characterizations of cell death induced by anti-IgM and Bz-423 co-treatment

12 h anti-IgM and Bz-423 co-treatment is required to establish full cell death by co-treatment: As previously shown, a persistent signaling induced by Bz-423 interacts with BCR signaling to establish cell death by co-treatment. How long this persistent signaling is required to establish cell death by co-treatment was determined. The result would define the time frame to study the potential points of intersection between Bz-423 signaling and anti-IgM signaling. After co-treatment, Bz-423 was removed at indicated time points and the consequences were determined 24 h after co-treatment. As previously observed [220], cells still underwent cell death when Bz-423 was removed up to 6 h after treatment with Bz-423 alone. In contrast, 12 h of co-treatment was required to achieve comparable cell death by co-treatment to unwashed cells (Figure 2.19). Co-treatment of anti-IgM and Bz-423 produced 60% cell death, which is comparable to 62% cell death induced if Bz-423 was removed 12 h after co-treatment. This result indicates 12 h co-treatment is required to reach the "point of no-return" for cell death by co-treatment. the percentage of cell death were 13%, 28%, 45%, 53% and 62% if Bz-423 was removed at 3, 6, 9, 10.5 and 12 h after co-treatment, respectively. Only 13% cell death was induced when Bz-423 was washed away 3 h after co-treatment (Figure 2.19), indicating the early synergistic cell signaling is not sufficient to induce cell death by co-treatment. 28%, 45%, and 53% cell death were induced when Bz-423 was removed at 6, 9, and 10.5 h after co-treatment. Comparing with the background cell death (3%) and cell death induced

by anti-IgM (6%) and Bz-423 (7%) alone, co-treatment for 6-11 h induced cell death by co-treatment.

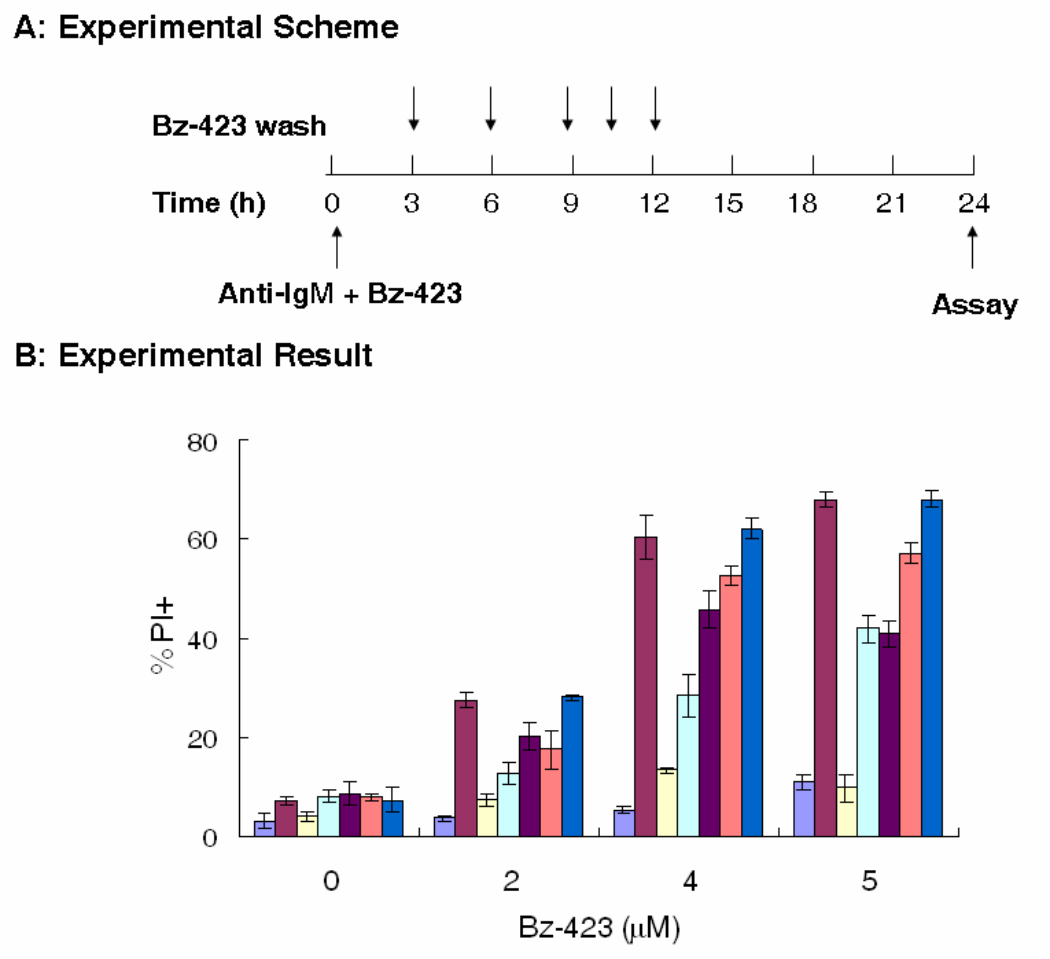

Figure 2.19: The effect of kinetic Bz-423 washout on cell death by co-treatment: (A) experimental scheme of kinetic Bz-423 washout. At indicated times after co-treatment, cells were washed and resuspended with 2% FBS media with anti-IgM (1 µg/mL). 24 h later, PI permeability was determined. The results are shown in panel B. Bz-423 was removed at 3 h ( ), 6 h( ), 9 h ( ), 10.5 h( ), and 12 h( ) after Bz-423 treatment. Control Ig (1 µg/mL,) and anti-IgM (1 µg/mL,) were added at the same time of Bz-423 treatment and no Bz-423 washout was performed. This experiment was repeated for three times. The absence of an error bar indicates ≤ 1 % standard deviation.

However, the cell death was lower than that induced by continuous co-treatment (60%). 6 h Bz-423 treatment while 12 h Bz-423 and anti-IgM co-treatment are required to reach the "points of no return", which indicates the kinetic of cell death by

co-treatment is therefore much slower than that of Bz-423 induced cell death [220]. However it is faster than that of anti-IgM induced cell death as 18 h anti-IgM stimulation is required to induce significant $\Delta\psi_m$ disruption [152]. $\Delta\psi_m$ disruption is indicative of "point of no return" in the effector phase of apoptosis [237]. This result also suggests anti-IgM and Bz-423 interacts at some points within 12 h co-treatment to amplify apoptotic signaling and reach a point of no return at 12 h co-treatment.

Cell death induced by co-treatment is kinetically different from cell death induced by Bz-423 or anti-IgM alone. Bz-423 washout experiment suggests cell death by co-treatment has a different kinetics from the cell death induced by Bz-423 or anti-IgM alone. The kinetics of cell death by co-treatment was further determined by multiple endpoints in effector phase of apoptosis. As mitochondrial membrane potential ($\Delta\psi_m$) disruption is a common feature of cell death [238], is observed during apoptosis induced by both anti-IgM stimulation [152] and Bz-423 treatment [220]. Therefore, $\Delta\psi_m$, PI permeability and subG0 DNA analysis were monitored at 8 h, 14 h, and 24 h after co-treatment. 8 h and 14 h were chosen based on previous observation that 12 h co-treatment is required to reach a point of no return for cell death by co-treatment. Two different probes 3,3'-dihexyloxacarbocyanine iodide ($DiOC_6(3)$) and tetramethylrhodamine ester (TMRM) were utilized to detect $\Delta\psi_m$ disruption [239]. There were 12-20% of live cells with low $\Delta\psi_m$ at 8 h, which was increased to 43-49% at 14 h after anti-IgM and Bz-423 co-treatment. By 24 h 63-86% of live cells had lost their $\Delta\psi_m$ (Figure 2.20). No change of $\Delta\psi_m$ was observed in live cells were treated with anti-IgM and Bz-423 alone or control Ig plus DMSO, which

indicated that $\Delta\psi_m$ is a converging point. In other words, anti-IgM and Bz-423 interacts at or upstream of $\Delta\psi_m$ disruption. Similar results were observed for cell death and apoptotic DNA.

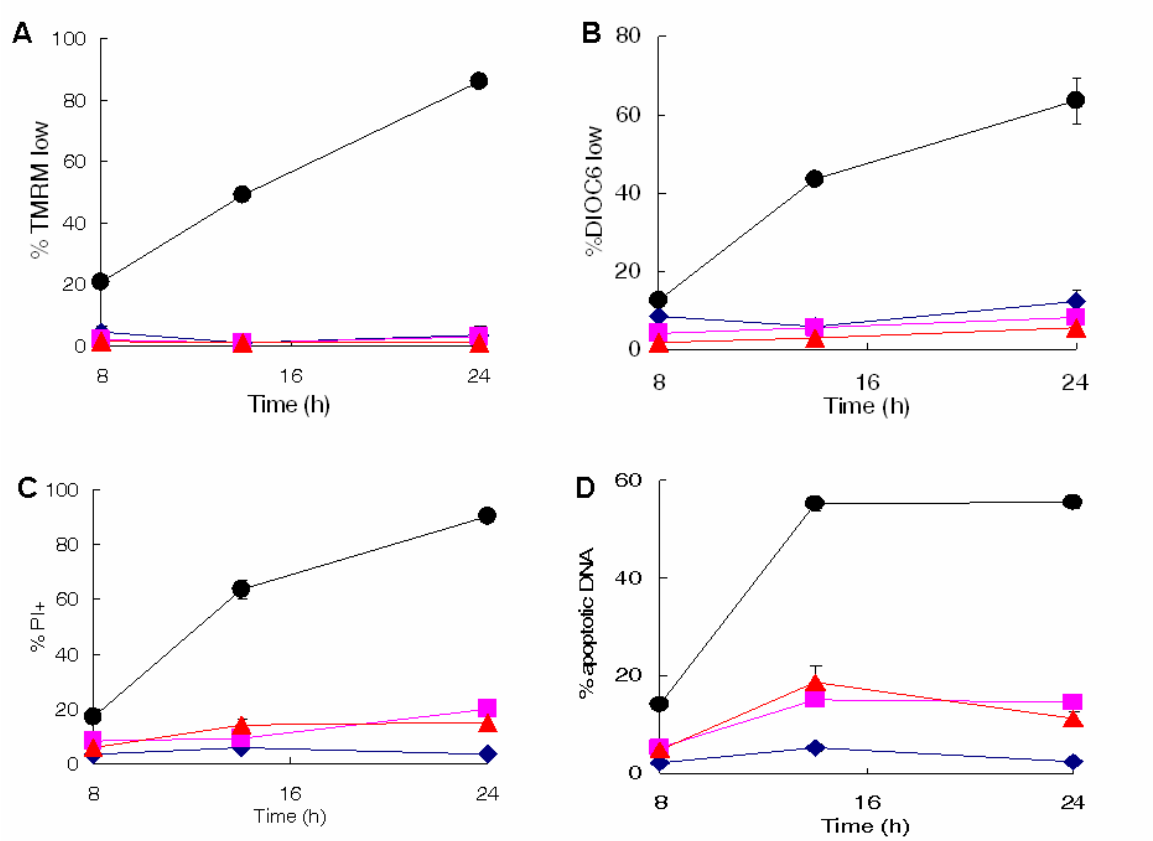

Figure 2.20: Kinetic changes of cell death by co-treatment. (A) Kinetic changes of $\Delta\psi_m$ were determined by TMRM staining. (B) Kinetic changes of $\Delta\psi_m$ were determined by DIOC6 staining. (C) Kinetics of cell death was determined by PI staining. (D) Kinetics of apoptosis was determined by subG0 analysis. The treatments were control Ig (1 µg/mL) + DMSO (◆), anti-IgM (1 µg/mL, ■), Bz-423 (5 µM, ▲), anti-IgM + Bz-423 (●). For panel A and panel B, only the live population was gated. This experiment was repeated for ≥ 2 times. The absence of an error bar indicates ≤ 1 % standard deviation.

Consistent with Bz-423 washout experiment, the kinetics of $\Delta\psi_m$ disruption and apoptotic cell death induced by anti-IgM and Bz-423 co-treatment are slower than high concentrations of Bz-423, which induces a significant $\Delta\psi_m$ disruption at 5 h, and apoptotic cell death at 8 h [217]. However, cell death by co-treatment has a relatively

faster kinetics when compared with high dose of anti-IgM, which induced $\Delta\psi_m$ disruption after 24 h and apoptotic cell death at 48 h [240]. This result confirmed that cell death by co-treatment has a slower kinetics than Bz-423 but a quicker kinetics than anti-IgM. Significant mitochondrial $\Delta\psi_m$ disruption is observed at 14 h after co-treatment, which is later than point of no return in cell death by co-treatment. $\Delta\psi_m$ disruption is not the point of no return for cell death by co-treatment but it is the converging point, where anti-IgM and Bz-423 co-treatment interact and induce a supra-additive effect.

The involvement of superoxide in cell death induced by anti-IgM and Bz-423 co-treatment

ROS is an early signal to cell death induced by co-treatment: Bz-423 binds to the oligomycin-sensitivity conferring protein (OSCP), a subunit of the mitochondrial F_0F_1-ATPase, inhibits mitochondrial F_0F_1-ATPase activity, and leads to mitochondrial hyper-permeablization (MHP), causing superoxide generation. Once above certain threshold, the superoxide signals cells to undergo apoptosis [220]. The superoxide dismutase mimetic Mn(III)tetrakis(4-Benzoic acid)porphyrin chloride (MnTBAP) and general anti-oxidant Vitamin E (VitE) inhibit cell death by co-treatment, indicating superoxide in cell death by co-treatment [221]. The superoxide produced by Bz-423 is not augmented by anti-IgM stimulation as an identical superoxide response was observed with or without anti-IgM co-stimulation [221]. Given the difference in kinetics of cell death by co-treatment compared with that of apoptosis induced by anti-IgM or Bz-423, it is possible that the timing of

superoxide production rather than its magnitude is altered under the co-tretment with anti-IgM and Bz-423. To test this hypothesis, the kinetics of superoxide production were monitored by the oxidation of dihydroethidium (DHE) to oxy-E in flow cytometry [241]. Anti-IgM stimulation failed to modulate the kinetics of superoxide induced by sub-apoptotic Bz-423 (Figure 2.21A). The

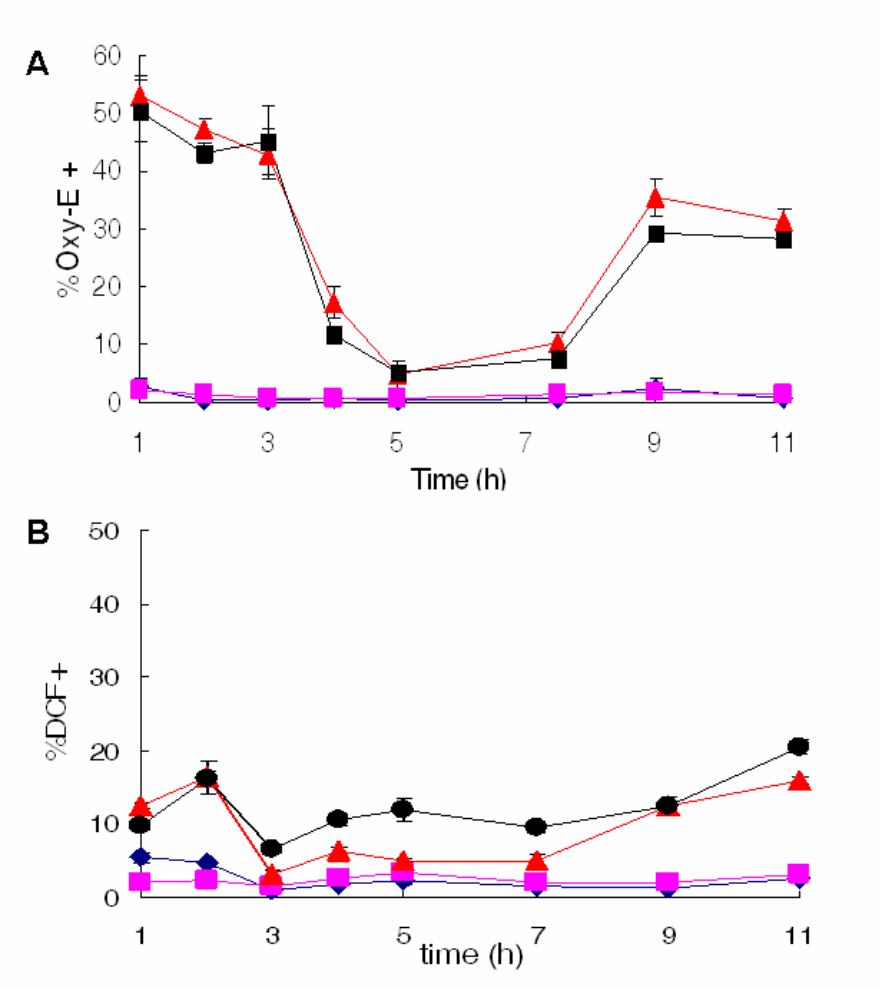

Figure 2.21: Anti-IgM co-treatment does not modulate Bz-423 induced ROS change in Ramos cells. (A) Kinetic superoxide change induced by anti-IgM and Bz-423 co-treatment was monitored by DHE assay. (B) Kinetic H_2O_2 change induced by Bz-423 induced by co-treatment was monitored by $DCFH_2$ assay. The treatments were control Ig (1 µg/mL) plus DMSO (◆), anti-IgM (1 µg/mL, ■), Bz-423 (5 µM, ▲), and anti-IgM plus Bz-423 (●). These experiments were repeated for ≥2 times. The absence of an error bar indicates ≤ 1 % standard deviation.

fluorescence intensity of oxy-E is also affected by the presence of DNA [242], and therefore an alternative dye, DCF, was used to monitor H_2O_2, the dismutation product of superoxide. Anti-IgM stimulation did not modulate the kinetics of Bz-423 induced H_2O_2 increase (Figure 2.21B). The protection of anti-oxidant against cell death by co-treatment suggests the involvement of ROS in cell death by co-treatment. However, There is no modulation of anti-IgM on Bz-423 induced reactive oxygen species (ROS) change, indicating that Bz-423 induced ROS increase acts proximally to induce cell death by co-treatment. Signals downstream of ROS will be the focus for identifying the critical mediator for the cell death by co-treatment.

Sustained superoxide increase is required to establish cell death induced by co-treatment: As shown in Figure 2.22, Bz-423 induced ROS peak at 1-3 h, decreases at 4-7 h, and peaks again at 9-11 h. Previous studies have shown that blocking Bz-423-induced ROS increase with antioxidants inhibits cell death by co-treatment. This leaves the question of which ROS peak is required for cell death by co-treatment especially in light of the slower death kinetics. Therefore, the role of Bz-423 induced ROS in cell death by co-treatment was further studied by varying the treatment time of anti-oxidants and studying their effects on cell death by co-treatment. When VitE was added 3, 6, 9 and 12 h after co-treatment, the protection against cell death by co-treatment is gradually lost (Figure 2.22). This result suggests a persistent role of ROS in establishing the cell death by co-treatment. Similar result was also observed when MnTBAP was applied.

General ROS-inducing reagents do not synergize with anti-IgM: As ROS

is required in cell death by co-treatment, it was thus brought up whether ROS increase alone is sufficient to synergize with anti-IgM stimulation and increase cell death is not known. This question was addressed by testing whether anti-IgM stimulation could sensitize Ramos B cells to other ROS producing reagents. Menadione generates ROS via redox cycling [243]. As shown in Figure 2.23, anti-IgM co-treatment only slight shifted the death response curve of menadione and H_2O_2 to the left and to the top.

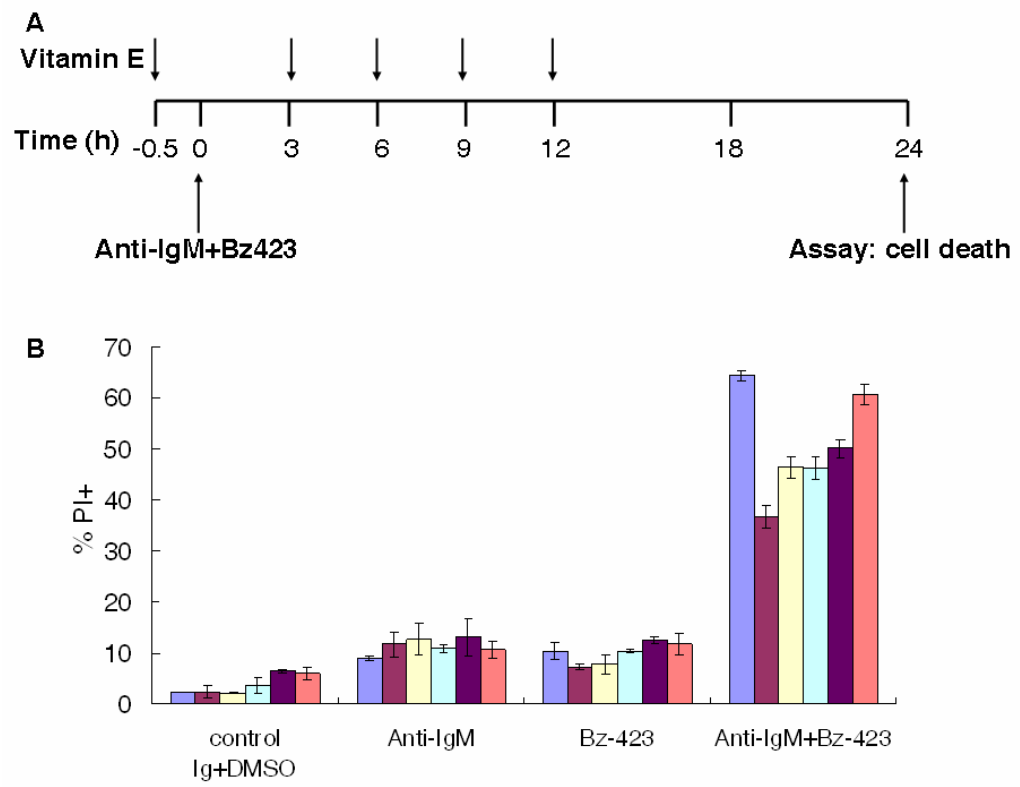

Figure 2.22: The effects of anti-oxidant Vitamin E (VitE) on cell death by co-treatment. (A) The scheme of the experimental design: At indicated time before or after the anti-IgM (1 µg/mL) and Bz-423 (5 µM) co-treatment, vitamin E (100 µM) was added. 24 h later, cell death was determined by PI permeability. The results are shown in panel B. Vitamin E was added at 30' before ( ), 3 h( ), 6 h( ), 9 h( ), and 12 h ( ) after treatment. No treatment of vitamin E was shown as This experiment was repeated for two times. The absence of an error bar indicates ≤ 1 % standard deviation.

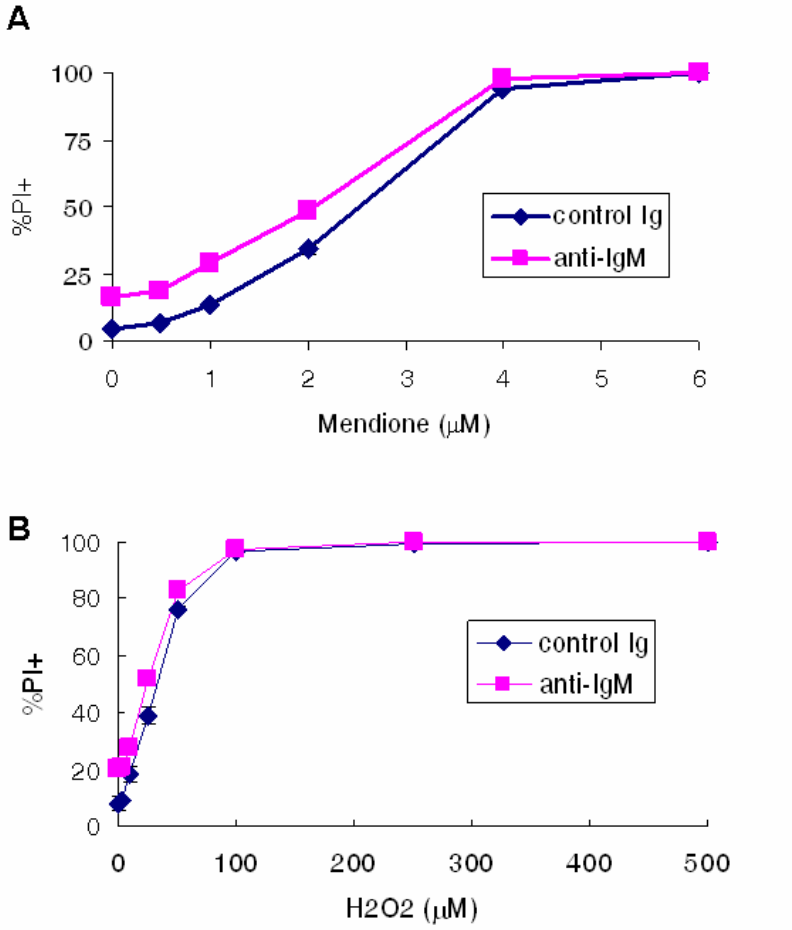

Figure 2.23: There is no synergy between anti-IgM stimulation and other ROS-inducing reagents. Ramos B cells were treated with a dose response of mendione (A) or H_2O_2 (B) in 2% FBS media. Control Ig (1 μg/mL,◆) or anti-IgM (1 μg/mL,■) was simultaneously added. 24 h later, cell death was determined through PI permeability. This experiment was at least repeated for two times. The absence of an error bar indicates ≤ 1 % standard deviation

This slightly shift was due to the cell death induced by anti-IgM. This result indicates that ROS is necessary but not sufficient to induce cell death by co-treatment with anti-IgM stimulation.

Antioxidant and an extra-cellular Ca^{2+} chelator together block cell death induced by anti-IgM and Bz-423 co-treatment: Pre-treating Ramos B cells with either antioxidant or an extra-cellular Ca^{2+} chelator 1,2-bis(2-Aminophenoxy)ethane-N,N,N',N'-tetraacetic acid, tetrapotassium salt

(BAPTA salt) partially inhibits cell death by co-treatment. It was therefore hypothesized that there were at least two independent pathways exist for cell death by co-treatment. One is possibly calcium-dependent; the other is possibly ROS-dependent. To test this hypothesis, the effect of a combination of antioxidant VitE and BAPTA salt on cell death by co-treatment was investigated. Co-treatment induced 62% cell death, which was reduced to 50%, 41% when VitE and BAPTA salt were applied alone. When VitE and BAPTA salt were added together, 18% cell death was induced (Figure 2.24). This result suggests that there were at least a ROS-dependent and calcium-dependent apoptotic pathway for cell death by co-treatment.

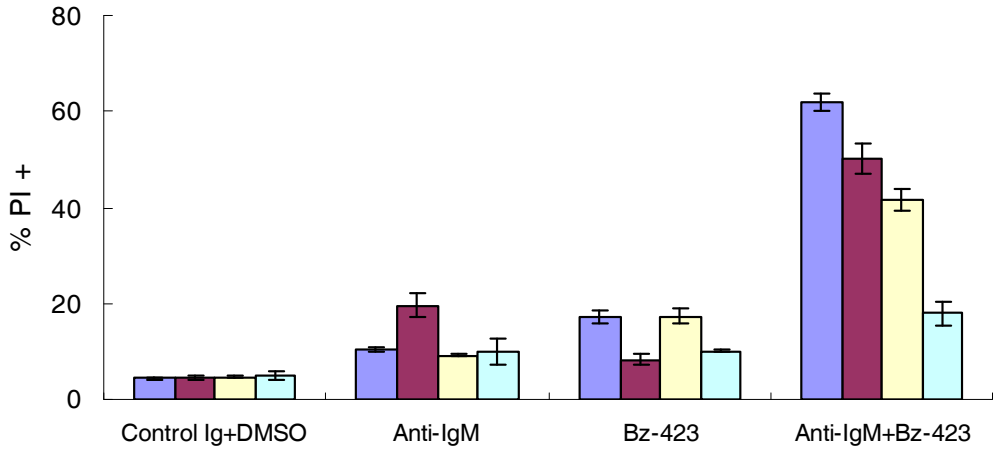

Figure 2.24: Anti-oxidant Vitamin E and extracellular Ca^{2+} chelator BAPTA salt together abolish cell death by co-treatment. Ramos B cells were pre-incubated with none (), vitamin E (100µM,), BAPTA salt (500µM,), and vitamin E plus BAPTA salt ( ) 30' before the treatment. The treatments were control Ig (1 µg/mL) plus DMSO, anti-IgM (1 µg/mL), Bz-423(5 µM), anti-IgM plus Bz-423. This experiment was repeated for two times. The absence of an error bar indicates ≤ 1 % standard deviation

Ca^{2+} involvement in the cell death by co-treatment: In the previous studies conducted in the lab, there are several pieces of evidence indicating Ca^{2+} is a critical

mediator for the cell death by co-treatment. Firstly, BAPTA salt inhibits cell death by co-treatment [221]. Secondly, Bz-423 enhanced and prolonged anti-IgM induced immediate calcium increase, indicating intracellular Ca^{2+} is a converging point. Pre-incubation of anti-oxidants inhibit this synergistic intracellular Ca^{2+} increase, indicating ROS modulate anti-IgM induced intracellular Ca^{2+} increase. As intracellular Ca^{2+} acts as second messenger to induce apoptosis [244], it is therefore hypothesized that this synergistic intracellular Ca^{2+} increase signal the apoptotic signaling pathway of cell death by co-treatment.

Early Ca^{2+} change is dispensable for cell death induced by anti-IgM and Bz-423 co-treatment: By studying the signaling pathway of BCR-induced calcium increase, Btk becomes an appealing candidate. It phosphorylates phospholipase Cγ (PLCγ) for subsequent calcium increase [245]. It is also involved in ROS-induced calcium signaling [246, 247]. It was therefore hypothesized that Btk is involved in the synergistic calcium increase induced by co-treatment. A specific Btk inhibitor LFM-A13 decreased the immediate $[Ca^{2+}]_i$ increase in response to anti-IgM stimulation or anti-IgM plus Bz-423 treatment (Figure 2.25), supporting this hypothesis. The involvement of Btk in cell death by co-treatment was further studied using LFM-A13. However, it did not inhibit cell death by co-treatment (Figure 2.25). These results suggest calcium increase, but not the immediate calcium increase upon treatment, may be involved in cell death by co-treatment. It was therefore hypothesized that early calcium increase is dispensable for the cell death by co-treatment. This hypothesis was studied by varying the addition time of BAPTA salt

and studying their effects on cell death by co-treatment. If the early synergistic Ca^{2+} change is required to induce cell death by co-treatment, addition of BAPTA salt 1 h after the co-treatment will not be able to protect against cell death by co-treatment since it does not inhibit the immediate Ca^{2+} increase. Co-treatment induced 68% cell death, which was reduced to 30%, 30%, 48% and 64% when BAPTA salt was added either 0.5 h before, 1, 6, and 12 h after co-treatment (Figure 2.26). There was comparable inhibition of synergistic

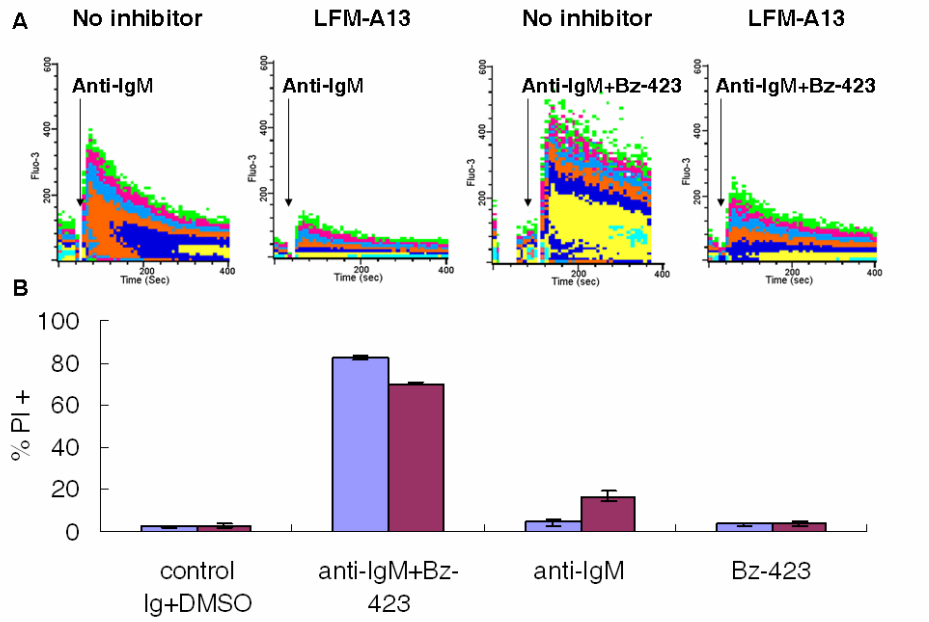

Figure 2.25: Btk inhibitor LFM-A13 inhibits anti-IgM induced calcium change but not cell death by co-treatment. (A) LFM-A13 inhibits $[Ca^{2+}]_i$ change by anti-IgM (1 µg/mL) alone and anti-IgM plus Bz-423 (5 µM). $[Ca^{2+}]_i$ change was monitored in fluo-3-loaded Ramos cells by flow cytometry. LFM-A13 (100 µM) was applied 30' before treatment. For anti-IgM plus Bz-423, fluo-3-loaded cells were first treated Bz-423 for 10', anti-IgM was added. Channels are colored according to cell density. Yellow cell number ≥50% of peak height (PH) > dark blue ≥25% PH > orange ≥12% PH > light blue ≥6% PH > pink ≥3% PH > green ≥1% PH. (B) LFM-A13 does not inhibit the cell death induced by co-treatment. Ramos B cells were pre-treated with LFM-A13 (■) or vehicle control (■) for 30 min, and then treated as indicated. 24 h later, cell death was determined by PI staining. These experiments were repeated ≥ 2 times. The absence of an error bar indicates ≤ 1 % standard deviation.

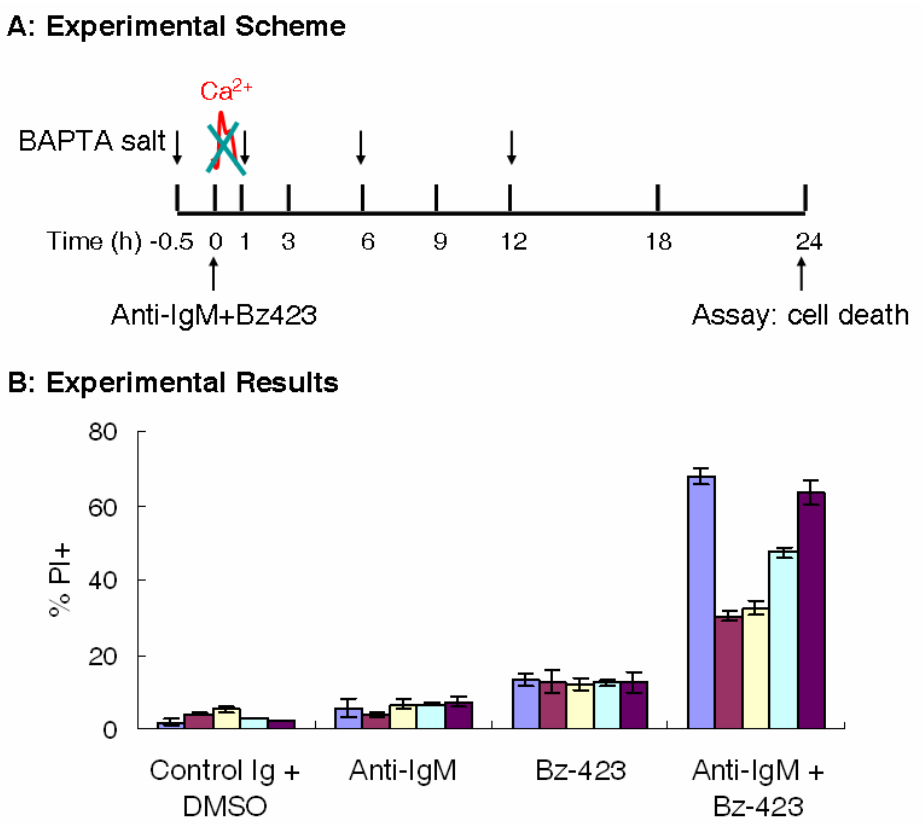

Figure 2.26: Early calcium change is dispensable for the cell death by co-treatment. (A) The scheme of this experiment. BAPTA salt (500 µM) is added at various time points of treatments. The effects of BAPTA salt are studied by determining cell death through PI permeability 24 h after the treatment. (B) The experimental results of BAPTA salt on cell death by co-treatment. BAPTA salt was added 0.5 h before (), 1 (), 6 (), 12 h () after treatment. No inhibitor was shown as . Control Ig (1 µg/mL), anti-IgM (1 µg/mL), and Bz-423 (5 µM) were used. This experiment was repeated three times. The absence of an error bar indicates ≤ 1 % standard deviation

cell death when BAPTA salt was added 0.5 h before or 1 h after treatment, showing that early Ca^{2+} increase observed within 15 min is not required for the cell death by co-treatment. The gradual loss protection by BAPTA salt suggests that calcium plays a sustained role in establishing cell death by co-treatment. This sustained Ca^{2+} change might activate several transcription factors and account for new protein synthesis required for cell death by co-treatment [248].

As the early Ca^{2+} change is dispensable for cell death by co-treatment, the

relative late Ca^{2+} change (>1 h) induced by anti-IgM and Bz-423 co-treatment was monitored. Bz-423 interferes with the background of Ca^{2+} indicators. After correcting Bz-423 background, any measurable Ca^{2+} change was not detected, although various methods (flow cytometry, plate reader, fluorometer) using different calcium indicator (Fura-2, Fura-red, Fluo-3, Indo-1) were attempted.

Ca^{2+} is sufficient to sensitize Ramos cells to Bz-423: Whether this intracellular Ca^{2+} increase is sufficient to sensitize Ramos B cells to Bz-423 was investigated. This was determined by co-treatment with Bz-423 and Ca^{2+} inducing agents, thapsigargin and ionomycin. Thapsigargin inhibits the specific sarco/endoplasmic reticulum Ca^{2+}-ATPase (SERCA) and blocks Ca^{2+} uptake by endoplasmic reticulum (ER), which causes activation of plasma membrane calcium channels allowing influx of Ca^{2+} to the cytosol [249]. Ionomycin is a non-specific ionophore that allows extracellular calcium into the cell. Both thapsigargin and ionomycin sensitized Ramos B cells to Bz-423 (Figure 2.27), indicating that a Ca^{2+} increase was sufficient to induce synergy with Bz-423. Pre-incubation with BAPTA salt abolished ionomycin induced synergy (Figure 2.27B), indicating this synergy induction was entirely caused by extracellular Ca^{2+} influx.

Anti-IgM induced Ca^{2+} increase is required for cell death induced by anti-IgM and Bz-423 co-treatment. Artificial Ca^{2+} increase by tharpsigargin or ionomycin sensitizes Ramos cells to Bz-423. To determine if the anti-IgM induced Ca^{2+} increase is responsible for sensitization of Ramos cells to Bz-423, inhibitors that specifically target anti-IgM induced Ca^{2+} change were used.

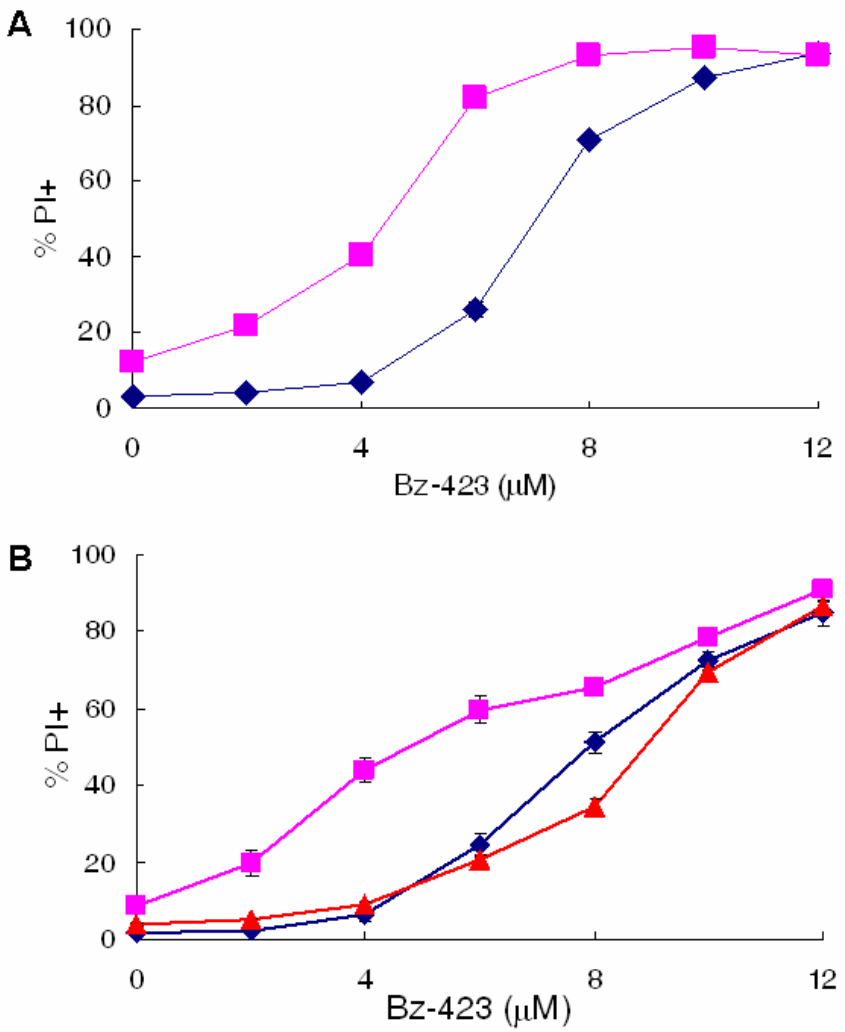

Figure 2.27: Reagents that increase $[Ca^{2+}]_i$ sensitize Ramos B cells to Bz-423. (A) SERCA inhibitor tharpsigargin synergizes with Bz-423 in cell death induction. Ramos B cells were co-treated with various concentrations of Bz-423 and tharpsigargin (5 nM,■) or its vehicle control DMSO (◆). (B) Ionophore ionomycin synergizes with Bz-423 in cell death induction. Ramos B cells were co-treated with various concentrations of Bz-423 and ionomycin (1 μM,■) or DMSO (◆). BAPTA salt (500 μM, ▲) was added 30 min before ionomycin and Bz-423 co-treatment. 24 h later, cell death was determined by PI permeability. These experiments were repeated for ≥ 2 times. The absence of an error bar indicates ≤ 1 % standard deviation

Ca^{2+} release activating Ca^{2+} channel (CRAC) is a common mechanism for cell receptor induced Ca^{2+} influx in lymphocytes [250]. A selective CRAC inhibitor YM-58483 (BTP-2) was used to study the role of Ca^{2+} influx in cell death by co-treatment [251]. YM-58483 partially inhibits cell death by co-treatment, which is

consistent with the partial protection of BAPTA salt on cell death by co-treatment (Fig 2.27A). This result confirms the observation that Ca^{2+} influx is involved in cell death by co-treatment and further suggests this Ca^{2+} influx is mediated through CRAC channel induced by co-treatment.

The PKC activator PMA decreases $[Ca^{2+}]_i$ by inhibiting phospholipase C-γ [252]. PMA is shown to ablate Ca^{2+} increase and to inhibit cell death induced by anti-IgM stimulation [253, 254]. PMA abolished anti-IgM induced cell death by co-treatment (Figure 2.26B). Its inhibition of anti-IgM induced Ca^{2+} change was also confirmed by using the Ca^{2+} sensitive dye Fura-2. Fura-2 is a ratiometric calcium indicator, the ratio of fluorescence excited at 340 nm to fluorescence excited at 380 nm (F340/F380) proportionally correlates with $[Ca^{2+}]_i$ [255]. Anti-IgM stimulation increases F340/F380, which indicates $[Ca^{2+}]_i$ increase. PMA blocks anti-IgM induced $[Ca^{2+}]_i$ increase (Figure 2.28C). In contrast, it did not affect ionomycin-induced $[Ca^{2+}]_i$ increase (Figure 2.28D). This result further supports the critical role of Ca^{2+} involvement in cell death by co-treatment.

In Summary, the protection against co-treatment-induced cell death by two additional inhibitors that suppress Ca^{2+} signaling suggested the involvement of anti-IgM induced Ca^{2+} increase in synergy.

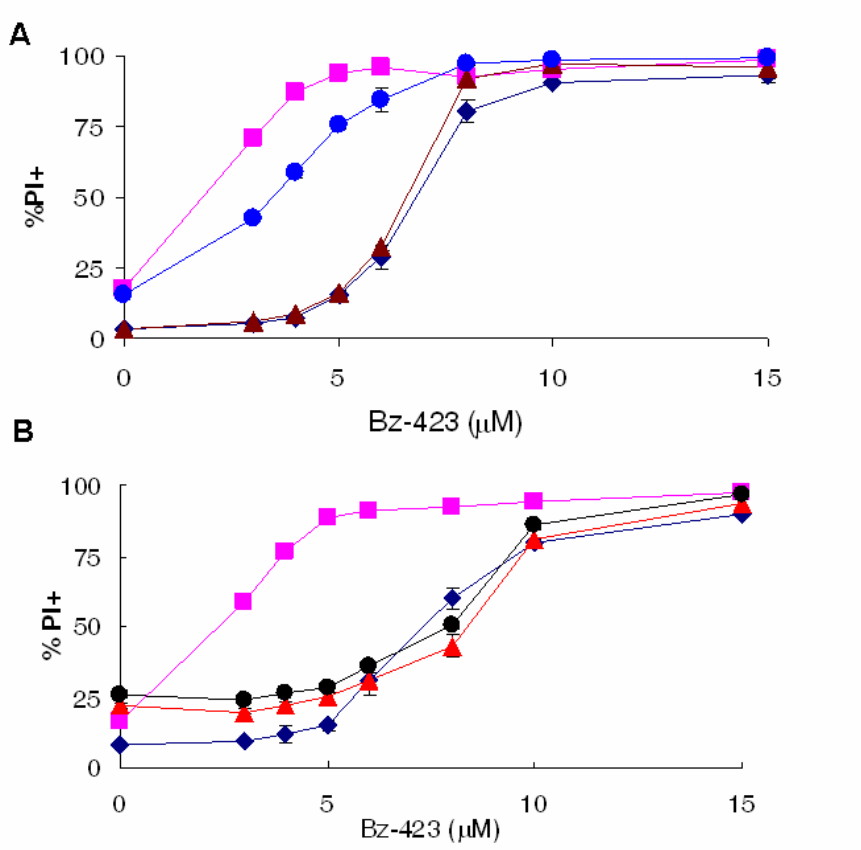
A
100
75
50
25
0
%PI+
0
5
10
15
Bz-423 (μM)
B
100
75
50
25
0
% PI+
0
5
10
15
Bz-423 (μM)

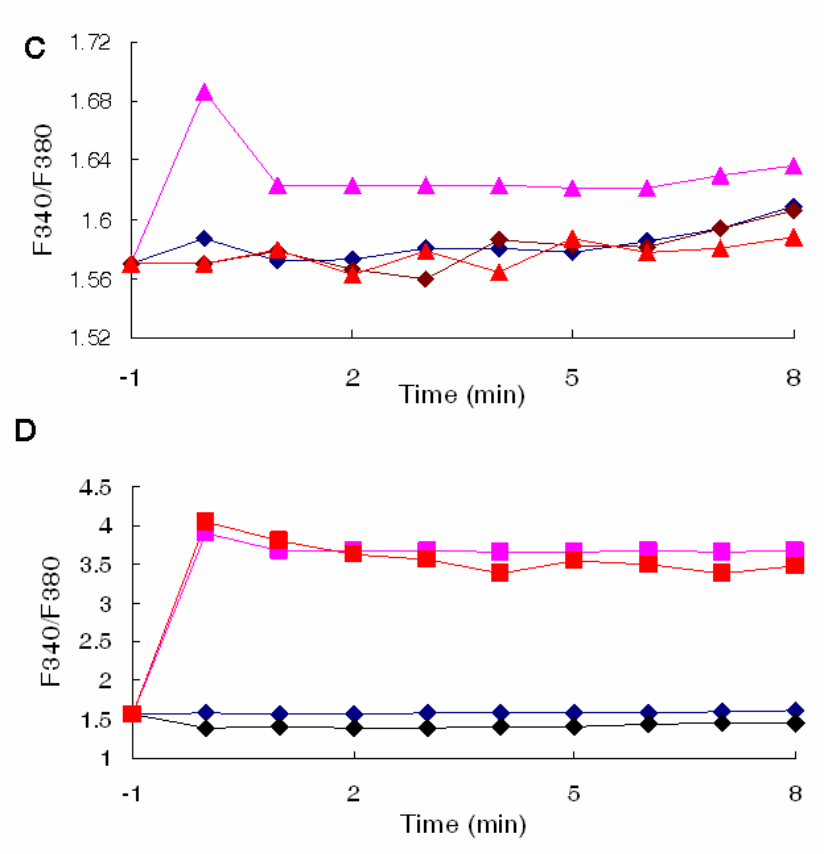
C
1.72
1.68
1.64
1.6
1.56
1.52
F340/F380
-1
2
5
8
Time (min)
D
4.5
4
3.5
3
2.5
2
1.5
1
F340/F380
-1
2
5
8
Time (min)

Figure 2.28: CRAC channel inhibitor YM-58483 and PKC activator PMA inhibited cell death by co-treatment through modulating anti-IgM induced calcium change. (A) YM-58483 (0.5 μM) inhibits anti-IgM induced synergy in Ramos B cells. (B) PMA (10 ng/mL) inhibits anti-IgM induced synergy in Ramos B cells. The legends for panel A and B are control Ig (1 μg/mL, ◆), anti-IgM (1 μg/mL, ■), YM-58483 plus control Ig (▲), YM-58483 plus anti-IgM (●), PMA plus control Ig (▲), and PMA plus anti-IgM(●). (C) PMA abolishes anti-IgM induced $[Ca^{2+}]_i$ increase. Fura-2 loaded Ramos B cells were treated with PMA (10 ng/mL) for 30 min. anti-IgM (1 μg/mL) was added and immediately the calcium change was monitored using plate reader. Increased F340/F380 indicates increased $[Ca^{2+}]_i$. (D) PMA does not affect ionomycin induced $Ca^{2+}]_i$ increase. Similar to panel C expect anti-IgM was replaced with ionomycin (0.5 μg/mL). The legends for panel C and B are control (DMSO or control Ig, ◆), anti-IgM (▲), PMA plus control Ig (◆) PMA plus anti-IgM (▲), ionomycin (■), PMA plus DMSO control (◆), PMA plus ionomycin (■).

Detailed cellular signaling pathway of cell death induced by Bz-423 and anti-IgM co-treatment

New protein is synthesized within 6 h of co-treatment to establish cell death.

Previous results have shown that the transcription inhibitor cycloheximide (CHX) blocks cell death by co-treatment, indicating that new protein synthesis is required [221]. Here, the timing of protein synthesis is investigated to determine when it occurs in the cell death pathway. CHX was added at various times relative to anti-IgM and Bz-423 co-treatment, and the effect of CHX on cell death by co-treatment was studied. If added after the completion of the necessary new protein synthesis, CHX will no longer block cell death by co-treatment. CHX failed to block cell death when added 6 h after the anti-IgM and Bz-423 co-treatment (Figure 2.29), suggesting that new protein is synthesized within 6 h. At 12 h, the apoptotic signaling reaches a point of no return, and cell death by co-treatment is therefore induced. This results further limits new protein is synthesized within 6 h of co-treatment, and anti-IgM signaling

and Bz-423 signaling must interact at the timepoints at this time range.

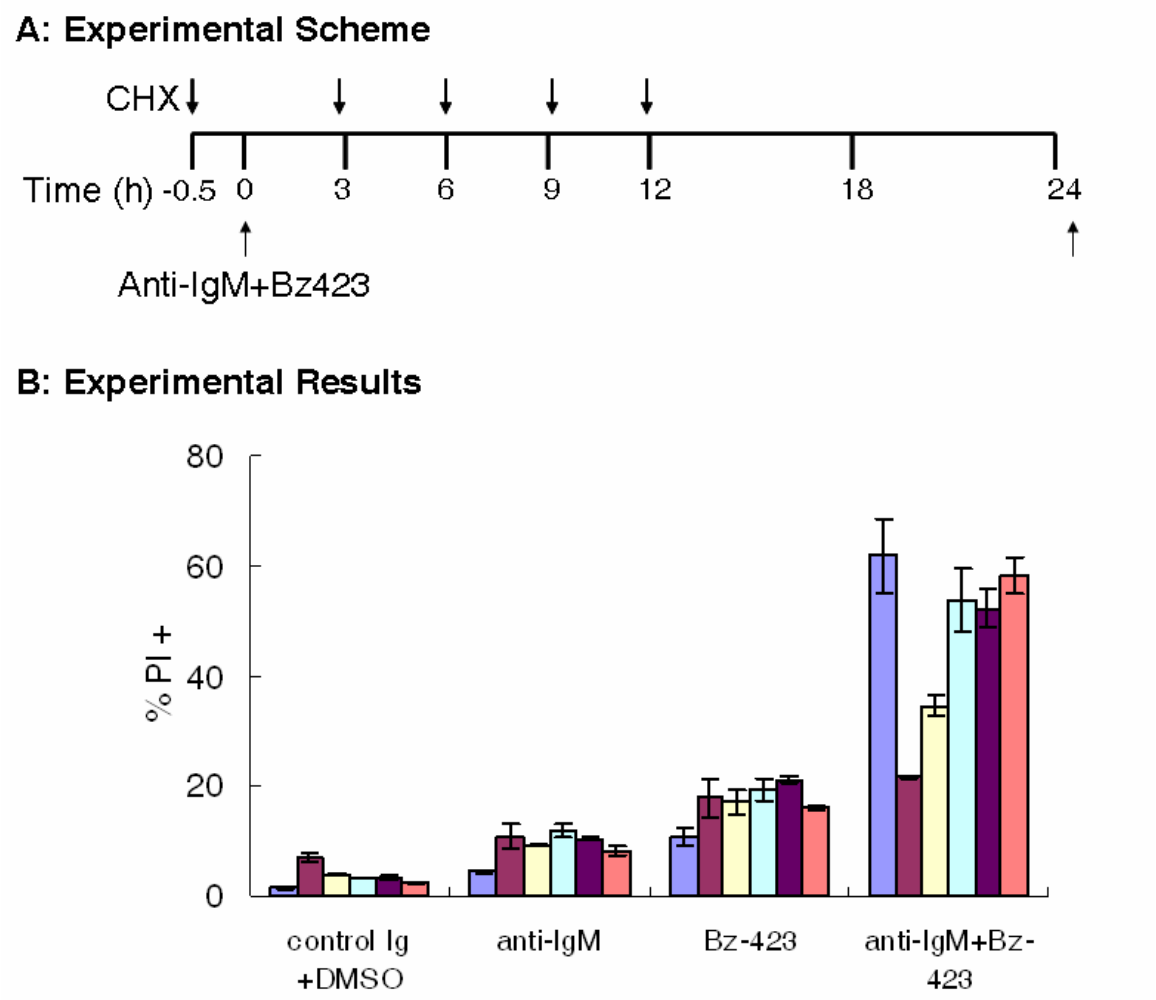

Figure 2.29: New protein is synthesized within 6 h of co-treatment to induce cell death in Ramos B cells. (A) The experimental scheme. Cycloheximide (CHX, 1 µg/mL) is added at various times relative to treatments. The effects of CHX are studied by determining cell death through PI permeability 24 h after the treatment. (B) The experimental results of CHX on cell death by co-treatment. CHX was added 0.5 h before ( ), 3 ( ), 6 ( ), 9 ( ) and 12 h ( ) after treatments. No inhibitor was shown as . Control Ig (1 µg/mL), anti-IgM (1 µg/mL), and Bz-423 (5 µM) were used. This experiment was repeated two times. The absence of an error bar indicates ≤ 1 % standard deviation

Cell death induced by co-treatment adopts mitochondria-dependent pathway: Converging point is an interaction point of two signaling pathway and it is amplified once these two signaling pathways are turned on. As previously identified, Ca^{2+} and ROS are two proximal signals to induce cell death by co-treatment, although

the early Ca^{2+} increase (<1 h) is dispensable for cell death by co-treatment. The next effort is to identify the detailed signaling pathway of synergistic apoptosis. Generally there are two pathways leading to apoptosis: the intrinsic and extrinsic pathways [256]. Mitochondria play a central role in the intrinsic pathway by sensing internal stress and releasing pro-apoptotic factors, which results in mitochondrial pro-apoptotic factors release and subsequent cell death. In the extrinsic pathway, death receptors, including Fas and TRAIL, respond to external stress signals and recruit caspases for activation, leading to cell death induction [257]. There is also cross-talk between these two pathways. Activated caspase cleaves the BH3-only protein Bid and its cleaved form tBid translocates to mitochondria, which triggers mitochondria dependent cell death [258].

The first question explored was which apoptotic pathway cell death by co-treatment adopts. As discussed previously, cell death by co-treatment requires new protein synthesis within 6 h of anti-IgM and Bz-423 co-treatment. Possible candidates for this new protein are Fas and FasL, which are involved in elimination of autoreactive B cells [259]. It was therefore hypothesized that synergistic treatment increases Fas or FasL expression, which results in the cell death by co-treatment. This hypothesis was tested by studying Fas and FasL expression levels induced by anti-IgM and Bz-423 co-treatment. Ramos B cells express both Fas and FasL on the cell surface as there are Fas and FasL staining over the background (Figure 2.30A). PMA plus ionomycin, which are known to cause increased Fas expression [260], induced 2.2-fold increase in the mean fluorescence intensity (MFI) of Fas surface

expression and 1.5-fold increase in MFI of FasL surface expression. In contrast, co-treatment does not modulate the MFI of Fas surface expression or MFI of FasL surface expression (Figure 2.30B). This result suggests that Fas and FasL increases are not required for cell death by co-treatment, suggesting that the extrinsic pathway is not used. This result is consistent with the observation that Fas is not responsible for B cell receptor (BCR)-mediated apoptosis [236].

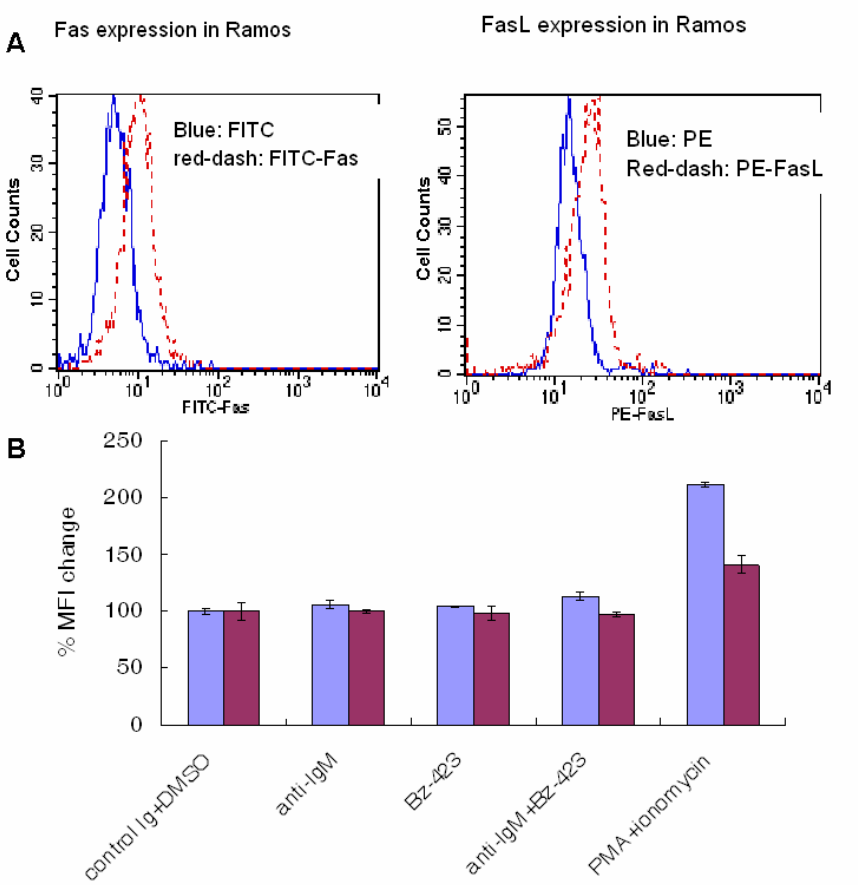

Figure 2.30: Fas and FasL expression changes induced by anti-IgM and Bz-423 co-treatment in Ramos B cells. (A) Fas and FasL are expressed in Ramos B cells. The histogram in solid line is the result from staining with isotype control antibody. The histogram in the dashed line is the result from staining with FITC-anti-Fas or PE-anti-FasL. (B) There is no change in the expression of Fas (▮) and FasL (▮) induced by co-treatment. Ramos B cells were treated with control Ig (1 µg/mL), anti-IgM (1 µg/mL) and Bz-423 (5 µM) for 8 h before staining with anti-Fas and anti-FasL. PMA (50 ng/mL) and ionomycin (1 µg/mL) were used as a positive control. This experiment was repeated for two times. The absence of an error bar indicates ≤ 1 % standard deviation.

Mitochondrial pro-apoptotic factors are released by co-treatment: The observation of $\Delta\psi_m$ disruption indicates the malfunction of mitochondria induced by co-treatment. Mitochondria are involved in apoptosis mediated both by BCR and by Bz-423 [175, 220]. Therefore, it was hypothesized that cell death by co-treatment adopts mitochondria-dependent pathway. This hypothesis was first studied by investigating pro-apoptotic factor release, such as cytochrome c, AIF, and Smac, from mitochondria induced by co-treatment. Cytochrome c binds to apaf-1 to form the apoptosome which activates caspase 9 and further apoptotic signaling. Smac binds to inhibitor of apoptosis protein (IAP) and assists in caspase activation. AIF is itself involved in caspase-independent nuclear DNA degradation [256]. Anti-IgM or Bz-423 alone did not increase cytochrome c signal in the cytosol fraction, or decrease cytochrome c signal in the mitochondria fraction, indicating they do not cause the release of cytochrome c from mitochondria to the cytosol (Figure 2.31A). Co-treatment induced significant cytochrome c increase in the cytosol at 8 h, which is correlated with significant decrease in the mitochondria (Figure 2.31A). Other mitochondrial pro-apoptotic factors AIF and Smac were also released into the cytosol (Figure 2.31B). This result indicates that mitochondria sense the apoptotic signaling induced by anti-IgM and Bz-423 then release pro-apoptotic factors. Moreover, single treatment does not induce cytochrome c release while the co-treatment does, indicating cytochrome is a converging point. This result indicates that Bz-423 signaling and BCR signaling interact at or upstream of mitochondria to induce cell death by co-treatment.

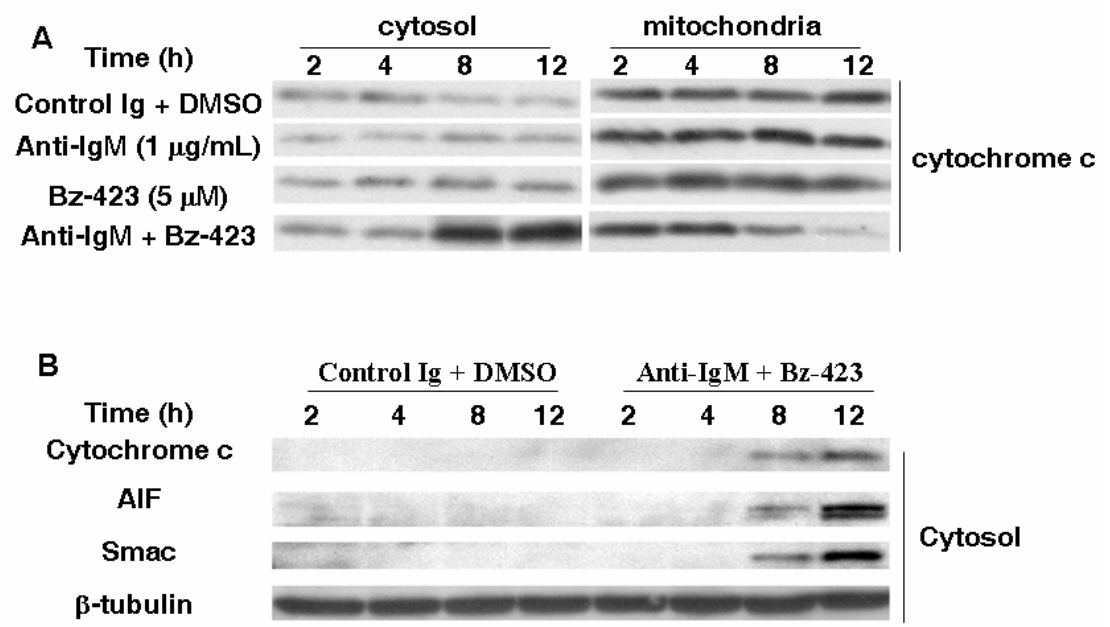

Figure 2.31: Pro-apoptotic factors release from mitochondria by Bz-423 and anti-IgM co-treatment in Ramos B cells. In A, mitochondria were isolated by passing the treated swollen B cells through needles. In B, separation of cytosol and organelles were done by digitonin permeablization. This experiment was at least repeated for four times.

The mechanism of synergistic pro-apoptotic factor release was studied using reagents shown to inhibit cell death by co-treatment. The inhibition of mitochondria pro-apoptotic factor release suggests that this specific signal acts at or upstream of mitochondria. Otherwise the signal acts downstream of mitochondria. Pre-treatment with VitE, BAPTA salt, and cycloheximide all inhibited the cytochrome c, Smac and AIF release (Figure 2.32). This demonstrates ROS, Ca^{2+}, and new protein synthesis occur at or upstream of mitochondrial pro-apoptotic factor release. Additionally, pan-caspase inhibitor z-VAD-fmk did not inhibit cytochrome c release at 8 h but it did attenuate cytochrome c release at 12 h. The caspase inhibitor only prevented only the late but not the early stage of cytochrome c release indicating that there is an amplification loop between cytochrome c release and activated caspase [261].

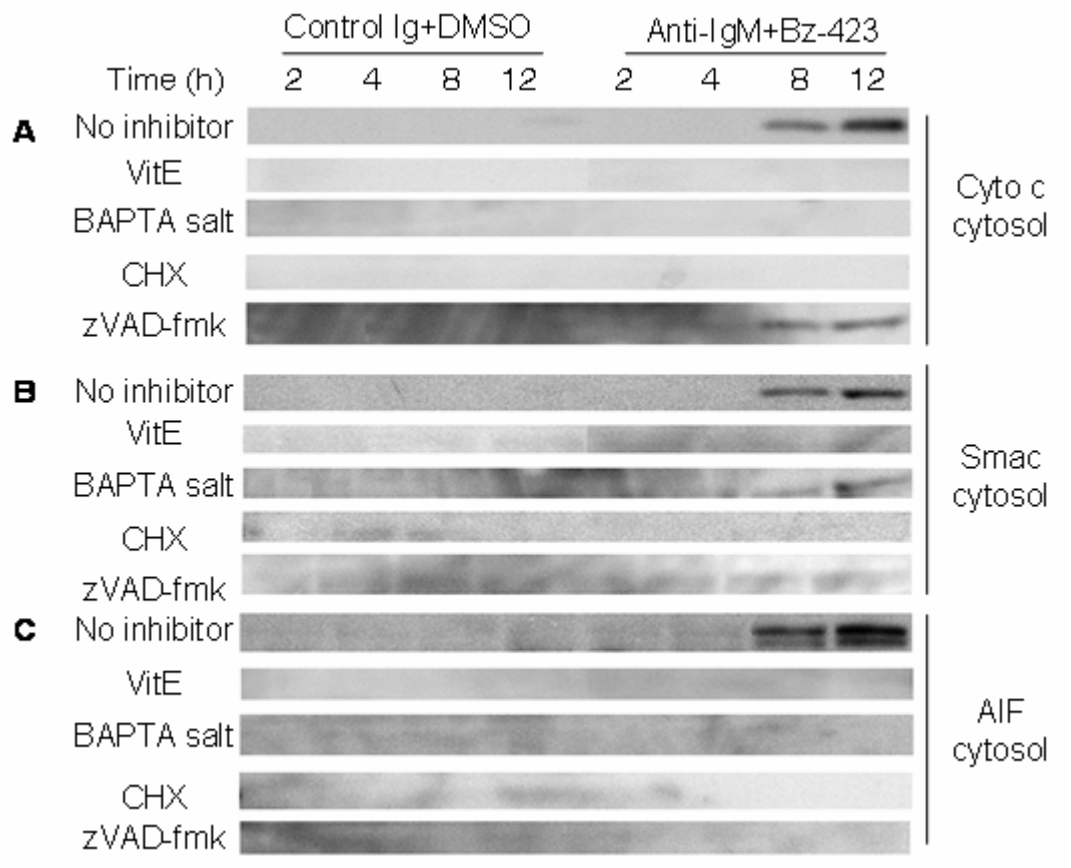

Figure 2.32: Inhibitors on mitochondrial pro-apoptotic factors release induced by anti-IgM and Bz-423 co-treatment in Ramos B cells. Ramos B cells were pre-treated with VitE (100 μM), BAPTA salt (500 μM), and CHX (1 μg/mL), and zVAD-fmk (100 μM) for 30' before treatment. At indicated times, cytosol fractions were obtained and the immunoblots were probed with specific antibodies. The treatments were control Ig (1 μg/mL) + DMSO, anti-IgM (1 μg/mL) + Bz-423 (5 μM). (A) The inhibitors on cytochrome c release induced by co-treatment. (B) The inhibitors on Smac release induced by co-treatment. (C) The inhibitors on AIF release induced by co-treatment. This experiment was repeated three times.

z-VAD-fmk did abolish Smac and AIF release, indicating that caspase activation acts upstream of Smac and AIF release (Figure 2.32). These results indicate slightly different release mechanism of these pro-apoptotic factors from mitochondria. This result is consistent with the observation that 12 h of co-treatment is required for cell death by co-treatment. Cytochrome c release act upstream of initial caspase activation. This observation not only suggests that cytochrome c may be the most critical factors

in the cell death by co-treatment, it also argues against the possible involvement of extrinsic pathway, in which caspases are initial triggers for apoptosis.

Bax and Bak are activated by anti-IgM and Bz-423 co-treatment. How ROS, Ca^{2+}, and protein synthesis act together to induce cytochrome c release induced by co-treatment was examined. There are two ways to release cytochrome c: mitochondrial permeability transition (MPT) and mitochondrial outer membrane permeablization (MOMP). As ROS and Ca^{2+} are well-established inducer for MPT [29], it was therefore hypothesized that co-treatment triggers the opening of MPT, which triggers the cell death by co-treatment. This hypothesis was studied by studying the effect of a specific MPT inhibitor bongkrekic acid on the cell death by co-treatment. Bongkrekic acid did not inhibit cell death by co-treatment, which supports that MPT is not involved in the cell death by co-treatment (Figure 2.33). The opening of MPT leads to $\Delta\psi_m$ disruption with subsequent OMM rupture and cytochrome c release [30]. $\Delta\psi_m$ disruption occurs either before cytochrome c release or at the same time. At 8 h, co-treatment induces a significant cytochrome c release while there was minimal $\Delta\psi_m$ disruption, indicating that the inner mitochondrial membrane is still intact. This result suggests that cytochrome c release occurs before $\Delta\psi_m$ disruption, which further supports that MPT is not involved in cell death by co-treatment.

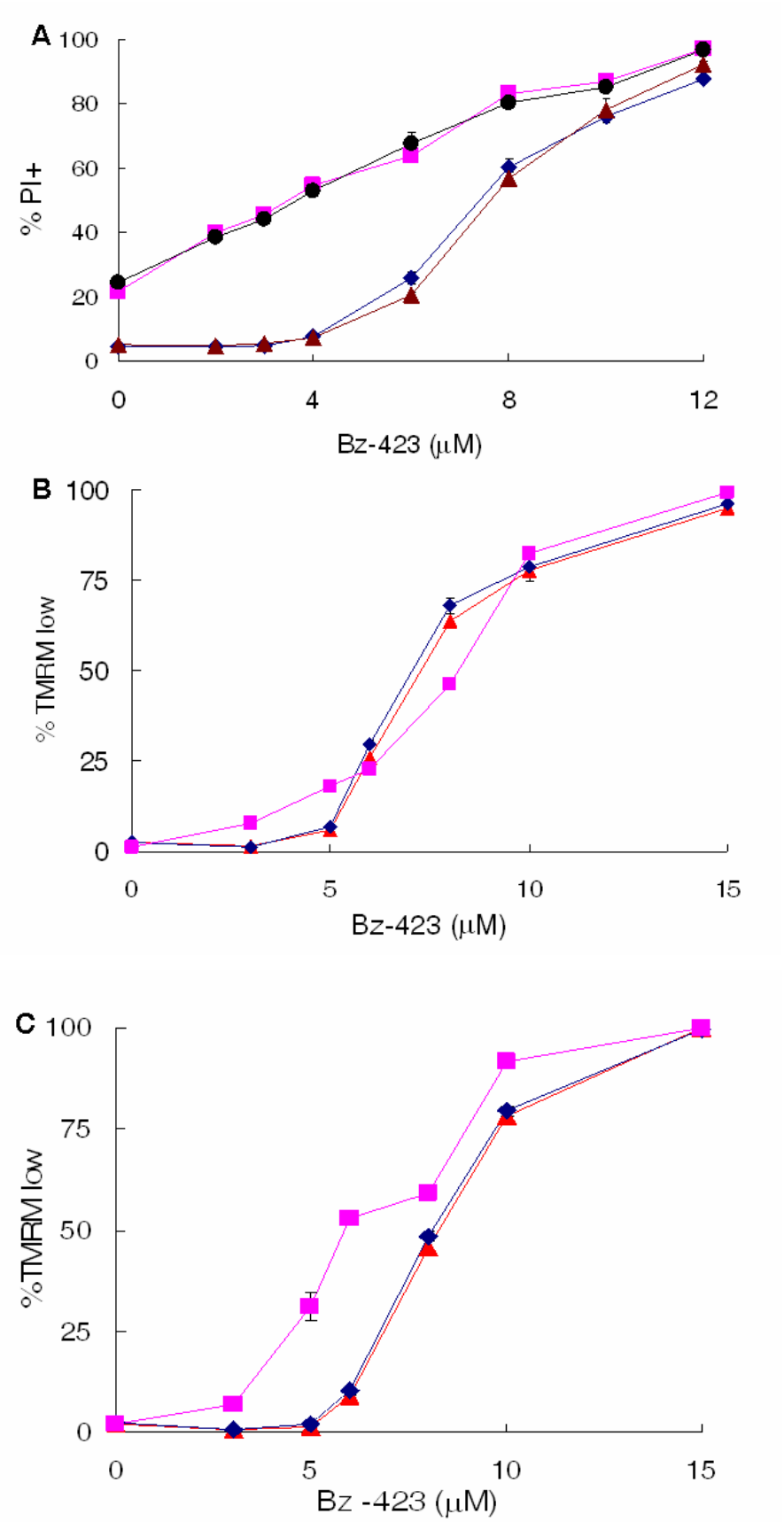
A
100
80
60
40
20
0
% PI+
0
4
8
12
Bz-423 (μM)
B
100
75
50
25
0
% TMRM low
0
5
10
15
Bz-423 (μM)
C
100
75
50
25
0
%TMRM low
0
5
10
15
Bz -423 (μM)

Figure 2.33: MPT is not involved in cell death by co-treatment. (A) Bongkrekic acid (BA) does not inhibit cell death by co-treatment. Ramos B cells were pre-treated with a specific ANT inhibitor BA (60 μM) for 30', and then co-treated with anti-IgM and increasing amount of Bz-423. Cell death was determined 24 h after the treatment. The treatments were control Ig (1 μg/mL, ◆), anti-IgM (1 μg/mL, ■), BA + control Ig (▲), and BA + anti-IgM (●). (B) $\Delta\psi_m$ changes at 8 h. (C) $\Delta\psi_m$ changes at 15 h. Ramos B cells were treated with series concentration of Bz-423 in the presence of none (▲), control Ig (◆), and anti-IgM (■). At 8 or 15 h, $\Delta\psi_m$ was measured by TMRM staining. These experiments were repeated ≥ 2 times.

On the other hand, cytochrome c release with an intact $\Delta\psi_m$ suggests the possible involvement of MOMP in cell death by co-treatment. Pro-apoptotic Bcl-2 proteins Bax and Bak are known to be involved in both Bz-423 induced cell death [220] and BCR stimulation-induced cell death [262]. Actived Bax and Bak undergo homo-oligomerization to form proteolipid pores, which allows cytochrome c release but not $\Delta\psi_m$ disruption [263]. It was therefore hypothesized that co-treatment activates Bax and Bak, which are responsible for the cytochrome c release and subsequent cell death. To test this hypothesis, Bax and Bak activation induced by anti-IgM and Bz-423 co-treatment were studied using antibodies that recognize only the activated forms of Bax and Bak [264]. Since cytochrome c release was detected at 8 h, the Bax and Bak activation were studied at both 6 h and 8 h after co-treatment. At 8 h, only 2% Bax and 1.5% Bak were activated under control treatment. Bz-423 alone induced 9% Bax activation and 10% Bak activation. Anti-IgM alone induced 6% Bax activation and 8% Bak activation. Co-treatment induced 37% Bax activation and 27% Bak activation (Figure 2.34). Similar results were also observed at 6 h. It is concluded that co-treatment induces a higher Bax and Bak activation than single treatment. This Bax and Bak activation suggests that Bz-423 signaling and BCR signaling interact at

or upstream of Bax and Bak to induce cell death by co-treatment.

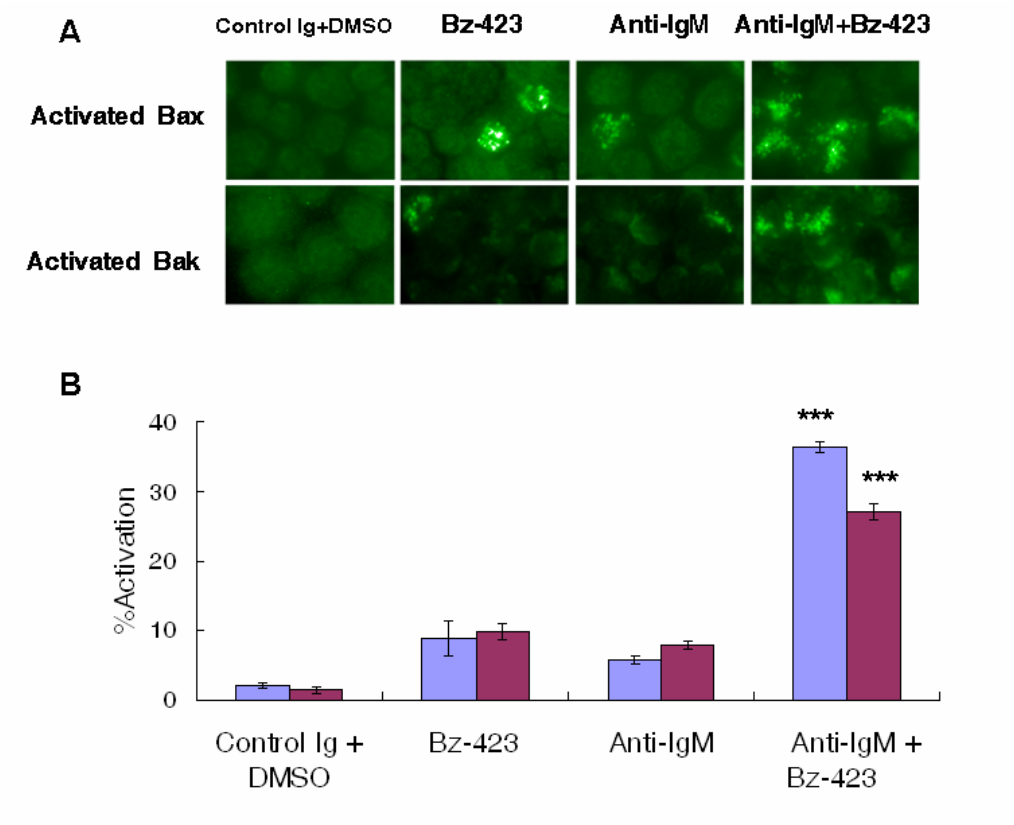

Figure 2.34: Bax and Bak activation by co-treatment. Ramos B cells were treated with either Bz-423 (5 μM), anti-IgM (1 μg/mL) alone or combined in 2% FBS media. After 8 h treatment, cells were fixed and stained with antibodies detecting activated form of Bax or Bak, respectively. (A) The representative immunofluorescence pictures of Bax and Bak activation were shown. (B) The percentages of activated Bax (■) and Bak (■) in treated Ramos cells were counted and the results were shown. This experiment was repeated ≥3 times.

As Bax and Bak are synergistically activated by co-treatment, it was hypothesized that the Bax and Bak activation induced by co-treatment leads to cytochrome c release and apoptosis. The involvement of Bax and Bak activation in cell death by co-treatment was studied using two methods: RNAi knockdown of Bax and/or Bak, and overexpression of the anti-apoptotic protein Bcl-2 or Bcl-xL. The inhibition of cell death by co-treatment will indicate the involvement of Bax and Bak

activation under synergistic condition. Introduction of interfering RNAs specific for Bax and/or Bak resulted in about 70% to 80% reduction in Bax and Bak protein levels (Figure 2.35A). Co-treatement induced 60% cell death, which was reduced to 36% and 42% cell death if either Bax or Bak were decreased, respectively. In cells with double Bax and Bak RNAi knockdown, the cell death was reduced to 25% (Figure 2.35A). Further protection by double Bax and Bak RNAis knockdown indicates that both Bax and Bak are involved in the cell death by co-treatment. The involvement of Bax and Bak was also confirmed using Bcl-2 and Bcl-xL overexpression. Bcl-2 and Bcl-xL exert their anti-apoptotic function through binding to Bax and Bak and preventing their activation [265]. Overexpression of Bcl-2 or Bcl-xL in stably transfected Ramos cells was confirmed by western blot (Figure 2.35B). Both Ramos B cells with Bcl-2 or Bcl-xL overexpression were resistant to anti-IgM and Bz-423 co-treatment (Figure 2.35B), confirming that Bax and Bak activations are critical for cell death by co-treatment. How Bcl-2 or Bcl-xL inhibits cell death by co-treatment was investigated by studying the effects of Bcl-2 or Bcl-xL overexpression on $\Delta\psi_m$ disruption, pro-apoptotic mitochondrial factor release, Bax and Bak activation induced by co-treatment. Bcl-2 overexpression and Bcl-xL overexpression inhibited $\Delta\psi_m$ disruption, mitochondrial pro-apoptotic factors release (cytochrome c and Smac), and Bax and Bak activation induced by co-treatment (Figure 2.36). These results indicate that Bcl-2 and Bcl-xL overexpression block cell death by co-treatment through inhibiting Bax and Bak activation and subsequent cytochrome c release and $\Delta\psi_m$ disruption. So how Bax and Bak are activated by anti-IgM and Bz-423

co-treatment becomes the next question to explore.

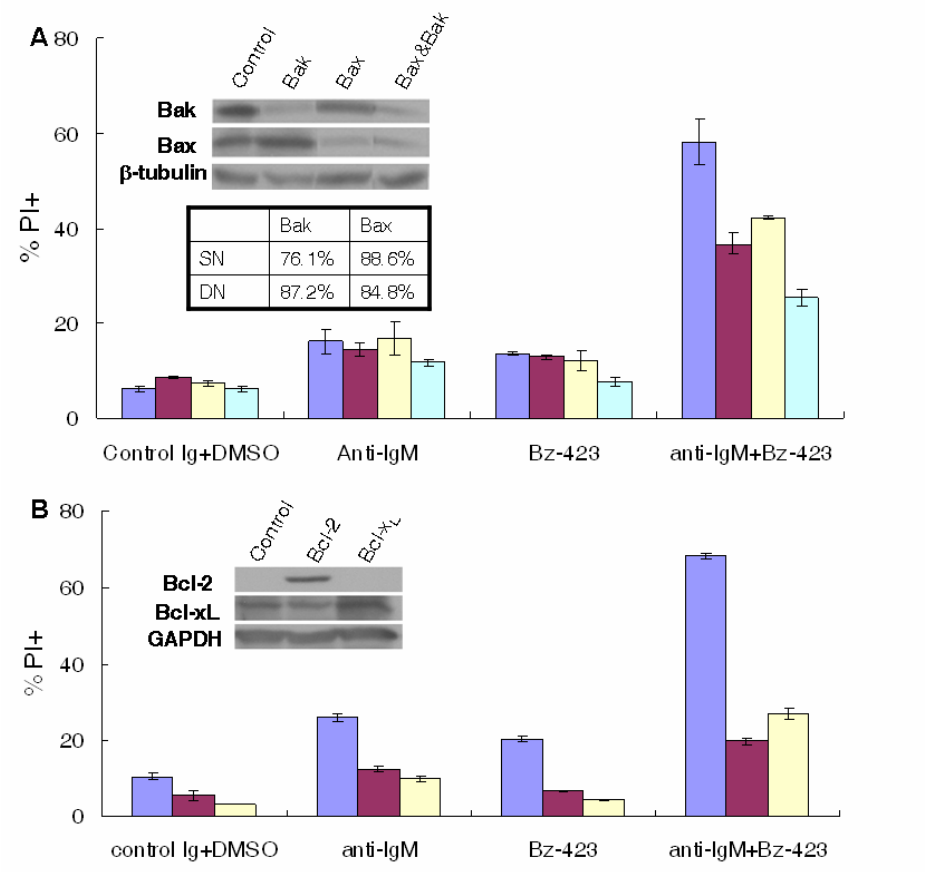

Figure 2.35: Bax and Bak are involved in cell death by co-treatment. (A) The effect of Bax and/or Bak RNAi knockdown on cell death by co-treatment induced by co-treatment. Ramos B cells were transiently transfected with negative control RNAi ( ), Bax RNAi ( ), Bak RNAi ( ) or combined ( ). Introduction of Bax and/or Bak RNAi results in ~80% decrease in the protein levels. The cell death was determined 24 h after treatment. (B) The effect of Bcl-2 and Bcl-xL overexpression on cell death by co-treatment induced by co-treatment. The overexpression of Bcl-2 and Bcl-xL was confirmed by western blot. Ramos B cells with stable transfection of pSFFV-control ( ), pSFFV-Bcl-2 ( ) and pSFFV-Bcl-xL ( ) were treated and cell death was determined by PI permeability 24 h later. Control Ig (1 µg/mL), anti-IgM (1 µg/mL) and Bz-423 (5 µM) were used. This experiment was repeated ≥ 2 times.

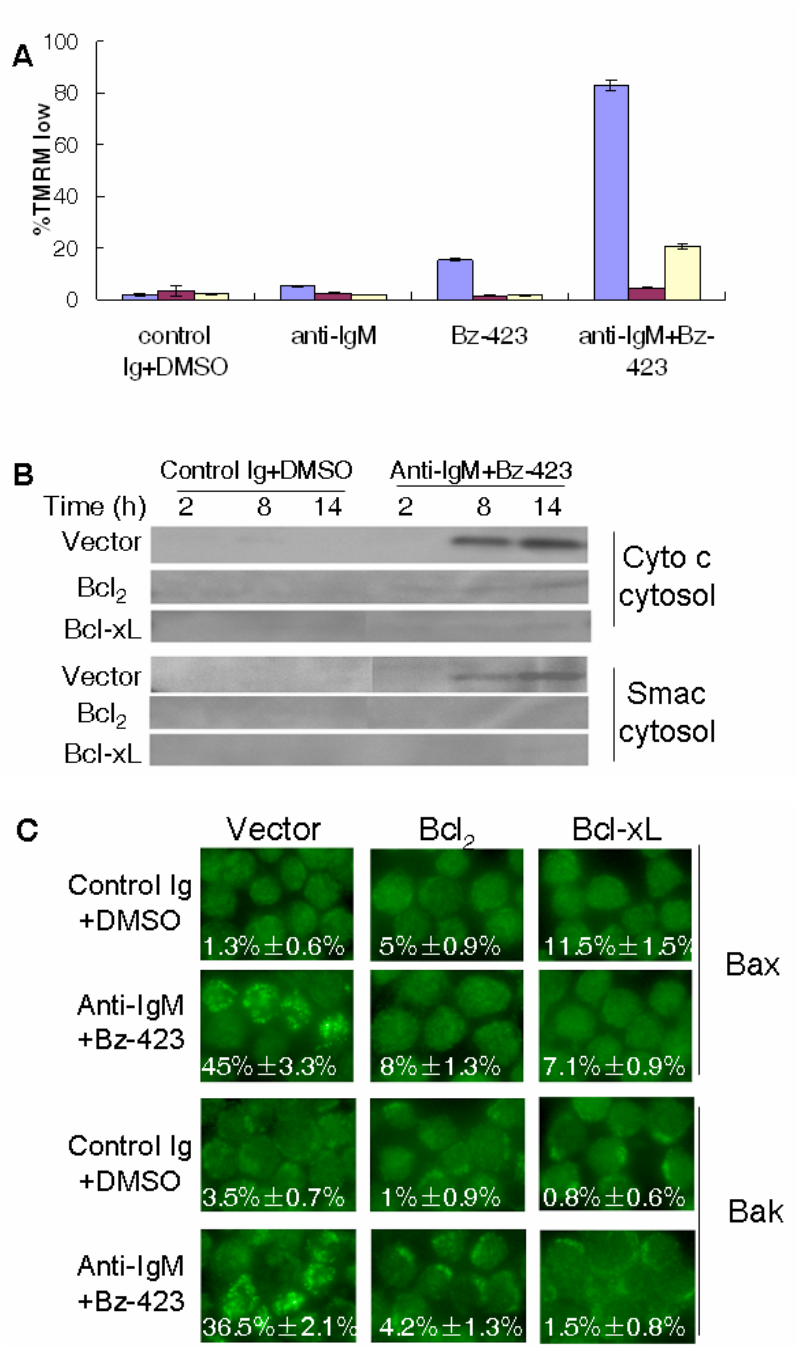

Figure 2.36: Bcl-2 and Bcl-xL overexpression on $\Delta\psi_m$ disruption, MOMP, and Bax and Bak activation by co-treatment in Ramos B cells. (A) Bcl-2 and Bcl-xL overexpression inhibit $\Delta\psi_m$ disruption induced by co-treatment. Ramos B cells with stably transfected with pSFFV-control ( ), pSFFV-Bcl-2 ( ) and pSFFV-Bcl-xL ( ) were treated and $\Delta\psi_m$ was measured at 18 h by TMRM. (B) Bcl-2 and Bcl-xL overexpression inhibit mitochondrial proapoptotic factors (cytochrome c and Smac) release induced by anti-IgM and Bz-423 co-treatment. (C) Bcl-2 and Bcl-xL overexpression inhibit Bax and Bak activation induced by co-treatment. The representative immunofluorescence of Bax and Bak activation, along with the percentage of activated Bax and Bak were shown. This experiment was repeated two times.

How Bax and Bak induced by anti-IgM and Bz-423 co-treatment are activated is was studied using inhibitor experiments. The inhibition of Bax and Bak activation suggests that this specific signal acts at or upstream of Bax and Bak. Otherwise the signal acts downstream of Bax and Bak. 36% of Bax was activated by co-treatment, which was reduced to 11%, 13%, 12% and 7% by MnTBAP, BAPTA salt, transcription inhibitor actinomycin D and translation inhibitor cycloheximide (Figure 2.37A). Similar results were also observed in Bak activation (Figure 2.37B).

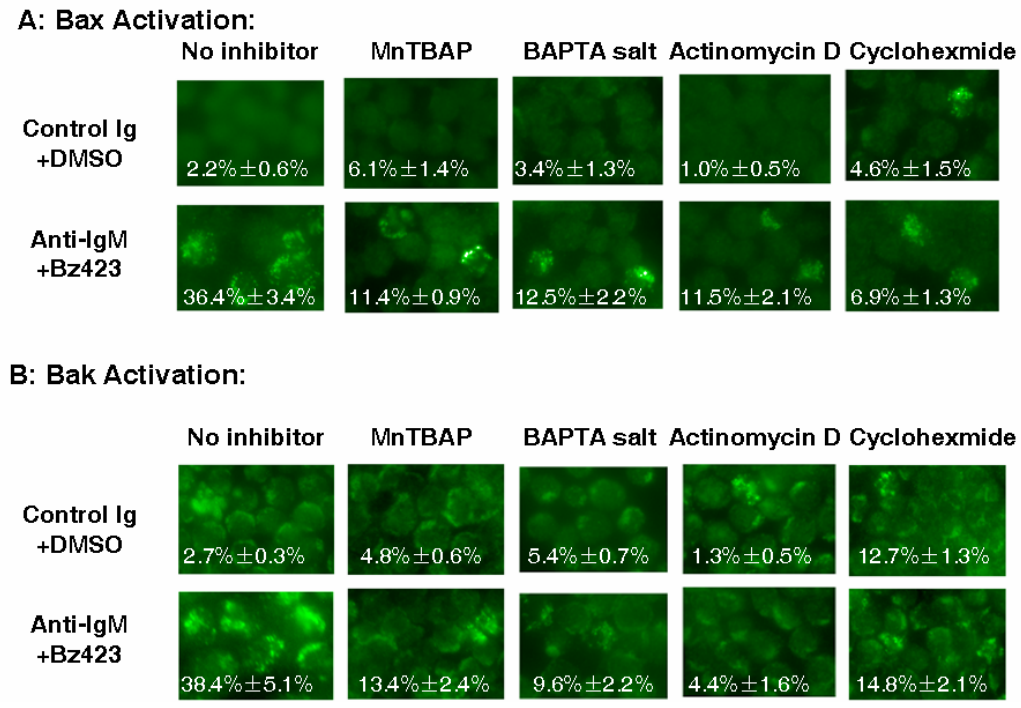

Figure 2.37: ROS, Ca^{2+}, and macromolecular synthesis are involved in Bax and Bak activations induced by co-treatment. (A) Inhibitors on Bax activation. (B) Inhibitors on Bak activation. The treatments were control Ig (1 μg/mL) + DMSO, anti-IgM (1 μg/mL) + Bz-423 (5 μM) in 2% FBS media. At 8 h, cells were fixed and Bax and Bak activation were measured by immunofluorescence. The percentages of activated Bax and activated Bak were indicated. MnTBAP (100 μM), BAPTA salt (500 μM), Actinomycin D (20 ng/mL), and cycloheximide (1 μg/mL) were added 30' before the treatment. This experiment was repeated three times.

These findings indicate ROS, calcium, and macromolecule synthesis all act upstream of Bax and Bak activations.

Co-treatment increases the expression level of Bim_S, Bmf and tBid. How ROS, Ca^{2+}, and macromolecular synthesis induce Bax and Bak activation by anti-IgM and Bz-423 co-treatment were studied. Bcl-2-like proteins (A1, MCl-1, Bcl-2 and Bcl-xL) can bind to Bax and Bak and directly inhibit Bax and Bak. They also can bind to BH3-only proteins and indirectly inhibit Bax and Bak [266]. Conversely, BH3-only proteins can activate Bax and Bak by interacting with Bax and Bak or by binding to Bcl-2-like proteins [266]. Bax and Bak can be activated by increasing the expression level of pro-apoptotic Bcl-2 protein (Bax, Bak, Bok and BH3-only proteins) or by decreasing the expression level of Bcl-2-like proteins. It was therefore hypothesized that co-treatment modulates the expression level of Bcl-2 family proteins, which are responsible for the cell death by co-treatment. The expression levels of these Bcl-2 proteins induced by anti-IgM and Bz-423 co-treatment were monitored. Bcl-2 was not included because Bcl-2 is undetectable in Ramos cells. There were no expression levels of anti-apoptotic A1, MCl-1, Bcl-xL and pro-apoptotic Bax, Bak, Bok (Figure 2.38), indicating that Bax and Bak induced by co-treatment are not activated through directly modulating the protein level of these multi-BH-domain Bcl-2 proteins.

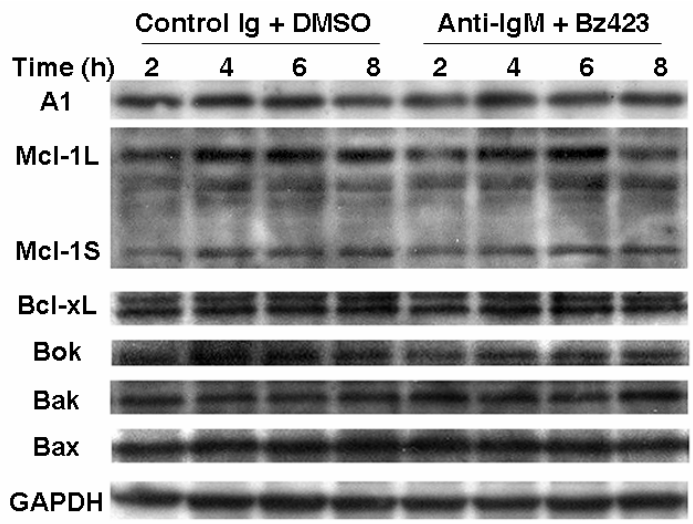

Figure 2.38: There are no expression level changes of Bcl-2-like proteins and Bax-like proteins induced by co-treatment. Ramos B cells were treated with control Ig (1 μg/mL) + DMSO, anti-IgM (1 μg/mL) + Bz-423 (5 μM) in 2% FBS. At indicated times, cell lysates were obtained, and immunoblots were probed with specific antibodies. This experiment was repeated two times.

The involvement of BH3-only proteins in Bax and Bak activation was studied by screening the expression level changes of BH3-only proteins by anti-IgM and Bz-423 co-treatment. Here the expression level of eight BH3-only proteins (Bad, Bmf, Bid, Bik, Bim, Puma, Noxa, Hrk) induced by co-treatment were studied. Among these eight proteins, co-treatment increased Bim_S by 3-fold at 4 h and by 6-fold at 6 h (Figure 2.39). And it increased Bmf by 1.5-fold at 2 h and by 2.1-fold at 4 h (Figure 2.39). As Bz-423 alone and anti-IgM alone did not increase Bim_S, Bmf, and tBid, it is concluded that co-treatment induced a synergistic increase in these BH3-only proteins. This result suggests Bim_S, Bmf, and tBid are critical mediators for Bax and Bak activation. Especially Bim-knockout mice develop lupus-like diseases [267], and there is a disturbance of B cell homeostasis in Bmf-knockout mice [268]. For further confirmation the involvement of these BH3-only proteins in cell death by co-treatment could be done using the RNAi knockdown of Bim and Bmf. In response

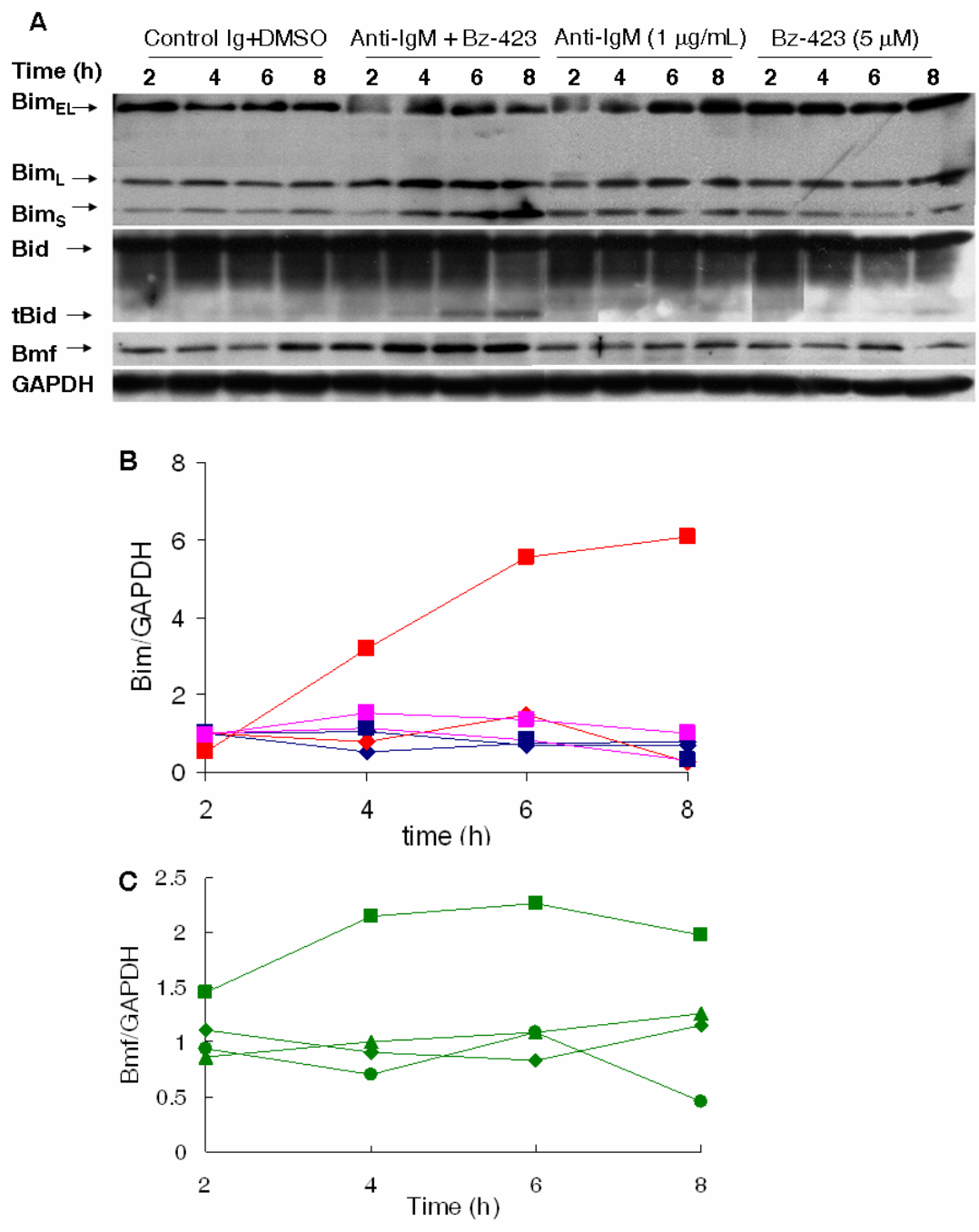

Figure 2.39: BH3-only protein changes by co-treatment in Ramos B cells. (A) The expression level of Bim_{EL}, Bim_L, and Bim_S, Bid cleavage to tBid, and Bmf changes induced by anti-IgM and Bz-423 co-treatment. (B) The quantitive expression level changes of three Bim isoforms by co-treatment. Control Ig + DMSO (◆) anti-IgM +Bz-423 (■).Bim_{EL}, Bim_L and Bim_S are in blue, magenta, red. (C) The quantitative expression level changes of Bmf. The treatments were control Ig (1 μg/mL) plus DMSO (◆), anti-IgM (1 μg/mL, ▲), Bz-423 (5 μM,●) and anti-IgM plus Bz-423 (■). At indicated times, cell lysates were obtained and the immunoblots were probed with specific antibodies. This experiment was repeated three times.

to BCR stimulation and ionomycin, Bim expression is increased [169]. This Bim increase is important for BCR-mediated apoptosis as the Bim-deficient cells are resistant to BCR ligation [169]. Calcineurin inhibitor cyclosporine A or FK506 blocks Bim up-regulation in response to TCR stimulation, suggesting the possible involvement of calcineurin in Bim increase. Therefore it is hypothesized that calcineurin is involved in cell death by co-treatment.

The involvement of calcineurin in cell death induced by Bz-423 and anti-IgM co-treatment

Calcineurin is involved in cell death induced by co-treatment: Calcineurin is a serine/threonine phosphatase, which is activated by cytosolic Ca^{2+} increases. Calcineurin is as a multifunctional regulator of diverse cellular function and is involved in multiple processes. The immunosuppressant drugs FK506 and cyclosporine A (CsA) inhibit calcineurin activity and subsequent T cell activation. This inhibition requires the binding of CsA to cyclohphilins and the binding of FK506 to FK506 binding protein (FKBP) [269]. The protection of FK506 and CsA against cell death indicated calcineurin involvement in cell death signaling [270]. It was therefore hypothesized that calcineurin is involved in cell death by anti-IgM and Bz-423 co-treatment. This hypothesis was tested by studying the effect of FK506 on cell death by co-treatment. FK506 partially inhibited cell death by co-treatment (Figure 2.40A), similar to the effect of BAPTA salt, which inhibits Ca^{2+} influx and acts upstream of calcineurin. Moreover, the inhibition by the nanomolar concentration of FK506 is consistent IC_{50} of FK506 for calcineurin, which is 2 nM [271]. These

results suggest that FK506 inhibits cell death by co-treatment through inhibition of calcineurin activity. To confirm this, an excess rapamycin, which binds tightly to FKBP, was used to compete with FK506. As binding of FK506 to FKBP is required for inhibition of calcineurin activity [269], to limit the availability of FKBP for FK506 binding is supposed to inhibit the effect of FK506 [272]. Before FK506 treatment, excess rapamycin was pre-incubated with cells, limiting the availability of FKBP to FK506. The inhibition by FK506 on cell death by co-treatment was reversed by excess rapamycin (Figure 2.40B), indicating the inhibition of cell death by FK506 is due to binding to FK506 binding protein (FKBP).

How calcineurin is involved in cell death by co-treatment was also investigated by studying the effects of FK506 on cytochrome c release, and Bax and Bak activation. FK506 attenuated cytochrome c, AIF and Smac release induced by anti-IgM and Bz-423 co-treatment (Figure 2.40C). Co-treatment induced 31.4% Bax activation and 36.5% Bak activation, respectively, which was decreased to 4.9% and 4.6%, respectively by FK506 pre-treatment (Figure 2.40D). All these results suggest that calcineurin acts upstream of Bax and Bak activation to induce cell death by co-treatment. Therefore, calcineurin leads to Bax and Bak activation, possibly via increasing Bim_S expression, which in turn causes MOMP, caspase activation and subsequent cell death.

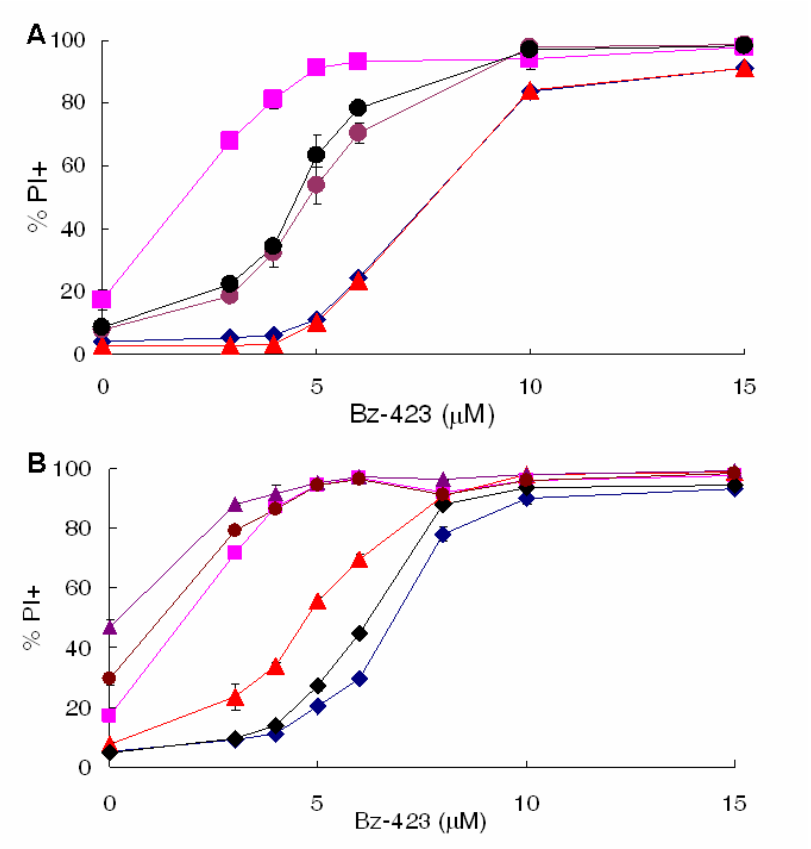
A
100
80
60
40
20
0
% PI+
0
5
10
15
Bz-423 (μM)
B
100
80
60
40
20
0
% PI+
0
5
10
15
Bz-423 (μM)

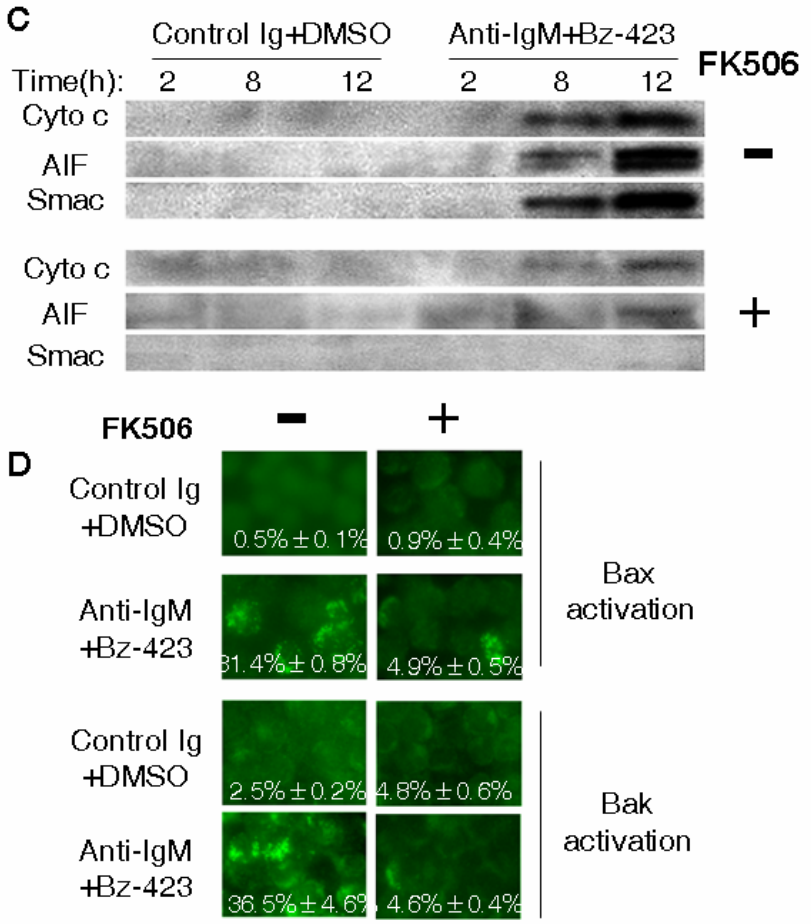
C
Control Ig+DMSO
Anti-IgM+Bz-423
FK506
Time(h):
2
8
12
2
8
12
Cyto c
AIF
Smac
-
Cyto c
AIF
Smac
+
D
FK506
-
+
Control Ig
+DMSO
0.5%±0.1%
0.9%±0.4%
Anti-IgM
+Bz-423
31.4%±0.8%
4.9%±0.5%
Bax
activation
Control Ig
+DMSO
2.5%±0.2%
4.8%±0.6%
Anti-IgM
+Bz-423
36.5%±4.6%
4.6%±0.4%
Bak
activation

Figure 2.40: Calcineurin inhibitor FK506 inhibits Bax & Bak activation, MOMP and cell death by co-treatment. (A) FK506 inhibits cell death by co-treatment. Ramos B cells were treated with series concentration of Bz-423 in presence of control Ig (1 µg/mL, ◆), anti-IgM (1 µg/mL, ■), control Ig plus FK506 (1 µM, ▲), anti-IgM plus FK506 (1 nM, ●), anti-IgM plus FK506 (1 µM, ●) for 24 h. Cell death was determined by PI permeability. (B) Rapamycin antagonizes the inhibition of FK506 against cell death by co-treatment. Ramos B cells were pre-treated with rapamycin (50 µM) for 30', were then treated with FK506 (1 nM) for 30' before Bz-423 treatment, The treatments were control Ig (1 µg/mL, ◆), anti-IgM (1 µg/mL, ■), anti-IgM plus FK506 (1 nM, ▲), control Ig plus rapamycin (50 µM, ◆), anti-IgM plus rapamycin (50 µM, ▲), and anti-IgM plus FK506 plus rapamycin (●). (C) FK506 inhibits pro-apoptotic factors release (cyto c, AIF, Smac) induced by anti-IgM and Bz-423 co-treatment. Treated cells were fractionated into cytosol and mitochondria. The cytosol fraction was monitored by western blot. (D) FK506 inhibits Bax and Bak activation induced by co-treatment. Activated Bax and Bak were monitored by immunofluorescence. On the bottom of the reprehensive pictures, the % cells with activated Bax and Bak were indicated. These experiments were repeated ≥ 2 times.

Calcineurin inhibitors FK506 and cyclosporine A (CsA) are also potent inhibitors of the MAPK signaling pathway [273]. Therefore, the effects of these inhibitors on cell death by co-treatment could be due to inhibiting either the Ca^{2+}-calcineurin pathway or the MAPK signaling. To exclude the possibility that MAPK pathway is involved in cell death by co-treatment, the MAP kinases p38 and JNK were investigated. The p38 inhibitor SB203580, SB202190 and JNK inhibitor II were used to test their effects on cell death by co-treatment. Pre-treatment with either p38 inhibitors (Figure 2.41A) or JNK inhibitor II (Figure 2.41B) did not affect the cell death by anti-IgM and Bz-423 co-treatment. These results suggested FK506 and CsA inhibited cell death induced by co-treatment through blocking the Ca^{2+}-calcineurin pathway, and not through inhibiting MAPK pathway.

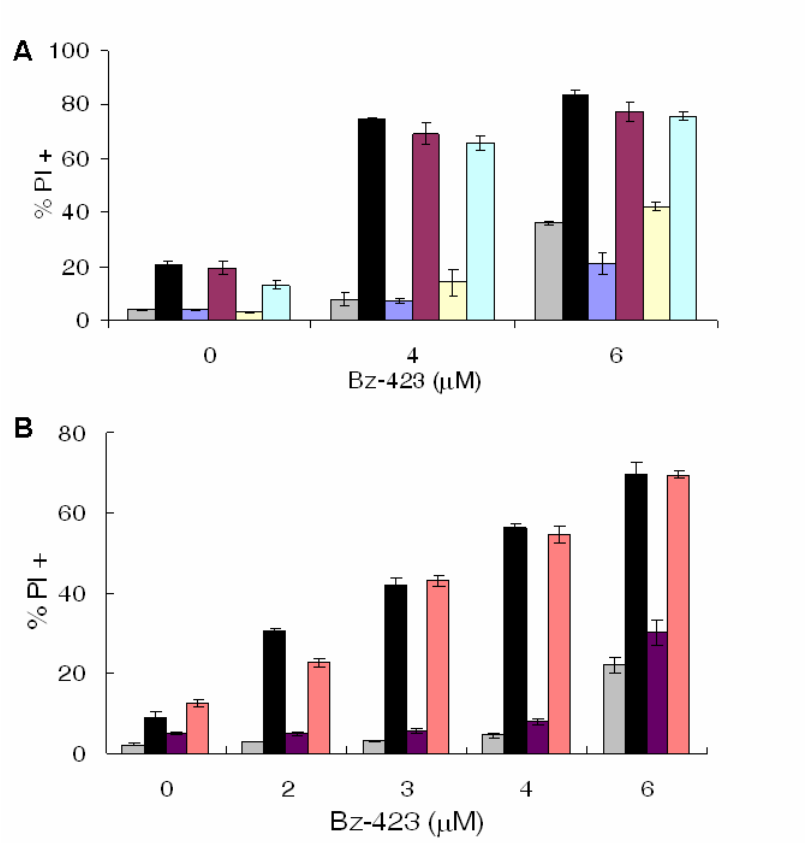

Figure 2.41: The p38 and JNK are not involved in cell death by co-treatment. (A) The specific p38 inhibitor (SB202190, SB203580) does not inhibit cell death by co-treatment. The treatments were control Ig (1 µg/ml,), anti-IgM (1 µg/ml,), control Ig + SB202190 (10 µM,), anti-IgM + SB202190 ( ), control Ig + SB203580 (10 µM,), anti-IgM + SB203580 ( ) (B) The specific JNK inhibitor II does not inhibit cell death by co-treatment. The treatments were control Ig (1 µg/ml,), anti-IgM (1 µg/ml,), control Ig + JNK inhibitor II (2.5 µM,), anti-IgM + JNK inhibitor II ( ). This experiment was repeated three times.

Co-treatment induces prolonged calcineurin activation: Since calcineurin is involved in cell death by co-treatment, it is hypothesized that Bz-423 and anti-IgM interact, which are responsible for the cell death by co-treatment. To test this hypothesis, the calcineurin activity induced by co-treatment was monitored. If there is a synergistic effect on calcineurin activity, calcineurin will be a converging point for anti-IgM and Bz-423 pathways. There are four ways to monitor calcineurin activity: *in vitro* calcineurin assay, NFAT dephosphorylation, NFAT nuclear translocation and

NFAT reporter assay (Figure 2.42B). The *in vitro* calcineurin assay takes advantage of the observation that calcineurin dephosphorylates the RII phosphopeptide [274]. The released phosphate can be detected by a classic malachite green assay [275]. Calcineurin activity can also be monitored through nuclear factor of activated T cells (NFAT), a transcription factor which calcineurin binds to and dephosphorylates ([276]; Figure 2.42A). Once NFAT is dephosphorylated, it translocates to the nucleus and initiates transcription activation of target genes ([276]; Figure 2.42A). Therefore, calcineurin activity can be monitored by studying the NFAT dephosphorylation or nuclear translocation by western blot or by studying transcription activation using the reporter plasmid pNFAT-SEAP ([276]; Figure 2.42B).

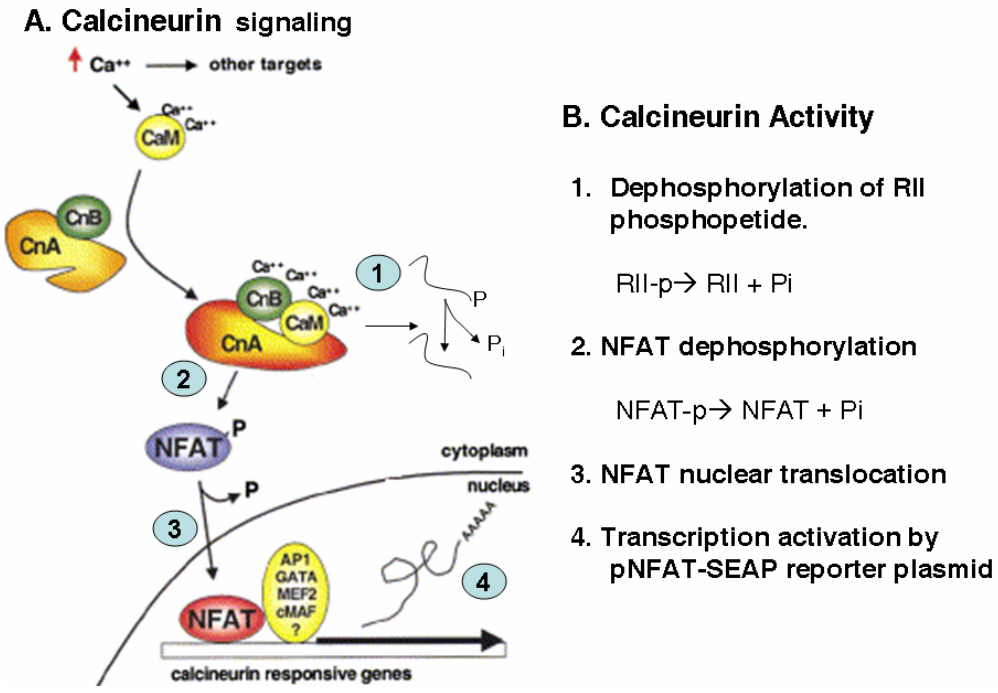

Figure 2.42: Ca^{2+}-calcineurin-NFAT signaling pathway and methods to measure calcineurin activity. (A) Ca^{2+}-calcineurin-NFAT signaling pathway. This is adapted from [276]. (B) four ways to measure calcineurin activity.

Calcineurin activity was first studied by monitoring NFAT dephosphorylation and translocation in Ramos cells. There is around 7.5% ± 2.5% NFAT dephosphorylated in resting Ramos B cells. This is consistent with a report of constitutively active NFAT in cells isolated from lymphoma and lymphoma cell lines such as Raji and Daudi [277]. In response to anti-IgM alone, 40 and 45% of NFAT was dephosphorylated at 1 and 2 h, respectively, and it returned to basal level at 4 and 6 h, indicating anti-IgM alone induces a transient NFAT dephosphorylation (Figure 2.43A). Both Bz-423 alone and co-treatment induced NFAT dephosphorylation at all the time monitored (Figure 2.43A). However, Bz-423 induced 20-40% NFAT dephosphorylation, and co-treatment induced 40-60% NFAT dephosphorylation. This observation suggests Bz-423 induces a low and sustained NFAT dephosphorylation and co-treatment induces an increased and sustained NFAT dephosphorylation. This increase in NFAT dephosphorylation results in immediate increase in nuclear fraction, as similar results were also observed in the NFAT nuclear translocation assay (Figure 2.43B). Phosphorylated NFAT was also present in the nuclear fractions, as it is decreased by ionomycin treatment and increased by cyclosporine A treatment. This presence of phosphorylated NFAT in the nuclear fraction is not due to the contamination of cytosol fraction as cytosol protein β-tubulin is not detected. It is possible due to a relatively rapid rephosphorylation. This would make it essential to have a sustained Ca^{2+}-calcineurin signaling to maintain NFAT activation for transcription activities [276].

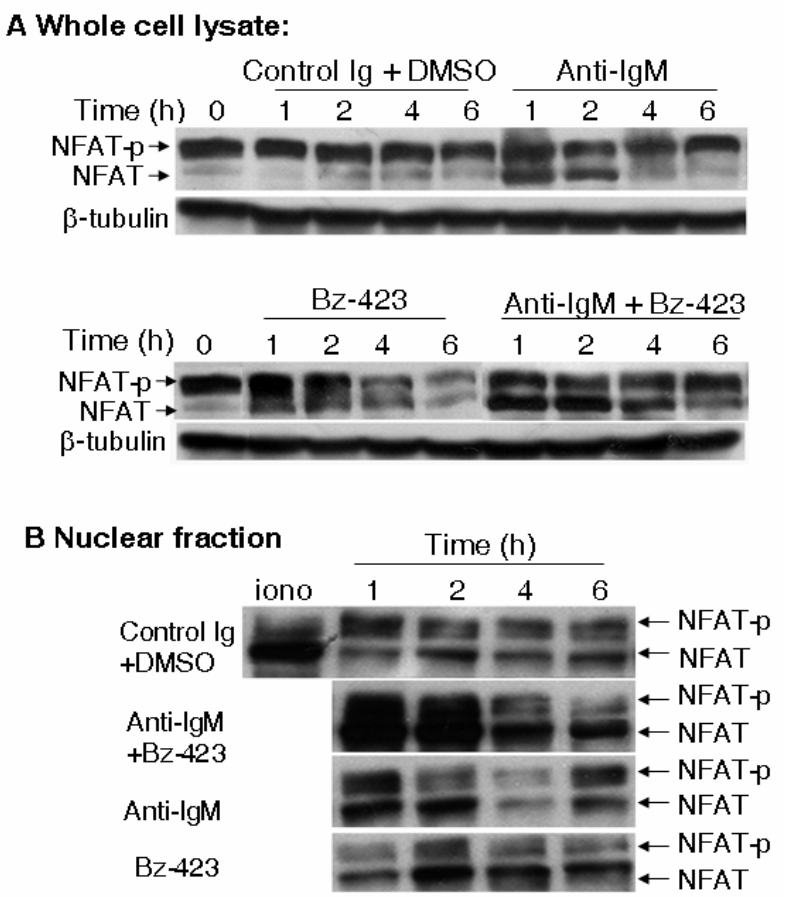

Figure 2.43: NFAT dephosphorylation and nuclear translocation induced by co-treatment in Ramos cells. (A) NFAT dephosphorylation induced by co-treatment. Whole cell lysates were isolated from treated Ramos B cells at indicated times, and immunoblots were performed with specific antibodies. (B) NFAT nuclear translocation was monitored. Nuclear fractions of treated Ramos B cells were obtained at indicated times. The immunoblots were performed with specific antibodies. The phosphorylated and de-phosphorylated forms of NFAT are indicated by arrow. The treatments were control Ig (1 μg/mL), anti-IgM (1 μg/mL) and Bz-423 (5 μM) in media with 2% FBS. The experiments were repeated ≥ 3 times.

Due to the qualitative nature of western blotting, it is difficult to decide whether anti-IgM and Bz-423 induced an additive or supra-additive effect on calcineurin activation. The reporter plasmid pNFAT-SEAP was used to quantify the calcineurin activity induced by co-treatment. In this system, the expression of secreted alkaline phosphatase (SEAP) is driven by activated NFAT through binding to three repetitive NFAT binding sites (3x NFAT) in the promoter region (Figure 2.44A).

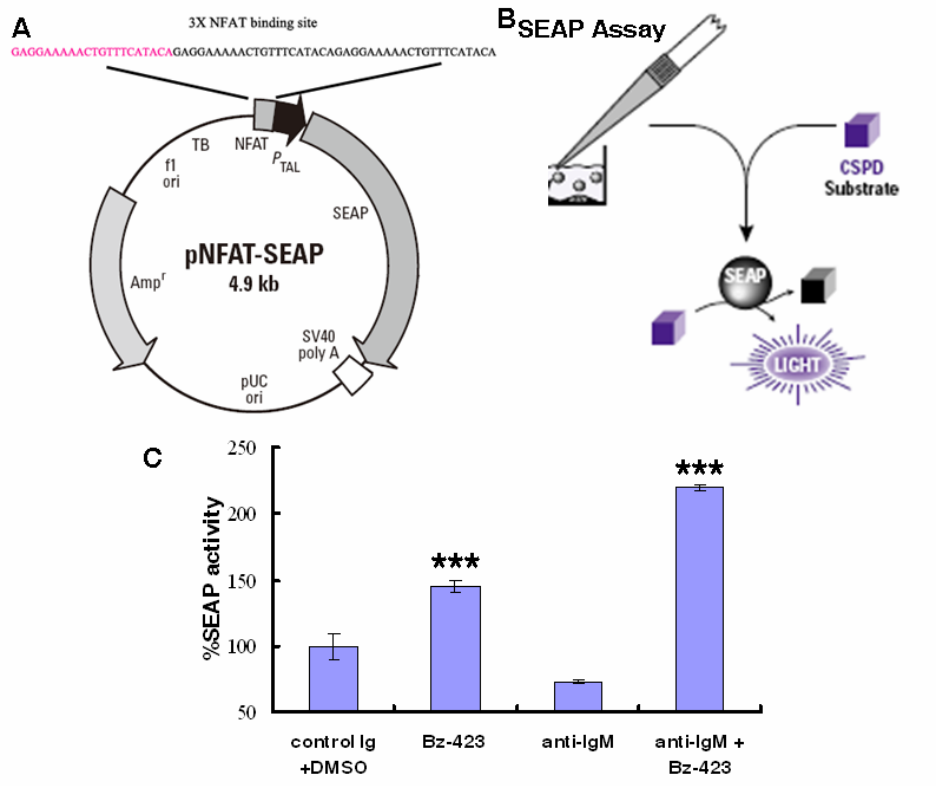

Figure 2.44: Co-treatment of anti-IgM and Bz-423 induces synergistic NFAT transcription activation in Ramos cells. (A) The construct of reporter plasmid pNFAT-SEAP. In the promoter region of pNFAT-SEAP, there are three repetitive NFAT binding sites. The DNA sequence in pink is that of one NFAT binding site. (B) The experimental scheme for SEAP assay: The SEAP collected from the media phosphorylates CSPD, producing light, which can be detected by chemiluminescence. (C) The SEAP activity induced by anti-IgM and Bz-423 co-treatment. Ramos B cells were transiently transfected with pNFAT-SEAP. After resting for 24 h, cells were treated with control Ig (1 μg/mL)+DMSO, Bz-423 (5 μM), anti-IgM (1 μg/mL), anti-IgM and Bz-423. 6 h later, the media was collected for assay. This experiment was repeated three times.

SEAP is secreted into the media, which is collected for measuring SEAP activity by chemiluminescence (Figure 2.44B). Ramos cells were transiently transfected with pNFAT-SEAP. After resting for 24 h, cells were treated with anti-IgM and Bz-423 alone or together. 6 h or 24 h later, media was collected for SEAP assay. The supernatant collected at 6 h or 24 h produced similar results, and 6 h data was shown in Figure 2.44C. Bz-423 alone induced a ~50% increase in NFAT-dependent SEAP

expression while anti-IgM did not increase any SEAP expression. Co-treatment induced ~150% increase in NFAT transcription activity. This result confirms Bz-423 and anti-IgM induced a synergistic NFAT transcription activation.

Mechanism of calcineurin activation by anti-IgM and Bz-423 co-treatment: The mechanism of NFAT activation induced by co-treatment was probed by studying the effect of inhibitors on NFAT dephosphorylation. As NFAT is activated by calcineurin [276], it was hypothesized that NFAT dephosphorylation is mediated by calcineurin. This hypothesis was tested by studying the effect of calcineurin inhibitors on NFAT dephosphorylation induced by co-treatment. As expected, the calcineurin inhibitor FK506 abolished NFAT dephosphorylation induced by co-treatment (Figure 2.45A). Calcineurin is activated by $[Ca^{2+}]_i$ increase [276], which possibly was induced by Ca^{2+} influx. Moreover, BAPTA salt blocks Ca^{2+} influx and inhibits cell death by co-treatment [221]. It is hypothesized that Ca^{2+} influx induced by co-treatment results in NFAT dephosphorylation. This hypothesis was tested by studying the effect of BAPTA salt on NFAT dephosphorylation induced by co-treatment. BAPTA salt inhibited NFAT dephosphorylation, showing Ca^{2+} influx is necessary to activate NFAT (Figure 2.45A). As anti-oxidants inhibit cell death by co-treatment, it was hypothesized that ROS might dephosphorylate NFAT [221]. This hypothesis was tested by studying the effect of anti-oxidants on NFAT dephosphorylation induced by co-treatment. The anti-oxidant MnTBAP surprisingly did not inhibit NFAT dephosphorylation (Figure 2.45A). This result suggests that early ROS (within 1 h) is not involved in NFAT dephosphorylation induced by co-treatment. The involvement

of ROS in NFAT dephosphorylation was further studied at later timepoints (after 1 h). MnTBAP inhibited sustained NFAT dephosphorylation at 4 h (Figure 2.45B). This result indicates that late ROS is involved in the sustained NFAT activation.

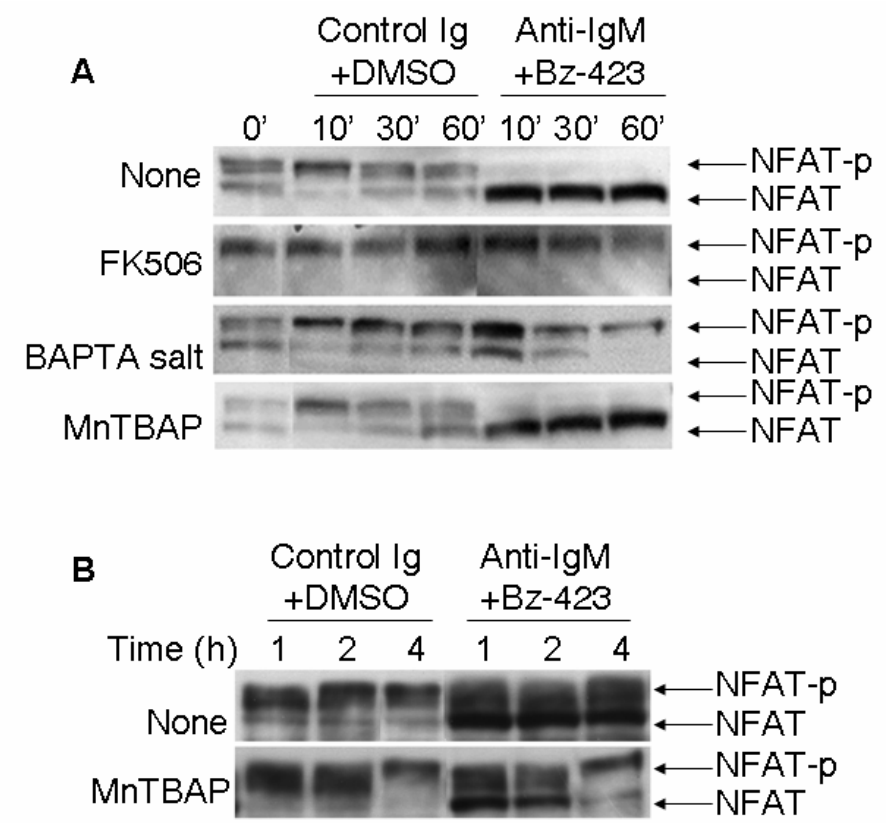

Figure 2.45: Inhibitors on NFAT dephosphorylation induced by co-treatment. (A) Inhibitors on NFAT dephosphorylation induced by co-treatment within 1 h. FK506 (1 μM), BAPTA salt (500 μM), or MnTBAP (100 μM) was added 30 min before the treatment in Ramos with 2% FBS. At indicated times, cell lysate were harvested and NFAT dephosphorylation was detected by western blot. The arrow indicated the position of phosphorylated and de-phosphorylated NFAT. Control Ig (1 μg/mL) plus DMSO, and anti-IgM (1 μg/mL) plus Bz-423 (5 μM) were used. The experiment in panel A was repeated two times, and the experiment in panel B was done once.

Bad and Nur77 are not involved in cell death induced by co-treatment: Besides NFAT, calcineurin also dephosphorylates Bad at Ser 112 and Ser 136, which results in its dissociation of 14-3-3, a sequestering protein for phosphorylated Bad [278]. After dissociating with protein 14-3-3, this dephosphorylated Bad binds to

anti-apoptotic Bcl-xL and Bcl-2, releasing pro-apoptotic Bax and Bak for subsequent apoptosis [278]. As Bad is involved in apoptosis and a substrate of calcineurin, it was hypothesized that Bad is dephosphorylated and dissociates with 14-3-3 during the co-treatment. To test this hypothesis, Bad dephosphorylation and dissociation with 14-3-3 were monitored. Anti-IgM and Bz-423 co-treatment did not change in the phosphorylation state of Bad or dissociation of 14-3-3 (Figure 2.46). This result argues against the involvement of Bad in cell death by co-treatment.

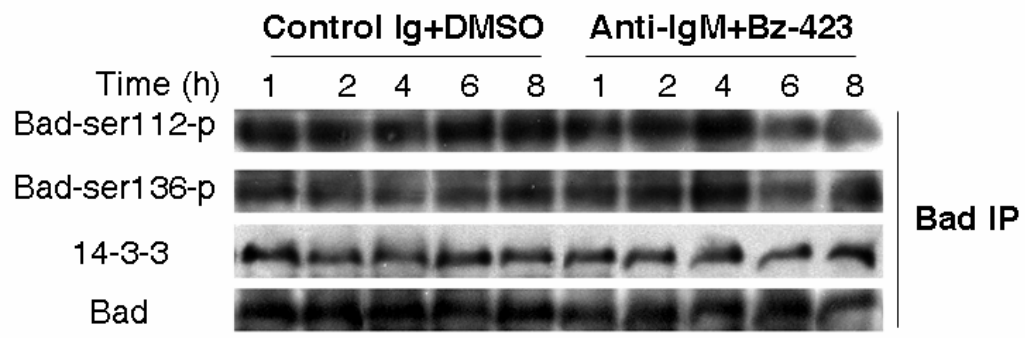

Figure 2.46: Bad is not activated by anti-IgM and Bz-423 co-treatment. The cell lysate from treated Ramos were immunoprecipitated by Bad antibody. The cell lysates from Bad immunoprecipitation (IP) were used to detect the levels of Bad phosphorylation at Ser 112 and Ser 136, and of the 14-3-3. The Bad were probed as the loading control. Bz-423 (5 μM), control Ig (1 μg/mL) and anti-IgM (1 μg/mL) were used. This experiment was repeated for two times.

In response to anti-IgM stimulation, Nur77 expression is increased in a NFAT-dependent manner, translocates into the mitochondria, and induces cell death [166]. Therefore, it was hypothesized that co-treatment increases Nur77 expression level, which may be responsible for the cell death. This hypothesis was first tested by studying the expression level changes of Nur77 by anti-IgM and Bz-423 co-treatment. Co-treatment did not increase the expression level of Nur77 (Fig 2.46), which

excludes its possible involvement of Nur77 in the cell death by co-treatment.

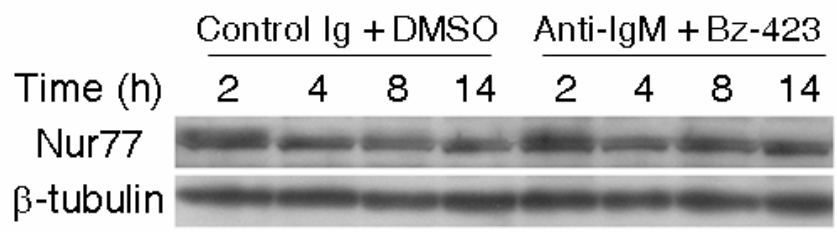

Figure 2.47: Nur77 expression level is not increased by anti-IgM and Bz-423 co-treatment. The treated cells were lysed and the immunoblots were probed for Nur77 expression. Bz-423 (5 μM), control Ig (1 μg/mL) and anti-IgM (1 μg/mL) were used. This experiment was repeated for two times.

Anti-IgM stimulation sensitizes Ramos cells to chemicals that target mitochondria: Bz-423 binds to the OSCP (oligomycin-sensitivity conferring protein) subunit of the mitochondrial F_0F_1-ATPase, inhibits mitochondrial F_0F_1-ATPase activity, and leads to mitochondrial hyper-permeablization (MHP), causing superoxide generation, which signals cells to undergo apoptosis. As shown previously, co-treatment of Bz-423 and anti-IgM synergistically activates Bax and Bak, which leads to cell death by co-treatment. Chemical reagents that inhibit the mitochondrial F_0F_1-ATPase, or the mitochondrial electron transport chain (ETC) were tested to determine whether anti-IgM stimulation sensitizes Ramos cells to these chemical reagents. Based on the 24 h cell death data, several interesting observation were made: Firstly, co-treatment of anti-IgM stimulation and mitochondrial F_0F_1-ATPase inhibitors oligomycin (Figure 2.48E) and 3,3'-diindolylmethane (DIM)

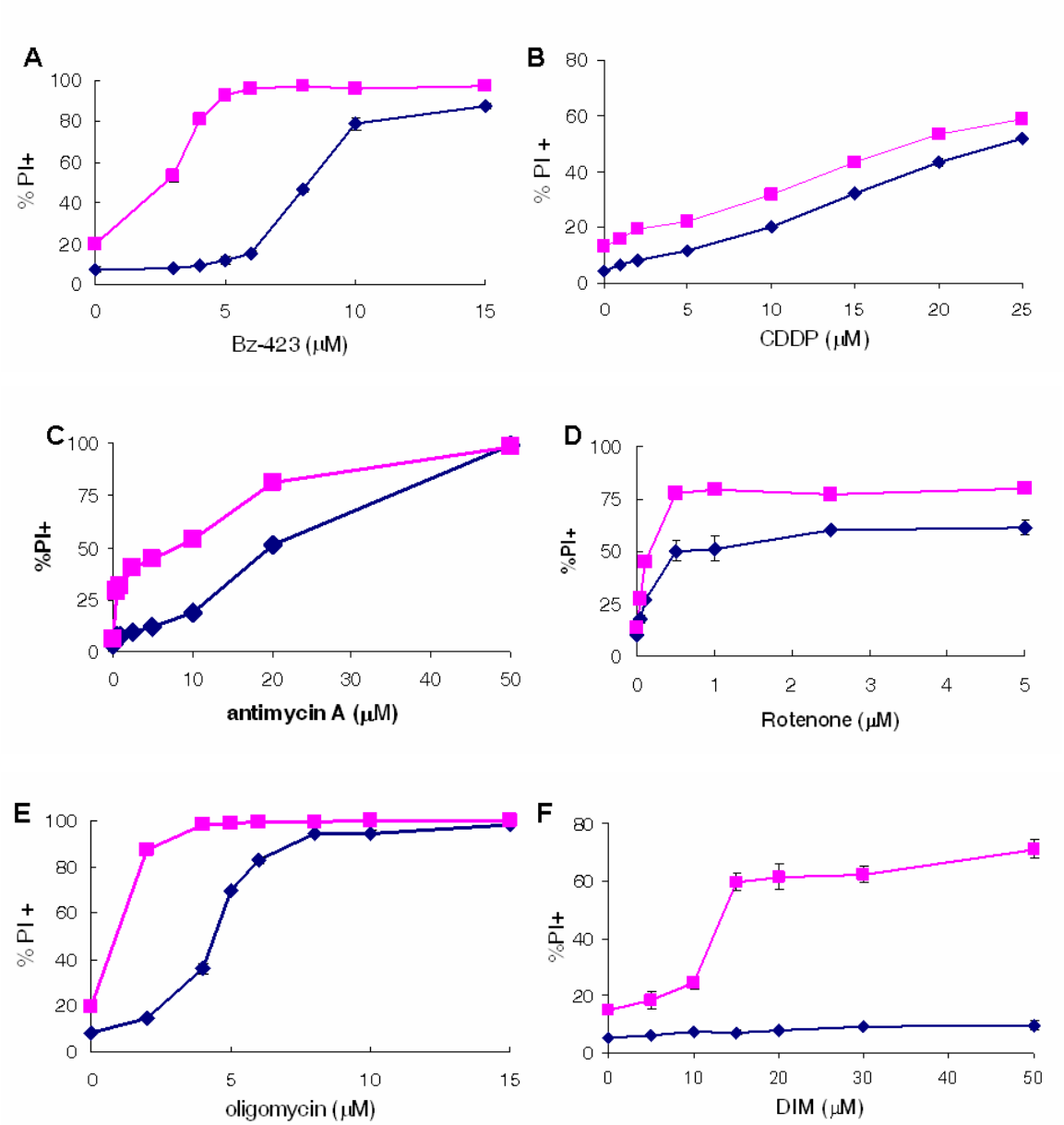

Figure 2.48: Several mitochondrial reagents synergize with anti-IgM in Ramos B cells. Ramos B cells in media with 2% FBS were treated with Bz-423 (A), CDDP (B), antimycin A (C), rotenone (D), oligomycin (E), and DIM (F) in the presence of anti-IgM (1 μg/mL, ■) or control Ig (1 μg/mL, ◆) for 24 h. And the cell death was measured by PI permeability. This experiment was repeated for ≥2 times. The absence of an error bar indicates ≤ 1 % standard deviation.

induced cell death by co-treatment (Figure 2.48F) . Secondly, anti-IgM stimulation sensitizes Ramos cells to the ETC complex I inhibitor rotenone (Fig 2.47D) and complex III inhibitor antimycin A (Figure 2.48C). In contrast, ROS-producing

reagents menadione and H_2O_2 were previously shown not to synergize with anti-IgM stimulation (Figure 2.23). Thirdly, anti-IgM stimulation did not modulate cellular sensitivity to DNA damaging reagent CDDP (Figure 2.48B), which induces cell death through Fas death receptor pathway [279]. These results indicate that anti-IgM stimulation does modulate cellular sensitivity to these chemicals against mitochondria, Although Bax and Bak is thought to be a common sensor for various signaling pathway, anti-IgM stimulation only sensitizes cells to chemicals target mitochondria suggests it specificity.

Since anti-IgM was found to cause cell death by co-treatment specifically with compounds targeting the mitochondria, inhibitor experiments were performed to probe the mechanism of synergy induced by these reagents. Antioxidants MnTBAP, VitE and the extracellular Ca^{2+} chelator BAPTA salt were used. Pretreatment of MnTBAP did not modulate cell death induced by antimycin A, rotenone or oligomycin alone. Nor did they modulate the cell death by co-treatment induced by antimycin A, rotenone or oligomycin (Table 2.2). This result suggests that superoxide does not mediate cell death induced by antimycin A or rotenone. Nor does superoxide mediate cell death by co-treatment with anti-IgM. Therefore, Bz-423 induced a superoxide increase plays a unique way in cell death by co-treatment. VitE, which decrease both superoxide and H_2O_2, protected oligomycin-induced cell death and synergy, indicating the involvement of H_2O_2. BAPTA salt, which inhibits anti-IgM induced sustained Ca^{2+} change, inhibits the cell death by co-treatment induced by all the reagents tested, suggesting the involvement of anti-IgM induced Ca^{2+} influx in

establishment of cell death by co-treatment. Although various chemicals that target mitochondria, especially those targeting mitochondrial ETC complex, synergized with anti-IgM in cell death induction in Ramos cells, their mechanisms are different.

	Bz-423		**oligomycin**		**Antimycin A**		**Rotenone**	
	Control Ig	Anti-IgM	Control Ig	Anti-IgM	Control Ig	Anti-IgM	Control Ig	Anti-IgM
No inhibitor	8	3	4	0.5	15	1	1	0.06
MnTBAP	12.5	8.5	4.5	2.5	14.5	1	1	0.05
VitE	10.5	6	> 8	> 8	15	1	1	0.06
BAPTA salt	8	7.5	4	2	17.5	7	1	0.1

Table 2.2: Comparison of Bz-423 with oligomycin, antimycin A and Rotenone in anti-IgM induced synergy. EC_{50} (μM) were obtained for 24 h cell death (PI) induced by co-treatment of control Ig (1 μg/mL) or anti-IgM (1 μg/mL) and increasing concentrations of compounds listed in the presence or absence of inhibitors.

Discussion

Self-reactive B cells play a central role in the pathogenesis of systemic lupus erythemosus (SLE) [280, 281]. Autoreactive B cells can secrete auto-antibodies, which mediate self-damage. They can also participate in self-damage by secreting cytokines or acting as antigen presenting cells (APCs), which activate self-reactive T cells [282]. Therefore, selective deletion of autoreactive B cells could be an effective and specific approach for SLE treatment. Various B cell-targeted strategies engaging different mechanisms have been developed and tested clinically [283]. Anti-CD20 and anti-CD22 were developed to induce apoptosis while anti-BAFF and TACI Ig were developed to block survivals [283]. Currently these agents are in phase III open trials studies [283].

Bz-423 is a non-anxiolytic benzodiazepine that binds to mitochondrial

F_0F_1-ATPase, resulting in ROS-dependent anti-proliferative and pro-apoptotic signaling pathways [217, 218, 284]. Abnormal expansion of germinal center (GC) B cells is observed in the spleen of NZB/NZW F1 lupus-prone mice, and is proposed to drive disease [217]. Bz-423 treatment of NZB/NZW F1 lupus-prone mice reduced both the numbers and the sizes of GCs in the spleen by 40% [217]. Additionally, terminal dUTP nick-end labeling (TUNEL) staining, a specific method to detect DNA fragmentation, the hallmark for apoptosis, demonstrated Bz-423 increases apoptosis in the spleen [217]. Thus, Bz-423 appears to selectively eliminate pathogenic lymphocytes in these lupus-prone mice. This *in vivo* observation was further studied *in vitro* using a B cell line with a GC-phenotype, Ramos B cell [221]. Since GC B cells are activated *in vivo*, and sustained activation of autoreactive B cells is important for the initiation and progress of SLE [285], it was hypothesized that activation could sensitize Ramos B cells to Bz-423 treatment. Co-treatment with sub-apoptotic anti-IgM and Bz-423 induced supra-additive cell death, confirming that activation can sensitize Ramos B cells to Bz-423 treatment [221]. This phenomenon is referred to anti-IgM-induced synergy. As shown in Figure 2.49, at low concentrations, Bz-423 did not kill Ramos B cells; however, these concentrations of Bz-423 caused significant cell death in the presence of anti-IgM, which binds to the B cell receptor (BCR) causing activation. This result suggests that Bz-423 selectively kills stimulated Ramos B cells over resting Ramos B cells. This could explain the *in vivo* selectivity of Bz-423 for pathogenic cells. In order to elucidate the mechanism of this cell death by co-treatment and to identify potential new targets, the signaling pathway of anti-IgM

induced synergy was studied in Ramos B cells.

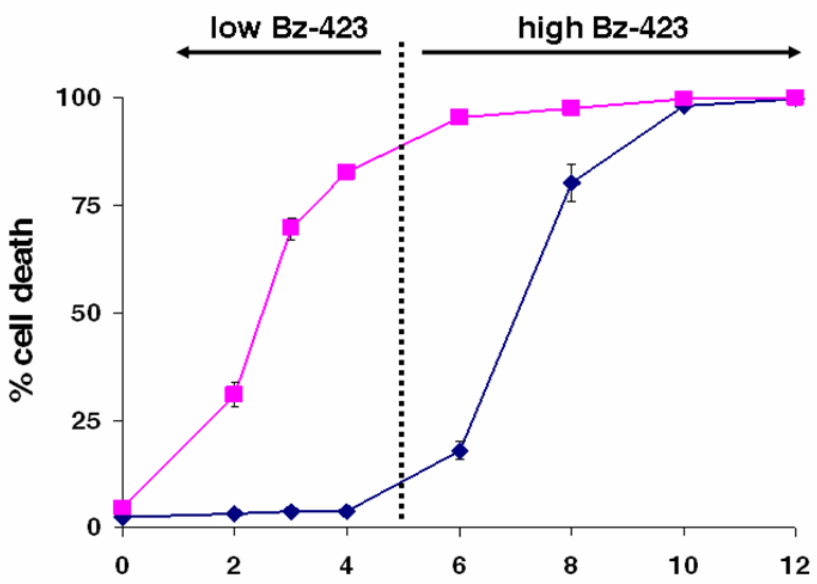

Figure 2.49: Bz-423 selectively kills anti-IgM stimulated Ramos B cells. Ramos B cells were treated with series concentrations of Bz-423 in the presence of control Ig (◆, 1 µg/mL) or anti-IgM (■, 1 µg/mL). 48 h later, cell death was determined by PI permeability assay.

Bz-423 selectively kills activated B cells with GC or immature B cells phenotypes: In NZB/NZW F1 mice, GC B cells are already activated before Bz-423 treatment. But in the *in vitro* model, anti-IgM and Bz-423 are co-treated simultaneously. Before studying the mechanism of anti-IgM induced synergy, this discrepancy was addressed. Cell death by co-treatment was still observed when Ramos B cells were pre-stimulated with anti-IgM for 14 h prior to Bz-423 treatment (Figure 2.49). This finding confirmed that low concentrations of Bz-423 selectively kill Ramos B cells regardless of whether they are pre-activated or con-currently activated by anti-IgM. Therefore this *in vitro* Ramos B cell model is appropriate for studying Bz-423 selectivity observed *in vivo*.

Disturbed peripheral B lymphocyte homeostasis is detected in SLE patients

[286-288]. There are increased percentages of transition B cells, plasma B cells and memory B cells detected in the peripheral blood of SLE patients [286-288]. The question of whether Bz-423 kills these B cell subsets was thus studied by screening for anti-IgM induced synergy in various B cell lines. Cell death by co-treatment was only observed in B cells with GC phenotype (Ramos, OCI-ly7) and in B cells with immature B cell characteristics (WEHI-231), but not in other Burkitt's lymphoma (BL) cell lines (ST486, CA46, Namalwa, Daudi, and Raji). This result suggests that Bz-423 not only selectively kills stimulated B cells over non-stimulated B cells, but also selectively kills activated B cells with GC phenotype and immature B cell characteristics. In the lupus-prone MRL-*lpr* mice which are responsive to Bz-423 treatment, B cells that bind to self antigens such as the ribonucleoprotein Sm and dsDNA displayed the immature phenotype [288, 289]. This suggests the possibility that Bz-423 may attenuate the disease by promoting cell death in these pathogenic immature B cells. Although GC B cells are rarely detected in peripheral blood, memory B cells, which arise from GC B cells as results of GC reactions, can be used to indicate GC B cell activity. CD27 is a maker of memory B cells. Upon activation, $CD27^{+}$ memory B cells can differentiate into $CD27^{high}$ plasma cells [290]. In human SLE patients, the percentages of $CD27^{+}$ memory B cells and $CD27^{high}$ plasma cells are significantly increased [286]. Moreover, a close correlation of $CD27^{high}$ plasma cells with disease activity was observed [286]. Upon immunosuppressive therapy, $CD27^{high}$ plasma cells were markedly decreased in the peripheral blood, further supporting that $CD27^{high}$ plasma cells are pathogenic and actively participate in

disease development [286]. The increased frequencies of memory B cells observed in human peripheral blood from SLE patients might be the result of intensive GC B cell activity [291]. As Bz-423 can selectively kill activated GC B cells, Bz-423 could reduce these abnormal B cell subsets thus providing an effective treatment for SLE.

Mechanism of cell death induced by anti-IgM and Bz-423 co-treatment: The above results show that anti-IgM induced synergy in Ramos B cells is an appropriate model system to study Bz-423 selectivity observed *in vivo*. And therefore it was used to delineate the apoptotic signaling pathway of anti-IgM induced cell death by co-treatment. An in depth understanding of anti-IgM induced synergy will help to identify the critical mediators of this phenomenon and help to explain Bz-423 selectivity. In addition, the results may help to design more specific treatment for autoimmune diseases.

Cell death induced by co-treatment is different from cell death induced by anti-IgM or Bz-423 alone: High concentration anti-IgM or Bz-423 induced cell death in a mitochondrial dependent pathway [217, 292]. Based on the kinetic changes of mitochondrial membrane potential ($\Delta\psi_m$) disruption and that of cell death, anti-IgM induced synergy is kinetically slower than Bz-423 induced cell death but faster than anti-IgM induced cell death. Bz-423 washout indicates 12 h co-treatment is required to reach "point of no return" in cell death by co-treatment while only 6 h Bz-423 treatment is required in Bz-423 induced cell death. These results are consistent with the observation that new protein synthesis is needed for anti-IgM induced synergy and anti-IgM induced cell death.

Inhibitors experiments also indicate anti-IgM induced synergy is different from cell death. Calcium, ROS, new protein synthesis and caspase are previously involved in cell death by co-treatment. In contrast, ROS is involved in Bz-423 induced cell death, and calcium, calcineurin, new protein synthesis and caspases are mediators for anti-IgM induced cell death [221]. Especially general caspase inhibitor zVAD-fmk does not inhibit Bz-423 induced cell death but inhibited cell death by co-treatment based on PI staining and cell morphology. This different protection by zVAD-fmk indicates that anti-IgM induced synergy and Bz-423 induced cell death adopted a different pathway to cause cell death, at least cell morphology and cell permeability changes.

It is possible that Bz-423 signaling and anti-IgM signaling converge at some points to induce cell death by co-treatment. At these intersection points, supraadditve changes are observed and therefore identified as converging points. Identification of converging points will help to understand how these two signaling pathways intersect. Anti-IgM and Bz-423 co-treatment does not further increase ROS change induced by Bz-423 [221], indicating they interact downstream of ROS.

MOMP is involved in cell death induced by Bz-423 and anti-IgM co-treatment: Anti-IgM and Bz-423 induce apoptosis in mitochondria-dependent pathways [217, 292]. Therefore mitochondrial pro-apoptotic factors (cytochrome c, AIF, Smac) release and mitochondrial membrane potential ($\Delta\psi_m$) disruption induced by anti-IgM and Bz-423 co-treatment were studied. At 8 h, mitochondrial pro-apoptotic factors are synergistically released but no significant $\Delta\psi_m$ disruption is

observed. Mitochondrial pro-apoptotic factors release in the presence of intact mitochondrial inner membrane is defined as mitochondrial outer membrane permeablization (MOMP) [31]. This result indicates that Bz-423 and anti-IgM signaling converged at or before MOMP. The involvement of MOMP in cell death by co-treatment was confirmed by inhibitor experiments. Inhibitors to block calcium influx, calcineurin activation, ROS increase, new protein synthesis prevent synergistic MOMP, suggesting they act upstream MOMP. At the concentration used to prevent cell death by co-treatment, general caspase inhibitor zVAD-fmk does not inhibit MOMP, indicating caspase activation is downstream MOMP.

Pro-apoptotic Bcl-2 proteins are activated by Bz-423 and anti-IgM co-treatment: The protection of Bcl-2 or Bcl-xL against MOMP suggests the possible involvement of Bax and Bak in cell death by co-treatment. Once activated, Bax and Bak could form pores in the OMM allowing MOMP [263]. Immunofluorescence was used to study Bax and Bak activation induced by anti-IgM and Bz-423 co-treatment through staining with activation-specific antibodies. Both proteins are synergistically activated at 6 h after co-treatment, suggesting that they are responsible for the synergistic MOMP observed at 8 h. Bax and Bak double RNAi knockdown blocks anti-IgM induced synergy, verifying the involvement of Bax and Bak. Since mouse embryonic fibroblasts with deficiency of Bax and Bak are resistant to multiple apoptotic stimuli, Bax and Bak are considered to be an essential gateway for various apoptotic signals [68]. Further study of Bax and Bak in lymphocytes indicates it is important in deleting of unwanted or autoreactive lymphocytes and therefore essential

in the lymphocytes homeostasis [293]. As Bax and Bak are activated by BH3-only proteins, the expression levels of BH3-only proteins induced by anti-IgM and Bz-423 co-treatment were studied. There is a synergistic increase in Bim, Bmf and truncated Bid (tBid) 4-6 h after anti-IgM and Bz-423 cotreatment, which might be responsible for the Bax and Bak activation (Figure 2.50). Bim, Bmf and tBid are shown to be involved in lymphocyte apoptosis induced by various apoptotic stimuli [294-296]. Lymphocytes from Bim-deficient mice are resistant to cell death induced by cell receptors [267, 293, 297]. Bmf-deficient mice develop a B cell-restricted lymphadenopathy due to the abnormal resistance to apoptosis induction [268]. Protein synthesis inhibitor cycloheximide is previously shown to inhibit cell death by co-treatment. When added 6 h after the co-treatment, it lost its inhibition of cell death by co-treatment. This result indicates that protein synthesis required for synergy occurs within 6 h. This is coincident with the increased expression of Bim, Bmf, indicating they could be the proteins required for synergy.

In summary, Bz-423 and anti-IgM co-treatment induced synergistic BH3-only proteins increase at 4-6 h, which is responsible for Bax and Bak activation at 6 h, MOMP at 8 h, caspases activation, and cell death by co-treatments at 24 h (Figure 2.50).

Ca^{2+}-calcineurin pathway is involved in cell death induced by anti-IgM and Bz-423 co-treatment: B cell receptor ligation induces a rapid calcium release from ER, which triggers CRAC channel opening and leads to a sustained calcium influx [107, 298]. In Ramos B cells anti-IgM alone rapidly increase $[Ca^{2+}]_i$ to ~120 nM and

calcium slowly declines to the resting level, which is ~50 nM. After 15 min, only 2% cells are above the resting level. Anti-IgM and Bz-423 cotreatment induced $[Ca^{2+}]_i$ reaches up to ~200 nM. 15 minutes later, 64% cells are above resting level. No significant calcium change is induced by Bz-423 alone [221]. This early calcium increase induced by Bz-423 and anti-IgM indicates that anti-IgM and Bz-423 signals converge at or upstream of the intracellular calcium increase.

In this chapter, the involvement of this early calcium increase in cell death by co-treatment was further studied. Btk is known to mediate the calcium increase induced by BCR ligation based on the result that a specific Btk inhibitor LFM-A13 inhibits this calcium change [299, 300]. Pre-incubation with LFM-A13 also inhibits the early intracellular Ca^{2+} increase induced by anti-IgM and Bz-423 co-treatment. However, LFM-A13 does not inhibit cell death by co-treatment, suggesting the possibility that early calcium increase is not required for cell death by co-treatment. This result is also confirmed using the extracellular calcium chelator BAPTA salt. When applied 1 h after co-treatment, BAPTA salt does not block the early calcium change, but it still inhibits cell death by co-treatment to the same level as it does when pre-incubated 30 minutes before co-treatment. These results suggest that early calcium increase is dispensable for cell death by co-treatment.

Despite the dispensable role of early calcium increase in cell death by co-treatment, the involvement of calcium in establishing cell death by co-treatment is well established. Extracellular calcium chelator BAPTA salt inhibits the cell death by co-treatment, suggesting the involvement of calcium influx. One mechanism for

extracellular calcium to enter cells is through calcium release activated calcium (CRAC) channel [301]. B cell receptor crosslinking induces sustained calcium change through CRAC channel [105, 302]. Deficiency in Orai1, one potent subunit of CRAC channel, results in decreased calcium influx in response to B cell receptor stimulation [302]. Therefore, the CRAC channel inhibitor YM-58483 was used to determine if CRAC is involved in cell death by co-treatment. Pre-incubation of Ramos B cells with YM-58483 inhibited anti-IgM induced synergy. This result not only confirms the critical role of calcium influx in cell death by co-treatment, but also indicates this calcium influx occurs through CRAC channel. As CRAC channel is involved in sustained calcium increase, it was hypothesized that the duration of calcium increase, but not the amplitude of calcium increase, is critical for cell death by co-treatment. The role of calcium in cell death by co-treatment was therefore studied by varying the addition time of BAPTA salt and studying its effect on cell death by co-treatment. BAPTA salt still inhibited cell death by co-treatment when added 1-8 h after co-treatment, suggested a sustained calcium change in establishing the cell death by co-treatment. Attempts to study this calcium change within 1-4 h after co-treatment are not successful. Part of the reasons is that Bz-423 interferes with calcium indicator.

As sustained calcium increase is critical for the cell death by co-treatment, it was therefore hypothesized that calcium itself could be sufficient to induce cell death by co-treatment with Bz-423 treatment. To test this hypothesis, cells were treated with reagents that induce sustained calcium influx along with Bz-423. Ionomycin is an ionophore which allows calcium to passively enter cells continuously [303, 304].

Tharpsigargin is an inhibitor for sacro/endoplasmic reticulum calcium ATPase (SERCA). Tharpsigargin depletes calcium in the ER, which subsequently opens CRAC channel for sustained calcium influx [305]. Both ionomycin and tharpsigargin synergize with Bz-423 in apoptosis induction, suggesting calcium increase is sufficient to sensitize cells to Bz-423. Although there are no literature reports of abnormal high calcium level in B cells from SLE patients, abnormal proximal B cell signaling is well established [186]. In response to anti-IgM stimulation, there is an enhanced calcium increase in lupus B cells [186]. Bz-423 treatment may enhance cell death by prolonging anti-IgM induced calcium change.

Calcium mediates a diverse array of cell functions by activating various transcription factors depending on its amplitude and duration [248]. A Low sustained calcium increase induced transcriptional activation of nuclear factor of activated T cells (NFAT) [248]. Calcium binds to calmodulin, which activates serine/threonine phosphatase calcineurin. The activated calcineurin then dephosphorylates NFAT, resulting in its nuclear translocation and increased transcription activation of target genes [106]. Dephosphorylated NFAT only has a lifetime of several minutes before it is rephosphorylated by constitutive active NFAT kinases [306]. Therefore, a prolonged calcium increase is therefore critical for NFAT-dependent transcription activation. Besides the translation inhibitor cycloheximide, the transcription inhibitor actinomycin D inhibits cell death by co-treatment. Together with the fact that sustained calcium increase is required for cell death by co-treatment, it is therefore hypothesized that cell death by co-treatment is induced by activating NFAT-dependent

transcription in a calcium-calcineurin manner. In fact, Bim, one of the BH3-only proteins whose expression is increased under synergistic condition, is also induced in response to cell receptor stimulation and ionomycin treatment [167, 169, 307].

T cell receptor mediated Bim increase was inhibited by pre-treatment of calcineurin inhibitor FK506 or cyclosporine A [167]. The involvement of calcineurin in cell death by co-treatment was studied using calcineurin inhibitors FK506 and cyclosporine A [308]. They inhibited anti-IgM induced Bax and Bak activation, MOMP, and cell death by co-treatment, confirming the hypothesis that calcineurin is involved in cell death by co-treatment. To determine if anti-IgM and Bz-423 co-treatment induces a synergistic effect on calcineurin activity, NFAT dephosphorylation, nuclear translocation and reporter plasmid pNFAT-SEAP were studied. Anti-IgM and Bz-423 co-treatement induced a sustained NFAT dephosphorylation, which results in a sustained NFAT nuclear translocation. The sustained NFAT activation leads to a synergistic effect on NFAT-dependent SEAP expression. Interestingly, anti-IgM induces transient NFAT activation and does not induce NFAT-dependent SEAP expression. Bz-423, which induces a low but sustained NFAT activation, does induce NFAT-dependent SEAP expression. These results highlight the critical role of sustained calcium increase and calcineurin activation in triggering NFAT-dependent transcription. This prolonged calcineurin activity may in part induce Bim transcription, which is responsible for Bax and Bak activation, cytochrome c release, and cell death (Figure 2.50). It is not clear yet whether this prolonged calcineurin activity is involved in Bmf increase or Bid cleavage. Further

experiments, including studying the effect of inhibitors for the cell death by co-treatment on the increases of BH3-only proteins, are needed to elucidate the mechanisms of BH3-only proteins changes induced by anti-IgM and Bz-423 co-treatment.

In summary, anti-IgM and Bz-423 co-treatment induces a sustained calcium increase, which activates calcineurin. This prolonged calcineurin activation may be responsible for transcriptional activation of BH3-only proteins Bim and Bmf, possibly through activated NFAT. Together with increased Bid cleavage to tBid through an unknown mechanism, Bim and Bmf activate Bax and Bak, which are responsible for the MOMP and subsequent cell death (Figure 2.50).

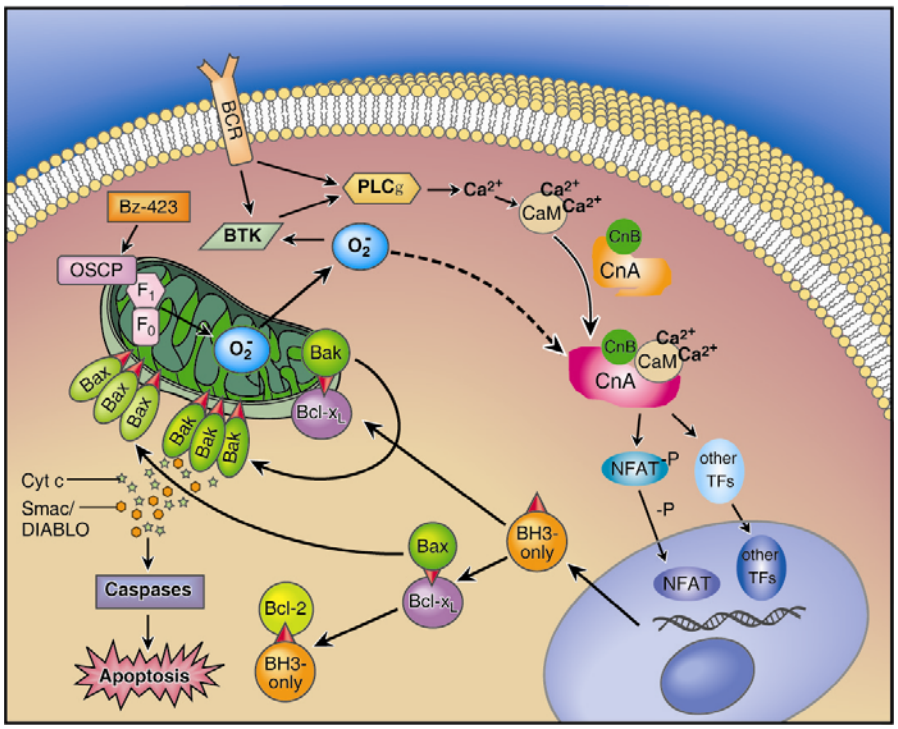

Figure 2.50: The apoptotic signaling pathway induced by co-treatment of Bz-423 and anti-IgM in Ramos B cells. Calcineurin A, CnA; calcineurin B, CnB; calmodulin, CaM; oligomycin sensitivity conferring protein, OSCP.

Bim and Bmf are potential therapeutic targets for autoimmune disease: It is well-established that pro-apoptotic BH3-only proteins regulates Bax and Bak activation [85, 90]. As a result of this activity, deletion of BH3-only proteins results in abnormal survival of autoreactive lymphocytes, leading to development of autoimmune disease [309]. Due to the redundancy of BH3-only proteins, not all mice with deficient BH3-only protein develop the autoimmune disease [309]. Mice deficient with Bad, Bik, Bid, Noxa or Hrk does not develop immune abnormalities [309]. In contrast, loss of Bim, Bmf or Puma affects the cellular sensitivity of lymphocytes to various apoptotic stimuli [309]. Bim-deficient mice and Bmf-deficient mice develop lupus-like disease, indicating their critical role of B cells homeostasis and normal function [67, 268]. The expression levels of Bim and Bmf are increased by anti-IgM and Bz-423 co-treatment. This finding is significant as it suggests Bz-423 may restore normal immune function by promoting apoptosis in B lymphocytes.

Bim is a potential target for SLE treatment as it is required for deletion of autoreactive lymphocytes: Bim was identified as a binding partner for the Bcl-2 like proteins Bcl-2 and MCl-1 [310-312]. *in vitro* studies showed that Bim can directly activate Bax and Bak [313], although the binding of Bim to Bax or Bak with high affinity has not yet been demonstrated under physiological conditions [309]. The Bim gene undergoes alternative splicing to produce three major isoforms: Bim extra long (Bim_{EL}), Bim long (Bim_{L}) and Bim short (Bim_{S}). They have different potency in apoptosis induction and various regulation mechanisms, which will be discussed below in details [314].

Studies of Bim-deficient mice have uncovered the key role of Bim in B cell homeostasis and function. Bim-deficient mice have a 3- to 5-fold increase in B cell numbers [267, 315]. Lymphocytes from Bim-/- mice are highly resistant to apoptosis induced by cytokine deprivation, ionomycin and cell receptor stimulation but not to phorbol ester treatment [267, 315]. These data indicate that different cytotoxic stimuli trigger apoptosis through activation of different BH3-only proteins (Figure 2.8) in introduction). Moreover, Bim-deficient mice develop lupus-like autoimmune disease [267], which suggests Bim might have a role in apoptosis of autoreactive B cells and T cells. Consistent with the *in vitro* observation that Bim-deficient B cells are refractory to BCR-induced apoptosis [169], Bim-deficient mice have defective autoreactive B cell deletion [316]. When lethally irradiated mHEL transgenic mice were reconstituted with bone marrow (BM) from Bim-deficient anti-HEL MD4 transgenic mice, 2-fold more donor B cells were recovered from BM and 6-fold more from spleen compared to the $Bim^{+/+}$ control mice. These results suggest that Bim deficiency increases the numbers of both immature B cells and mature B cells [169]. When lethally irradiated sHEL transgenic mice were reconstituted with BM from Bim-deficient MD4, 17-fold more self-reactive B cells in the spleens of $Bim^{-/-}$ recipients compared with $Bim^{+/+}$ control [169]. These results show that Bim is essential for deletion of autoreactive B cells.

Due to it critical role in Bax and Bak activation, Bim is tightly regulated at the transcriptional and post-translational levels. In response to survival factor withdrawal and cell receptor stimulation, the mRNA and protein levels of Bim

increase [169, 317, 318]. Loss of cytokine-receptor stimulation causes inactivation of the kinase AKT, which in turn leads to activation of the transcription factor forkhead box O3A (FoxO3A), resulting in the increased level of Bim mRNA [318]. In response to T-cell or B-cell receptors stimulation, increased Bim mRNA and protein have been observed [169, 317]. Pre-treatment with FK506 and cyclosporine A inhibit Bim increase induced by T cell receptor stimulation, indicating that calcineurin activity is necessary for Bim increase [167]. In addition to transcriptional regulation, Bim can be post-translationally regulated. Bim_{EL} and Bim_{L} can be sequestered by the microtubular dynein-motor complex through binding to the dynein light chain (DLC1). Bim_{EL} and Bim_{L} could be regulated by phosphorylation by MAPK kinases including JNK and ERK (Figure 2.51; [319-321]).

Among the three major Bim isoforms, Bim_{S} is the most potent. Unlike Bim_{EL} and Bim_{L}, Bim_{S} can not be sequestered by microtubular dynein-motor complex (Figure 2.51, [319]). Bim_{S} lacks of ERK1/2 and JNK binding domain and could not be regulated by these MAPK phosphorylation (Figure 2.51, [319]). Bim_{S} is selectively induced by anti-IgM and Bz-423 co-treatment. Although the detailed mechanism of the Bim_{S} induction induced by anti-IgM and Bz-423 co-treatment is not clear, it is proposed that calcium-calcineurin may be responsible because calcineurin is known to be necessary in Bim expression increase in response to TCR stimulation and ionomycin treatment [167]. As Bim plays a critical role in deleting autoreactive B cells [169, 316], it is highly possible that Bz-423 can selectively induce cell death of autoreactive B cells through increasing Bim_{S}.

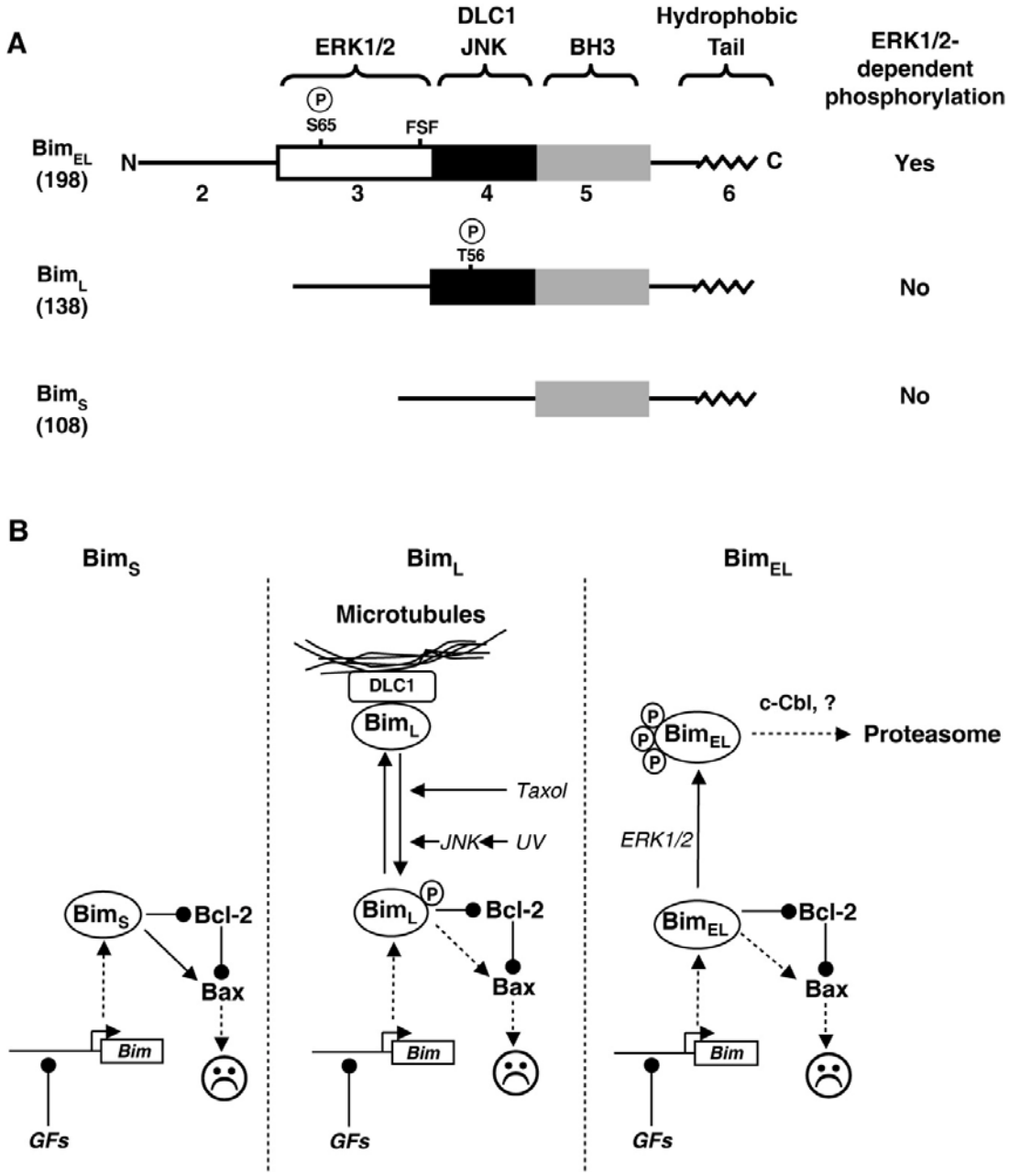

Figure 2.51: Bim isoforms and their regulations. (A) The carton structure of three isoforms of Bim. The numbers below Bim_{EL} are the exon numbers. Exon 3 is the region for ERK phosphorylation. and Exon 4 is the region binding to DLC1 and phosphorylation site inside this region is labeled. Exon 5 is BH3 region. Exon 6 is the region for hydrophobic tail. (B) regulation of different isoforms. They are transcriptionally regulated. In response to taxol treatment or JNK phosphorylation, BimL can be dissociated with DLC1 for its pro-apoptotic activity. Bim_{EL} can be phosphorylated by ERK to signal the proteasomal degradation. Both panel A and Panel B are adapted from [319].

Bmf is a potential target for SLE treatment as it is important for B cell homeostasis: Bmf is a BH3-only protein that shares a conserved amino-terminal DLC binding motif with Bim [322]. It is sequestered by the myosin V motors [322]. Phosphorylation of Bmf by MAPK increases binding to DLC2 in the cytoskeleton. MAPK inhibition induces translocation of Bmf from DLC2 to cytosol or mitochondria and promotes apoptosis [94]. Bmf expression is also preferentially upregulated in response to histone deacetylase inhibitors, suggesting that histone hyperacetylation causes Bmf transcription activation [296]. In response to oxidative stress by arsenic trioxide (ATO), Bmf expression is increased and results in cell death [323]. Glutathione (GSH) depletion and anti-oxidant N-acetylcysteine (NAC) regulated ATO-induced Bmf level and subsequent cell death [323], indicating the critical role of ROS in Bmf transcription activation.

Bmf-deficient mice develop a B cell-restricted lymphadenopathy [268], which is consistent with high expression in B cells [324]. Analysis of various B cell subsets revealed significant increases in pre-B cells, transitional T1 cells, and mature B cells in Bmf-deficient mice [268]. This result shows the critical role of Bmf in B cell homeostasis. Pre-B cells isolated from Bmf-deficient mice are resistant to a range of apoptotic stimuli such as dexamethasome and the histone deacetylase inhibitor (SAHA). This phenotype may be responsible for B cell hyperplasia observed in the Bmf-deficient mice [268]. ATO induces apoptosis through transcriptional activation of Bmf in a ROS dependent manner [323]. Interestingly, apoptotic Bz-423 also induces ROS production and Bmf increase [316]. Thus Bz-423 might increase Bmf in a

ROS-dependent way similar to ATO. Although Bz-423 at low concentrations (≤ 5 μM in 2% FBS media) alone did not increase Bmf expression, co-treatment with anti-IgM induced a Bmf increase, possible by modulating ROS-mediated Bmf increase. How oxidative stress induced by ATO and Bz-423 increases Bmf is not clear. However, the correlation of ROS increase to Bmf expression suggests the possible role of ROS in the Bmf increase. Considering the critical role of Bmf in B cell homeostasis, Bmf increase induced by anti-IgM and Bz-423 co-treatment may contribute to Bz-423 efficacy observed *in vivo*.

In addition to the Bim and Bmf increases induced by co-treatment, there is a tBid increase. As Bid can be cleaved and activated to tBid by calpain, caspases, granzyme B and cathepsins [99]. General caspase inhibitor zVAD-fmk does block Bid cleavage, excluding caspase involvement in Bid cleavage. Calpain can be activated by calcium [325, 326]. Therefore it is possible calpain is activated by anti-IgM and Bz-423 co-treatment and contributes to Bid cleavage. However, calpain inhibitor II did not inhibit Bid cleavage, which eliminates the involvement of calpain in tBid increase. At high concentration both Bz-423 and anti-IgM also induce Bid cleavage, although the mechanisms are still elusive. More studies are needed to answer the following questions: How is Bid cleaved by anti-IgM and Bz-423 co-treatment? Does Bid cleavage by co-treatment adopt the same mechanism as Bz-423 or anti-IgM induced Bid cleavage? Although Bik is upregulated by anti-IgM stimulation (this thesis, [91]) and is involved in anti-IgM induced cell death [91], co-treatment with Bz-423 does not further increase Bik, indicating it is not a converging point. However,

this does not exclude the involvement of Bik in cell death induced by anti-IgM and Bz-423 co-treatment.

Bmf activates Bax and Bak by neutralizing Bcl-2 and Bcl-xL, tBid activates Bax and Bak by neutralizing to Mcl-1 and A1, and Bik activates Bax and Bak by neutralizing Bcl-xL and A1 [90]. Considering Bmf, tBid and Bik are weak activators of Bax and Bak and each of them alone might be insufficient to activate Bax and Bak. Therefore, Bmf, tBid and Bik may work together to activate Bax and Bak, which provides another interaction point for Bz-423 signaling and anti-IgM signaling to work together to activate Bax and Bak. The collaborative actions by BH3-only proteins were also reported in the literatures [327-329]. During neisseria gonorrhoeae infection, Bim and Bmf synergize to induce apoptosis [327]. Bid and Bim act together to induced apoptosis [328, 329].

Data presented in this chapter show that BH3-only proteins (Bim, Bmf, tBid and Bik) are induced by anti-IgM and Bz-423 co-treatment. They may work together to activate Bax and Bak, which is responsible for the cell death by co-treatment. Among these BH3-only proteins, Bim and Bmf are particularly interesting as their deficiency leads to the development of autoimmune diseases. BH3 mimetics, peptides and small molecules such as ABT-737, are cytotoxic to B lymphoid tumors and chronic lymphocyte leukemia [85]. ABT-737, which binds to Bcl-2 and Bcl-xL in low nanomolar affinity [330], kill acute myeloid leukemia (AML) cells but not normal hematopoietic progenitor cells *in vitro*, and delay leukemia in xenografts without collateral damage [331]. Due to the specific role of Bim in deleting autoreactive

lymphocyte and non-redundant function of Bmf in B cells homeostasis, small molecules mimicking Bim and Bmf or selectively increasing their expression may be effective and selective for the autoimmune therapies. Recently a BH3 peptideomimetic for Bim was shown to selectively kill pathogenic lymphocytes from B-cell chronic lymphocyte leukemia (B-CCL) over those from healthy individuals [332]. Adenoviral vector with Bim_S induces apoptosis in tumor cells C666-1 in a time- and dose-dependent manner. C666-1 cells with overexpressed Bim_S do not form tumors in severe combined immunodeficient (SCID) mice [333].

Calcineurin is a potential therapeutic target for lupus treatment: FK506 and cyclosporine A suppress immune function by inhibiting calcineurin [334, 335]. During lymphocyte activation, the rise in $[Ca^{2+}]_i$ activates calcineurin, a phosphatase which activates the transcription factor NFAT by dephosphorylation [336]. NFAT is responsible for the transcription of genes involved in activation such as IL-2, IL-4 [337]. As a result, calcineurin inhibitors FK506 and cyclosporine A block lymphocyte activation, and are used to treat a range of immune diseases [334, 338-340]. Due to their renal toxicity, FK506 and cyclosporine A are rarely used alone for SLE nephritis treatment [341]. Instead, calcineurin inhibitors are used in combination with other immunosuppressant reagents to minimize their side effects [342]. Compared to other conventional immunosuppressive treatments, calcineurin inhibitors are general immunosuppressants and do not have much advantage when for SLE [343].

Further studies suggest calcineurin mediates apoptosis induced by agents that increase $[Ca^{2+}]_i$ [244]. In both T cells and B cells, calcineurin activity is increased

during the apoptosis induced by receptor ligation and ionomycin [344, 345]. This observation suggests the possible involvement of calcineurin in apoptosis. FK506 and cyclosporine A inhibit calcineurin activity and prevent calcium-dependent cell death [166, 344-347], which confirms the involvement of calcineurin in apoptosis. Activated calcineurin may dephosphorylate and activate BH3-only protein Bad, which may be responsible for apoptosis [170]. Moreover, Bim and Bik are increased in response to cell receptor stimulation [91, 167]. Calcineurin inhibitors antagonize the increased expression of Bim and Bik, suggesting the involvement of calcineurin in Bim and Bik expression [91, 167]. Co-treatment of anti-IgM and Bz-423 induced NFAT-dependent transcription in a synergistic manner, indicating that co-treatment induces a synergistic increase in the calcineurin activity. Moreover, the cell death induced by co-treatment was inhibited by FK506 and cyclosporine A. These results suggest the involvement of calcineurin, which might be responsible for Bim and Bik increase by anti-IgM and Bz-423 co-treatment, possible through activating transcription factor NFAT. However, the involvement of other transcription factors could not be excluded.

In addition to regulating BH3-only proteins, the N-terminus of calcineurin can directly bind to BH4 domain of Bcl-2 [348], which suggests the possibility that calcineurin mediates apoptosis through simply sequestering Bcl-2 protein to inhibit synergy. NFAT, one substrate of calcineurin, is involved in apoptosis by inducing transcription of molecules involved in apoptosis, including FasL and Nur77 [166, 349]. Anti-IgM stimulation increases Nur77 expression, which then translocates to the

mitochondria and triggers cytochrome c release and apoptosis [166]. FK506 and the NFAT inhibitor VIVIT peptide block anti-IgM-induced Nur77 expression and subsequent cell death [166]. Being substrates of calcium-calcineurin signaling, Bad dephosphorylation, Nur77 expression and FasL expression induced by anti-IgM and Bz-423 co-treatment were studied. However, no Bad dephosphorylation, Nur77 or FasL increase were observed, limiting their involvement in cell death by co-treatment. More experiments need to be conducted to identify NFAT-regulated proteins involved in cell death by co-treatment. For example, the effects of calcineurin inhibitor FK506 and cyclosporine A on Bim, tBid and Bmf increase by anti-IgM and Bz-423 co-treatment could be conducted to confirm whether calcineurin is involved in activating these BH3-only proteins.

The observation that activated calcineurin can mediate apoptosis in lymphocytes suggests another strategy for autoimmune disease treatment. Instead of suppressing its activity to block lymphocytes activation, calcineurin can be activated to promote lymphocyte apoptosis. Compared with immunosuppression, this strategy is more selective in that calcium signaling is abnormal in pathogenic lymphocyte. In response to BCR stimulation, enhanced and sustained calcium increase was induced in lupus B cells [185, 350]. However, this hyperactivity of BCR signaling does not lead to apoptosis as lupus B cells are refractory to BCR-induced apoptosis [351]. Bz-423 may promote apoptosis mediated by BCR ligation. In SLE patients or lupus mice, self-antigen binds to self-reactive B cells. As anti-IgM sensitizes Ramos B cells to Bz-423, the binding of self-antigen to self-reactive B cells may also sensitizes cells

to Bz-423. Calcineurin expression was increased in PBMCs from SLE patients [352]. This increased calcineurin expression may be responsible for Bz-423 sensitivity as Bz-423 activates calcineurin. Moreover, estrogen stimulation is shown to increase calcineurin expression in a dose-dependent manner [353].

Materials and Methods

Materials: Chemicals were obtained from Sigma-Aldrich unless indicated. The basic information on inhibitors and several chemicals is listed in Table 2.3.

Cell lines and culture: Human Burkitt's lymphoma cell lines Ramos, ST486, Raji, Daudi, Namalwa, CA46 and the mouse immature B cell line WEHI-231, were purchased from American Type Culture Collection (ATCC). Ramos, ST486, Raji, Daudi, Namalwa, and CA46 were maintained in RPMI 1640 (Mediatech) supplemented with 10% heat-inactivated fetal bovine serum (10% FBS, Mediatech), penicillin (100 U/mL), streptomycin (100 μg/mL) and L-glutamine (290 μg/mL) (1x PSG, Mediatech) in a humidified incubator (37^{o}C, 5% CO_2). WHEI-231 were cultured in ATCC-formulated Dulbecco's modified Eagle's medium supplemented with 10% FBS, 1x PSG, non-essential amino acid (Mediatech) and 0.05 mM 2-mercaptoethanol. The Bcl-2 over-expressing and Bcl-xL over-expressing Ramos cells were maintained in complete media containing 1.5 mg/mL G418 (Gibco). Human diffuse large B-cell lymphoma (HDLBL) OCI-Ly7 was kindly provided by Dr. H. A. Messner [354], and was cultured in Iscove's modified Dulbecco's medium supplemented with 10% human serum and 1x PSG. Chicken DT40 B cells and Btk deficient DT40 B cells were purchased from ARIKEN bioresource center and were cultured in RPMI1640

Reagent	Final Conc.	Source	Stock solution
11R-VIVIT peptide	100 µM	Calbiochem	10mM in dH_2O
Actinomycin D	2 ng/mL	Sigma-Aldrich	1 mg/mL in DMSO
BAPTA salt	500 µM	Sigma-Aldrich	500mM in water
Bongkrekic Acid	50 µM	Calbiochem	100 mM in DMSO
cycloheximide	1 µg/mL	Sigma-Aldrich	1mg/mL in dH_2O
Cyclosporin A	0.5 µM	Sigma-Aldrich	10 mM in DMSO
DCFH-DA	5 µM	Invitrogen	10 mM in DMSO, freshly prepared
Dihydroethidium (DHE)	7.5 µM	Invitrogen	10 mM in DMSO, protected from light
$DIOC_6(3)$	20 nM	Invitrogen	10 mM in DMSO, protected from light
FK506	0.5 µM	Tecoland corporation	12.4 mM in EtOH
Fluo-3 AM	2 µM	Invitrogen	2 mM in DMSO, protected from light
Fura-2 AM	2 µM	Invitrogen	2 mM in DMSO, protected from light
JNK inhibitor II	2.5 µM	Calbiochem	5 mM in DMSO
LFM-A13	100 µM	Sigma-Aldrich	100 mM in DMSO
LY-58483	0.5 µM	Sigma-Aldrich	10 mM in DMSO
MnTBAP	100 µM	Alexis Biochemicals	100 mM in 50% EtOH, freshly prepared
PMA	10 ng/mL	Sigma-Aldrich	1 mg/mL in DMSO
TMRM	50 nM	Invitrogen	10 mM in DMSO, protected from light
Vitamin E	100 µM	Sigma-Aldrich	30 mM in EtOH, freshly prepared
zVAD-fmk	100 µM	Sigma-Aldrich	100 mM in DMSO

Table 2.3: Effective concentration, source, stock preparation for chemical reagents.

containing 4 mM Glutamine, 10% FBS, 1% chicken serum, and 50 µM 2-mercaptoethanol.

Treatments: To detect ROS, mitochondrial membrane potential ($\Delta\psi_m$) change and cell death (PI and $subG_0$ analysis) induced by anti-IgM and Bz-423 co-treatment, cells were plated in 96-well plates at a density of $5x10^5$ cells /mL in media containing 2% FBS, were then treated with a dose response of chemicals in the presence of 1 µg/mL anti-IgM (Cat#109-006-129, Jackson ImmunoResearch), using 1 µg/mL control Ig (Cat#005-000-036, Jackson ImmunoResearch) as a negative control. At indicated timepoints, cells were processed for specific assay. Inhibitors were pre-incubated for 30 min before treatment.

Detection of dead cells and hypodiploid DNA: At the endpoint, cells were stained with 1 µg/mL propidium iodide (PI) for 10 min at room temperature. Unlike live cells, dead cells are permeable to PI. Once PI binds to DNA, its fluorescence is enhanced. This enhanced PI fluorescence was measured by the FACSCalibur flow cytometry (BD Biosicence, San Diego,CA) in the FL3 channel. SubG0 peak analysis is able to detect the apoptotic cells in the dead cells. Cells were first stained in $subG_0$ buffer [50 µg/mL PI, 0.2% (v/v) Triton-X, 10 µg/mL RNase A in phosphate buffered saline (PBS)] for at least 12 h at 4^oC. Then the apoptotic hypodiploid $subG_0$ peak was detected by the flow cytometry in the FL2 channel on a linear scale. For each sample, 5000 events were recorded and the data were analyzed by cellquest software.

ROS measurement: Dihydroethidium (DHE) and 4', 7'-dichlorodihydrofluorescin diacetate (DCFH-DA) were used to monitor superoxide and hydrogen peroxide, respectively. For superoxide measurement, 30' before the reading, DHE (7.5 μM) was applied to treated cells. The conversion of DHE to oxy-E by superoxide was detected in the FL2 channel of flow cytometry. For hydrogen peroxide measurement, cells were pre-loaded with DCFH-DA (5 μM) at 37^{o}C for 30 min. After one wash with excess PBS, the DCFH-DA pre-loaded cells were treated. At the desired timepoints, the fluorescence of the oxidized product 2', 7'-dichlorofluorescin (DCF) was monitored in the FL1 channel of flow cytometry. For each sample, 3000 events were recorded and the data were analyzed by the cellquest software.

Mitochondrial membrane potential ($\Delta\psi_m$) measurement: $\Delta\psi_m$ was measured either by tetramethyl rhodamine methyl ester (TMRM) or by 3, 3'-dihexyloxacarbocyanine, iodide [$DIOC_6$ (3)]. 30 min before reading in the flow cytometry, either $DIOC_6$(3) (20 nM) or TMRM (50 nM) was loaded to treated cells. The fluorescence of $DIOC_6$ (3) was measured by FL1 channel while that of TMRM was monitored in FL2 channel. Mitochondria uncoupler carbonylcyanide-p-trifluoromethoxyphenylhydrazone (FCCP) was used as a positive control for $\Delta\psi_m$ disruption. For each sample, 5000 events were recorded and the data were analyzed by the cellquest software.

Bz-423 washout Experiment: Ramos cells were plated in the round-bottom 96-well plates at density of 5x10^5 cells /mL in media containing 2% FBS. And the

cells were treated with a series concentration of Bz-423 in the presence of 1 μg/mL anti-IgM or 1 μg/mL control Ig. At indicated time, cells were spun at 1000 g for 7 min, and were washed once with media containing 10% FBS. The After being resuspended in 2% FBS media containing either 1 μg/mL anti-IgM or 1 μg/mL control Ig, the washed cells were then incubated for the remainder of the experiment, and viability was determined by PI permeability assay and $subG_0$ peak analysis.

Cell surface staining: Half a million of treated Ramos cells were harvested and resuspended in 100 μL staining buffer [PBS + 2% FBS + 0.02% (w/v) NaN_3]. FITC-conjugated anti-IgM or FITC-conjugated anti-Fas was applied to cells and cells were incubated on ice for 30 min. After washing once with staining buffer, the FITC fluorescence was measured in the FL1 channel of flow cytometry. FasL on the cell surface was stained with mouse anti-human FasL in 100 μL staining buffer on ice for 30 min. After three washes, cells were incubated with PE-conjugated anti-mouse IgG_1 in 100 μL staining buffer on ice for another 30 min. After one wash, FasL expression was determined by measuring the PE fluorescence in the FL2 channel of flow cytometry. For each sample, 6000 events were recorded.

Continuous Ca^{2+} measurement: The kinetic intracellular [Ca^{2+}] change induced by anti-IgM and Bz-423 co-treatment was measured using either ratiometric Ca^{2+} indicator fura-2 in a fluorescence plate reader or another Ca^{2+} indicator fluo-3 through the flow cytometry. Fura-2 is excited at 340 nm and 380 nm and the ratio of the emission at those wavelengths is directly correlated to [Ca^{2+}]. The ratiometric character of Fura-2 corrects artificial difference in the fluorescence signal due to

unequal dye loading and dye bleaching [355]. Another Ca^{2+} indicator fluo-3 is excited at 506 nm and emitted at 526 nm, which is used for Ca^{2+} measure in the flow cytometry. The ester forms (AM) of both dyes were used to assist the dye loading into the cells, where they were de-esterified by esterase, causing them to be retained in the cells. Ramos cells ($1x10^6$ cells /mL) were loaded with calcium indicator (fluo-3 AM, fura-2 AM) in loading buffer (1 mM $CaCl_2$, 1 mM $MgCl_2$ and 2% FBS in PBS) at 37^oC for 30 min. After dye-loaded cells were washed with PBS, they were resuspended in the loading buffer at $5x10^5$ cells /mL and ready for treatment. For intracellular [Ca^{2+}] measurement by flow cytometry, fluo-3-loaded Ramos cells were firstly incubated with 5 μM Bz-423 or its vehicle control DMSO. Right before stimulation by anti-IgM, the baseline of fluo-3 fluorescence was monitored in the FL1 channel. Immediately following anti-IgM stimulation, fluo-3 fluorescence change was recorded for 8-10 min. For intracellular [Ca^{2+}] measurement by plate reader, fura-2 loaded cells were plated in the 96 black-well plate (cat# 237108, Fisher). 10 min after 5 μM Bz-423 or DMSO incubation with cells at 37^oC for 10 min, the baseline was read. Immediately after addition of 1 μg/mL control Ig or 1μg/mL anti-IgM, fura-2 fluorescence change was monitored. The fluorescence at maximal [Ca^{2+}] was determined by the addition of ionophore Br-A23187 (2 μg/mL) and the fluorescence at minimum [Ca^{2+}] was determined by addition of 5 mM ethylene glycol tetraacetic acid (EGTA) to Br-A23187-treated cells. The [Ca^{2+}] was calculated based on the following equation: $[Ca^{2+}] = K_d*Q*[(R-R_{min})/(R_{max}-R)]$, In this equation, K_d is the dissociation constant, which was measured to be 120 nM in Ramos cells using Ca^{2+}

calibration buffer kit #1 (c-3008, Invitrogen) based on the manufacture's protocol; R represents the ratio of the fluorescence intensity at 340 nm over that at 380 nm, that is F_{340}/F_{380}; R_{min} and R_{max} correspond to F_{340}/F_{380} at the minimum and maximum $[Ca^{2+}]$, respectively; Q is the ratio of fluorescence intensity excited by 380 nm at minimum $[Ca^{2+}]$ over that at maximum $[Ca^{2+}]$, that is F_{min}/F_{max} at 380 nm.

Mitochondria isolation: Two methods were used to isolate mitochondria: the needle method and the digitonin permeablization method. The needle method produces relative purer mitochondria while the digitonin method produces cytosol fraction with less contamination of broken mitochondria. For both methods, the purity of fractions was tested by immunoblotting with cytosol specific antibody β-tubulin and mitochondria specific antibody β-subunit of F_0F_1-ATPase.

The needle method takes advantage of the size difference between swollen cells and mitochondria. When passed through a needle, the swollen cells are broken open while mitochondria are kept intact. $5x10^6$ Cells were swollen on ice for 20 min in 100 μL hypotonic Buffer A (20 mM Hepes-KOH, pH7.5, 10 mM KCl, 10 mM β-glycerophophate, 5 mM NaF, 1.5 mM $MgCl_2$, 1 mM EDTA, 1 mM EGTA, 1 mM DTT, 1 mM Na_3VO_4, 250 mM sucrose, 0.1 mM PMSF) with complete cocktail protein inhibitors (Roche). The swollen cells were disrupted by 8 strokes through a 28.5 gauge needle. The homogenate was spun down at 500x g for 10 min at 4^oC to pellet nuclei and unbroken cells. The supernatant was centrifuged at maximum speed in a microcentrifuge for 30 min at 4^oC to yield supernatant (cytosol fraction) and pellet (mitochondria fraction). The mitochondria pellet was further lysed in 50 μL 1x

WCE buffer (25 mM Hepes, pH 7.7, 150 mM NaCl, 2.5 mM $MgCl_2$, 0.2 mM EDTA, 0.1% Triton X-100, 20 mM β-glycerophophate, 0.5 mM DTT, 3.3 mM NaF, 0.1 mM Na_3VO_4, 1 mM PMSF) with protease inhibitor.

At the proper concentration, digitonin selectively permeablizes plasma membrane and could be used for isolating cytosolic fraction [356]. The digitonin permeablization method was adopted from the method measuring cytochrome c release using the flow cytometry [357]. At harvested time point, 5 x 10^6 Cells were harvest, rinsed with PBS, and permeablized in 100 μL of ice-cold cell lysis and mitochondria intact (CALMI) buffer (120 mM KCl, 1 mM EDTA, 175 μg/mL digitonin) on ice for 5 min. Then the permeablized cells were centrifuged at 500 g for 10 min at 4°C. The cytosolic fraction (supernatant) was removed. The pellet containing mitochondria was lysed in 50 μL 1x WCE buffer. The efficiency of plasma membrane permeablization by digitonin was verified by trypan blue staining to be greater than 95%.

Cytosol and nuclear fractionation: At indicated treatment times, 1x10^7 cells were washed once with ice-cold PBS, resuspended in 200 μL ice-cold low-salt buffer (10 mM Hepes-KOH pH 7.9, 10 mM KCl, 0.2 mM EDTA, 1 mM DTT, 0.5 mM PMSF plus protease inhibitor cocktail), and incubated on ice for 20 min. The homogenate was then centrifuged at 500 g for 10 min at 4°C. The supernatant (cytosolic fraction) was removed, and the nuclear pellet was resuspended in 200 μL ice-cold high-salt buffer (20 mM Hepes-KOH pH 7.9, 400 mM NaCl, 0.2 mM EDTA, 1 mM DTT, 0.5 mM PMSF plus protease inhibitor cocktail). The nuclear fraction was

vigorously vortexed for 5 min, followed by incubation on ice for another 5 min. This vortexing and ice-incubation steps were repeated for 5 times. This nuclear extracts were spun down and the supernatants were collected as the nuclear fractions. The successful separation between cytosol and nuclear was confirmed by immunoblotting for cytosol-specific antibody β-tubulin and nucleus-specific antibody CREB.

Western Blot: $5x10^6$ treated cells were harvested and washed once in ice-cold PBS and lysed in 50 µL 1x WCE buffer with complete protease inhibitor cocktail. Following incubation on ice for 30 min, the supernatant was collected by centrifugation at full speed for 30 min. The protein concentration was quantified by bradford protein assay, using bovine serum albumin (BSA) to make a standard curve. Equal amounts of the whole cell lysates were heat-denatured at 95^oC for 5 min in 30 µL total volume containing 5 µL of 6x SDS loading buffer (350 mM Tris-HCl pH 6.8, 10.28 % SDS, 36 % (v/v) glycerol, 0.6 M DTT, 0.012 % (w/v) bromophenol blue). The heated sample was loaded to polyacrylamide gel. After transferring into the PVDF membrane (Bio-Rad), it was blocked in 5% milk in PBS containing 0.5% (v/v) tween 20. Primary antibody was incubated at 4^oC overnight in 1% non-fat milk in 1x PBS plus 0.5% (v/v) tween 20. After 3 extensive 5 min washing in 1x PBS plus 0.5% (v/v) tween 20, secondary antibody (GE healthcare) was applied and incubated for 1 h at room temperature. The blots were then developed using ECL^{TM} western blotting detection reagents (GE healthcare). The detailed information of antibodies used was

Reagent	dilution	Source	Catalog #
FITC-conjugated anti-IgM	1:50	Jackson ImmunoResearch	109-096-043
FITC-conjugated Fas	1:50	BD Bioscience	340479
PE-conjugated anti-mouse IgG1	1:50	BD Bioscience	555749
Mouse anti-human FasL	1:100	BD Bioscience	556374
CREB	1:2000	Millipore	AB3006
Cytochrome c	1:1000	BD Bioscience	556432
AIF	1:1000	BD Bioscience	551429
Smac	1:1000	Alexis Biochemicals	210-788-C100
β-subunit of F0F1-ATPase	1:3000	Invitrogen	A-21351
Bcl-2	1:1000	Dakocytomation	M0887
Bcl-xL	1:1000	BD Bioscience	556361
Bmf	1:1000	abgent	AP1309a
Bad	1:1000	BD Bioscience	610392
Blk	1:1000	Santa Cruz Biotech	sc-329
Bid	1:1000	Cell Signaling Technology	2002
Bim	1:1000	BD Bioscience	559685
Noxa	1:1000	Calbiochem	OP180
Puma	1:1000	eBioscience	14-6041
Bak	1:2000	Millipore	06-536
Bax	1:2000	Millipore	06-499
Mcl-1	1:1000	Santa Cruz Biotech	sc-12756
A1	1:1000	Santa Cruz Biotech	sc-8351
Calcineurin	1:1000	BD Bioscience	556350
NFATc2 (4G6-G5)	1:250	Santa Cruz Biotech	sc-7296
NFAT1	1:1500	BD Bioscience	610702
β-tubulin	1:3000	Sigma-Aldrich	T4026
Nur77	1:1000	Santa Cruz Biotech	sc-5569

GAPDH	1:10000	Chemicon	MAB374
Bad	1:40	Santa Cruz Biotech	sc-942
14-3-3	1:1000	Santa Cruz Biotech	sc-629
Phospho-Bad at Ser 112	1:1000	Upstate biotech	06-853
Phosphor-Bad at Ser 136	1:1000	Upstate biotech	06-846

Table 2.4: Information of antibodies applied in western blots, immunoprecipitation, immunofluorescence and flow cytometry.

listed in Table 2.4. Specifically, for detection of NFATc2 using antibody from Santa cruz biotech, to maximize the NFATc2 signaling and to minimize background, the membrane were blocked in 5% non-fat milk overnight followed by 2 h incubation of NFATc2 antibody (1:200 dilution) at room temperature.

Immunoprecipitation: At the indicated time, $1x10^7$ Ramos cells were lysed for 30 min on ice in 200 μL of Nondiet P-40 lysis buffer (50 mM Tris, pH 7.5, 140 mM NaCl, 0.1% Nondiet P-40, 5 mM EDTA, 5 mM NaF, 1 mM Na_3VO_4, 0.1 mM PMSF with complete cocktail protein inhibitors). The whole cell lysate was collected after 30 min spin at max speed in the microcentrifuge at 4^oC. Before immunoprecipitation with Bad antibody, the lysate was first pre-cleared with 20 μL protein A/G plus agarose beads (sc-2003, Santa Cruz Biotech). After 30' incubation at 4^oC with gentle agitation, the cell lysate was spun down and the supernatant was kept for immunoprecipitation. The pre-cleared cell lysate was incubated with 1 μg anti-Bad antibody (sc-942, Santa Cruz Biotech) overnight at 4^oC with gentle agitation, using normal rabbit IgG (sc-2027, Santa Cruz Biotech) as a negative control. 20 μL of protein A/G plus agarose beads were then added to each sample. After 4 h incubation

of lysate-beads at 4^{o}C with gentle agitation, lysate were centrifuged to remove the supernatant. After 10 min washing beads with lysis buffer for three times, they were resuspended 80 µL of 2x loading buffer (0.125 M Tris-Cl, pH 6.8, 2% SDS, 10% glycerol, 5% (v/v) 2-mercaptoethanol, 0.0025% (w/v) bromophenol blue). The samples were then boiled at 95^{o}C for 5 min to release the pulled-down proteins from the protein-A/G beads and to denature them. In each gel, 25 µL per sample were loaded for western blot. The antibodies detecting phosphor-Bad at Ser 112 and Ser 136 were used for bad de-phosphorylation. And dissociation of Bad with 14-3-3 was studied using 14-3-3 antibody. The detailed information of antibodies used was shown in table 2.4.

Immunofluorescence to detect activated Bax and Bak: At indicated times, treated Ramos cells were harvested and dried on slides. Cells were then fixed by 2% paraformaldehye in PBS (16% solution, cat # 15710, Electron Microscopy Science) for 15 min at room temperature. To remove the fixative and to block the non-specific binding, cells were washed for 6 times, each time 5 min, with blocking buffer [0.05 % (w/v) saponin, 5% FBS in PBS]. Cells were then stained with 1 µg/mL antibody against activated Bax (06-499, Upstate) or 1 µg/mL antibody against activated Bak (06-536, upstate) in the blocking buffer overnight at 4^{o}C. The following day, after six 5-min extensive washes with blocking buffer, the cells were incubated with FITC-conjugated anti-rabbit antibody (554020, BD bioscience) for 30 min at room temperature. After the same washing step, the samples were mounted in prolong anti-fade kit (p7481, invitrogen). Images (630x) were captured using SPOT advance

program and a SPOT RS slider digital camera (Diagnostic Instruments Inc) in a Leica DM-LB microscope.

Transient transfection for Bax and Bak RNAi knockdown: siGENOME SMARTpool regents for human Bax and Bak were purchased from Dharmacon. siGENOME. And none-targeting siRNA#1 (D-001210-01-05, Dharmacon) was used as a negative control. These siRNA oligos were dissolved in 1x siRNA buffer (0.2 mM $MgCl_2$, 60 mM KCl, and 6 mM Hepes-pH 7.5) at a concentration of 20 μM, aliquoted and kept at -80^{o}C. Before electroporation, 8x10^{6} Ramos cells were washed once with ice-cold PBS and then resuspended in 100 μL of electroporation buffer T (Amaxa) with 5 μL of 20 μM Bax RNAi or Bak RNAi. Cells were electroporated using program N-16 on the amaxa nucleofector apparatus. The shocked Ramos cells recovered in the pre-warm RPMI1640 media containing 10% FBS at 37^{o}C for at least 8 h before the following shock. Electroporation was done twice during the 1st day, once the 2nd day. 24 h after the final shock, Ramos cells were treated. RNAi knockdown efficiency was determined by western blotting for Bax and Bak expression level.

Transient transfection and SEAP activity measurement: pNFAT-SEAP, pNFκB-SEAP, pAP1-SEAP are mammalian expression vectors (clontech) for reporting specific transcription activities, in which transcription of secreted alkaline phosphatase (SEAP) is driven by 3 copies of NFAT response element, 4 copies of NFκB consensus sequence and 4 copies of AP1 enhancer, respectively. 8x10^{6} cells were washed with ice-cold PBS, resuspended in 100 μL electroporation buffer T

(Amaxa) with 2 μg of indicated reporter plasmids, and subjected to electroporation using amaxa nucleofector apparatus using program G-16. Immediately electroporated cells were transferred into media with 10% FBS and recovered for 24 h. The following day, cells were then resuspended in 2% FBS media for treatment. At the indicated time, the supernatant was harvested for the SEAP activity measurement, which was performed using the Great EscAPe SEAP chemiluminescence kit (clontech) according to the manufacture instruction.

Statement of collaboration: Dr. Tom Sunderberg constructed Bcl-2 overexpressing Ramos cells and Bcl-xL overexpressing Ramos cells. Costas A Lyssiotis tested cell death induced by anti-IgM and Bz-423 co-treatment in OCI-Ly7 cell line.

Bibliography

1. Walker, N.I., Harmon, B.V., Gobe, G.C., Kerr, J.F. (1988). Patterns of cell death. Methods Achiev Exp Pathol *13*, 18-54.

2. Arends, M.J., Wyllie, A.H. (1991). Apoptosis: mechanisms and roles in pathology. Int Rev Exp Pathol *32*, 223-54.

3. Green, D.R., Cotter, T.G. (1992). Introduction: apoptosis in the immune system. Semin Immunol *4*, 355-62.

4. Kang, M.H., Reynolds, C.P. (2009). Bcl-2 inhibitors: targeting mitochondrial apoptotic pathways in cancer therapy. Clin Cancer Res *15*, 1126-32.

5. Merino, D., Bouillet, P. (2009). The Bcl-2 family in autoimmune and degenerative disorders. Apoptosis *14*, 570-83.

6. Riedl, S.J., Salvesen, G.S. (2007). The apoptosome: signalling platform of cell death. Nat Rev Mol Cell Biol *8*, 405-13.

7. Salvesen, G.S., Dixit, V.M. (1997). Caspases: intracellular signaling by proteolysis. Cell *91*, 443-6.

8. Scaffidi, C., Krammer, P.H., Peter, M.E. (1999). Isolation and analysis of components of CD95 (APO-1/Fas) death-inducing signaling complex. Methods *17*, 287-91.

9. Zou, H., Li, Y., Liu, X., Wang, X. (1999). An APAF-1.cytochrome c multimeric complex is a functional apoptosome that activates procaspase-9. J Biol Chem *274*, 11549-56.

10. Bredesen, D.E. (2000). Apoptosis: overview and signal transduction pathways. J Neurotrauma *17*, 801-10.

11. Ow, Y.P., Green, D.R., Hao, Z., Mak, T.W. (2008). Cytochrome c: functions beyond respiration. Nat Rev Mol Cell Biol *9*, 532-42.

12. Muzio, M., Chinnaiyan, A.M., Kischkel, F.C., O'Rourke, K., Shevchenko, A., Ni, J., Scaffidi, C., Bretz, J.D., Zhang, M., Gentz, R., Mann, M., Krammer, P.H., Peter, M.E., Dixit, V.M. (1996). FLICE, a novel FADD-homologous ICE/CED-3-like protease, is recruited to the CD95 (Fas/APO-1) death--inducing signaling complex. Cell *85*, 817-27.

13. Chinnaiyan, A.M., O'Rourke, K., Tewari, M., Dixit, V.M. (1995). FADD, a novel death domain-containing protein, interacts with the death domain of Fas and initiates apoptosis. Cell *81*, 505-12.

14. Xu, G., Shi, Y. (2007). Apoptosis signaling pathways and lymphocyte homeostasis. Cell Res *17*, 759-71.

15. Verhagen, A.M., Ekert, P.G., Pakusch, M., Silke, J., Connolly, L.M., Reid, G.E., Moritz, R.L., Simpson, R.J., Vaux, D.L. (2000). Identification of DIABLO, a mammalian protein that promotes apoptosis by binding to and antagonizing IAP proteins. Cell *102*, 43-53.

16. Du, C., Fang, M., Li, Y., Li, L., Wang, X. (2000). Smac, a mitochondrial protein that promotes cytochrome c-dependent caspase activation by eliminating IAP inhibition. Cell *102*, 33-42.

17. Susin, S.A., Lorenzo, H.K., Zamzami, N., Marzo, I., Snow, B.E., Brothers, G.M., Mangion, J., Jacotot, E., Costantini, P., Loeffler, M., Larochette, N., Goodlett, D.R., Aebersold, R., Siderovski, D.P., Penninger, J.M., Kroemer, G. (1999). Molecular characterization of mitochondrial apoptosis-inducing factor. Nature *397*, 441-6.

18. van Loo, G., Schotte, P., van Gurp, M., Demol, H., Hoorelbeke, B., Gevaert, K., Rodriguez, I., Ruiz-Carrillo, A., Vandekerckhove, J., Declercq, W., Beyaert, R., Vandenabeele, P. (2001). Endonuclease G: a mitochondrial protein released in apoptosis and involved in caspase-independent DNA degradation. Cell Death Differ *8*, 1136-42.

19. Li, L.Y., Luo, X., Wang, X. (2001). Endonuclease G is an apoptotic DNase when released from mitochondria. Nature *412*, 95-9.

20. Nagata, S., Nagase, H., Kawane, K., Mukae, N., Fukuyama, H. (2003). Degradation of chromosomal DNA during apoptosis. Cell Death Differ *10*, 108-16.

21. Li, H., Zhu, H., Xu, C.J., Yuan, J. (1998). Cleavage of BID by caspase 8 mediates the mitochondrial damage in the Fas pathway of apoptosis. Cell *94*,

491-501.

22. Crompton, M. (1999). The mitochondrial permeability transition pore and its role in cell death. Biochem J *341 (Pt 2)*, 233-49.

23. Kinnally, K.W., Antonsson, B. (2007). A tale of two mitochondrial channels, MAC and PTP, in apoptosis. Apoptosis *12*, 857-68.

24. Brustovetsky, N., Brustovetsky, T., Jemmerson, R., Dubinsky, J.M. (2002). Calcium-induced cytochrome c release from CNS mitochondria is associated with the permeability transition and rupture of the outer membrane. J Neurochem *80*, 207-18.

25. Yang, J.C., Cortopassi, G.A. (1998). Induction of the mitochondrial permeability transition causes release of the apoptogenic factor cytochrome c. Free Radic Biol Med *24*, 624-31.

26. Sparagna, G.C., Gunter, K.K., Gunter, T.E. (1994). A system for producing and monitoring in vitro calcium pulses similar to those observed in vivo. Anal Biochem *219*, 96-103.

27. Zamzami, N., Kroemer, G. (2001). The mitochondrion in apoptosis: how Pandora's box opens. Nat Rev Mol Cell Biol *2*, 67-71.

28. Gogvadze, V., Zhivotovsky, B. (2007). Alteration of mitochondrial function and cell sensitization to death. J Bioenerg Biomembr *39*, 23-30.

29. Javadov, S., Karmazyn, M. (2007). Mitochondrial permeability transition pore opening as an endpoint to initiate cell death and as a putative target for cardioprotection. Cell Physiol Biochem *20*, 1-22.

30. Kowaltowski, A.J., Castilho, R.F., Vercesi, A.E. (2001). Mitochondrial permeability transition and oxidative stress. FEBS Lett *495*, 12-5.

31. Green, D.R., Kroemer, G. (2004). The pathophysiology of mitochondrial cell death. Science *305*, 626-9.

32. Zoratti, M., Szabo, I., De Marchi, U. (2005). Mitochondrial permeability transitions: how many doors to the house? Biochim Biophys Acta *1706*, 40-52.

33. Gunter, T.E., Yule, D.I., Gunter, K.K., Eliseev, R.A., Salter, J.D. (2004). Calcium and mitochondria. FEBS Lett *567*, 96-102.

34. Halestrap, A.P., Connern, C.P., Griffiths, E.J., Kerr, P.M. (1997). Cyclosporin A binding to mitochondrial cyclophilin inhibits the permeability transition pore and protects hearts from ischaemia/reperfusion injury. Mol Cell Biochem *174*, 167-72.

35. Baines, C.P., Kaiser, R.A., Purcell, N.H., Blair, N.S., Osinska, H., Hambleton, M.A., Brunskill, E.W., Sayen, M.R., Gottlieb, R.A., Dorn, G.W., Robbins, J., Molkentin, J.D. (2005). Loss of cyclophilin D reveals a critical role for mitochondrial permeability transition in cell death. Nature *434*, 658-62.

36. Dubinsky, J.M., Levi, Y. (1998). Calcium-induced activation of the mitochondrial permeability transition in hippocampal neurons. J Neurosci Res *53*, 728-41.

37. Li, V., Brustovetsky, T., Brustovetsky, N. (2009). Role of cyclophilin D-dependent mitochondrial permeability transition in glutamate-induced calcium deregulation and excitotoxic neuronal death. Exp Neurol

38. Bernardes, C.F., Meyer-Fernandes, J.R., Basseres, D.S., Castilho, R.F., Vercesi, A.E. (1994). Ca(2+)-dependent permeabilization of the inner mitochondrial membrane by 4,4'-diisothiocyanatostilbene-2,2'-disulfonic acid (DIDS). Biochim Biophys Acta *1188*, 93-100.

39. Siliprandi, D., Scutari, G., Zoccarato, F., Siliprandi, N. (1974). Action of 'diamide' on some energy linked processes of rat liver mitochondria. FEBS Lett *42*, 197-9.

40. Lenartowicz, E., Bernardi, P., Azzone, G.F. (1991). Phenylarsine oxide induces the cyclosporin A-sensitive membrane permeability transition in rat liver mitochondria. J Bioenerg Biomembr *23*, 679-88.

41. Vieira, H.L., Haouzi, D., El Hamel, C., Jacotot, E., Belzacq, A.S., Brenner, C., Kroemer, G. (2000). Permeabilization of the mitochondrial inner membrane during apoptosis: impact of the adenine nucleotide translocator. Cell Death Differ *7*, 1146-54.

42. Valle, V.G., Fagian, M.M., Parentoni, L.S., Meinicke, A.R., Vercesi, A.E. (1993). The participation of reactive oxygen species and protein thiols in the mechanism of mitochondrial inner membrane permeabilization by calcium plus prooxidants. Arch Biochem Biophys *307*, 1-7.

43. Halestrap, A.P., Woodfield, K.Y., Connern, C.P. (1997). Oxidative stress, thiol reagents, and membrane potential modulate the mitochondrial permeability

transition by affecting nucleotide binding to the adenine nucleotide translocase. J Biol Chem *272*, 3346-54.

44. Manon, S., Roucou, X., Guerin, M., Rigoulet, M., Guerin, B. (1998). Characterization of the yeast mitochondria unselective channel: a counterpart to the mammalian permeability transition pore? J Bioenerg Biomembr *30*, 419-29.

45. Castilho, R.F., Kowaltowski, A.J., Meinicke, A.R., Bechara, E.J., Vercesi, A.E. (1995). Permeabilization of the inner mitochondrial membrane by Ca2+ ions is stimulated by t-butyl hydroperoxide and mediated by reactive oxygen species generated by mitochondria. Free Radic Biol Med *18*, 479-86.

46. Sullivan, P.G., Thompson, M.B., Scheff, S.W. (1999). Cyclosporin A attenuates acute mitochondrial dysfunction following traumatic brain injury. Exp Neurol *160*, 226-34.

47. Feldmann, G., Haouzi, D., Moreau, A., Durand-Schneider, A.M., Bringuier, A., Berson, A., Mansouri, A., Fau, D., Pessayre, D. (2000). Opening of the mitochondrial permeability transition pore causes matrix expansion and outer membrane rupture in Fas-mediated hepatic apoptosis in mice. Hepatology *31*, 674-83.

48. Kroemer, G., Dallaporta, B., Resche-Rigon, M. (1998). The mitochondrial death/life regulator in apoptosis and necrosis. Annu Rev Physiol *60*, 619-42.

49. Budd, S.L., Tenneti, L., Lishnak, T., Lipton, S.A. (2000). Mitochondrial and extramitochondrial apoptotic signaling pathways in cerebrocortical neurons. Proc Natl Acad Sci U S A *97*, 6161-6.

50. Tafani, M., Schneider, T.G., Pastorino, J.G., Farber, J.L. (2000). Cytochrome c-dependent activation of caspase-3 by tumor necrosis factor requires induction of the mitochondrial permeability transition. Am J Pathol *156*, 2111-21.

51. Jacotot, E., Ravagnan, L., Loeffler, M., Ferri, K.F., Vieira, H.L., Zamzami, N., Costantini, P., Druillennec, S., Hoebeke, J., Briand, J.P., Irinopoulou, T., Daugas, E., Susin, S.A., Cointe, D., Xie, Z.H., Reed, J.C., Roques, B.P., Kroemer, G. (2000). The HIV-1 viral protein R induces apoptosis via a direct effect on the mitochondrial permeability transition pore. J Exp Med *191*, 33-46.

52. Massari, P., Ho, Y., Wetzler, L.M. (2000). Neisseria meningitidis porin PorB

interacts with mitochondria and protects cells from apoptosis. Proc Natl Acad Sci U S A *97*, 9070-5.

53. Chipuk, J.E., Green, D.R. (2008). How do BCL-2 proteins induce mitochondrial outer membrane permeabilization? Trends Cell Biol *18*, 157-64.

54. Schlesinger, P.H., Gross, A., Yin, X.M., Yamamoto, K., Saito, M., Waksman, G., Korsmeyer, S.J. (1997). Comparison of the ion channel characteristics of proapoptotic BAX and antiapoptotic BCL-2. Proc Natl Acad Sci U S A *94*, 11357-62.

55. Antonsson, B., Conti, F., Ciavatta, A., Montessuit, S., Lewis, S., Martinou, I., Bernasconi, L., Bernard, A., Mermod, J.J., Mazzei, G., Maundrell, K., Gambale, F., Sadoul, R., Martinou, J.C. (1997). Inhibition of Bax channel-forming activity by Bcl-2. Science *277*, 370-2.

56. Saito, M., Korsmeyer, S.J., Schlesinger, P.H. (2000). BAX-dependent transport of cytochrome c reconstituted in pure liposomes. Nat Cell Biol *2*, 553-5.

57. Wei, M.C., Lindsten, T., Mootha, V.K., Weiler, S., Gross, A., Ashiya, M., Thompson, C.B., Korsmeyer, S.J. (2000). tBID, a membrane-targeted death ligand, oligomerizes BAK to release cytochrome c. Genes Dev *14*, 2060-71.

58. Lalier, L., Cartron, P.F., Juin, P., Nedelkina, S., Manon, S., Bechinger, B., Vallette, F.M. (2007). Bax activation and mitochondrial insertion during apoptosis. Apoptosis *12*, 887-96.

59. Wolter, K.G., Hsu, Y.T., Smith, C.L., Nechushtan, A., Xi, X.G., Youle, R.J. (1997). Movement of Bax from the cytosol to mitochondria during apoptosis. J Cell Biol *139*, 1281-92.

60. Gross, A., Jockel, J., Wei, M.C., Korsmeyer, S.J. (1998). Enforced dimerization of BAX results in its translocation, mitochondrial dysfunction and apoptosis. Embo J *17*, 3878-85.

61. Antignani, A., Youle, R.J. (2006). How do Bax and Bak lead to permeabilization of the outer mitochondrial membrane? Curr Opin Cell Biol *18*, 685-9.

62. Ihrlund, L.S., Hernlund, E., Viktorsson, K., Panaretakis, T., Barna, G., Sabapathy, K., Linder, S., Shoshan, M.C. (2006). Two distinct steps of Bak regulation during apoptotic stress signaling: different roles of MEKK1 and

JNK1. Exp Cell Res *312*, 1581-9.

63. Danial, N.N., Korsmeyer, S.J. (2004). Cell death: critical control points. Cell *116*, 205-19.

64. Strasser, A., O'Connor, L., Dixit, V.M. (2000). Apoptosis signaling. Annu Rev Biochem *69*, 217-45.

65. Wang, X. (2001). The expanding role of mitochondria in apoptosis. Genes Dev *15*, 2922-33.

66. Knudson, C.M., Tung, K.S., Tourtellotte, W.G., Brown, G.A., Korsmeyer, S.J. (1995). Bax-deficient mice with lymphoid hyperplasia and male germ cell death. Science *270*, 96-9.

67. Lindsten, T., Ross, A.J., King, A., Zong, W.X., Rathmell, J.C., Shiels, H.A., Ulrich, E., Waymire, K.G., Mahar, P., Frauwirth, K., Chen, Y., Wei, M., Eng, V.M., Adelman, D.M., Simon, M.C., Ma, A., Golden, J.A., Evan, G., Korsmeyer, S.J., MacGregor, G.R., Thompson, C.B. (2000). The combined functions of proapoptotic Bcl-2 family members bak and bax are essential for normal development of multiple tissues. Mol Cell *6*, 1389-99.

68. Wei, M.C., Zong, W.X., Cheng, E.H., Lindsten, T., Panoutsakopoulou, V., Ross, A.J., Roth, K.A., MacGregor, G.R., Thompson, C.B., Korsmeyer, S.J. (2001). Proapoptotic BAX and BAK: a requisite gateway to mitochondrial dysfunction and death. Science *292*, 727-30.

69. Shimizu, S., Narita, M., Tsujimoto, Y. (1999). Bcl-2 family proteins regulate the release of apoptogenic cytochrome c by the mitochondrial channel VDAC. Nature *399*, 483-7.

70. Marzo, I., Brenner, C., Zamzami, N., Jurgensmeier, J.M., Susin, S.A., Vieira, H.L., Prevost, M.C., Xie, Z., Matsuyama, S., Reed, J.C., Kroemer, G. (1998). Bax and adenine nucleotide translocator cooperate in the mitochondrial control of apoptosis. Science *281*, 2027-31.

71. Nutt, L.K., Pataer, A., Pahler, J., Fang, B., Roth, J., McConkey, D.J., Swisher, S.G. (2002). Bax and Bak promote apoptosis by modulating endoplasmic reticular and mitochondrial Ca2+ stores. J Biol Chem *277*, 9219-25.

72. Oakes, S.A., Opferman, J.T., Pozzan, T., Korsmeyer, S.J., Scorrano, L. (2003). Regulation of endoplasmic reticulum Ca2+ dynamics by proapoptotic BCL-2 family members. Biochem Pharmacol *66*, 1335-40.

73. Scorrano, L., Oakes, S.A., Opferman, J.T., Cheng, E.H., Sorcinelli, M.D., Pozzan, T., Korsmeyer, S.J. (2003). BAX and BAK regulation of endoplasmic reticulum Ca2+: a control point for apoptosis. Science *300*, 135-9.

74. Di Paola, M., Zaccagnino, P., Montedoro, G., Cocco, T., Lorusso, M. (2004). Ceramide induces release of pro-apoptotic proteins from mitochondria by either a Ca2+ -dependent or a Ca2+ -independent mechanism. J Bioenerg Biomembr *36*, 165-70.

75. Kinsey, G.R., McHowat, J., Patrick, K.S., Schnellmann, R.G. (2007). Role of Ca2+-independent phospholipase A2gamma in Ca2+-induced mitochondrial permeability transition. J Pharmacol Exp Ther *321*, 707-15.

76. Voehringer, D.W., Meyn, R.E. (2000). Redox aspects of Bcl-2 function. Antioxid Redox Signal *2*, 537-50.

77. Hacker, G., Weber, A. (2007). BH3-only proteins trigger cytochrome c release, but how? Arch Biochem Biophys *462*, 150-5.

78. Motoyama, N., Wang, F., Roth, K.A., Sawa, H., Nakayama, K., Nakayama, K., Negishi, I., Senju, S., Zhang, Q., Fujii, S., et al. (1995). Massive cell death of immature hematopoietic cells and neurons in Bcl-x-deficient mice. Science *267*, 1506-10.

79. Veis, D.J., Sorenson, C.M., Shutter, J.R., Korsmeyer, S.J. (1993). Bcl-2-deficient mice demonstrate fulminant lymphoid apoptosis, polycystic kidneys, and hypopigmented hair. Cell *75*, 229-40.

80. Opferman, J.T., Letai, A., Beard, C., Sorcinelli, M.D., Ong, C.C., Korsmeyer, S.J. (2003). Development and maintenance of B and T lymphocytes requires antiapoptotic MCL-1. Nature *426*, 671-6.

81. Dai, Y., Grant, S. (2007). Targeting multiple arms of the apoptotic regulatory machinery. Cancer Res *67*, 2908-11.

82. Kuwana, T., Mackey, M.R., Perkins, G., Ellisman, M.H., Latterich, M., Schneiter, R., Green, D.R., Newmeyer, D.D. (2002). Bid, Bax, and lipids cooperate to form supramolecular openings in the outer mitochondrial membrane. Cell *111*, 331-42.

83. Kuwana, T., Bouchier-Hayes, L., Chipuk, J.E., Bonzon, C., Sullivan, B.A., Green, D.R., Newmeyer, D.D. (2005). BH3 domains of BH3-only proteins differentially regulate Bax-mediated mitochondrial membrane

permeabilization both directly and indirectly. Mol Cell *17*, 525-35.

84. Willis, S.N., Fletcher, J.I., Kaufmann, T., van Delft, M.F., Chen, L., Czabotar, P.E., Ierino, H., Lee, E.F., Fairlie, W.D., Bouillet, P., Strasser, A., Kluck, R.M., Adams, J.M., Huang, D.C. (2007). Apoptosis initiated when BH3 ligands engage multiple Bcl-2 homologs, not Bax or Bak. Science *315*, 856-9.

85. Adams, J.M., Cory, S. (2007). Bcl-2-regulated apoptosis: mechanism and therapeutic potential. Curr Opin Immunol *19*, 488-96.

86. Willis, S.N., Chen, L., Dewson, G., Wei, A., Naik, E., Fletcher, J.I., Adams, J.M., Huang, D.C. (2005). Proapoptotic Bak is sequestered by Mcl-1 and Bcl-xL, but not Bcl-2, until displaced by BH3-only proteins. Genes Dev *19*, 1294-305.

87. Imaizumi, K., Benito, A., Kiryu-Seo, S., Gonzalez, V., Inohara, N., Lieberman, A.P., Kiyama, H., Nunez, G. (2004). Critical role for DP5/Harakiri, a Bcl-2 homology domain 3-only Bcl-2 family member, in axotomy-induced neuronal cell death. J Neurosci *24*, 3721-5.

88. Oda, E., Ohki, R., Murasawa, H., Nemoto, J., Shibue, T., Yamashita, T., Tokino, T., Taniguchi, T., Tanaka, N. (2000). Noxa, a BH3-only member of the Bcl-2 family and candidate mediator of p53-induced apoptosis. Science *288*, 1053-8.

89. Nakano, K., Vousden, K.H. (2001). PUMA, a novel proapoptotic gene, is induced by p53. Mol Cell *7*, 683-94.

90. Willis, S.N., Adams, J.M. (2005). Life in the balance: how BH3-only proteins induce apoptosis. Curr Opin Cell Biol *17*, 617-25.

91. Jiang, A., Clark, E.A. (2001). Involvement of Bik, a proapoptotic member of the Bcl-2 family, in surface IgM-mediated B cell apoptosis. J Immunol *166*, 6025-33.

92. Spender, L.C., O'Brien, D.I., Simpson, D., Dutt, D., Gregory, C.D., Allday, M.J., Clark, L.J., Inman, G.J. (2009). TGF-beta induces apoptosis in human B cells by transcriptional regulation of BIK and BCL-X(L). Cell Death Differ

93. Barreyro, F.J., Kobayashi, S., Bronk, S.F., Werneburg, N.W., Malhi, H., Gores, G.J. (2007). Transcriptional regulation of Bim by FoxO3A mediates hepatocyte lipoapoptosis. J Biol Chem *282*, 27141-54.

94. VanBrocklin, M.W., Verhaegen, M., Soengas, M.S., Holmen, S.L. (2009). Mitogen-activated protein kinase inhibition induces translocation of Bmf to promote apoptosis in melanoma. Cancer Res *69*, 1985-94.

95. Takada, E., Hata, K., Mizuguchi, J. (2006). Requirement for JNK-dependent upregulation of BimL in anti-IgM-induced apoptosis in murine B lymphoma cell lines WEHI-231 and CH31. Exp Cell Res *312*, 3728-38.

96. Bergmann, A. (2002). Survival signaling goes BAD. Dev Cell *3*, 607-8.

97. Masters, S.C., Subramanian, R.R., Truong, A., Yang, H., Fujii, K., Zhang, H., Fu, H. (2002). Survival-promoting functions of 14-3-3 proteins. Biochem Soc Trans *30*, 360-5.

98. Klumpp, S., Krieglstein, J. (2002). Serine/threonine protein phosphatases in apoptosis. Curr Opin Pharmacol *2*, 458-62.

99. Yin, X.M. (2006). Bid, a BH3-only multi-functional molecule, is at the cross road of life and death. Gene *369*, 7-19.

100. Walensky, L.D., Pitter, K., Morash, J., Oh, K.J., Barbuto, S., Fisher, J., Smith, E., Verdine, G.L., Korsmeyer, S.J. (2006). A stapled BID BH3 helix directly binds and activates BAX. Mol Cell *24*, 199-210.

101. Sanchez, M., Misulovin, Z., Burkhardt, A.L., Mahajan, S., Costa, T., Franke, R., Bolen, J.B., Nussenzweig, M. (1993). Signal transduction by immunoglobulin is mediated through Ig alpha and Ig beta. J Exp Med *178*, 1049-55.

102. Reth, M. (1989). Antigen receptor tail clue. Nature *338*, 383-4.

103. Wang, L.D., Clark, M.R. (2003). B-cell antigen-receptor signalling in lymphocyte development. Immunology *110*, 411-20.

104. Satterthwaite, A.B., Li, Z., Witte, O.N. (1998). Btk function in B cell development and response. Semin Immunol *10*, 309-16.

105. Oh-hora, M., Rao, A. (2008). Calcium signaling in lymphocytes. Curr Opin Immunol *20*, 250-8.

106. Gwack, Y., Feske, S., Srikanth, S., Hogan, P.G., Rao, A. (2007). Signalling to transcription: store-operated Ca2+ entry and NFAT activation in lymphocytes.

Cell Calcium *42*, 145-56.

107. Weiss, A., Littman, D.R. (1994). Signal transduction by lymphocyte antigen receptors. Cell *76*, 263-74.

108. Yankee, T.M., Clark, E.A. (2000). Signaling through the B cell antigen receptor in developing B cells. Rev Immunogenet *2*, 185-203.

109. Kurosaki, T., Maeda, A., Ishiai, M., Hashimoto, A., Inabe, K., Takata, M. (2000). Regulation of the phospholipase C-gamma2 pathway in B cells. Immunol Rev *176*, 19-29.

110. Knox, K.A., Finney, M., Milner, A.E., Gregory, C.D., Wakelam, M.J., Michell, R.H., Gordon, J. (1992). Second-messenger pathways involved in the regulation of survival in germinal-centre B cells and in Burkitt lymphoma lines. Int J Cancer *52*, 959-66.

111. Shambharkar, P.B., Blonska, M., Pappu, B.P., Li, H., You, Y., Sakurai, H., Darnay, B.G., Hara, H., Penninger, J., Lin, X. (2007). Phosphorylation and ubiquitination of the IkappaB kinase complex by two distinct signaling pathways. Embo J *26*, 1794-805.

112. Niiro, H., Maeda, A., Kurosaki, T., Clark, E.A. (2002). The B lymphocyte adaptor molecule of 32 kD (Bam32) regulates B cell antigen receptor signaling and cell survival. J Exp Med *195*, 143-9.

113. Petro, J.B., Khan, W.N. (2001). Phospholipase C-gamma 2 couples Bruton's tyrosine kinase to the NF-kappaB signaling pathway in B lymphocytes. J Biol Chem *276*, 1715-9.

114. Petro, J.B., Rahman, S.M., Ballard, D.W., Khan, W.N. (2000). Bruton's tyrosine kinase is required for activation of IkappaB kinase and nuclear factor kappaB in response to B cell receptor engagement. J Exp Med *191*, 1745-54.

115. Saijo, K., Mecklenbrauker, I., Santana, A., Leitger, M., Schmedt, C., Tarakhovsky, A. (2002). Protein kinase C beta controls nuclear factor kappaB activation in B cells through selective regulation of the IkappaB kinase alpha. J Exp Med *195*, 1647-52.

116. Su, T.T., Guo, B., Kawakami, Y., Sommer, K., Chae, K., Humphries, L.A., Kato, R.M., Kang, S., Patrone, L., Wall, R., Teitell, M., Leitges, M., Kawakami, T., Rawlings, D.J. (2002). PKC-beta controls I kappa B kinase lipid raft recruitment and activation in response to BCR signaling. Nat

Immunol *3*, 780-6.

117. Baldwin, A.S., Jr. (1996). The NF-kappa B and I kappa B proteins: new discoveries and insights. Annu Rev Immunol *14*, 649-83.

118. Anderson, J.S., Teutsch, M., Dong, Z., Wortis, H.H. (1996). An essential role for Bruton's [corrected] tyrosine kinase in the regulation of B-cell apoptosis. Proc Natl Acad Sci U S A *93*, 10966-71.

119. Grumont, R.J., Rourke, I.J., O'Reilly, L.A., Strasser, A., Miyake, K., Sha, W., Gerondakis, S. (1998). B lymphocytes differentially use the Rel and nuclear factor kappaB1 (NF-kappaB1) transcription factors to regulate cell cycle progression and apoptosis in quiescent and mitogen-activated cells. J Exp Med *187*, 663-74.

120. Joyce, D., Albanese, C., Steer, J., Fu, M., Bouzahzah, B., Pestell, R.G. (2001). NF-kappaB and cell-cycle regulation: the cyclin connection. Cytokine Growth Factor Rev *12*, 73-90.

121. Fruman, D.A., Snapper, S.B., Yballe, C.M., Davidson, L., Yu, J.Y., Alt, F.W., Cantley, L.C. (1999). Impaired B cell development and proliferation in absence of phosphoinositide 3-kinase p85alpha. Science *283*, 393-7.

122. Pogue, S.L., Kurosaki, T., Bolen, J., Herbst, R. (2000). B cell antigen receptor-induced activation of Akt promotes B cell survival and is dependent on Syk kinase. J Immunol *165*, 1300-6.

123. Hodson, D.J., Turner, M. (2009). The role of PI3K signalling in the B cell response to antigen. Adv Exp Med Biol *633*, 43-53.

124. Ravetch, J.V., Lanier, L.L. (2000). Immune inhibitory receptors. Science *290*, 84-9.

125. Datta, S.R., Dudek, H., Tao, X., Masters, S., Fu, H., Gotoh, Y., Greenberg, M.E. (1997). Akt phosphorylation of BAD couples survival signals to the cell-intrinsic death machinery. Cell *91*, 231-41.

126. Gold, M.R., Scheid, M.P., Santos, L., Dang-Lawson, M., Roth, R.A., Matsuuchi, L., Duronio, V., Krebs, D.L. (1999). The B cell antigen receptor activates the Akt (protein kinase B)/glycogen synthase kinase-3 signaling pathway via phosphatidylinositol 3-kinase. J Immunol *163*, 1894-905.

127. Piatelli, M.J., Doughty, C., Chiles, T.C. (2002). Requirement for a hsp90

chaperone-dependent MEK1/2-ERK pathway for B cell antigen receptor-induced cyclin D2 expression in mature B lymphocytes. J Biol Chem *277*, 12144-50.

128. Iwanaga, R., Ohtani, K., Hayashi, T., Nakamura, M. (2001). Molecular mechanism of cell cycle progression induced by the oncogene product Tax of human T-cell leukemia virus type I. Oncogene *20*, 2055-67.

129. Richards, J.D., Dave, S.H., Chou, C.H., Mamchak, A.A., DeFranco, A.L. (2001). Inhibition of the MEK/ERK signaling pathway blocks a subset of B cell responses to antigen. J Immunol *166*, 3855-64.

130. Forssell, J., Nilsson, A., Sideras, P. (2000). Reduced formation of phosphatidic acid upon B-cell receptor triggering of mouse B-lymphocytes lacking Bruton's tyrosine kinase. Scand J Immunol *52*, 30-8.

131. Hashimoto, A., Okada, H., Jiang, A., Kurosaki, M., Greenberg, S., Clark, E.A., Kurosaki, T. (1998). Involvement of guanosine triphosphatases and phospholipase C-gamma2 in extracellular signal-regulated kinase, c-Jun NH2-terminal kinase, and p38 mitogen-activated protein kinase activation by the B cell antigen receptor. J Exp Med *188*, 1287-95.

132. Mikula, M., Schreiber, M., Husak, Z., Kucerova, L., Ruth, J., Wieser, R., Zatloukal, K., Beug, H., Wagner, E.F., Baccarini, M. (2001). Embryonic lethality and fetal liver apoptosis in mice lacking the c-raf-1 gene. Embo J *20*, 1952-62.

133. Huser, M., Luckett, J., Chiloeches, A., Mercer, K., Iwobi, M., Giblett, S., Sun, X.M., Brown, J., Marais, R., Pritchard, C. (2001). MEK kinase activity is not necessary for Raf-1 function. Embo J *20*, 1940-51.

134. Weng, W.K., Jarvis, L., LeBien, T.W. (1994). Signaling through CD19 activates Vav/mitogen-activated protein kinase pathway and induces formation of a CD19/Vav/phosphatidylinositol 3-kinase complex in human B cell precursors. J Biol Chem *269*, 32514-21.

135. Cherukuri, A., Shoham, T., Sohn, H.W., Levy, S., Brooks, S., Carter, R., Pierce, S.K. (2004). The tetraspanin CD81 is necessary for partitioning of coligated CD19/CD21-B cell antigen receptor complexes into signaling-active lipid rafts. J Immunol *172*, 370-80.

136. Phillips, N.E., Parker, D.C. (1983). Fc-dependent inhibition of mouse B cell activation by whole anti-mu antibodies. J Immunol *130*, 602-6.

137. Pan, C., Baumgarth, N., Parnes, J.R. (1999). CD72-deficient mice reveal nonredundant roles of CD72 in B cell development and activation. Immunity *11*, 495-506.

138. Dal Porto, J.M., Gauld, S.B., Merrell, K.T., Mills, D., Pugh-Bernard, A.E., Cambier, J. (2004). B cell antigen receptor signaling 101. Mol Immunol *41*, 599-613.

139. Gary-Gouy, H., Bruhns, P., Schmitt, C., Dalloul, A., Daeron, M., Bismuth, G. (2000). The pseudo-immunoreceptor tyrosine-based activation motif of CD5 mediates its inhibitory action on B-cell receptor signaling. J Biol Chem *275*, 548-56.

140. Niiro, H., Clark, E.A. (2002). Regulation of B-cell fate by antigen-receptor signals. Nat Rev Immunol *2*, 945-56.

141. O'Keefe, T.L., Williams, G.T., Davies, S.L., Neuberger, M.S. (1996). Hyperresponsive B cells in CD22-deficient mice. Science *274*, 798-801.

142. Saito, Y., Miyagawa, Y., Onda, K., Nakajima, H., Sato, B., Horiuchi, Y., Okita, H., Katagiri, Y.U., Saito, M., Shimizu, T., Fujimoto, J., Kiyokawa, N. (2008). B-cell-activating factor inhibits CD20-mediated and B-cell receptor-mediated apoptosis in human B cells. Immunology *125*, 570-90.

143. Kehry, M.R. (1996). CD40-mediated signaling in B cells. Balancing cell survival, growth, and death. J Immunol *156*, 2345-8.

144. Komada, Y., Zhang, X.L., Zhou, Y.W., Tanaka, S., Higashigawa, M., Ido, M., Sakurai, M. (1994). Apoptotic cell death induced by anti-IgM antibody and phorbol esters is inhibited by interleukin-4 in human B lymphoma cell line MBC-1. Cell Immunol *159*, 280-93.

145. Donjerkovic, D., Scott, D.W. (2000). Activation-induced cell death in B lymphocytes. Cell Res *10*, 179-92.

146. Bireland, M.L., Monroe, J.G. (1997). Biochemistry of antigen receptor signaling in mature and developing B lymphocytes. Crit Rev Immunol *17*, 353-85.

147. Benhamou, L.E., Cazenave, P.A., Sarthou, P. (1990). Anti-immunoglobulins induce death by apoptosis in WEHI-231 B lymphoma cells. Eur J Immunol *20*, 1405-7.

148. Koncz, G., Bodor, C., Kovesdi, D., Gati, R., Sarmay, G. (2002). BCR mediated signal transduction in immature and mature B cells. Immunol Lett *82*, 41-9.

149. Parry, S.L., Hasbold, J., Holman, M., Klaus, G.G. (1994). Hypercross-linking surface IgM or IgD receptors on mature B cells induces apoptosis that is reversed by costimulation with IL-4 and anti-CD40. J Immunol *152*, 2821-9.

150. Tsubata, T., Murakami, M., Honjo, T. (1994). Antigen-receptor cross-linking induces peritoneal B-cell apoptosis in normal but not autoimmunity-prone mice. Curr Biol *4*, 8-17.

151. Parry, S.L., Holman, M.J., Hasbold, J., Klaus, G.G. (1994). Plastic-immobilized anti-mu or anti-delta antibodies induce apoptosis in mature murine B lymphocytes. Eur J Immunol *24*, 974-9.

152. Trujillo, M.A., Eberhardt, N.L. (2003). Kinetics of the apoptotic response induced by anti-IgM engagement of the B cell receptor is dependent on the density of cell surface immunoglobulin M expression. DNA Cell Biol *22*, 525-31.

153. Doi, T., Motoyama, N., Tokunaga, A., Watanabe, T. (1999). Death signals from the B cell antigen receptor target mitochondria, activating necrotic and apoptotic death cascades in a murine B cell line, WEHI-231. Int Immunol *11*, 933-41.

154. Yoshida, T., Higuchi, T., Hagiyama, H., Strasser, A., Nishioka, K., Tsubata, T. (2000). Rapid B cell apoptosis induced by antigen receptor ligation does not require Fas (CD95/APO-1), the adaptor protein FADD/MORT1 or CrmA-sensitive caspases but is defective in both MRL-+/+ and MRL-lpr/lpr mice. Int Immunol *12*, 517-26.

155. Berard, M., Mondiere, P., Casamayor-Palleja, M., Hennino, A., Bella, C., Defrance, T. (1999). Mitochondria connects the antigen receptor to effector caspases during B cell receptor-induced apoptosis in normal human B cells. J Immunol *163*, 4655-62.

156. Herold, M.J., Kuss, A.W., Kraus, C., Berberich, I. (2002). Mitochondria-dependent caspase-9 activation is necessary for antigen receptor-mediated effector caspase activation and apoptosis in WEHI 231 lymphoma cells. J Immunol *168*, 3902-9.

157. Bouchon, A., Krammer, P.H., Walczak, H. (2000). Critical role for mitochondria in B cell receptor-mediated apoptosis. Eur J Immunol *30*, 69-77.

158. Nomura, T., Han, H., Howard, M.C., Yagita, H., Yakura, H., Honjo, T., Tsubata, T. (1996). Antigen receptor-mediated B cell death is blocked by signaling via CD72 or treatment with dextran sulfate and is defective in autoimmunity-prone mice. Int Immunol *8*, 867-75.

159. Fang, W., Rivard, J.J., Ganser, J.A., LeBien, T.W., Nath, K.A., Mueller, D.L., Behrens, T.W. (1995). Bcl-xL rescues WEHI 231 B lymphocytes from oxidant-mediated death following diverse apoptotic stimuli. J Immunol *155*, 66-75.

160. Nisitani, S., Tsubata, T., Murakami, M., Okamoto, M., Honjo, T. (1993). The bcl-2 gene product inhibits clonal deletion of self-reactive B lymphocytes in the periphery but not in the bone marrow. J Exp Med *178*, 1247-54.

161. Norvell, A., Mandik, L., Monroe, J.G. (1995). Engagement of the antigen-receptor on immature murine B lymphocytes results in death by apoptosis. J Immunol *154*, 4404-13.

162. Ishigami, T., Kim, K.M., Horiguchi, Y., Higaki, Y., Hata, D., Heike, T., Katamura, K., Mayumi, M., Mikawa, H. (1992). Anti-IgM antibody-induced cell death in a human B lymphoma cell line, B104, represents a novel programmed cell death. J Immunol *148*, 360-8.

163. Aagaard-Tillery, K.M., Jelinek, D.F. (1995). Differential activation of a calcium-dependent endonuclease in human B lymphocytes. Role in ionomycin-induced apoptosis. J Immunol *155*, 3297-307.

164. Sugawara, H., Kurosaki, M., Takata, M., Kurosaki, T. (1997). Genetic evidence for involvement of type 1, type 2 and type 3 inositol 1,4,5-trisphosphate receptors in signal transduction through the B-cell antigen receptor. Embo J *16*, 3078-88.

165. Higashigawa, M., Komada, Y., Shimono, Y., Nagata, T., Inamochi, H., Mao, X.Y., M'Soka, T., Hori, H., Kawasaki, H., Sakurai, M. (1997). FK506 inhibits anti-IgM antibody-induced apoptosis and 17 kD endonuclease activity in the human B-cell line, MBC-1, established from Burkitt's lymphoma. Br J Haematol *99*, 908-13.

166. Kondo, E., Harashima, A., Takabatake, T., Takahashi, H., Matsuo, Y., Yoshino, T., Orita, K., Akagi, T. (2003). NF-ATc2 induces apoptosis in Burkitt's lymphoma cells through signaling via the B cell antigen receptor. Eur J Immunol *33*, 1-11.

167. Sandalova, E., Wei, C.H., Masucci, M.G., Levitsky, V. (2004). Regulation of expression of Bcl-2 protein family member Bim by T cell receptor triggering. Proc Natl Acad Sci U S A *101*, 3011-6.

168. Mouhamad, S., Besnault, L., Auffredou, M.T., Leprince, C., Bourgeade, M.F., Leca, G., Vazquez, A. (2004). B cell receptor-mediated apoptosis of human lymphocytes is associated with a new regulatory pathway of Bim isoform expression. J Immunol *172*, 2084-91.

169. Enders, A., Bouillet, P., Puthalakath, H., Xu, Y., Tarlinton, D.M., Strasser, A. (2003). Loss of the pro-apoptotic BH3-only Bcl-2 family member Bim inhibits BCR stimulation-induced apoptosis and deletion of autoreactive B cells. J Exp Med *198*, 1119-26.

170. Malissein, E., Verdier, M., Ratinaud, M.H., Troutaud, D. (2003). Changes in bad phosphorylation are correlated with BCR-induced apoptosis of WEHI-231 immature B cells. Biochimie *85*, 733-40.

171. Gauld, S.B., Blair, D., Moss, C.A., Reid, S.D., Harnett, M.M. (2002). Differential roles for extracellularly regulated kinase-mitogen-activated protein kinase in B cell antigen receptor-induced apoptosis and CD40-mediated rescue of WEHI-231 immature B cells. J Immunol *168*, 3855-64.

172. Graves, J.D., Draves, K.E., Craxton, A., Saklatvala, J., Krebs, E.G., Clark, E.A. (1996). Involvement of stress-activated protein kinase and p38 mitogen-activated protein kinase in mIgM-induced apoptosis of human B lymphocytes. Proc Natl Acad Sci U S A *93*, 13814-8.

173. Graves, J.D., Draves, K.E., Craxton, A., Krebs, E.G., Clark, E.A. (1998). A comparison of signaling requirements for apoptosis of human B lymphocytes induced by the B cell receptor and CD95/Fas. J Immunol *161*, 168-74.

174. Lee, J.R., Koretzky, G.A. (1998). Extracellular signal-regulated kinase-2, but not c-Jun NH2-terminal kinase, activation correlates with surface IgM-mediated apoptosis in the WEHI 231 B cell line. J Immunol *161*, 1637-44.

175. Eeva, J., Pelkonen, J. (2004). Mechanisms of B cell receptor induced apoptosis. Apoptosis *9*, 525-31.

176. Carey, G.B., Scott, D.W. (2001). Role of phosphatidylinositol 3-kinase in anti-IgM- and anti-IgD-induced apoptosis in B cell lymphomas. J Immunol

166, 1618-26.

177. Ku, P.T., You, M., Bose, H.R., Jr. (2000). Role and regulation of Rel/NF-kappaB activity in anti-immunoglobulin-induced apoptosis in WEHI-231 B lymphoma cells. Cell Signal *12*, 245-53.

178. Yung, S., Chan, T.M. (2008). Anti-DNA antibodies in the pathogenesis of lupus nephritis--the emerging mechanisms. Autoimmun Rev *7*, 317-21.

179. Shlomchik, M.J., Madaio, M.P., Ni, D., Trounstein, M., Huszar, D. (1994). The role of B cells in lpr/lpr-induced autoimmunity. J Exp Med *180*, 1295-306.

180. Jenks, S.A., Sanz, I. (2009). Altered B cell receptor signaling in human systemic lupus erythematosus. Autoimmun Rev *8*, 209-13.

181. Desai-Mehta, A., Lu, L., Ramsey-Goldman, R., Datta, S.K. (1996). Hyperexpression of CD40 ligand by B and T cells in human lupus and its role in pathogenic autoantibody production. J Clin Invest *97*, 2063-73.

182. Liossis, S.N., Kovacs, B., Dennis, G., Kammer, G.M., Tsokos, G.C. (1996). B cells from patients with systemic lupus erythematosus display abnormal antigen receptor-mediated early signal transduction events. J Clin Invest *98*, 2549-57.

183. Sarmay, G., Koncz, G., Pecht, I., Gergely, J. (1997). Fc gamma receptor type IIb induced recruitment of inositol and protein phosphatases to the signal transductory complex of human B-cell. Immunol Lett *57*, 159-64.

184. March, M.E., Ravichandran, K. (2002). Regulation of the immune response by SHIP. Semin Immunol *14*, 37-47.

185. Enyedy, E.J., Mitchell, J.P., Nambiar, M.P., Tsokos, G.C. (2001). Defective FcgammaRIIb1 signaling contributes to enhanced calcium response in B cells from patients with systemic lupus erythematosus. Clin Immunol *101*, 130-5.

186. Pugh-Bernard, A.E., Cambier, J.C. (2006). B cell receptor signaling in human systemic lupus erythematosus. Curr Opin Rheumatol *18*, 451-5.

187. Liossis, S.N., Tsokos GC (2001). *B-cell abonormalities in systemic lupus erythematosus. In "Dubois" lupus Erythematossu*. Philiadelphia: Lippinocott, Williams & Wilkins. pp 205-18.

188. Shrivastava, P., Katagiri, T., Ogimoto, M., Mizuno, K., Yakura, H. (2004). Dynamic regulation of Src-family kinases by CD45 in B cells. Blood *103*, 1425-32.

189. Flores-Borja, F., Kabouridis, P.S., Jury, E.C., Isenberg, D.A., Mageed, R.A. (2007). Altered lipid raft-associated proximal signaling and translocation of CD45 tyrosine phosphatase in B lymphocytes from patients with systemic lupus erythematosus. Arthritis Rheum *56*, 291-302.

190. Roy, V., Chang, N.H., Cai, Y., Bonventi, G., Wither, J. (2005). Aberrant IgM signaling promotes survival of transitional T1 B cells and prevents tolerance induction in lupus-prone New Zealand black mice. J Immunol *175*, 7363-71.

191. Kozono, Y., Kotzin, B.L., Holers, V.M. (1996). Resting B cells from New Zealand Black mice demonstrate a defect in apoptosis induction following surface IgM ligation. J Immunol *156*, 4498-503.

192. Mohan, C., Morel, L., Yang, P., Wakeland, E.K. (1997). Genetic dissection of systemic lupus erythematosus pathogenesis: Sle2 on murine chromosome 4 leads to B cell hyperactivity. J Immunol *159*, 454-65.

193. Subramanian, S., Tus, K., Li, Q.Z., Wang, A., Tian, X.H., Zhou, J., Liang, C., Bartov, G., McDaniel, L.D., Zhou, X.J., Schultz, R.A., Wakeland, E.K. (2006). A Tlr7 translocation accelerates systemic autoimmunity in murine lupus. Proc Natl Acad Sci U S A *103*, 9970-5.

194. Fairhurst, A.M., Hwang, S.H., Wang, A., Tian, X.H., Boudreaux, C., Zhou, X.J., Casco, J., Li, Q.Z., Connolly, J.E., Wakeland, E.K. (2008). Yaa autoimmune phenotypes are conferred by overexpression of TLR7. Eur J Immunol *38*, 1971-8.

195. Kumar, K.R., Li, L., Yan, M., Bhaskarabhatla, M., Mobley, A.B., Nguyen, C., Mooney, J.M., Schatzle, J.D., Wakeland, E.K., Mohan, C. (2006). Regulation of B cell tolerance by the lupus susceptibility gene Ly108. Science *312*, 1665-9.

196. Hibbs, M.L., Tarlinton, D.M., Armes, J., Grail, D., Hodgson, G., Maglitto, R., Stacker, S.A., Dunn, A.R. (1995). Multiple defects in the immune system of Lyn-deficient mice, culminating in autoimmune disease. Cell *83*, 301-11.

197. Chan, V.W., Meng, F., Soriano, P., DeFranco, A.L., Lowell, C.A. (1997). Characterization of the B lymphocyte populations in Lyn-deficient mice and the role of Lyn in signal initiation and down-regulation. Immunity *7*, 69-81.

198. Savino, M.T., Ortensi, B., Ferro, M., Ulivieri, C., Fanigliulo, D., Paccagnini, E., Lazzi, S., Osti, D., Pelicci, G., Baldari, C.T. (2009). Rai acts as a negative regulator of autoimmunity by inhibiting antigen receptor signaling and lymphocyte activation. J Immunol *182*, 301-8.

199. Saito, E., Fujimoto, M., Hasegawa, M., Komura, K., Hamaguchi, Y., Kaburagi, Y., Nagaoka, T., Takehara, K., Tedder, T.F., Sato, S. (2002). CD19-dependent B lymphocyte signaling thresholds influence skin fibrosis and autoimmunity in the tight-skin mouse. J Clin Invest *109*, 1453-62.

200. Sato, S., Ono, N., Steeber, D.A., Pisetsky, D.S., Tedder, T.F. (1996). CD19 regulates B lymphocyte signaling thresholds critical for the development of B-1 lineage cells and autoimmunity. J Immunol *157*, 4371-8.

201. Engel, P., Zhou, L.J., Ord, D.C., Sato, S., Koller, B., Tedder, T.F. (1995). Abnormal B lymphocyte development, activation, and differentiation in mice that lack or overexpress the CD19 signal transduction molecule. Immunity *3*, 39-50.

202. Inaoki, M., Sato, S., Weintraub, B.C., Goodnow, C.C., Tedder, T.F. (1997). CD19-regulated signaling thresholds control peripheral tolerance and autoantibody production in B lymphocytes. J Exp Med *186*, 1923-31.

203. Smith, K.G., Tarlinton, D.M., Doody, G.M., Hibbs, M.L., Fearon, D.T. (1998). Inhibition of the B cell by CD22: a requirement for Lyn. J Exp Med *187*, 807-11.

204. O'Keefe, T.L., Williams, G.T., Batista, F.D., Neuberger, M.S. (1999). Deficiency in CD22, a B cell-specific inhibitory receptor, is sufficient to predispose to development of high affinity autoantibodies. J Exp Med *189*, 1307-13.

205. Nishizumi, H., Horikawa, K., Mlinaric-Rascan, I., Yamamoto, T. (1998). A double-edged kinase Lyn: a positive and negative regulator for antigen receptor-mediated signals. J Exp Med *187*, 1343-8.

206. Hibbs, M.L., Harder, K.W., Armes, J., Kountouri, N., Quilici, C., Casagranda, F., Dunn, A.R., Tarlinton, D.M. (2002). Sustained activation of Lyn tyrosine kinase in vivo leads to autoimmunity. J Exp Med *196*, 1593-604.

207. Schmidt, K.N., Hsu, C.W., Griffin, C.T., Goodnow, C.C., Cyster, J.G. (1998). Spontaneous follicular exclusion of SHP1-deficient B cells is conditional on the presence of competitor wild-type B cells. J Exp Med *187*, 929-37.

208. Kozlowski, M., Mlinaric-Rascan, I., Feng, G.S., Shen, R., Pawson, T., Siminovitch, K.A. (1993). Expression and catalytic activity of the tyrosine phosphatase PTP1C is severely impaired in motheaten and viable motheaten mice. J Exp Med *178*, 2157-63.

209. Tsui, H.W., Siminovitch, K.A., de Souza, L., Tsui, F.W. (1993). Motheaten and viable motheaten mice have mutations in the haematopoietic cell phosphatase gene. Nat Genet *4*, 124-9.

210. Cyster, J.G., Healy, J.I., Kishihara, K., Mak, T.W., Thomas, M.L., Goodnow, C.C. (1996). Regulation of B-lymphocyte negative and positive selection by tyrosine phosphatase CD45. Nature *381*, 325-8.

211. Bolland, S., Ravetch, J.V. (2000). Spontaneous autoimmune disease in Fc(gamma)RIIB-deficient mice results from strain-specific epistasis. Immunity *13*, 277-85.

212. Bolland, S., Yim, Y.S., Tus, K., Wakeland, E.K., Ravetch, J.V. (2002). Genetic modifiers of systemic lupus erythematosus in FcgammaRIIB(-/-) mice. J Exp Med *195*, 1167-74.

213. Do, R.K., Chen-Kiang, S. (2002). Mechanism of BLyS action in B cell immunity. Cytokine Growth Factor Rev *13*, 19-25.

214. Higuchi, T., Aiba, Y., Nomura, T., Matsuda, J., Mochida, K., Suzuki, M., Kikutani, H., Honjo, T., Nishioka, K., Tsubata, T. (2002). Cutting Edge: Ectopic expression of CD40 ligand on B cells induces lupus-like autoimmune disease. J Immunol *168*, 9-12.

215. Gross, J.A., Johnston, J., Mudri, S., Enselman, R., Dillon, S.R., Madden, K., Xu, W., Parrish-Novak, J., Foster, D., Lofton-Day, C., Moore, M., Littau, A., Grossman, A., Haugen, H., Foley, K., Blumberg, H., Harrison, K., Kindsvogel, W., Clegg, C.H. (2000). TACI and BCMA are receptors for a TNF homologue implicated in B-cell autoimmune disease. Nature *404*, 995-9.

216. Bednarski, J.J., Warner, R.E., Rao, T., Leonetti, F., Yung, R., Richardson, B.C., Johnson, K.J., Ellman, J.A., Opipari, A.W., Jr., Glick, G.D. (2003). Attenuation of autoimmune disease in Fas-deficient mice by treatment with a cytotoxic benzodiazepine. Arthritis Rheum *48*, 757-66.

217. Blatt, N.B., Bednarski, J.J., Warner, R.E., Leonetti, F., Johnson, K.M., Boitano, A., Yung, R., Richardson, B.C., Johnson, K.J., Ellman, J.A., Opipari, A.W., Jr., Glick, G.D. (2002). Benzodiazepine-induced superoxide signals B cell

apoptosis: mechanistic insight and potential therapeutic utility. J Clin Invest *110*, 1123-32.

218. Boitano, A., Ellman, J.A., Glick, G.D., Opipari, A.W., Jr. (2003). The proapoptotic benzodiazepine Bz-423 affects the growth and survival of malignant B cells. Cancer Res *63*, 6870-6.

219. Johnson, K.M., Chen, X., Boitano, A., Swenson, L., Opipari, A.W., Jr., Glick, G.D. (2005). Identification and validation of the mitochondrial F1F0-ATPase as the molecular target of the immunomodulatory benzodiazepine Bz-423. Chem Biol *12*, 485-96.

220. Boitano, A. (2005). Mechanisms of pro-apoptotic Benzodiazepine. thesis

221. Bednarski, J.J., Lyssiotis, C.A., Roush, R., Boitano, A.E., Glick, G.D., Opipari, A.W., Jr. (2004). A novel benzodiazepine increases the sensitivity of B cells to receptor stimulation with synergistic effects on calcium signaling and apoptosis. J Biol Chem *279*, 29615-21.

222. Luzina, I.G., Atamas, S.P., Storrer, C.E., daSilva, L.C., Kelsoe, G., Papadimitriou, J.C., Handwerger, B.S. (2001). Spontaneous formation of germinal centers in autoimmune mice. J Leukoc Biol *70*, 578-84.

223. Gregory, C.D., Edwards, C.F., Milner, A., Wiels, J., Lipinski, M., Rowe, M., Tursz, T., Rickinson, A.B. (1988). Isolation of a normal B cell subset with a Burkitt-like phenotype and transformation in vitro with Epstein-Barr virus. Int J Cancer *42*, 213-20.

224. Tuscano, J.M., Riva, A., Toscano, S.N., Tedder, T.F., Kehrl, J.H. (1999). CD22 cross-linking generates B-cell antigen receptor-independent signals that activate the JNK/SAPK signaling cascade. Blood *94*, 1382-92.

225. Guzman-Rojas, L., Sims-Mourtada, J.C., Rangel, R., Martinez-Valdez, H. (2002). Life and death within germinal centres: a double-edged sword. Immunology *107*, 167-75.

226. Hasler, P., Zouali, M. (2001). B cell receptor signaling and autoimmunity. Faseb J *15*, 2085-98.

227. Drake, L., McGovern-Brindisi, E.M., Drake, J.R. (2006). BCR ubiquitination controls BCR-mediated antigen processing and presentation. Blood *108*, 4086-93.

228. Chang, N.H., McKenzie, T., Bonventi, G., Landolt-Marticorena, C., Fortin, P.R., Gladman, D., Urowitz, M., Wither, J.E. (2008). Expanded population of activated antigen-engaged cells within the naive B cell compartment of patients with systemic lupus erythematosus. J Immunol *180*, 1276-84.

229. Alizadeh, A.A., Eisen, M.B., Davis, R.E., Ma, C., Lossos, I.S., Rosenwald, A., Boldrick, J.C., Sabet, H., Tran, T., Yu, X., Powell, J.I., Yang, L., Marti, G.E., Moore, T., Hudson, J., Jr., Lu, L., Lewis, D.B., Tibshirani, R., Sherlock, G., Chan, W.C., Greiner, T.C., Weisenburger, D.D., Armitage, J.O., Warnke, R., Levy, R., Wilson, W., Grever, M.R., Byrd, J.C., Botstein, D., Brown, P.O., Staudt, L.M. (2000). Distinct types of diffuse large B-cell lymphoma identified by gene expression profiling. Nature *403*, 503-11.

230. Kerr, W.G., Hendershot, L.M., Burrows, P.D. (1991). Regulation of IgM and IgD expression in human B-lineage cells. J Immunol *146*, 3314-21.

231. Wilson, B.E., Mochon, E., Boxer, L.M. (1996). Induction of bcl-2 expression by phosphorylated CREB proteins during B-cell activation and rescue from apoptosis. Mol Cell Biol *16*, 5546-56.

232. Mazer, B.D., Toledano, B., Saririan, M., Bastien, Y. (1998). Dose-dependent agonist and antagonist effects of the platelet-activating factor analogue 1-palmitoyl-2-acetoyl-sn-glycero-3-phosphocholine on B lymphocytes. J Allergy Clin Immunol *102*, 231-7.

233. Sasaki, S., Ito, E., Toki, T., Maekawa, T., Kanezaki, R., Umenai, T., Muto, A., Nagai, H., Kinoshita, T., Yamamoto, M., Inazawa, J., Taketo, M.M., Nakahata, T., Igarashi, K., Yokoyama, M. (2000). Cloning and expression of human B cell-specific transcription factor BACH2 mapped to chromosome 6q15. Oncogene *19*, 3739-49.

234. Xu, Z., Duan, B., Croker, B.P., Wakeland, E.K., Morel, L. (2005). Genetic dissection of the murine lupus susceptibility locus Sle2: contributions to increased peritoneal B-1a cells and lupus nephritis map to different loci. J Immunol *175*, 936-43.

235. Tan, P.L., Pang, G.T., Cullinane, G., Wilson, J.D. (1980). Immunoglobulin-secreting cells in SLE: correlation with disease activity. J Rheumatol *7*, 807-13.

236. Lens, S.M., den Drijver, B.F., Potgens, A.J., Tesselaar, K., van Oers, M.H., van Lier, R.A. (1998). Dissection of pathways leading to antigen receptor-induced and Fas/CD95-induced apoptosis in human B cells. J Immunol *160*, 6083-92.

237. Perl, A., Banki, K. (2000). Genetic and metabolic control of the mitochondrial transmembrane potential and reactive oxygen intermediate production in HIV disease. Antioxid Redox Signal *2*, 551-73.

238. Petit, P.X., Susin, S.A., Zamzami, N., Mignotte, B., Kroemer, G. (1996). Mitochondria and programmed cell death: back to the future. FEBS Lett *396*, 7-13.

239. Le, S.B., Holmuhamedov, E.L., Narayanan, V.L., Sausville, E.A., Kaufmann, S.H. (2006). Adaphostin and other anticancer drugs quench the fluorescence of mitochondrial potential probes. Cell Death Differ *13*, 151-9.

240. Azuma, Y., Higurashi, K., Matsumoto, K. (2007). Immobilized alpha2,6-linked sialic acid suppresses caspase-3 activation during anti-IgM antibody-induced apoptosis in Ramos cells. Biochim Biophys Acta *1770*, 279-85.

241. Fink, B., Laude, K., McCann, L., Doughan, A., Harrison, D.G., Dikalov, S. (2004). Detection of intracellular superoxide formation in endothelial cells and intact tissues using dihydroethidium and an HPLC-based assay. Am J Physiol Cell Physiol *287*, C895-902.

242. Georgiou, C.D., Papapostolou, I., Patsoukis, N., Tsegenidis, T., Sideris, T. (2005). An ultrasensitive fluorescent assay for the in vivo quantification of superoxide radical in organisms. Anal Biochem *347*, 144-51.

243. Criddle, D.N., Gillies, S., Baumgartner-Wilson, H.K., Jaffar, M., Chinje, E.C., Passmore, S., Chvanov, M., Barrow, S., Gerasimenko, O.V., Tepikin, A.V., Sutton, R., Petersen, O.H. (2006). Menadione-induced reactive oxygen species generation via redox cycling promotes apoptosis of murine pancreatic acinar cells. J Biol Chem *281*, 40485-92.

244. Krebs, J. (1998). The role of calcium in apoptosis. Biometals *11*, 375-82.

245. Mohamed, A.J., Yu, L., Backesjo, C.M., Vargas, L., Faryal, R., Aints, A., Christensson, B., Berglof, A., Vihinen, M., Nore, B.F., Smith, C.I. (2009). Bruton's tyrosine kinase (Btk): function, regulation, and transformation with special emphasis on the PH domain. Immunol Rev *228*, 58-73.

246. Lindvall, J., Islam, T.C. (2002). Interaction of Btk and Akt in B cell signaling. Biochem Biophys Res Commun *293*, 1319-26.

247. Qin, S., Chock, P.B. (2001). Bruton's tyrosine kinase is essential for hydrogen

peroxide-induced calcium signaling. Biochemistry *40*, 8085-91.

248. Dolmetsch, R.E., Lewis, R.S., Goodnow, C.C., Healy, J.I. (1997). Differential activation of transcription factors induced by Ca2+ response amplitude and duration. Nature *386*, 855-8.

249. Lytton, J., Westlin, M., Hanley, M.R. (1991). Thapsigargin inhibits the sarcoplasmic or endoplasmic reticulum Ca-ATPase family of calcium pumps. J Biol Chem *266*, 17067-71.

250. Hajnoczky, G., Davies, E., Madesh, M. (2003). Calcium signaling and apoptosis. Biochem Biophys Res Commun *304*, 445-54.

251. He, L.P., Hewavitharana, T., Soboloff, J., Spassova, M.A., Gill, D.L. (2005). A functional link between store-operated and TRPC channels revealed by the 3,5-bis(trifluoromethyl)pyrazole derivative, BTP2. J Biol Chem *280*, 10997-1006.

252. Rao, A. (1991). Signaling mechanisms in T cells. Crit Rev Immunol *10*, 495-519.

253. Valentine, M.A., Licciardi, K.A. (1992). Rescue from anti-IgM-induced programmed cell death by the B cell surface proteins CD20 and CD40. Eur J Immunol *22*, 3141-8.

254. Scott, D.W., Livnat, D., Whitin, J., Dillon, S.B., Snyderman, R., Pennell, C.A. (1987). Lymphoma models for B cell activation and tolerance. V. Anti-Ig mediated growth inhibition is reversed by phorbol myristate acetate but does not involve changes in cytosolic free calcium. J Mol Cell Immunol *3*, 109-20.

255. Paredes, R.M., Etzler, J.C., Watts, L.T., Zheng, W., Lechleiter, J.D. (2008). Chemical calcium indicators. Methods *46*, 143-51.

256. van Gurp, M., Festjens, N., van Loo, G., Saelens, X., Vandenabeele, P. (2003). Mitochondrial intermembrane proteins in cell death. Biochem Biophys Res Commun *304*, 487-97.

257. Gupta, S. (2000). Molecular steps of cell suicide: an insight into immune senescence. J Clin Immunol *20*, 229-39.

258. Sun, X.M., MacFarlane, M., Zhuang, J., Wolf, B.B., Green, D.R., Cohen, G.M. (1999). Distinct caspase cascades are initiated in receptor-mediated and chemical-induced apoptosis. J Biol Chem *274*, 5053-60.

259. Rathmell, J.C., Cooke, M.P., Ho, W.Y., Grein, J., Townsend, S.E., Davis, M.M., Goodnow, C.C. (1995). CD95 (Fas)-dependent elimination of self-reactive B cells upon interaction with CD4+ T cells. Nature *376*, 181-4.

260. Stel, A.J., Ten Cate, B., Jacobs, S., Kok, J.W., Spierings, D.C., Dondorff, M., Helfrich, W., Kluin-Nelemans, H.C., de Leij, L.F., Withoff, S., Kroesen, B.J. (2007). Fas receptor clustering and involvement of the death receptor pathway in rituximab-mediated apoptosis with concomitant sensitization of lymphoma B cells to fas-induced apoptosis. J Immunol *178*, 2287-95.

261. Chen, Q., Gong, B., Almasan, A. (2000). Distinct stages of cytochrome c release from mitochondria: evidence for a feedback amplification loop linking caspase activation to mitochondrial dysfunction in genotoxic stress induced apoptosis. Cell Death Differ *7*, 227-33.

262. Takeuchi, O., Fisher, J., Suh, H., Harada, H., Malynn, B.A., Korsmeyer, S.J. (2005). Essential role of BAX,BAK in B cell homeostasis and prevention of autoimmune disease. Proc Natl Acad Sci U S A *102*, 11272-7.

263. James, D., Parone, P.A., Terradillos, O., Lucken-Ardjomande, S., Montessuit, S., Martinou, J.C. (2007). Mechanisms of mitochondrial outer membrane permeabilization. Novartis Found Symp *287*, 170-6; discussion 6-82.

264. Zhong, Y., Weininger, M., Pirbhai, M., Dong, F., Zhong, G. (2006). Inhibition of staurosporine-induced activation of the proapoptotic multidomain Bcl-2 proteins Bax and Bak by three invasive chlamydial species. J Infect *53*, 408-14.

265. Nunez, G., Merino, R., Simonian, P.L., Grillot, D.A. (1996). Regulation of lymphoid apoptosis by Bcl-2 and Bcl-XL. Adv Exp Med Biol *406*, 75-82.

266. Levine, B., Sinha, S., Kroemer, G. (2008). Bcl-2 family members: dual regulators of apoptosis and autophagy. Autophagy *4*, 600-6.

267. Bouillet, P., Metcalf, D., Huang, D.C., Tarlinton, D.M., Kay, T.W., Kontgen, F., Adams, J.M., Strasser, A. (1999). Proapoptotic Bcl-2 relative Bim required for certain apoptotic responses, leukocyte homeostasis, and to preclude autoimmunity. Science *286*, 1735-8.

268. Labi, V., Erlacher, M., Kiessling, S., Manzl, C., Frenzel, A., O'Reilly, L., Strasser, A., Villunger, A. (2008). Loss of the BH3-only protein Bmf impairs B cell homeostasis and accelerates gamma irradiation-induced thymic lymphoma development. J Exp Med *205*, 641-55.

269. Liu, J., Farmer, J.D., Jr., Lane, W.S., Friedman, J., Weissman, I., Schreiber, S.L. (1991). Calcineurin is a common target of cyclophilin-cyclosporin A and FKBP-FK506 complexes. Cell *66*, 807-15.

270. Shibasaki, F., Hallin, U., Uchino, H. (2002). Calcineurin as a multifunctional regulator. J Biochem *131*, 1-15.

271. O'Keefe, S.J., Tamura, J., Kincaid, R.L., Tocci, M.J., O'Neill, E.A. (1992). FK-506- and CsA-sensitive activation of the interleukin-2 promoter by calcineurin. Nature *357*, 692-4.

272. Dumont, F.J., Melino, M.R., Staruch, M.J., Koprak, S.L., Fischer, P.A., Sigal, N.H. (1990). The immunosuppressive macrolides FK-506 and rapamycin act as reciprocal antagonists in murine T cells. J Immunol *144*, 1418-24.

273. Matsuda, S., Koyasu, S. (2003). Regulation of MAPK signaling pathways through immunophilin-ligand complex. Curr Top Med Chem *3*, 1358-67.

274. Fruman, D.A., Pai, S.Y., Klee, C.B., Burakoff, S.J., Bierer, B.E. (1996). Measurement of Calcineurin Phosphatase Activity in Cell Extracts. Methods *9*, 146-54.

275. Attin, T., Becker, K., Hannig, C., Buchalla, W., Wiegand, A. (2005). Suitability of a malachite green procedure to detect minimal amounts of phosphate dissolved in acidic solutions. Clin Oral Investig *9*, 203-7.

276. Rothermel, B.A., Vega, R.B., Williams, R.S. (2003). The role of modulatory calcineurin-interacting proteins in calcineurin signaling. Trends Cardiovasc Med *13*, 15-21.

277. Marafioti, T., Pozzobon, M., Hansmann, M.L., Ventura, R., Pileri, S.A., Roberton, H., Gesk, S., Gaulard, P., Barth, T.F., Du, M.Q., Leoncini, L., Moller, P., Natkunam, Y., Siebert, R., Mason, D.Y. (2005). The NFATc1 transcription factor is widely expressed in white cells and translocates from the cytoplasm to the nucleus in a subset of human lymphomas. Br J Haematol *128*, 333-42.

278. Wang, H.G., Pathan, N., Ethell, I.M., Krajewski, S., Yamaguchi, Y., Shibasaki, F., McKeon, F., Bobo, T., Franke, T.F., Reed, J.C. (1999). Ca2+-induced apoptosis through calcineurin dephosphorylation of BAD. Science *284*, 339-43.

279. Rebillard, A., Lagadic-Gossmann, D., Dimanche-Boitrel, M.T. (2008).

Cisplatin cytotoxicity: DNA and plasma membrane targets. Curr Med Chem *15*, 2656-63.

280. Chan, O.T., Madaio, M.P., Shlomchik, M.J. (1999). The central and multiple roles of B cells in lupus pathogenesis. Immunol Rev *169*, 107-21.

281. Mandik-Nayak, L., Ridge, N., Fields, M., Park, A.Y., Erikson, J. (2008). Role of B cells in systemic lupus erythematosus and rheumatoid arthritis. Curr Opin Immunol *20*, 639-45.

282. Chan, O., Madaio, M.P., Shlomchik, M.J. (1997). The roles of B cells in MRL/lpr murine lupus. Ann N Y Acad Sci *815*, 75-87.

283. Karim, M.Y., Pisoni, C.N., Khamashta, M.A. (2009). Update on immunotherapy for systemic lupus erythematosus--what's hot and what's not! Rheumatology (Oxford)

284. Sundberg, T.B., Ney, G.M., Subramanian, C., Opipari, A.W., Jr., Glick, G.D. (2006). The immunomodulatory benzodiazepine Bz-423 inhibits B-cell proliferation by targeting c-myc protein for rapid and specific degradation. Cancer Res *66*, 1775-82.

285. Lampe, M.A., Patarca, R., Iregui, M.V., Cantor, H. (1991). Polyclonal B cell activation by the Eta-1 cytokine and the development of systemic autoimmune disease. J Immunol *147*, 2902-6.

286. Odendahl, M., Jacobi, A., Hansen, A., Feist, E., Hiepe, F., Burmester, G.R., Lipsky, P.E., Radbruch, A., Dorner, T. (2000). Disturbed peripheral B lymphocyte homeostasis in systemic lupus erythematosus. J Immunol *165*, 5970-9.

287. Sims, G.P., Ettinger, R., Shirota, Y., Yarboro, C.H., Illei, G.G., Lipsky, P.E. (2005). Identification and characterization of circulating human transitional B cells. Blood *105*, 4390-8.

288. Arce, E., Jackson, D.G., Gill, M.A., Bennett, L.B., Banchereau, J., Pascual, V. (2001). Increased frequency of pre-germinal center B cells and plasma cell precursors in the blood of children with systemic lupus erythematosus. J Immunol *167*, 2361-9.

289. Santulli-Marotto, S., Retter, M.W., Gee, R., Mamula, M.J., Clarke, S.H. (1998). Autoreactive B cell regulation: peripheral induction of developmental arrest by lupus-associated autoantigens. Immunity *8*, 209-19.

290. Agematsu, K., Hokibara, S., Nagumo, H., Komiyama, A. (2000). CD27: a memory B-cell marker. Immunol Today *21*, 204-6.

291. Grammer, A.C., Slota, R., Fischer, R., Gur, H., Girschick, H., Yarboro, C., Illei, G.G., Lipsky, P.E. (2003). Abnormal germinal center reactions in systemic lupus erythematosus demonstrated by blockade of CD154-CD40 interactions. J Clin Invest *112*, 1506-20.

292. Goodnow, C.C., Sprent, J., Fazekas de St Groth, B., Vinuesa, C.G. (2005). Cellular and genetic mechanisms of self tolerance and autoimmunity. Nature *435*, 590-7.

293. Deming, P.B., Rathmell, J.C. (2006). Mitochondria, cell death, and B cell tolerance. Curr Dir Autoimmun *9*, 95-119.

294. Mann, J.J., Fraker, P.J. (2005). Zinc pyrithione induces apoptosis and increases expression of Bim. Apoptosis *10*, 369-79.

295. Shelton, S.N., Shawgo, M.E., Robertson, J.D. (2009). Cleavage of bid by executioner caspases mediates feed forward amplification of mitochondrial outer membrane permeabilization during genotoxic stress-induced apoptosis in jurkat cells. J Biol Chem

296. Zhang, Y., Adachi, M., Kawamura, R., Imai, K. (2006). Bmf is a possible mediator in histone deacetylase inhibitors FK228 and CBHA-induced apoptosis. Cell Death Differ *13*, 129-40.

297. Snow, A.L., Oliveira, J.B., Zheng, L., Dale, J.K., Fleisher, T.A., Lenardo, M.J. (2008). Critical role for BIM in T cell receptor restimulation-induced death. Biol Direct *3*, 34.

298. Walshe, C.A., Beers, S.A., French, R.R., Chan, C.H., Johnson, P.W., Packham, G.K., Glennie, M.J., Cragg, M.S. (2008). Induction of cytosolic calcium flux by CD20 is dependent upon B Cell antigen receptor signaling. J Biol Chem *283*, 16971-84.

299. Glassford, J., Soeiro, I., Skarell, S.M., Banerji, L., Holman, M., Klaus, G.G., Kadowaki, T., Koyasu, S., Lam, E.W. (2003). BCR targets cyclin D2 via Btk and the p85alpha subunit of PI3-K to induce cell cycle progression in primary mouse B cells. Oncogene *22*, 2248-59.

300. Mahajan, S., Ghosh, S., Sudbeck, E.A., Zheng, Y., Downs, S., Hupke, M., Uckun, F.M. (1999). Rational design and synthesis of a novel anti-leukemic

agent targeting Bruton's tyrosine kinase (BTK), LFM-A13 [alpha-cyano-beta-hydroxy-beta-methyl-N-(2, 5-dibromophenyl)propenamide]. J Biol Chem *274*, 9587-99.

301. Ishikawa, J., Ohga, K., Yoshino, T., Takezawa, R., Ichikawa, A., Kubota, H., Yamada, T. (2003). A pyrazole derivative, YM-58483, potently inhibits store-operated sustained Ca2+ influx and IL-2 production in T lymphocytes. J Immunol *170*, 4441-9.

302. Gwack, Y., Srikanth, S., Oh-Hora, M., Hogan, P.G., Lamperti, E.D., Yamashita, M., Gelinas, C., Neems, D.S., Sasaki, Y., Feske, S., Prakriya, M., Rajewsky, K., Rao, A. (2008). Hair loss and defective T- and B-cell function in mice lacking ORAI1. Mol Cell Biol *28*, 5209-22.

303. Liu, C., Hermann, T.E. (1978). Characterization of ionomycin as a calcium ionophore. J Biol Chem *253*, 5892-4.

304. Morgan, A.J., Jacob, R. (1994). Ionomycin enhances Ca2+ influx by stimulating store-regulated cation entry and not by a direct action at the plasma membrane. Biochem J *300 (Pt 3)*, 665-72.

305. Inesi, G., Hua, S., Xu, C., Ma, H., Seth, M., Prasad, A.M., Sumbilla, C. (2005). Studies of Ca2+ ATPase (SERCA) inhibition. J Bioenerg Biomembr *37*, 365-8.

306. Tomida, T., Hirose, K., Takizawa, A., Shibasaki, F., Iino, M. (2003). NFAT functions as a working memory of Ca2+ signals in decoding Ca2+ oscillation. Embo J *22*, 3825-32.

307. Gomez-Vicente, V., Doonan, F., Donovan, M., Cotter, T.G. (2006). Induction of BIM(EL) following growth factor withdrawal is a key event in caspase-dependent apoptosis of 661W photoreceptor cells. Eur J Neurosci *24*, 981-90.

308. Hemenway, C.S., Heitman, J. (1999). Calcineurin. Structure, function, and inhibition. Cell Biochem Biophys *30*, 115-51.

309. Strasser, A. (2005). The role of BH3-only proteins in the immune system. Nat Rev Immunol *5*, 189-200.

310. Chen, L., Willis, S.N., Wei, A., Smith, B.J., Fletcher, J.I., Hinds, M.G., Colman, P.M., Day, C.L., Adams, J.M., Huang, D.C. (2005). Differential targeting of prosurvival Bcl-2 proteins by their BH3-only ligands allows complementary

apoptotic function. Mol Cell *17*, 393-403.

311. O'Connor, L., Strasser, A., O'Reilly, L.A., Hausmann, G., Adams, J.M., Cory, S., Huang, D.C. (1998). Bim: a novel member of the Bcl-2 family that promotes apoptosis. Embo J *17*, 384-95.

312. Hsu, S.Y., Lin, P., Hsueh, A.J. (1998). BOD (Bcl-2-related ovarian death gene) is an ovarian BH3 domain-containing proapoptotic Bcl-2 protein capable of dimerization with diverse antiapoptotic Bcl-2 members. Mol Endocrinol *12*, 1432-40.

313. Marani, M., Tenev, T., Hancock, D., Downward, J., Lemoine, N.R. (2002). Identification of novel isoforms of the BH3 domain protein Bim which directly activate Bax to trigger apoptosis. Mol Cell Biol *22*, 3577-89.

314. Strasser, A., Puthalakath, H., Bouillet, P., Huang, D.C., O'Connor, L., O'Reilly, L.A., Cullen, L., Cory, S., Adams, J.M. (2000). The role of bim, a proapoptotic BH3-only member of the Bcl-2 family in cell-death control. Ann N Y Acad Sci *917*, 541-8.

315. Villunger, A., Scott, C., Bouillet, P., Strasser, A. (2003). Essential role for the BH3-only protein Bim but redundant roles for Bax, Bcl-2, and Bcl-w in the control of granulocyte survival. Blood *101*, 2393-400.

316. Oliver, P.M., Vass, T., Kappler, J., Marrack, P. (2006). Loss of the proapoptotic protein, Bim, breaks B cell anergy. J Exp Med *203*, 731-41.

317. Bouillet, P., Purton, J.F., Godfrey, D.I., Zhang, L.C., Coultas, L., Puthalakath, H., Pellegrini, M., Cory, S., Adams, J.M., Strasser, A. (2002). BH3-only Bcl-2 family member Bim is required for apoptosis of autoreactive thymocytes. Nature *415*, 922-6.

318. Dijkers, P.F., Medema, R.H., Lammers, J.W., Koenderman, L., Coffer, P.J. (2000). Expression of the pro-apoptotic Bcl-2 family member Bim is regulated by the forkhead transcription factor FKHR-L1. Curr Biol *10*, 1201-4.

319. Ley, R., Ewings, K.E., Hadfield, K., Cook, S.J. (2005). Regulatory phosphorylation of Bim: sorting out the ERK from the JNK. Cell Death Differ *12*, 1008-14.

320. Akiyama, T., Bouillet, P., Miyazaki, T., Kadono, Y., Chikuda, H., Chung, U.I., Fukuda, A., Hikita, A., Seto, H., Okada, T., Inaba, T., Sanjay, A., Baron, R., Kawaguchi, H., Oda, H., Nakamura, K., Strasser, A., Tanaka, S. (2003).

Regulation of osteoclast apoptosis by ubiquitylation of proapoptotic BH3-only Bcl-2 family member Bim. Embo J *22*, 6653-64.

321. Luciano, F., Jacquel, A., Colosetti, P., Herrant, M., Cagnol, S., Pages, G., Auberger, P. (2003). Phosphorylation of Bim-EL by Erk1/2 on serine 69 promotes its degradation via the proteasome pathway and regulates its proapoptotic function. Oncogene *22*, 6785-93.

322. Puthalakath, H., Villunger, A., O'Reilly, L.A., Beaumont, J.G., Coultas, L., Cheney, R.E., Huang, D.C., Strasser, A. (2001). Bmf: a proapoptotic BH3-only protein regulated by interaction with the myosin V actin motor complex, activated by anoikis. Science *293*, 1829-32.

323. Morales, A.A., Gutman, D., Lee, K.P., Boise, L.H. (2008). BH3-only proteins Noxa, Bmf, and Bim are necessary for arsenic trioxide-induced cell death in myeloma. Blood *111*, 5152-62.

324. Morales, A.A., Olsson, A., Celsing, F., Osterborg, A., Jondal, M., Osorio, L.M. (2004). Expression and transcriptional regulation of functionally distinct Bmf isoforms in B-chronic lymphocytic leukemia cells. Leukemia *18*, 41-7.

325. Mandic, A., Viktorsson, K., Strandberg, L., Heiden, T., Hansson, J., Linder, S., Shoshan, M.C. (2002). Calpain-mediated Bid cleavage and calpain-independent Bak modulation: two separate pathways in cisplatin-induced apoptosis. Mol Cell Biol *22*, 3003-13.

326. Gil-Parrado, S., Fernandez-Montalvan, A., Assfalg-Machleidt, I., Popp, O., Bestvater, F., Holloschi, A., Knoch, T.A., Auerswald, E.A., Welsh, K., Reed, J.C., Fritz, H., Fuentes-Prior, P., Spiess, E., Salvesen, G.S., Machleidt, W. (2002). Ionomycin-activated calpain triggers apoptosis. A probable role for Bcl-2 family members. J Biol Chem *277*, 27217-26.

327. Kepp, O., Gottschalk, K., Churin, Y., Rajalingam, K., Brinkmann, V., Machuy, N., Kroemer, G., Rudel, T. (2009). Bim and Bmf synergize to induce apoptosis in Neisseria gonorrhoeae infection. PLoS Pathog *5*, e1000348.

328. Mandal, M., Crusio, K.M., Meng, F., Liu, S., Kinsella, M., Clark, M.R., Takeuchi, O., Aifantis, I. (2008). Regulation of lymphocyte progenitor survival by the proapoptotic activities of Bim and Bid. Proc Natl Acad Sci U S A *105*, 20840-5.

329. Weber, S.U., Schewe, J.C., Lehmann, L.E., Muller, S., Book, M., Klaschik, S., Hoeft, A., Stuber, F. (2008). Induction of Bim and Bid gene expression during

accelerated apoptosis in severe sepsis. Crit Care *12*, R128.

330. Oltersdorf, T., Elmore, S.W., Shoemaker, A.R., Armstrong, R.C., Augeri, D.J., Belli, B.A., Bruncko, M., Deckwerth, T.L., Dinges, J., Hajduk, P.J., Joseph, M.K., Kitada, S., Korsmeyer, S.J., Kunzer, A.R., Letai, A., Li, C., Mitten, M.J., Nettesheim, D.G., Ng, S., Nimmer, P.M., O'Connor, J.M., Oleksijew, A., Petros, A.M., Reed, J.C., Shen, W., Tahir, S.K., Thompson, C.B., Tomaselli, K.J., Wang, B., Wendt, M.D., Zhang, H., Fesik, S.W., Rosenberg, S.H. (2005). An inhibitor of Bcl-2 family proteins induces regression of solid tumours. Nature *435*, 677-81.

331. Konopleva, M., Contractor, R., Tsao, T., Samudio, I., Ruvolo, P.P., Kitada, S., Deng, X., Zhai, D., Shi, Y.X., Sneed, T., Verhaegen, M., Soengas, M., Ruvolo, V.R., McQueen, T., Schober, W.D., Watt, J.C., Jiffar, T., Ling, X., Marini, F.C., Harris, D., Dietrich, M., Estrov, Z., McCubrey, J., May, W.S., Reed, J.C., Andreeff, M. (2006). Mechanisms of apoptosis sensitivity and resistance to the BH3 mimetic ABT-737 in acute myeloid leukemia. Cancer Cell *10*, 375-88.

332. Ghiotto, F., Fais, F., Tenca, C., Tomati, V., Morabito, F., Casciaro, S., Mumot, A., Zoppoli, G., Ciccone, E., Parodi, S., Bruno, S. (2009). Apoptosis of B-cell chronic lymphocytic leukemia cells induced by a novel BH3 peptidomimetic. Cancer Biol Ther *8*

333. Yip, K.W., Li, A., Li, J.H., Shi, W., Chia, M.C., Rashid, S.A., Mocanu, J.D., Louie, A.V., Sanchez, O., Huang, D., Busson, P., Yeh, W.C., Gilbert, R., O'Sullivan, B., Gullane, P., Liu, F.F. (2004). Potential utility of BimS as a novel apoptotic therapeutic molecule. Mol Ther *10*, 533-44.

334. Halloran, P.F. (1996). Molecular mechanisms of new immunosuppressants. Clin Transplant *10*, 118-23.

335. Wiederrecht, G., Lam, E., Hung, S., Martin, M., Sigal, N. (1993). The mechanism of action of FK-506 and cyclosporin A. Ann N Y Acad Sci *696*, 9-19.

336. Martinez-Martinez, S., Redondo, J.M. (2004). Inhibitors of the calcineurin/NFAT pathway. Curr Med Chem *11*, 997-1007.

337. Savignac, M., Mellstrom, B., Naranjo, J.R. (2007). Calcium-dependent transcription of cytokine genes in T lymphocytes. Pflugers Arch *454*, 523-33.

338. Sardy, M., Ruzicka, T., Kuhn, A. (2009). Topical calcineurin inhibitors in cutaneous lupus erythematosus. Arch Dermatol Res *301*, 93-8.

339. Mok, C.C., Tong, K.H., To, C.H., Siu, Y.P., Au, T.C. (2005). Tacrolimus for induction therapy of diffuse proliferative lupus nephritis: an open-labeled pilot study. Kidney Int *68*, 813-7.

340. Fu, L.W., Yang, L.Y., Chen, W.P., Lin, C.Y. (1998). Clinical efficacy of cyclosporin a neoral in the treatment of paediatric lupus nephritis with heavy proteinuria. Br J Rheumatol *37*, 217-21.

341. Ryffel, B., Weber, E., Mihatsch, M.J. (1994). Nephrotoxicity of immunosuppressants in rats: comparison of macrolides with cyclosporin. Exp Nephrol *2*, 324-33.

342. Ranchin, B., Fargue, S. (2007). New treatment strategies for proliferative lupus nephritis: keep children in mind! Lupus *16*, 684-91.

343. Dooley, M.A., Ginzler, E.M. (2006). Newer therapeutic approaches for systemic lupus erythematosus: immunosuppressive agents. Rheum Dis Clin North Am *32*, 91-102, ix.

344. Fruman, D.A., Mather, P.E., Burakoff, S.J., Bierer, B.E. (1992). Correlation of calcineurin phosphatase activity and programmed cell death in murine T cell hybridomas. Eur J Immunol *22*, 2513-7.

345. Bonnefoy-Berard, N., Genestier, L., Flacher, M., Revillard, J.P. (1994). The phosphoprotein phosphatase calcineurin controls calcium-dependent apoptosis in B cell lines. Eur J Immunol *24*, 325-9.

346. Liu, W., Youn, H.D., Liu, J.O. (2001). Thapsigargin-induced apoptosis involves Cabin1-MEF2-mediated induction of Nur77. Eur J Immunol *31*, 1757-64.

347. Jayaraman, T., Marks, A.R. (2000). Calcineurin is downstream of the inositol 1,4,5-trisphosphate receptor in the apoptotic and cell growth pathways. J Biol Chem *275*, 6417-20.

348. Shibasaki, F., Kondo, E., Akagi, T., McKeon, F. (1997). Suppression of signalling through transcription factor NF-AT by interactions between calcineurin and Bcl-2. Nature *386*, 728-31.

349. Kalivendi, S.V., Konorev, E.A., Cunningham, S., Vanamala, S.K., Kaji, E.H., Joseph, J., Kalyanaraman, B. (2005). Doxorubicin activates nuclear factor of activated T-lymphocytes and Fas ligand transcription: role of mitochondrial reactive oxygen species and calcium. Biochem J *389*, 527-39.

350. Tsokos, G.C., Kovacs, B., Liossis, S.N. (1997). Lymphocytes, cytokines, inflammation, and immune trafficking. Curr Opin Rheumatol *9*, 380-6.

351. Tsubata, T. (2005). B cell abnormality and autoimmune disorders. Autoimmunity *38*, 331-7.

352. Lu, M.C., Lai, N.S., Yu, H.C., Hsieh, S.C., Tung, C.H., Yu, C.L. (2008). Nifedipine suppresses Th1/Th2 cytokine production and increased apoptosis of anti-CD3 + anti-CD28-activated mononuclear cells from patients with systemic lupus erythematosus via calcineurin pathway. Clin Immunol *129*, 462-70.

353. Rider, V., Foster, R.T., Evans, M., Suenaga, R., Abdou, N.I. (1998). Gender differences in autoimmune diseases: estrogen increases calcineurin expression in systemic lupus erythematosus. Clin Immunol Immunopathol *89*, 171-80.

354. Chang, H., Blondal, J.A., Benchimol, S., Minden, M.D., Messner, H.A. (1995). p53 mutations, c-myc and bcl-2 rearrangements in human non-Hodgkin's lymphoma cell lines. Leuk Lymphoma *19*, 165-71.

355. Dustin, L. (2000). Ratiometric analysis of calcium mobilization. clinical and Applied Immunology Reviews 1, 5-15.

356. Vercesi, A.E., Bernardes, C.F., Hoffmann, M.E., Gadelha, F.R., Docampo, R. (1991). Digitonin permeabilization does not affect mitochondrial function and allows the determination of the mitochondrial membrane potential of Trypanosoma cruzi in situ. J Biol Chem *266*, 14431-4.

357. Campos, C.B., Paim, B.A., Cosso, R.G., Castilho, R.F., Rottenberg, H., Vercesi, A.E. (2006). Method for monitoring of mitochondrial cytochrome c release during cell death: Immunodetection of cytochrome c by flow cytometry after selective permeabilization of the plasma membrane. Cytometry A *69*, 515-23.

CHAPTER 3

ACTIVATION OF NFAT BY BZ-423

Introduction

A diverse lymphocyte repertoire is critical for immunity against pathogens. However, diversity increases the chances of these cell receptors to be self-reactive. Therefore, balance between diversity and self-reactivity is tightly regulated [1]. About 50-75% of newly produced B cells are self-reactive [2]. During B cell development, a series of checkpoints must exist to maintain tolerance to self antigens [2, 3]. These checkpoints mainly include receptor editing, clonal deletion and functional inactivation (anergy, regulatory T cells, inhibitory cytokines) [2, 3]. Among these tolerance mechanisms, 15-40% self-reactive cells are silenced by anergy [2] .

Anergy: There are a portion of autoreactive B cells detected in the periphery, but they do not generate autoantibodies as autoantibodies are detected. This observation suggests these autoreactive B cells are functionally inactivated [4]. Although these autoreactive cells retain their ability to bind to self antigen, their response to antigenic stimulation is greatly reduced [4], which may be responsible for the functional inactivation observed. This hypo-responsive state to antigen stimulation of autoreactive lymphocytes is defined as anergy [4]. Anergy is usually caused by

incomplete activation, such as chronic self-antigen stimulation in the absence of co-stimulation [5]. B cell receptor (BCR) ligation mediates tolerance by prompting receptor editing, apoptosis, or anergy [6]. Apoptosis and receptor editing are likely induced if self-antigen binds to BCR in a high affinity or avidity while anergy is likely induced if the self-antigen binds to BCR with a low affinity or avidity [6]. Unlike apoptosis and receptor editing, which permanently eliminates self-reactive BCRs and reduces cell receptor diversity, anergy maintains BCR diversity by functionally inactivating self-reactive BCRs with low affinity or avidity [7]. Anergy can also be reversed quickly by displacement of antigen [7].

Transgenic mouse models for anergy: Numerous transgenic mouse models have been developed to study B cell or T cell anergy under physiological and pathological conditions [7-18]. In these models, an engineered cell receptor for known antigen is introduced to produce the immunoglobulin (Ig) transgenic mouse, which produces sufficient lymphocytes with the desired specificity and affinity for given antigens [19]. The antigens used to study anergy are either foreign antigens (e.g. hen egg lysozyme (HEL), ovalbumin (OVA)) or derived from the pathogenic antigens involved in autoimmune diseases (e.g. dsDNA, ssDNA, Sm, insulin) ([9, 20-23]; Table 3.1). Below, two examples of transgenic mouse models for B cell anergy are discussed: one is HEL-specific model; the other one is DNA-specific model.

B cells from MD4 transgenic mice express BCR with a high affinity for HEL [8, 24], and soluble HEL (sHEL) is produced in ML5 transgenic mice [8, 24]. Breeding MD4 and ML5 generates double transgenic mice MD4 x ML5, the most

widely studied transgenic mouse model used to study B cell anergy [10]. In this model, sHEL is the neo-self antigen and anti-HEL B cells are self-reactive [10]. Co-expression of sHEL evidently increases the percentage of transitional 3 (T3) B cells [10]. As T3-B cells display reduced response to BCR stimulation, they are anergic B cells in these transgenic mice. Consistent with the reduced BCR response observed in T3 B cells, these mice fail to secrete anti-HEL antibodies following immunization with exogenous HEL plus adjuvant [10]. The presence of self-reactive cells but no production of autoantibodies suggests that they are functionally inactivated.

The presence of autoantibodies for double-stranded DNA (dsDNA) and single-stranded DNA (ssDNA) autoantibodies is a defining feature for both SLE patients and lupus-prone mice [25, 26]. Transgenic mice with engineered BCRs to bind self-antigens including dsDNA and ssDNA are generated, which are physiologically more mimic self-reactive B cells observed in the SLE patients [27]. A DNA-specific immunoglobulin-heavy-chain variable region (3H9) is derived from MRL-lpr mice [27], and B cells from V_H3H9 mice have a polyclonal B-cell repertoire enriched for ssDNA and dsDNA [11]. When the V_H3H9 heavy chain is forced to pair with ssDNA-specific light chain (V_κB) in V_H3H9 x V_κB double transgenic mice, self-reactive B cells for ssDNA are generated [12, 13]. Similarly, self-reactive B cells for dsDNA are generated in V_H3H9 x V_λ2 double transgenic mice [12]. In all these three DNA-specific transgenic mouse models for anergy, there are no autoantibodies for ssDNA, dsDNA detected [11-13], indicating these self-reactive B cells are

rendered anergic. DNA-specific autoantibodies were detected in the V_H3H9 x MRL-lpr mice, which mirrors the autoantibodies in non-transgenic MRL-lpr mice and can be used to study the anergy mechanism [28].

Anergy is observed in both mature and immature B cells [4]. Heterogeneous phenotypic characteristics of anergic B cells have been reported from various transgenic mouse models [8]. The specific increase in certain B cell population observed in immunoglobulin transgenic mice indicates that self-reactive B cells are arrested at several stage of B-cell development. This inhibition of self-reactive differentiation will limit the generation of high affinity pathogenic autoantibodies. As shown in Table 3.1, dsDNA-specific B cells from V_H3H9 and V_H3H9 x V_λ2 mice arrest at an immature and/or transitional stage, limiting self-reactive B cells entering the mature B-cell population. In MD4 x ML5 and Ars/A1 mice, self-reactive B cells are arrested at the T3 B-cell stage. Similarly, Sm-specific B cells arrest at early pre-plasma cells; interestingly, self-reactive B cells for ssDNA and Sm-specific B cells from V_H3H9 x V_κB mice and V_H2-12 x V_κB, which have a low affinity for self-antigens, do not exhibit a block in development. The detailed mechanism of these heterogeneous observations is not clear. The cell stage at which anergic B cells are arrested likely depends on the affinity of BCR for self-antigens, the nature and availability of self-antigens and the differentiation state of auto-reactive lymphocytes. It seems likely that B cells with low affinity and/or avidity for self antigen, such as V_H125 x V_κ125, V_H3H9 x V_κ8, V_H2-12 mice, are allowed to proceed through development [8].

Mouse model	Resting Anergic cells	*In vivo* observation (phenotype)	Response of anergic B cells to *in vitro* stimulation
MD4 x ML5 (nM affinity for HEL) [10]	High $[Ca^{2+}]_i$ and high ERK phosphorylation low IgM, low CD86, short life span	No anti-HEL autoantibodies Growth arrest at T3 B cells	Reduced phosphorylation of Igα, Igβ, SYK; no Ca^{2+} mobilization; no activation marker expression; no proliferation
V_H3H9 x V_λ2 (dsDNA) [11, 12]	Reduced IgM, $CD80^-$, $CD86^-$, reduced life span HSA /CD44 /MHC class II increase,	No anti-dsDNA autoantibodies, Growth arrest at immature B-cell stage	Reduced SYK phosphorylation, no activation marker expression, no proliferation
V_H3H9 x V_κ8 (ssDNA) [11, 13]	Reduced IgM and IgD, normal life span	No autoantibody secretion	Normal SYK phosphorylation, normal Ca^{2+} mobilization, intermediate proliferation No autoantibody secretion
Ars/A1 (μM affinity for ssDNA) [7, 14]	High $[Ca^{2+}]_i$ and high ERK phosphorylation, reduced IgM, high CD80/MHC class II	Growth arrest at T3 B cells No autoantibody secretion	Reduced Igα and Igβ and SYK phosphorylation, no Ca^{2+} mobilization, no activation marker expression, no proliferation, no autoantibody secretion
V_H2-12 (various affinity for ssDNA, Sm) [15, 16]	Increased CD80, CD40 and slight increase in ERK phosphorylation Reduced IgM	No autoantibody secretion, growth arrest at pre-plasma-cell stage	Normal SYK phosphorylation, weak proliferation
V_H2-12 x V_κ8 (low affinity for Sm) [17]	Increased MHC class II, reduced IgM	No autoantibody secretion, reduced marginal-zone B cells	Normal SYK phosphorylation
V_H125 x V_κ125 (μM affinity for insulin)[18]	reduced IgM	No autoantibody secretion	Normal Igα/Igβ/SYK phosphorylation and Ca^{2+} mobilization, no proliferation
An1 (mixed antigen) [3]	reduced IgM	No autoantibody secretion, growth arrest at T3 B cells	Reduced Ca^{2+} mobilization, no activation marker expression

Table 3.1: Summary of transgenic mouse models for B cell anergy. In the mouse model column, the mouse model name is followed by the self-antigen in parenthesis and citation. The 2nd column is the phenotype of resting anergic B cells. The 3rd column is the phenotype observed *in vivo* and the 4th column is the response of anergic B cells to IgM–specific antibodies.

Characteristics of anergic B cells: Anergic B cells have elevated intracellular calcium levels [10, 29], reduced membrane immunoglobulin expression [30], and/or shortened life span [8, 31]. In response to stimulation, reduced calcium mobilization and decreased tyrosine phosphorylation are observed [7, 14]. The attenuated proximal BCR signaling may leads to reduced proliferation (growth arrest *in vivo*), diminished activation marker, and decreased immunoglobulin production [7, 14].

As anergy is reversible, reduced survival is important for maintaining tolerance. Anergic B cells have a half-life of 1-5 days [20], which is considerably shorter than non-self-reactive mature B cells (40 days) [32]. This decreased survival in anergic B cells might be due to their increased dependence on B cell activating factor belonging to the TNF family (BAFF), coupled with their inability to compete with non-self-reactive cells for this survival factor [33]. Elevated BAFF can rescue anergic B cells from rapid elimination, which is confirmed by the observation that BAFF overexpression increases the numbers of autoreactive B cells [34]. However, Mice with BAFF overexpression do not develop SLE-like disease [34], indicating that BAFF is involved in pathogenesis of autoimmune disease, but not sufficient for the onset of autoimmune disease. Autoreactive B cells, which normally arrest at various stages in normal mice, develop into the mature B cells and produce autoantibodies in mice with defective apoptotic signaling pathway, such as MRL/*lpr* mice [35] and Bim-deficient mice [36]. These results indicate that abnormally extended survival of anergic B cells predisposes to autoimmune disease.

Anergic B cells display abnormal proximal BCR signaling in response to stimulation [7, 14]. As both the affinity of the BCR and the nature of self-antigen regulate anergy induction, the down-regulation of the BCR observed in anergic B cells may be partially responsible for diminished downstream signaling and immuno-responses [37]. In anergic B cells, dampened proximal BCR signaling of anergic B cells may also result from dysregulated immunoreceptor tyrosine-based activated motifs (ITAMs) phosphorylation [8]. Normal BCR stimulation induces phosphorylation of two tyrosine residues in the Igα and Igβ ITAMs, which recruits and activates the tyrosine kinase SYK, resulting in productive BCR signaling ([8]; Figure 3.1A). However, in anergic B cells, BCR stimulation only induces monophosphorylation of tyrosines, which does not support the recruitment of SYK and the subsequent SYK-dependent signaling pathway. Instead, ITAM monophosphorylation leads to constitutive engagement of RasGAP-associated docking protein p62 (Dok) and SHIP-1 [8], which negatively regulates BCR signaling and prevents any productive BCR signaling ([31, 38]; Figure 3.1B). Moreover, higher basal phosphorylation levels of the tyrosine phosphatase SHIP and SHP-1 were observed in anergic B cells from MD4 x ML5 and Ars/A1 transgenic mice [39, 40]. Anergy is lost in SHIP-1 deficient self-reactive B cells from Ars/A1 [31]. How monophosphorylation of ITAM occurs in anergic B cells is not clear. It may result from ineffective BCR aggregation. It may also result from the increased dissociation of Igα/Igβ from the BCR, as decreased co-immunoprecipitation of membrane Ig with Igα /Igβ signal-transducing complex is observed in anergic B cells [31, 41].

Mutations in other molecules involved in BCR signaling also interfere with anergy induction. For example, in the absence of CD72, which negatively regulates BCR signaling, autoreactive B cells are inappropriately expanded [24]. Similar anergy breakdown is observed in mice defective in negative BCR regulator CD5 [42] and in mice overexpressing the positive BCR regulator CD19 [43].

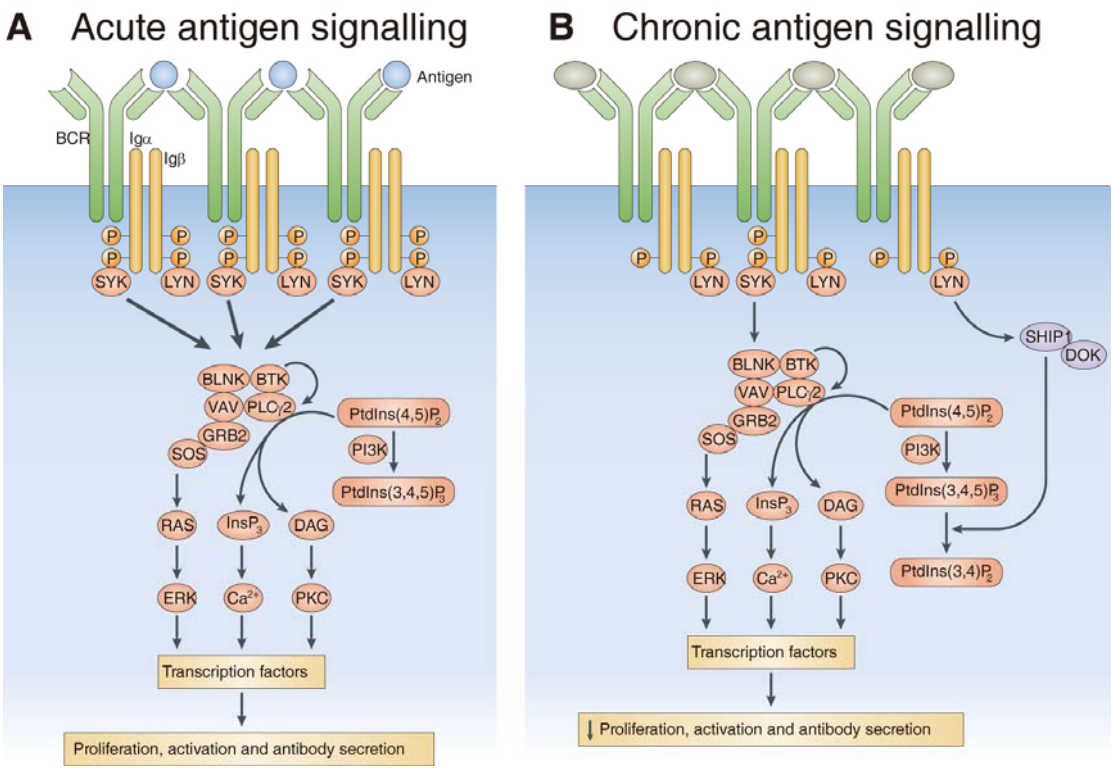

Figure 3.1: B-cell signaling in response to acute foreign antigen or chronic self-antigen stimulation. A: Foreign antigen binds to BCR and induces phosphorylation of two tyrosine residues in the ITAMs of Igα and Igβ by LYN. This results in subsequent recruitment and activation of SYK, BLNK, BTK, resulting a productive BCR signaling. B: In anergic B cells, chronic binding of self-antigen triggered a monophosphorylation of ITAM tyrosines by LYN, which limits the recruitment and activation of SYK. LYN also enhances the activation of an inhibitory complex containing SHIP1 and DOK. These proteins acts as negative regulators for BCR signaling and dampen any productive BCR signaling. This picture is adapted from [8]

***Identification of anergic B cells in normal mice*:** The physiological importance of anergy in silencing self-reactive B cells was highlighted by the identification of naturally occurring anergic B cells. Through an unique sets of cell surface markers, T3 cells ($B220^+$ $CD93^+$ $CD23^+$ IgM^{low}) were identified as anergic B cells within a wild-type repertoire [3]. Instead of being a development intermediates, they are a major population of anergic B cells. Therefore these T3 cells are renamed as An1 B cells [44]. An1 B cells have the characteristics of anergic B cells from transgenic mouse models: they have high basal $[Ca^{2+}]_i$ and short half-life time (4-5 d) [30]; and they display diminished BCR proximal signaling and reduced immune responses to BCR stimulation [3]. Further analysis the BCR from An1 cells indicates an enrichment of BCR reactive with dsDNA, indicating they are self-reactive [3]. All these characteristics suggest An1 cells are naturally occurring anergic B cells. They can be detected in the spleen, lymph nodes, and peripheral blood, which account for 5-10% of peripheral blood B cells in wild type mice [3]. As the half-life of An1 cells is 4-5 d, comparing to 40 d of normal peripheral B cells, it is estimated as many as 50% of newly produced B cells are expected to become anergic [3].

An1 might not be the only physiologically existed anergic B cells, as they are negligible in Sm- and insulin-specific models [3]. To support this, a subpopulation of naïve B cells expressing IgD but not IgM is identified as anergic B cells in healthy humans [45]. They display several characteristics of anergic B cells [45]. For example, in response to BCR stimulation, a reduced capacity to mobilize calcium and decreased levels of tyrosine phosphorylation were observed [45]. A pool of DNA-reactivate B

cells or anti-nuclear reactive memory cells with several characteristics of anergic B cells were also detected in peripheral blood of healthy humans [2, 46]

Characteristics of anergic T cells: Anergy is induced as a result of incomplete or suboptimal T cell activation [47, 48]. Unlike B cells, naïve T cells are more resistant to anergy induction than memory T cells both *in vivo* and *in vitro* [49-51]. The first description of anergic T cells arose from the observation that T cell clones that were initially stimulated with formaldehyde fixed APCs failed to proliferate or produce IL-2 upon rechallenged with live APCs plus peptide [52]. Similar to anergic B cells, elevated basal $[Ca^{2+}]_i$ is also observed in anergic T cells. In response to stimulation, they display attenuated proximal TCR signaling, including reduced calcium mobilization and decreased tyrosine phosphorylation [48, 53-55]. The hallmarks of anergic T cells are reduced proliferation and cytokine production (IL-2) in response to receptor activation such as anti-CD3 and anti-CD28 co-stimulation [56]. Similar to the anergy induction in B cells, anergy can be developed *in vivo* by applying soluble self-antigen. For example, intravenous administration of soluble ovalbumin (OVA) peptide renders OVA-specific T cells tolerant, as defective proliferation response and decreased IL-2 production are observed following OVA plus adjuvant CFA stimulation [57]. *In vitro* they can be induced by delivery of a strong T cell receptor stimulation in the absence of co-stimulation, by calcium ionophore ionomycin, or by weak agonist and altered peptide ligand [58].

Molecular mechanism of anergy induction and maintenance:

Desensitized cell receptor signaling: In several anergic T cells and B cells, attenuated cell receptor-mediated signaling is observed. Chronic stimulation of lymphocytes leads to constitutive $[Ca^{2+}]_i$ increase and high basal level of tyrosine phosphorylation [3, 55]. These changes lead to biased activation of inhibitory signaling [55, 59, 60]. Similar to anergic B cells, increased LYN activity also be observed in anergic T cells [55]. Moreover, studies of TCR signaling in anergic T cells indicate the involvement of other TCR signaling molecules [61, 62]. Increased Diacylglycerol kinase (DGK) is observed in anergic T cells [61]. DGK phosphorylates diacylglycerol (DAG) and inhibits the subsequent DAG-mediated signaling. This observation suggests DGK may participate in anergy by modulating DAG-mediated signaling. Consistent with this observation, DGKα-overexpressed T cells are anergic while DGKα-deficient T cells are resistant to anergy induction [61]. Two key signaling proteins PKCθ and PLCγ were also diminished in anergic T cells [62]. At the same time, increased E3 ubiquitin ligases (Itch, Cbl-B) were observed [62]. As PKCθ and PLCγ are targets of E3 ubiquitin ligases Itch, Cbl-B, decreased PKCθ and PLCγ1 are possibly due to increased proteolytic degradation by E3 ubiquitin ligases Itch, Cbl-B, which leads to attenuated TCR signaling observed in anergic T cells [62].

The involvement of Calcium-calcineurin-NFAT in anergy: Elevated $[Ca^{2+}]_i$ is observed in anergic T cells and B cells [3, 55], suggesting Ca^{2+} plays a critical role in anergy induction. Ionomycin, an ionophore to increase $[Ca^{2+}]_i$, induces anergy in T cells in vitro [63], confirming the critical role of calcium. Calcineurin inhibitor cyclosporine A (CsA) or FK506 blocks anergy [48, 63-65], suggesting calcineurin is

involved in anergy. Overexpression of a active form of calcineurin promotes anergy induction [66], further supporting essential role of calcineurin in anergy. Anergy induction is compromised in both NFATc2-deficient T cells and NFATc2-deficient B cells [63, 67], indicating the involvement of NFAT. In addition, Jurkat T cells transfected with vectors encoding constitutively active NFATc2 mutant are resistant to anti-CD3 plus anti-CD28 stimulation, a characteristic of anergic T cells [68]. In summary, calcium-calcineurin-NFAT signaling pathway is involved in both anergy induction in T cells and B cells.

Anergy-associated genes: Transcription inhibitor actinomycin D and protein inhibitor cycloheximide inhibit anergy, suggesting macromolecular synthesis is required for anergy induction and maintenance [69]. What genes are transcribed and post-translated under anergic conditions has been studied [70]. By studying gene expression in both anergic T cells and B cells, a set of anergy-associated genes was identified ([71, 72]; Table 3.2). The majority of anergy-associated genes are regulated by activated NFAT in the absence of AP-1 activation [63, 68, 73]. This selective NFAT activation is induced by low sustained $[Ca^{2+}]_i$, which is not sufficient to activate other transcription factors such as NFκB and AP-1 [39]. Furthermore, Primary T cells with a retroviral expression of a constitutively active NFATc2 that is unable to interact with AP-1 results in strong anergy induction [63]. In response to anti-CD3 and anti-CD28 stimulation, both NFATc2 and AP-1 are activated [63]. However, the defective interaction between NFATc2 and AP-1 makes it impossible for NFATc2 to form transcriptional complex with AP-1, which resulted in diminished IL-2 production and

proliferation [63]. Several anergy associated genes are also induced, which indicates anti-CD3 and anti-CD28 induce anergy instead of activation in these mutant cells. These results suggest that NFAT alone induces synergy and AP-1 binding is not necessary as well [63].

Both upregulated and downregulated anergy genes were identified [3, 71, 73, 74]. In anergic T cells, the upregulated anergy associated genes collectively act to repress TCR signaling [58]. Based on their function, they are divided into 3 categories: E3 ubiquitin ligases (gene related to anergy in lymphocytes (GRAIL), Casitas B cell lymphoma-b (Cbl-b), Itch) [75], transcriptional repressor (GRG4, Ikaros, Jumonji, EGR2, EGR3), and receptor involved in T cell receptor signaling such as receptor tyrosine phosphatase and diacylglycerol kinase (DAKα) [74]. Similar to the transcription program in T cell anergy, a subset of anergy genes are identified in anergic B cell, although their functions in anergy induction and maintenance are not clear [3, 71, 73]. Among these anergy-associated genes identified in anergic B cells, EGR-2, NAB-2 and neurogranin are induced via a calcineurin-NFAT pathway [3, 71, 73].

E3 ubiquitin ligases are most studied anergy associated gene. E3 ubiquitin ligase transfers ubiquitin to target proteins to mark them for degradation [76]. In response to tolerant stimuli, E3 ubiquitin ligases, including Itch, Cbl-b and GRAIL, are upregulated in a CsA-sensitive manner [77]. *Cbl-b*- or *Itch*-knockout mice develop SLE-like disease, suggesting a breakdown of tolerance contributes to the development of autoimmune disease [77]. T cells from those mice are resistant to anergy induction

at low doses of ionomycin [77], suggesting that E3 ligases are necessary for tolerance.

Gene	category	Activation Modes	Reference
Itch *Cbl-b* *Grail*	E3 ubiquitin ligases	Ca^{2+}-calcineurin for activation, increased in anergic lymphocytes, involved in anergy induction and maintenance by enhanced proteolytic degradation of PKCθ and PLCγ1. *Itch*-deficient mice develops autoimmune disease	[77-80]
Ikaros	Transcriptional repressor	Ca^{2+}-calcineurin-NFAT for activation, increased in anergic T cells. It inhibits IL-2 transcription by binding to IL-2 promoter and inducing histone deacetylation,	[63, 81, 82]
Grg4	Transcriptional repressor	Ca^{2+}-calcineurin-NFAT for activation increased in anergic T cells. It acts as co-repressor. In lymphocytes, it binds to Pax5 to convert it from activator to repressor	[63, 83]
Rptp-κ *Ptp1b*	Protein tyrosine phosphatase	Ca^{2+}-calcineurin-NFAT for activation increased in anergic T cells. It may antagonize protein tyrosine kinase, therefore, inhibiting proximal TCR signaling	[63]
Diacylglycerol kinase (DGK)	to repress DAG signaling and GTPase-Ras signaling	Ca^{2+}-calcineurin-NFAT for activation increased in anergic T cells. It phosphorylates DAG and inhibits its subsequent signaling. It also inhibits GTPase Ras signaling. DGKα overexpression induces synergy and anergy induction is impaired in DGKα-deficient mice	[63, 84, 85]
Egr2/Egr3	NFAT partners for repression	Ca^{2+}-calcineurin-NFAT for activation, increased in anergic B cells and T cells. Negative regulator for T cell activation, impaired anergy induction if *EGR2* reduced. Increased EGR2/3 associated with effective lupus treatment.	[61, 86-88]

Table 3.2: Anergy-associated genes.

GRAIL overexpression also renders T cells anergic [80]. Recently, a B cell specific ablation of both c-*Cbl* and *Cbl-b* results in enhanced BCR-proximal signaling and defective B cell tolerance, which might be responsible for SLE-like symptoms observed in the these *Cbl* double-deficient mice [89].

E3 ubiquitin ligases play a critical role in maintaining the anergic state by promoting proteolytic degradation [62]. The accelerated degradation of PLC-γ1 and PKC-θ expression by E3 ubiquitin ligases leads to attenuated proximal T cell signaling, which eventually results in IL-2 production in response to stimulation [62]. Overexpression of Itch or Nedd4 led to the ubiquitination and degradation of PLC-γ1 and PKC-θ in HEK293 cells [80, 90]. PLC-γ1 cleaves phosphatidylinositol 4,5-biphosphate (PIP2) to produce diacyl glycerol (DAG) and inositol 1,4,5-triphosphate (InsP3), important for DAG- and calcium-mediated signaling [91]. PKC-θ is activated by DAG and important for activations of AP-1 and NFκB [92]. In addition to signaling for proteasome degradation, ubiquitin modification is also involved in the endocytosis pathway of protein tyrosine kinases (PTKs) for lysosomal degradation [93], further suppressing TCR signaling. *Cbl-b* downregulates TCR surface expression by promoting its endocytosis via mono-ubiquitination, which may be partially responsible for T cell receptor downregulation in anergic T cells [94].

Transcription factors including early growth response gene 2 (EGR2) and early growth response gene 3 (EGR3) are upregulated in tolerant lymphocytes in a Ca^{2+}-calcineurin dependent manner [86, 87]. Their increase expression in turn regulates transcription of anergy-associated genes. For example, EGR2 may activate

Cbl-b as overexpression of EGR2 or EGR3 leads to increased Cbl-b while EGR3 deficiency results in lower expression of Cbl-b [86]. EGR2 also up-regulates cell cycle inhibitors p21 and p27, which may be associated with reduced proliferation in anergic lymphocytes [95]. *EGR2* reduction by *EGR2*-specific RNA interference (RNAi) rendered cells resistant to anergy induction [87], suggesting the critical role of EGR2 in anergy induction. However, anti-CD3 induces anergy is normal in EGR3-deficent T cells, possibly because of functional redundancy between EGR2 and EGR3 [86].

NFAT in regulatory T cells: regulatory T cells (Tregs, $Foxp3^+CD4^+CD25^+$) actively suppress T cell activation and play an important role in T cell anergy [96]. NFAT plays a critical role in the suppressor function of regulatory T cells (Treg, $Foxp3^+CD4^+CD25^+$) cells [97]. NFAT interacts with Foxp3 and forms the transcription complex, which binds to the promoters to repress *IL-2* expression and to activate transcription of Treg markers *CTLA4* and *CD25* [98]. Structure-based mutation of Foxp3, disrupts its interaction with NFAT and decreases the transcription activity of Foxp3, which results in the impairment of Tregs' regulatory function and leads to the development of autoimmune disease [98]. In mice lacking NFATc2 and NFATc3, $CD4^+$ T cells are resistant to suppression mediated by wild type Treg cells [99], which further supports the critical role of NFAT in the suppressor functions of Treg cells..

Nuclear factor of activated T cells (NFAT) family: In addition to its involvement in tolerance, activated NFAT participates in lymphocyte development

and effector function. There are five members of the NFAT family: NFATc1 (NFAT2, NFATc), NFATc2 (NFAT1, NFATp), NFATc3 (NFAT4, NFATx), NFATc4 (NFAT3) and NFAT5 [100-103] (Figure 3.2). Among them, NFATc1-4 are dephosphorylated and activated by serine/threonine phosphatase calcineurin [104]. NFATc1a, one isoform of NFATc1, is under control of an NFAT-dependent inducible promoter [105]. Therefore, activated NFAT binds to the promoter of NFATc1a and promotes to its expression [105, 106]. Although NFATc1-3 are expressed in peripheral lymphocytes [104], NFATc2 accounts for 80-90% of total NFAT activity in resting lymphocytes [63]. NFATc3 is highly expressed in thymocytes [107]. NFATc4 is implicated mainly in cardiac hypertrophy [108].

NFAT proteins contain a transactivation domain (TAD), a moderately conserved regulatory domain and a highly conserved DNA binding domain (RSD) (Figure 3.2). Within the regulatory domain, there is a conserved calcineurin binding region, a nuclear localization sequence (NLS) and a series of conserved serine-rich sites. NFAT kinase and calcineurin tightly regulates NFAT activity by phosphorylating and dephosphorylating these serine residues, respectively ([109, 110]; Figure 3.2).

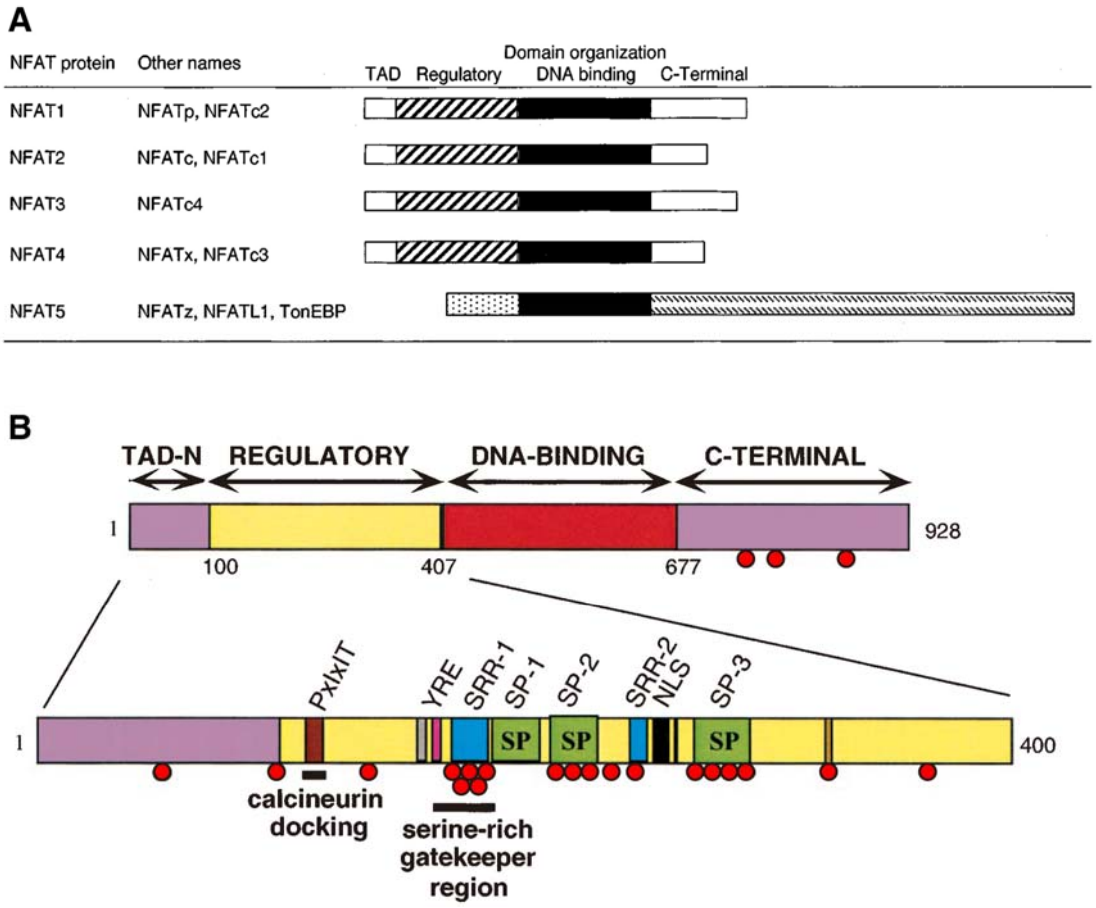

Figure 3.2: NFAT family proteins and their structures. Panel A shows schematic structures of NFAT member proteins. Panel B is the detailed domain structure of NFAT. The N-terminal transactivation domain (TAD-N), regulatory domain, DNA binding domain and c-terminal domain are indicated. The regulatory domain is enlarged to show conserved sequence motif as colored boxes. PxIxIT is a major calcineurin docking site. NLS is the nuclear localization sequence. The phosphorylation sites are indicated as red filled circle based on study results from NFATc2 [111]. This figure is adapted from [112].

NFAT activation signaling pathway: Calcineurin is a heterodimeric protein of a catalytic subunit (CnA) and a regulatory subunit (CnB). The autoinhibitory domain in CnB obscures the phosphatase domain CnA [113]. In resting cells, calcineurin is inactivated, and NFAT is phosphorylated, with low affinity for DNA, and located in the cytoplasm [114]. $[Ca^{2+}]_i$ can be increased by immunoreceptor ligation (BCR, TCR, CD40, and etc), calcium ionophores (ionomycin, A23187), or

the endoplasmic reticulum calcium-ATPase (SERCA) inhibitor (tharpsigargin) [114]. Tharpsigargin inhibits SERCA and causes calcium release of ER stores [114]. The increased Ca^{2+} then binds to calmodulin, which activates the serine/threonine phosphatase activity of calcineurin by displacing the autoinhibitory domain in CnB and exposing the active sites in the CnA [115]. The activated calcineurin activates NFATs in three steps: dephosphorylation, nuclear import and promoter binding (Figure 3.3; [114]). Activated calcineurin first dephosphorylates 13 or more residues in the regulatory domain of NFAT, which triggers a conformational change, unmasking its NLS resulting in nuclear translocation [104]. Once in the nucleus, as dephosphorylated NFAT has higher affinity for DNA, it binds to the promoter of target genes and activates transcription [104, 116-118]. FK506 and CsA inhibit calcineurin-mediated NFAT dephosphorylation and block all three steps of activation, indicating that dephosphorylation is the initial and critical step of activation [116]. NFAT returns to its original phosphorylated state with 5-15 min upon addition of calcium chelator EGTA or CsA [116, 117, 119]. This rapid reversal of NFAT activation implies that sustained calcium influx and calcineurin activity are required for NFAT-mediated transcription [114]. This re-phosphorylation of NFAT is mediated by constitutive NFAT kinases, including glycogen synthase kinase 3 (GSK3) [111], casein kinase 1 (CK1) [120] and dual-specificity tyrosine-phosphorylation regulated kinase (DYRK1 and DYRK2) [121].

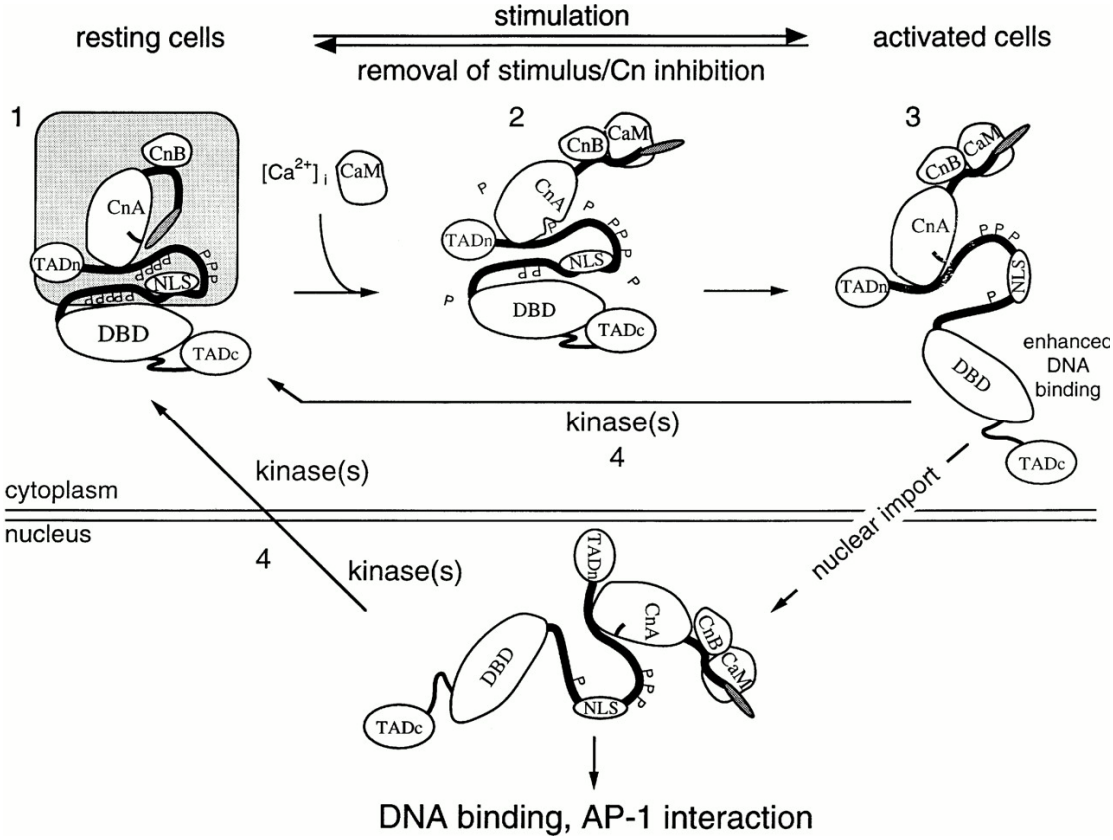

Figure 3.3: NFAT activation. See text for details. TAD (transcription activation domain), NLS (nuclear localization sequence), DBD (DNA binding domain), CnA (calcineurin A), CnB (calcineurin B), CaM (calmodulin). This picture is adapted from [114].

The activity of calcineurin is not only regulated by calcineurin B and calmodulin, but also by several endogenous calcineurin inhibitors [122] including calcineurin-binding protein 1 (cabin1, cain) [123], A-kinase anchoring protein AKAP79 [124], calcineurin B homolog protein (CHP) [125], and modulatory calcineurin-interacting proteins (MCIPs, calcipressin) [126-128]. These proteins bind to calcineurin and inhibit its phosphatase activity [122]. For example, calcipressin 1 (Csp1) binds to CnA and inhibits calcineurin activity [128]. Csp1 deficiency will presumably lower the threshold for calcineurin activation. In response to TCR stimulation, T cells from Csp1-deficient mice produce more cytokines and display

increased FasL expression [128]. As FasL expression is controlled by NFAT, increased FasL expression indicates increased NFAT activation. It is therefore concluded that Csp1 deficiency lowers the threshold for calcineurin activation and subsequent NFAT activity, which leads to increased FasL expression in response to TCR stimulation [128].

CRAC channel in calcium influx of lymphocytes: In lymphocytes, the calcium release activated calcium (CRAC) channel is the main mechanism for calcium influx across the plasma membrane (Figure 3.4; [129, 130]). The importance of calcium influx through CRAC channel is highlighted by three families of patients with severe combined immunodeficiency (SCID), who have major defects in CRAC channel function and display severely compromised lymphocyte function [131-133]. As the molecular composition of the CRAC channel is not totally resolved, the CRAC channel is defined by its unique electrophysiological characteristic: high selectivity of calcium over other cations, activation by depletion of intracellular calcium stores (such as ER depletion), low single channel current, and inhibition by heavy metals such as La^{3+} and intracellular calcium [110].

Three independent groups have identified Orai as a pore subunit of CRAC channel [134-136]. So far, three isoforms (Orai1, Orai2, and Orai3) have been identified (Figure 3.5B, [110]). A single mismutation R91W in Orai1 is detected in SCID patients, which may contribute to the reduced calcium influx [134]. Expression of wild type Orai1 in SCID T cells restores SOCE, confirming the involvement of Orai in calcium influx [134]. Using genome-wide RNA interference screen, stromal

interaction molecule (STIM) was also identified to participate in regulation of CRAC

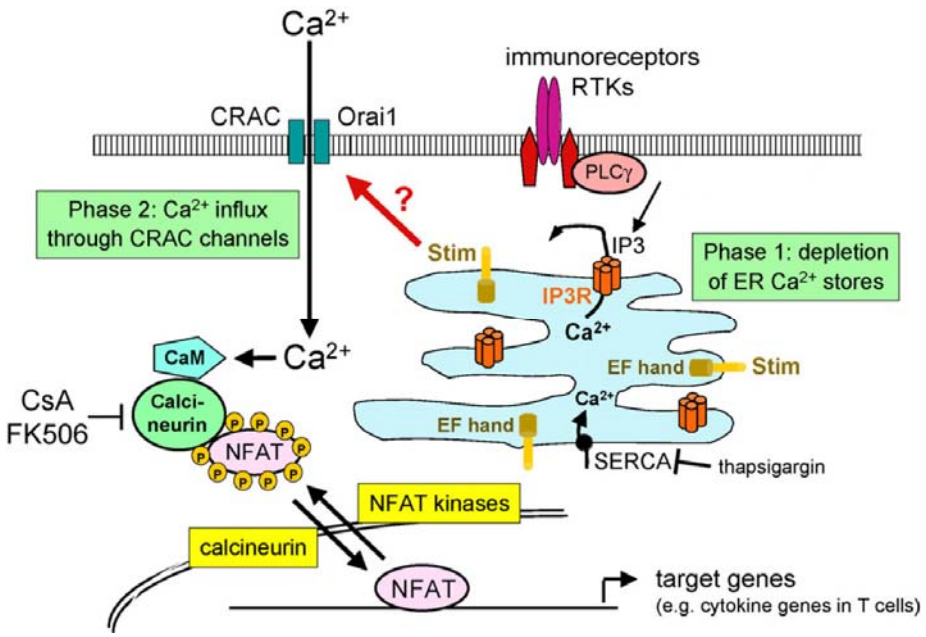

Figure 3.4: NFAT activation signaling. Cell receptor ligation leads to increased production of inositol triphosphate (IP3), which binds to IP3 receptor located in the ER, leading to the depletion of ER calcium store. The ER depletion triggers the opening of CRAC, resulting extracellular calcium influx and sustained intracellular calcium increase. The increased calcium binds to calmodulin (CaM), which activated calcineurin. Activated calcineurin dephosphorylated NFAT, resulting in its nuclear translocation and subsequent NFAT-dependent gene expression. The depleted ER is refilled with calcium using SERCA. Thapsigargin, a specific inhibitor for SERCA, prolongs calcium increase by inhibiting ER calcium refilling. CsA and FK506 inhibit calcineurin activity. The dephosphorylated NFAT returns to its resting level by constitutive active NFAT kinase. This figure is adapted from [110]

channel opening [135, 136]. STIM (STIM1 and STIM2) is located in the ER lumen, where the N-terminal EF hand, a helix-loop-helix structure domain found in calcium binding proteins, binds to calcium and senses calcium change in the ER (Figure 3.5 A; [137, 138]). Following ER calcium depletion, STIM1 aggregates into small clusters in the ER membrane [139], which signals opening of the CRAC channel (Figure 3.5C). Further studies are needed to answer whether there are other proteins in the CRAC

channels.

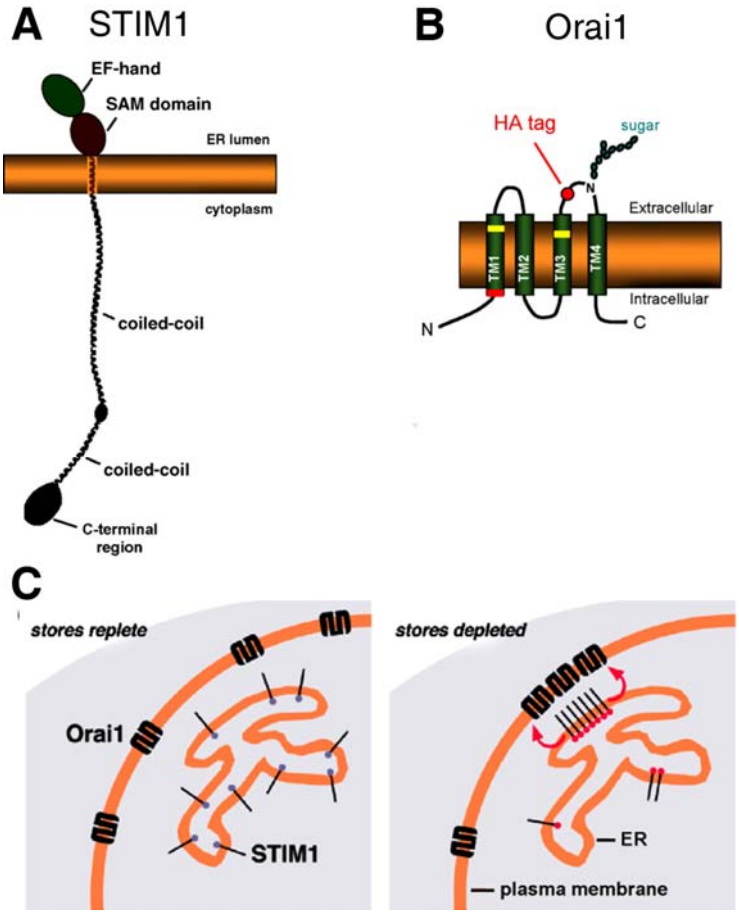

Figure 3.5: Proposed model of STIM and Orai in CRAC channel opening. Panel A is the schematic structure of STIM1. In the ER lumen side, there is an EF-hand, which binds to and senses ER calcium level, and it is followed by a sterile α-motif (SAM) domain, which possible transmit the ER calcium binding signals to cytosol. The STIM structure on cytosol side is not clear. Pane B is the schematic structure of Orai1. It is a plasma membrane protein with four transmembrane domains (TM). The red rectangle indicates R91W mutation identified in SCID patients. Panel C is the proposed model of STIM-orai signaling. The ER calcium sensor STIM1 is distributed throughout the ER in the resting cells. Once the ER is depleted from ER, bound calcium dissociates from STIM1, which results in conformational changes in the STIM1 and aggregation. At sites of ER-plasma membrane, signal from STIM1 (red arrows) activate calcium influx through CRAC channel. This picture is adapted from [110].

In addition to Orai, bioinformatics approaches for potential CRAC channel subunit have identified transient receptor potential (TRP) proteins [140]. However, further detailed studies reveal that their effects on CRAC channel activity are only

modulatory [141]. TRPC1 is shown to interact both STIM and Orai, therefore, it is proposed to serve as a molecular link [142]. 3,5-bis(trifluoromethyl)pyrazole derivative YM-58483 (BTP2) specifically inhibit CRAC channel, as it inhibited calcium influx through CRAC channel by 30-fold increase when compared with voltage-operated calcium channels [143]. YM-58483 inhibits calcium influx with an IC_{50} of approximately 10-300 nM [143-145], and it also inhibits calcium influx through TRPC with an IC_{50} of approximately 300 nM [145]. Based on these findings, it is proposed that TRP proteins may modulate CRAC channel and can be a regulatory site for CRAC channel.

NFAT transcriptional regulation: NFATs are transcription factors that can activate and repress gene transcription. NFAT was discovered through studying IL-2 expression. In the promoter of IL-2, there are two high-affinity and several low-affinity NFAT binding sites [146]. Introduction of mutations that abolish NFAT binding to the two high-affinity NFAT-binding sites results in a dramatic reduction in the promoter activity [147], indicating the critical activating role of NFAT in IL-2 expression. The IL-2 transcription activation requires cooperative interaction between NFAT and AP-1, as cells harboring NFAT1 mutant that are unable to interact with AP-1 but still bind to DNA do not produce IL-2 in response to stimulation [148]. In addition to IL-2, NFAT can also induce other cytokines and co-stimulating molecules (CD40L, CTLA-4, FasL), which are crucial for lymphocytes activation, differentiation and cell death induction [149-152].

In addition to activating transcription, NFATs can repress transcription [58].

NFATs can repress IL-2 expression by upregulating Ikaros [82]. The increased Ikaros binds to the IL-2 promoter and recruits histone deacetylase (HDAC). HDAC then removes acetyl groups from core nucleosome histones, decreasing the accessibility of transcription factors to the IL-2 promoter and reducing IL-2 transcription [82]. NFAT itself negatively regulates the expression of cyclin-dependent kinase 4 (CDK4) [153, 154]. NFATc2-deficient mice have elevated CDK4 protein levels, and this elevated CDK4 expression is inhibited by ectopic expression of NFATc2 [153]. Being an important protein in regulating cell cycle, the increased CDK4 is proposed to be associated with hyperproliferative phenotype in NFATc2-deficient mice [153].

The role of NFAT in immune response: Inhibition of NFAT activation by CsA significantly suppresses T cell proliferation in response to stimulation, indicating its critical role in T cell activation [155]. Due to their redundant role, single knockout of calcineurin catalytic domain *CnA*α or *CnA*β does not affect the overall lymphocyte functions (Table 3.3; [156, 157]). It is surprising that knockout of calcineurin regulatory domain *CnB* does not induce dramatic defects in lymphocyte function either [158]. Knockout mice that lack individual *NFAT* isoform show only mild alteration in immune function, and severe changes become apparent only when more than one *NFAT* isoforms is deleted, indicating functional redundancy in the NFAT family (Table 3.3; [159-166]). However, single *NFAT* deletion causes a variety of phenotype. This observation indicates that individual isoforms have distinct immune functions. For example, NFATc1 was induced upon activation, and its knockout attenuated T-cell proliferative response [160, 167], indicating the positive role of

Gene	Null phenotype associated with immune function
NFATc1 (NFATc, NFAT2)	Embryonic Lethal due to failure of cardiac morphogenesis [159] Reduced B and T cell proliferative response, impaired Th2 response, defective T cell development and Th2 differentiation [160],
NFATc2 (NFATp, NFAT1)	Enhanced B and T cell response, Th2 bias with increased Th2 cytokine [161, 162]
NFATc3 (NFATx, NFAT4)	Impaired $CD4^+/CD8^+$ SP thymocytes due to increased $CD4^+CD8^+$ DP apoptosis, hyperactive peripheral T cells response [163].
NFATc4 (NFAT3)	Viable, no apparent defects in immune function[164]
NFATc3/c4	Embryonic lethal due to vascular developmental abnormalities [164].
NFATc1/c2	Hyperactive B cells with elevated antibodies, expanded plasma cells and filtration while hypoactive in response to activation, impaired T cell function (reduced Th1 and Th2 cytokines) [166].
NFATc2/c3	Lymphoproliferative disorder (hyper-reactive TCR, defect in T cell apoptosis) [165]
CnAα	Normal T cell and B cell development, normal overall T cell function, slightly defective antigen-specific T cell response [156]. CnAα accounts for 70-80% of overall calcineurin activity in T cells [168]
CnAβ	Defective T cell development (decreased CD3, $CD4^+/CD8^+$ SP), slightly impaired T cell function [157]
CnB	Abnormal immunogenic B cell response [158]

Table 3.3: The phenotypes of calcineurin- and NFAT-deficient mice.

NFATc1 in lymphocyte proliferation. In contrast, deficiency of NFATc2 and/or NFATc3 results in increased B cell and T cell proliferation in response to antigen stimulation, and an increased percentage of activated cells in observed in these mutant mice [161, 162, 165]. As FasL expression is reduced, together with defective anti-CD3-induced apoptosis, the increase in activated cells is possibly due to lack of activation-induced cell death (AICD) [169]. These observations indicate a negative role of NFATc2 or NFATc3 in lymphocytes proliferation and activation.

Results

Bz-423 induces NFATc2 activation

Bz-423 induces NFATc2 dephosphorylation in a dose- and time-dependent manner. NFATc2 (NFAT1/NFATp) is a member of the nuclear factor of activated T cells (NFAT) family plays a central role in transcriptional activation of numerous genes concerned with the immune response [152]. In B cells, NFATc2 regulates cytokine production [162], suppresses B cell proliferation [170], and promotes B cell tolerance [67]. Bz-423 induces NFATc2 dephosphorylation in Ramos B cells (Chapter 2). Considering the critical role of NFAT in modulating immune function, Bz-423 induced NFAT dephosphorylation was studied.

First, the concentration dependence and the timecourse of Bz-423 induced NFAT dephosphorylation were investigated. As serum reduction from 10 to 2% induces transient NFAT dephosphorylation, media containing 10% (v/v) fetal bovine serum (FBS) was used for these experiments. As Bz-423 binds to serum protein and its effective concentration is reduced [171], [Bz-423] was increased for those studies. The effective concentration of 16 μM Bz-423 in 10% FBS is equivalent to that of 5 μM Bz-423 in 2% FBS as they both induces equivalent amount of cell death in anti-IgM-stimulated Ramos B cells (Figure 3.6). In Ramos cells, Bz-423 induces NFATc2 dephosphorylation in a dose-dependent manner (Figure 3.7A). At 15 min, 20% of NFATc2 was dephosphorylated by Bz-423 (8 μM), and 35% of NFATc2 was dephosphorylated by Bz-423 (16 μM). Bz-423 also induced NFATc2 dephosphorylation in a time-dependent manner. At 15 min, 35% of NFATc2 was

dephosphorylated by Bz-423. Then it declined to the resting level at 0.5 and 1 h. At 2 to 6 h, the dephosphorylated NFAT maintained at around 20-30% (Figure 3.7B).

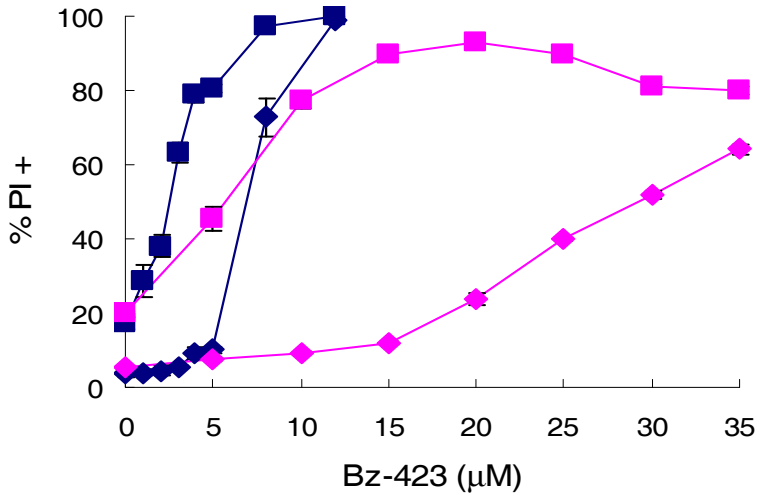

Figure 3.6: Anti-IgM induced synergy in media with different [serum]. Ramos B cells in media with either 2% FBS (blue) or 10% FBS (magenta) were treated with various concentration of Bz-423 in the presence of control Ig (1 μg/mL,◆) or anti-IgM (1 μg/mL,■). 24 h later, cell death were determined by PI permeability. This experiment was repeated for 2 times. The absence of an error bar indicates ≤ 1 % standard deviation

Bz-423 induces NFATc2 nuclear translocation in Ramos cells: Once dephosphorylated, NFAT translocates into the nucleus and initiates transcription of NFAT-dependent genes [110]. To test the hypothesis that dephosphorylated NFATc2 translocates from cytosol to nucleus, the cytosol and nuclear fractions of Bz-423 treated Ramos cells were immunoblotted with NFATc2 specific antibody to study the sub-cellular distribution change. β-tubulin and cAMP response element binding (CREB) were used as cytosol and nuclear marker, respectively. Ionomycin, an ionophore which increases $[Ca^{2+}]_i$ increase, and activates calcineurin and NFAT [172],

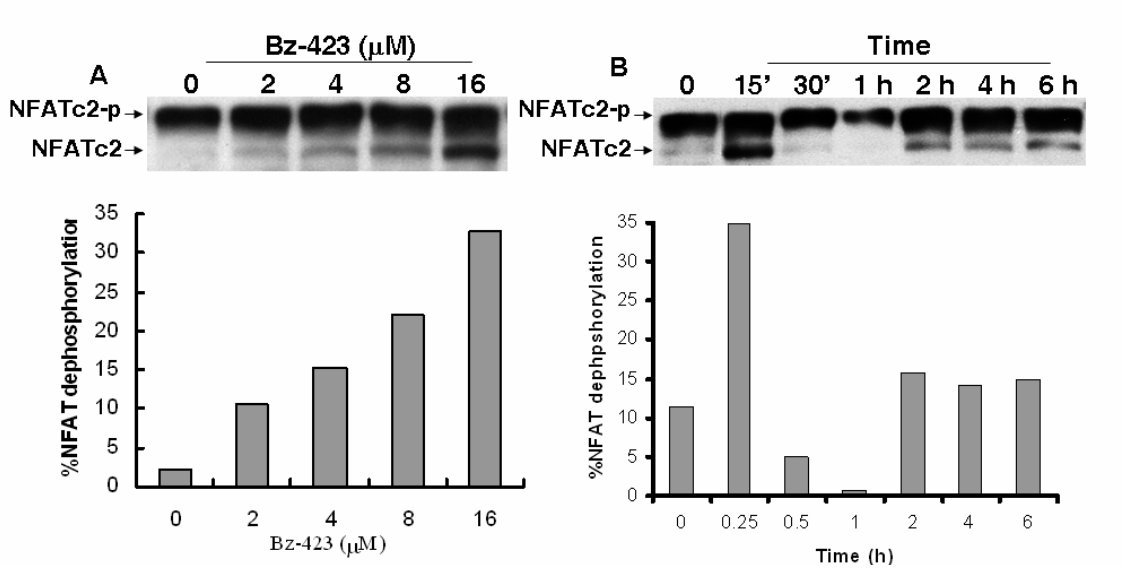

Figure 3.7: Bz-423 induces NFATc2 dephosphorylation in Ramos cells. (A) Ramos cells were treated with a dose response of Bz-423 in media containing 10% FBS. 15 min later, the whole cell lysate was harvested and NFATc2 dephosphorylation was detected in western blot. Both the phosphorylated and dephosphorylated NFAT are quantified using Image J program and the % NFAT dephosphorylation was calculated by the equation 100%*dephosphorylated NFAT / (dephosphorylated NFAT + phosphorylated NFAT). The dose response of Bz-423 induced NFAT dephosphorylation at 15 min was shown. (B) Ramos cells were treated with Bz-423 (16 μM) in media containing 10% FBS. At indicated times the whole cell lysate was harvested for immunoblotting using NFATc2. The time course of Bz-423 induced NFAT dephosphorylation and the quantification of % NFAT dephosphorylation are shown. Both panels are representative of two experiments.

was used as a positive control. In whole cell lysates, ionomycin induced NFATc2 dephosphorylation. This dephosphorylated NFAT translocated into the nucleus as dephosphorylated NFATc2 disappeared in the cytosol fraction and was increased in the nuclear fraction (Figure 3.8A). Absence of β-tubulin in the nuclear fraction and CREB in the cytosol fraction demonstrated the fraction obtained were pure (Figure 3.8A). Some dephosphorylated form of NFAT was detected in the nucleus of untreated Ramos cells (Figure 3.8A), suggesting NFATc2 is partially activated in Ramos B cells. This finding is consistent with the literature reports that constitutive

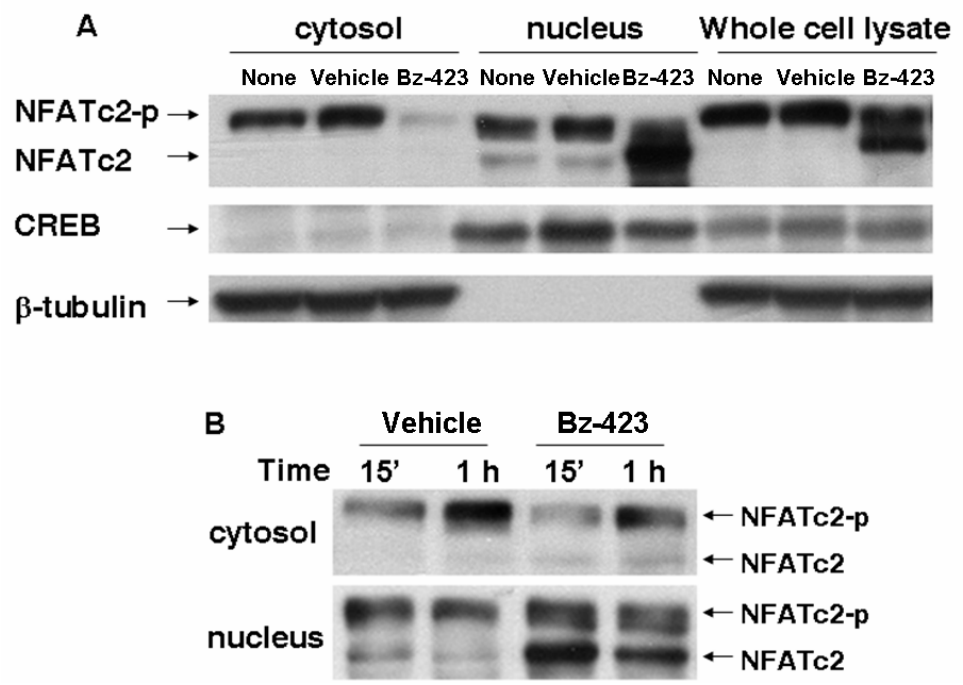

Figure 3.8: Bz-423 induces NFATc2 nuclear translocation in Ramos cells. (A) Ionomycin induced NFAT nuclear translocation in Ramos B cells: Ramos cells were treated ionomycin (iono, 1 μg/mL) for 20 min, using DMSO as a vehicle control. Then non-treated-, vehicle- and ionomycin-treated Ramos cells were harvested, and whole cell lysate, cytosol and nuclear fractions were obtained. The cell lysates were immunoblotted with antibodies specific for NFATc2, nuclear specific protein CREB, cytosol specific β-tubulin. (B) The cytosol and nuclear fractions from vehicle /Bz-423 (16 μM) treated for 15 min or 1 h were immunoblotted with NFATc2. Panel A is from a single experiment and Panel B is representative of three experiments.

NFAT activation and nuclear translocation is observed in diffuse large B-cell lymphomas (DLBCL) and Burkitt's lymphomas [173]. In addition, phosphorylated NFAT was also observed in the nucleus of Ramos cells (Figure 3.7A), which is blocked by CsA. This presence of dephosphorylated NFAT in the nucleus has been previously reported in T cells during ionomycin removal or EGTA addition [117]. As NFAT can be rephosphorylated by NFAT kinase and translocates back to the cytosol, the phosphorylated form of NFAT observed in the nucleus is possibly due to the relative slow NFAT nuclear export as NFAT nuclear export is a relatively slower than NFAT rephosphorylation [174]. Therefore, to maintain a sustained NFAT activation, a

sustained NFAT activating signal is required. Bz-423 also induced NFAT nuclear translocation as increased dephosphorylated NFAT was detected in the nucleus (Figure 3.8B). At 15 min, Bz-423 induces ~10-fold increase in dephosphorylated NFAT over vehicle control. Thus, these results confirm that Bz-423 induced NFAT dephosphorylation, which translocates to the nucleus.

Bz-423 induces NFAT-dependent transcription: NFAT activated by Bz-423 is expected to induce transcription. A commercially available NFAT reporter plasmid pNFAT-SEAP was used to test the hypothesis. As described in Chapter 2, in the plasmid pNFAT-SEAP, three copies of consensus NFAT binding element are constructed in the promoter region of reporter gene secreted alkaline phosphatase (SEAP) (Figure 2.44). Activated NFAT binds to these consensus NFAT-binding elements and induce SEAP expression [175]. SEAP is secreted into the media and its activity can be measured [176]. Hence, in this reporter plasmid, SEAP activity directly reflects the NFAT transcription activity. Ramos B cells were transiently transfected with pNFAT-SEAP. After 24 h, B cells were treated with Bz-423 in media with 2% FBS. Lower FBS was used here because serum is reported to interfere SEAP assay (communication with Clonetch). At indicated times, the media of treated cells were collected and the SEAP activity was measured. Bz-423 (5 μM) only induces 35% increase in SEAP expression after 8 h treatment (Figure 3.9), which is significantly lower than the literature reported 3-20 folds changes in response to NFAT activation [177].

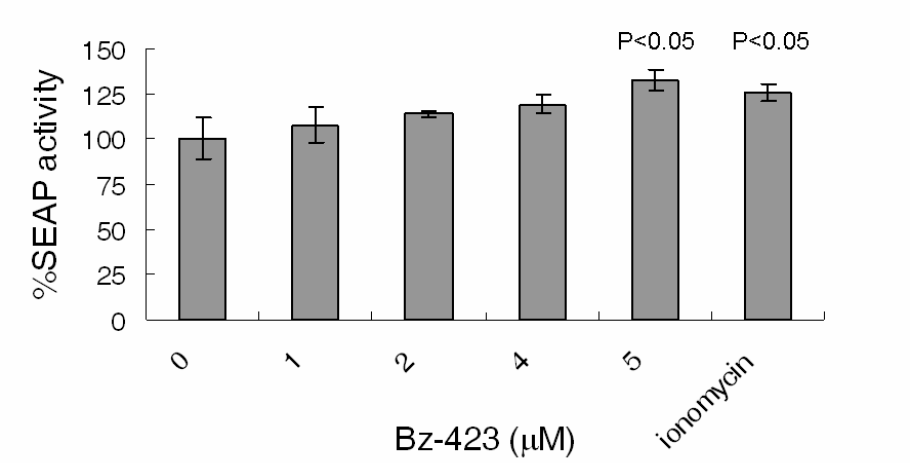

Figure 3.9: Bz-423 induces NFAT-dependent transcriptional activation using pNFAT-reporter plasmid. Ramos cells were transiently electroporated with pNFAT-SEAP. 24 h later, cells was treated with various concentrations of Bz-423 and ionomycin (0.5 μg/mL) in 2% FBS media. 8 h later, the supernatant was harvested and SEAP activity was monitored. The SEAP activity change were shown, assuming SEAP activity of vehicle treated Ramos is 100%. This panel is one representative experimental data of four experiments.

There are several possibilities to explain the low level of SEAP expression. First, Bz-423 is not a strong activator for NFAT activation. As Bz-423 only induced 35% NFAT dephosphorylation at 16 μM, it was hypothesized that a strong NFAT activator would induce a higher increase in SEAP transcription. However, ionomycin (0.5 μg/mL), which induces 75% NFATc2 dephosphorylation, only induced a 25% increase in SEAP activity (Figure 3.9), which is comparable to SEAP activity increase by Bz-423. This result eliminates this possibility that Bz-423 induces small NFAT-dependent transcription due to the fact that it is a weak NFAT activator. Second, co-treatment of protein kinase C (PKC) activator PMA and ionomycin induces IL-2 expression. In contrast, ionomycin alone does not increase IL-2 expression [178]. This observation suggests that both PKC activation and calcineurin activation are required for IL-2 expression. As the consensus NFAT binding element is derived from human

IL-2 enhancer sequences between -286 and -257 [179], it was thus hypothesized that pNFAT-SEAP is not optimized for transcriptional activity only induced by NFAT. To test this hypothesis, CCRF-CEM T cell line was chosen based on two reasons. First, NFAT dependent transcription in the reporter plasmid is well-established in T cells [180]. Second, Bz-423 induces NFAT dephosphorylation in CCRF-CEM T cells (Figure 3.27B). PKC activator PMA plus ionomycin co-treatment was shown to increase IL-2 level and pNFAT-SEAP transcription activation [177], and was used as a positive control. Consistent to ionomycin-induced low NFAT-dependent SEAP transcription in Ramos cells, ionomycin alone only induces 50% increase in SEAP activity (Figure 3.10). Although PMA does not further enhance ionomycin-induced NFAT dephosphorylation, PMA plus ionomycin co-treatment increases SEAP activity by 23-fold (Figure 3.10), which is similar to literature reports [177]. PMA activates transcription factor AP-1 [181] and NFκB [182], which form a transcription complex with NFAT [58]. This finding suggests that NFAT-mediated transcription in this plasmid can be increased significantly assisted by other transcription factors like NFκB, AP-1. Although PMA itself does not activate NFAT [183], it is surprised to observe that PMA alone induces the NFAT-dependent SEAP expression in CCRF-CEM T cells (Figure 3.10). This is possible due to the fact that there is several portion of constitutively active NFATc2 in CCRF-CEM cells [173]. This constitutive active NFATc2 may interact with NFκB or/and AP-1 activatedby PMA, which result in a SEAP expression. This result confirms the speculation that low transcription activation of pNFAT-SEAP induced by Bz-423 may be due to the low sensitivity of

this plasmid to NFAT activation.

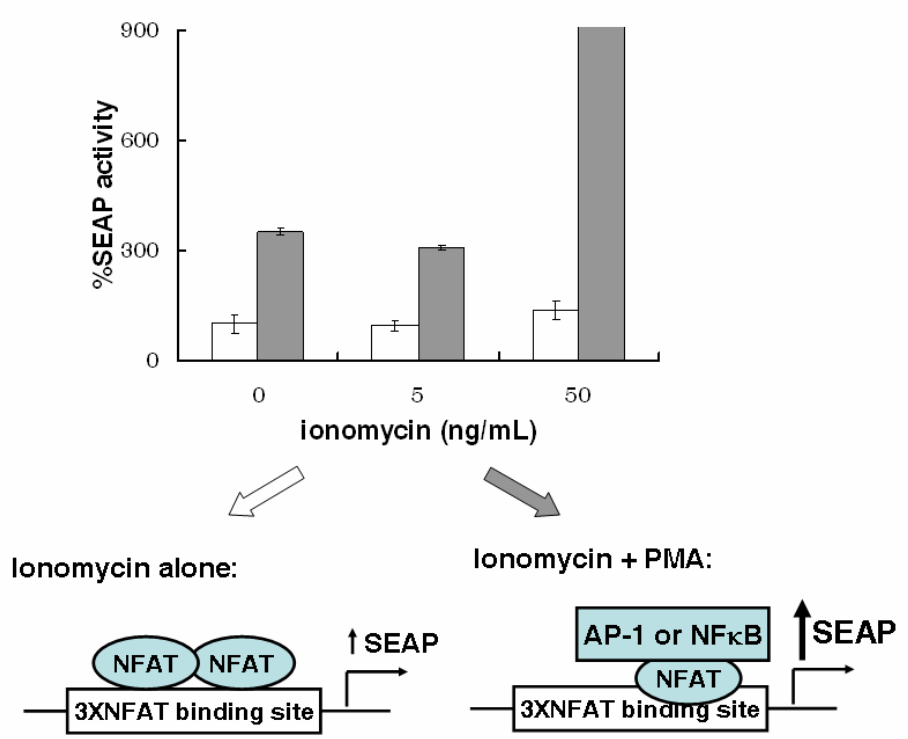

Figure 3.10: The plasmid pNFAT-SEAP responds poorly to ionomycin stimulation but well to PMA and ionomycin co-stimulation. CCRF-CEM cells were transiently transfected with pNFAT-SEAP, 24 h later, cells in 2% FBS were treated with ionomycin in the presence (gray bar) or absence (blank bar) of PMA. 6 h later, supernatants were harvested for SEAP activity. The SEAP activity change by the treatment was shown. Cartoons are proposed to explain transcription activity of pNFAT-SEAP in response to stimulation by ionomycin alone or PMA plus ionomycin. This panel is from one experiment. This experiment was repeated 2 times.

As pNFAT-SEAP responds poorly to NFAT activation alone, this pNFAT-SEAP system was modified to study the concentration dependence of Bz-423 on NFAT-dependent transcription activation. During the Bz-423 treatment, PMA was concurrently applied. Consistent with previous findings, Bz-423 (5 μM) increased SEAP activity by 39% over the vehicle control. When compared with SEAP increase by PMA alone, co-treatment induced a 28% increase at 2 μM, 85% increase at 4 μM, and 114% increase in SEAP activity at 5 μM (Figure 3.11). These results confirm that

Bz-423 promotes transcriptional activation in a NFAT-dependent pathway.

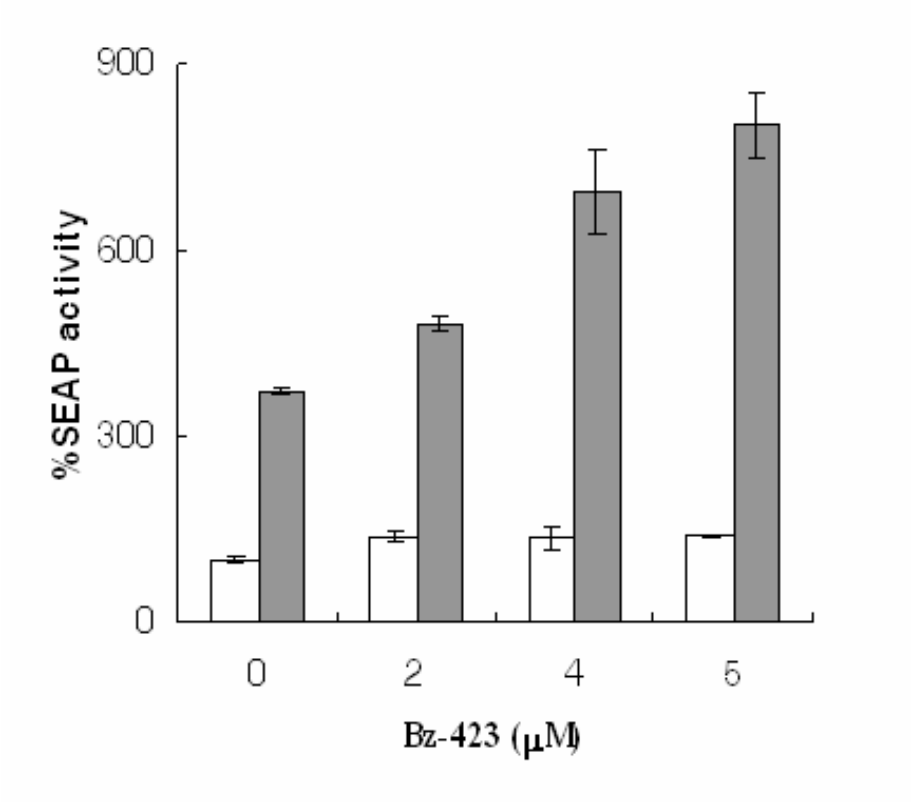

Figure 3.11: Bz-423 induces NFAT-dependent transcription. CCRF-CEM cells were transiently transfected with pNFAT-SEAP, 24 h later, cells in 2% FBS were treated with a dose response of Bz-423 in the presence (gray bar) or absence (white bar) of PMA. 8 h later, supernatants were harvested for SEAP activity. The SEAP activity change by the treatment is shown. This panel is from one experiment. This experiment was repeated 2 times.

As Bz-423 induced NFAT-dependent gene transcription *in vitro*, changes in mRNA levels of NFAT-dependent endogenous genes by Bz-423 are expected. To test this hypothesis, several NFAT-dependent genes were chosen and the effects of Bz-423 on mRNA changes of these genes were studied. By studying the potent NFAT binding in the promoter region of Bz-423 modulated genes from HGU133A Affymetrix gene chips (Table 3.4; [184]), 19 NFAT-responsive genes were identified. Among these genes, interferon regulatory factor 4 (IRF4, LSIRF/MUM1), myxovirus resistance 1

(MX1, MxA), interleukin 8 (IL-8, CXCL8), myristoylated alanine-rich protein kinase C substrate (MRACKs) and FMS-related tryrosine kinase 1 (FLT1) were chosen because the availability of validated primers for real-time reverse transcription polymerase chain reaction (RT-PCR) analysis. Promoter analysis of these selected genes using on-line program TESS (http://www.cbil.upenn.edu/cgi-bin/tess/tess?RQ=WELCOME) revealed potent NFAT binding sites in the promoter region. There was no detectable *MARCKs* or *FLT1* mRNA in Ramos cells as there was no difference between sample undergoing reverse transcription and sample not undergoing reverse transcription. The positive control ionomycin did not alter *MX-1* or *IL-8* mRNA levels, but it increases *IRF4* mRNA by 4-fold. This increase was inhibited by CsA, indicating *IRF4* mRNA increase is due to calcineurin activation (Figure 3.12A). Similar to ionomycin, Bz-423 did not significantly alter *MX-1* or *IL-8* mRNA levels (Figure 3.12A). Bz-423 increased *IRF4* mRNA level in a dose-dependent manner (2.5-fold increase by 8 μM Bz-423, and 4-fold increase by 16 μM Bz-423) (Figure 3.12A). At all the time points tested, Bz-423 induced *IRF4* mRNA increase (Figure 3.12A), with the greatest increase at 2 h (Figure 3.12B). These results suggest Bz-423 activated *IRF4* transcription in a dose- and time-dependent manner.

Gene	Function	Potent NFAT binding site	Fold induction
Interferon regulatory factor 4	Transcription factor	Yes	8.5
Paired box 3	Transcription factor	Yes	0.59
Forkhead box P3	Transcription factor	Yes	0.59
Zic family member 1 (odd-paired homolog, Drosophila)	Transcription factor	Yes	0.59
Trichorhinophalangeal syndrome I	Transcription factor	Yes	0.36
Short stature homeobox 2	Transcription factor	Yes	0.50
Tenascin XB, Ehlers-Danlos syndrome type IV	Extracellular matrix protein	Yes	0.54
Collagen, type III, alpha 1 (Ehlers-Danlos syndrome type IV, autosomal dominant)	Extracellular matrix protein	Yes	0.51
Poliovirus receptor-related 1 (herpesvirus entry mediator C)	Extracellular matrix protein	Yes	0.44
SPARC-like 1 (mast9, hevin)	Extracellular matrix protein	Yes	0.40
Myristoylated alanine-rich protein kinase C substrate	Calcium signaling	Yes	0.59
Guanine nucleotide binding protein (G protein), alpha activating activity polypeptide O	Receptor signaling	Yes	0.50
Microtubule associated serine/threonine kinase 2	Serine/threonine kinase	Yes	0.52
FMS-related tyrosine kinase 1	Tyrosine kinase, apoptosis	Yes	0.59
Myxovirus resistance 1	Apoptosis	Yes	1.5
Jumonji, AT rich interactive domain 2	Cell cycle	Yes	0.50
Transcription factor Dp-2 (E2F dimerization partner 2)	Cell cycle	Yes	2.19
ADP-ribosylation factor 6	endocytosis	Yes	0.25
Interleukin 8	pro-inflammatory cytokine	Yes	0.55

Table 3.4: The lists of genes modulated by Bz-423 and with potent NFAT binding sites in the promoter. RNA was isolated from Ramos B cells treated with Bz-423 (10 μM) for 4 h in complete media containing 2% FBS and vehicle control, and hybridized to a HGU133A affymetrix gene chip. Whether the promoter region contains NFAT binding is indicated. Fold mRNA increase is relative to vehicle. Fold changes represent the mean of two separate experiments.

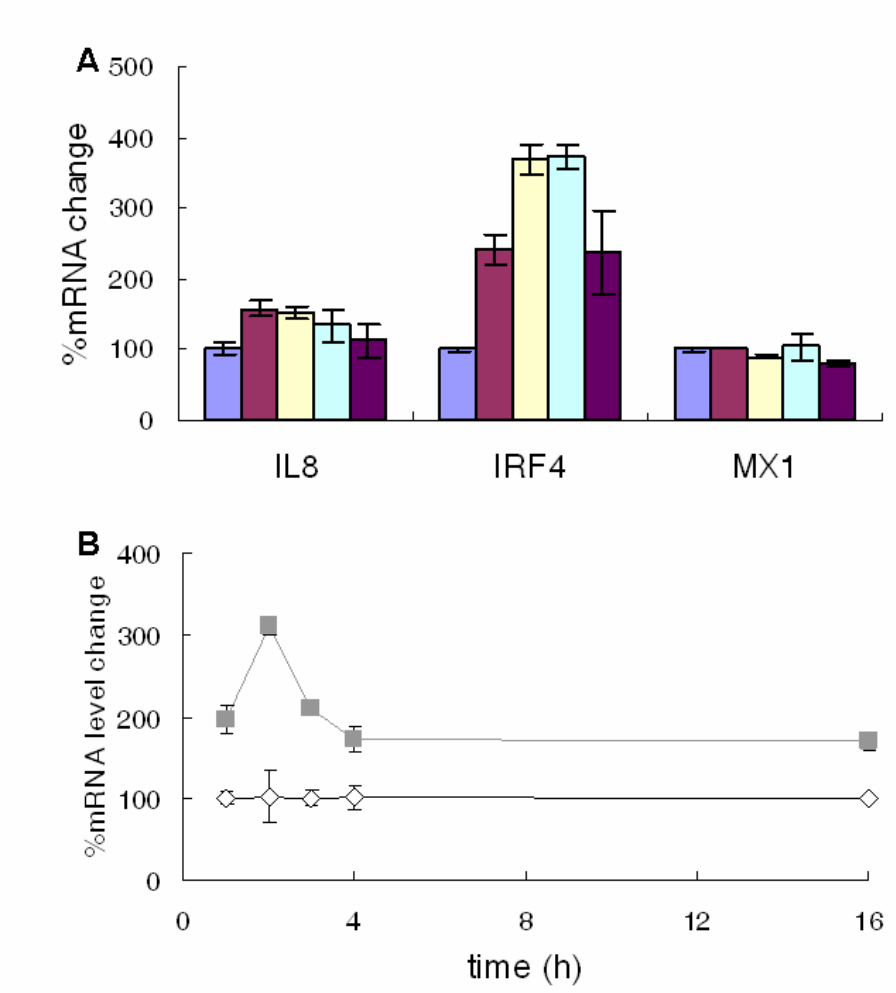

Figure 3.12: Bz-423 induces *IRF4* mRNA increase in a time-dependent and dose-dependent manner. (A) The RNAs were obtained from Ramos cells treated with vehicle control ( ), Bz-423 (8 µM , 16 µM), ionomycin (0.5 µg/mL), CsA (250 nM) plus ionomycin ( ) for 2 h. Then *IRF4* mRNA levels were then determined through RT-PCR. (B)The RNAs were extracted from Ramos cells treated with vehicle control (◇) or Bz-423 (, 16 µM) at various time points. RNAs were first converted to cDNA using reverse transcriptase, and real-time RT-PCR was performed to evaluate *IRF4* mRNA levels. β-actin was used as internal loading control. The cycle threshold (C_T) for IRF4 was first normalized by C_T for β-actin. The normalized C_T was used to calculate the *IRF4* mRNA level change based on the equation 100 x $2^{(C_{T\text{-vehicle}}-C_{T\text{-Bz-423}})}$ [185].

IRF4 transcription is regulated by NFAT [158, 186]. As CsA inhibits ionomycin-induced *IRF4* mRNA increases, it was hypothesized that Bz-423 induced *IRF4* increase through activating NFAT. Due to lack of a specific NFAT inhibitor, CsA was used to probe the involvement of calcineurin in Bz-423 induced *IRF4* increase.

CsA inhibited Bz-423 induced *IRF4* mRNA increases both at 2 and 6 h (Figure 3.13), confirming the involvement of calcineurin in *IRF4* increase induced by Bz-423 treatment.

The data so far showed that Bz-423 activates NFAT transcription, and increases *IRF4* mRNA levels in a calcineurin dependent manner. These data, together with the presence of potent NFAT binding sites in the *IRF4* promoter region [158, 186], suggest that Bz-423 induces *IRF4* gene transcription via NFAT activation. To test this hypothesis, a chromatin immunoprecipitation (CHIP) assay was performed. The CHIP assay is a method used to determine the location of DNA binding sites for the interested protein. An antibody for the interested protein is used to pull-down a

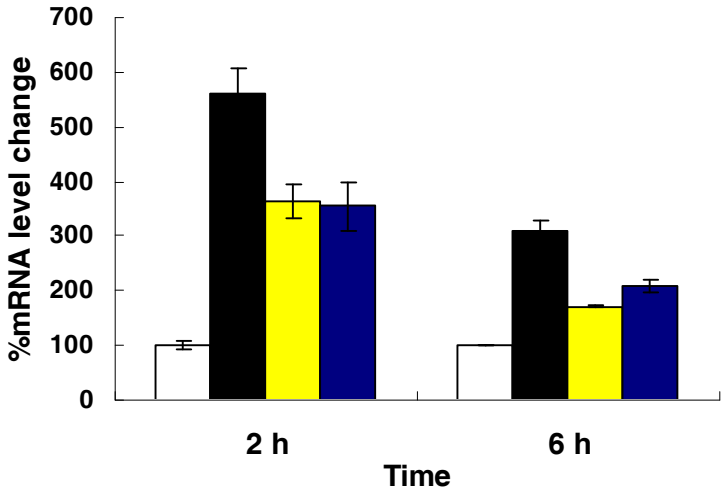

Figure 3.13: Bz-423 increases *IRF4* mRNA level via calcineurin. CsA (250 ng/mL) was pre-treated with Ramos B cells for 30 min, and then treated with Bz-423 (16 μM) and vehicle. At indicated time point, cells were harvested and RNA was extracted. The *IRF4* mRNA levels were studied by RT-PCR. β-actin was used as internal loading control. The mRNA level changes are shown as vehicle (white bar), Bz-423 (black bar), vehicle plus CsA (yellow bar), Bz-423 plus CsA (blue bar). C_T was used to for IRF4 was first normalized by C_T for β-actin. The normalized C_T was used to calculate the *IRF4* mRNA level change based on the equation 100 x 2^($C_{T\text{-vehicle}}$-$C_{T\text{-Bz-423}}$) [185]. This experiment is representative of two independent experiments.

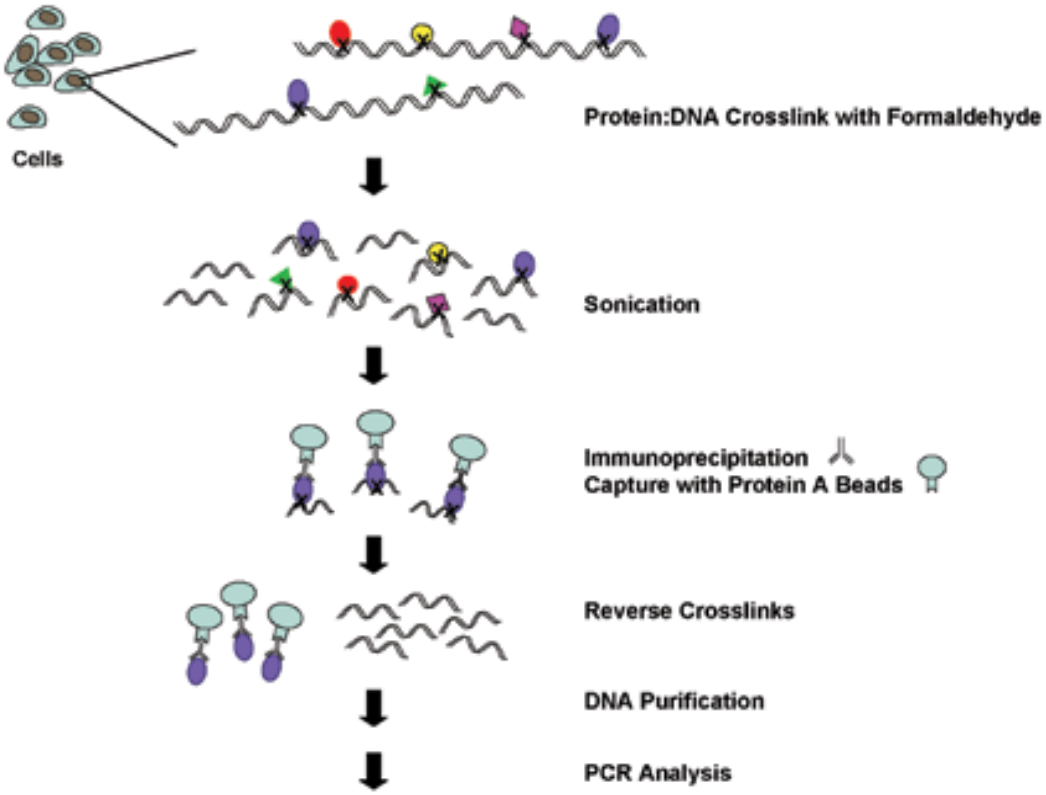

Figure 3.14: Outlines of chromatin Immunoprecipitation (CHIP) assay. Protein:DNA crosslinks are formed in treated cells with formaldehyde, followed by the sonication to break DNA into 0.2-1 kb in length. By using an antibody of interesting protein, the protein-DNA complex is pulled out. The purified protein-DNA complexes are reversed by heating. The identity and quantity of the DNA fragments are then determined by PCR. This picture was adopted from USB web site (http://www.usbweb.com/category.asp?cat=252&id=78460)

crosslinked DNA-protein complex, and the immunoprecipitated DNA is then amplified by PCR using specific primers (Figure 3.14). In our case, CHIP assay was used to study the binding of transcription factor NFATc2 to the *IRF4* promoter region. An increase of NFATc2 binding to the *IRF4* promoter regions after Bz-423 treatment suggests the role of activated NFAT in Bz-423 induced *IRF4* mRNA increases. Quantitative PCR using Syber Green revealed a 2.5- to 5-fold increase of NFATc2

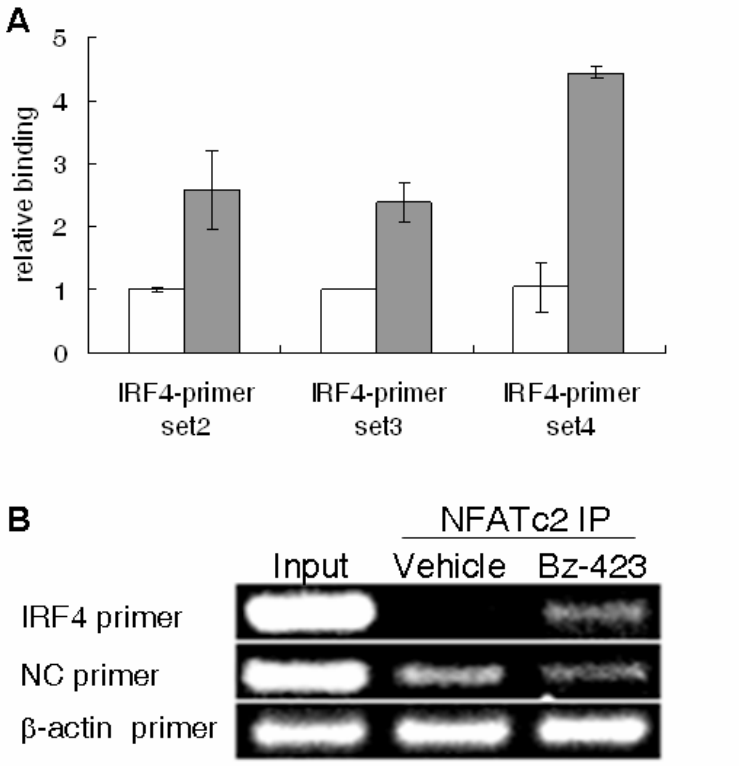

Figure 3.15: Bz-423 increases NFATc2 binding to *IRF4* promoter. Ramos B cells were treated with Bz-423 (16 μM). At 2 h, CHIP was performed to obtain the DNA pooled down by anti-NFATc2 Ab. (A) The DNA was quantified by RT-PCR. Ct was first normalized by NC primer, and the relative binding increase by Bz-423 (gray bar) to vehicle control (white bar) was then calculated based on the equation 100 x $2^{(C_{T\text{-vehicle}} - C_{T\text{-Bz-423}})}$ [185]. (B)The agarose gel electrophoresis results of PCR products using IRF4 primer set 4, NC primer, and β-actin primer were shown. This experiment is representative of two independent experiments.

binding to *IRF4* promoter region by Bz-423 (Figure 3.15A). The IRF4 primer set1 was eliminated because it produced multiple PCR products. The results from agarose gel electrophoresis of PCR products were shown in Figure 3.15B. A primer that flanks a region of genomic DNA between GAPDH genes and CNAP1 (NC primer, [187]) and β-actin primer were used as negative controls. The input before the NFATc2 immunoprecipitation was used as a positive control. Bz-423 enriched the DNA

containing *IRF4* promoter but it did not increase the amount of DNA containing the region that targeted by NC primer and β-actin primer (Figure 3.15B). This result indicates that Bz-423 increases the binding of NFATc2 to *IRF4* promoter, suggesting that Bz-423 increases *IRF4* mRNA level by increasing NFATc2 binding to its promoter region.

CsA pre-incubation blocks Bz-423-induced *IRF4* mRNA increases (Figure 3.13), indicating the involvement of calcineurin in inducing *IRF4* mRNA expression. As CsA inhibits NFAT activation via calcineurin, it is likely that Bz-423 increases NFATc2 binding to *IRF4* promoter regions through calcineurin. To test this hypothesis, the effect of CsA on Bz-423 induced NFATc2 binding to the *IRF4* promoter was explored. Bz-423 treatment induced 3-fold increase in NFATc2 binding to *IRF4* promoter region, which was abolished by CsA pre-treatment (Figure 3.16A). Agarose gel electrophoresis of the PCR products also showed CsA inhibited Bz-423 induced increase of PCR products in the *IRF4* promoter region (Figure 3.16B). The observation suggests that calcineurin is involved in *IRF4* mRNA increase by activating NFATc2 and its subsequent NFATc2 binding to the *IRF4* promoter.

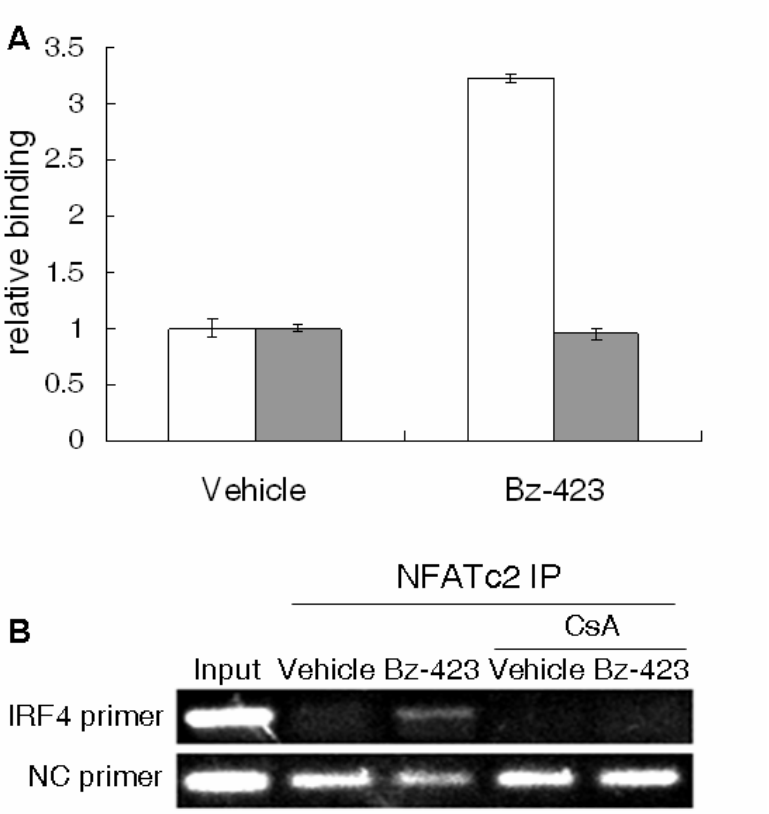

Figure 3.16: Bz-423 treatment increases NFAT binding to *IRF4* promoter region, which is abolished by CsA pre-incubation. (A) Before Bz-423 treatment, calcineurin inhibitor CsA (250 nM, gray bar) was pre-treated for 30 min. Ramos B cells were then treated with Bz-423 (16 μM, 2 h). The crosslinks of protein and DNA complex were subjected to CHIP using anti-NFATc2 for immunoprecipitation. The *IRF4* promoter was amplified by RT-PCR using primers targeting *IRF4* promoter. The products were quantified using Sybr Green Ct was first normalized by NC primer, and the relative binding to vehicle control was then calculated based on the equation 100 x $2^{(C_{T\text{-}vehicle}-C_{T\text{-}Bz\text{-}423})}$ [185]. (B) The agarose gel electrophoresis results of PCR products using IRF4 primer set 4 were shown. Both panels are from one experiment.

In summary, Bz-423 activates NFAT, increases NFAT binding to the *IRF4* promoter region and initiates transcriptions of the *IRF4* genes. Calcineurin inhibitor blocks Bz-423 induced NFAT increase in NFATc2 binding to the *IRF4* promoter and its subsequent mRNA level, validating the involvement of the calcineurin-NFAT pathway.

Mechanism of Bz-423 induced NFAT dephosphorylation: Bz-423 induced NFAT activation leads to transcription of genes critical for immune function, which may contribute to the efficacy of Bz-423 in lupus mice. A better understanding of the upstream signaling events leading to Bz-423 induced NFAT dephosphorylation will help to define the *in vivo* mechanism of action and potential application against autoimmune disease.

An inhibitor strategy was used to study how Bz-423 induces NFAT dephosphorylation. As calcineurin is involved in NFAT-dependent *IRF4* transcription, whether it is involved in Bz-423 induced NFAT dephosphorylation was explored. CsA blocked Bz-423 induced NFAT dephosphorylation (Figure 3.17A), confirming that calcineurin activity is required for NFAT dephosphorylation. This result indicates that Bz-423 activated NFAT and its subsequent transcription through calcineurin. Being a well-known activator for calcineurin, the role of Ca^{2+} in Bz-423 induced NFAT dephosphorylation was studied next. As Bz-423 interferes with various calcium indicators, its effect on intracellular [Ca^{2+}] change has not been identified despite considerable effort. The involvement of Ca^{2+} was therefore studied by the extracellular Ca^{2+} chelating agent ethylene glycol tetraacetic acid (EGTA). EGTA blocked Bz-423 induced NFAT dephosphorylation, indicating the involvement of extracellular Ca^{2+} (Figure 3.17A). To confirm the involvement of Ca^{2+} influx and to further study the mechanism of Ca^{2+} influx, a specific Ca^{2+} release activated Ca^{2+} (CRAC) channel inhibitor YM-58483 was applied to study its effect on NFAT dephosphorylation [143]. YM-58483 blocked Bz-423 induced NFAT

dephosphorylation (Figure 3.17A),

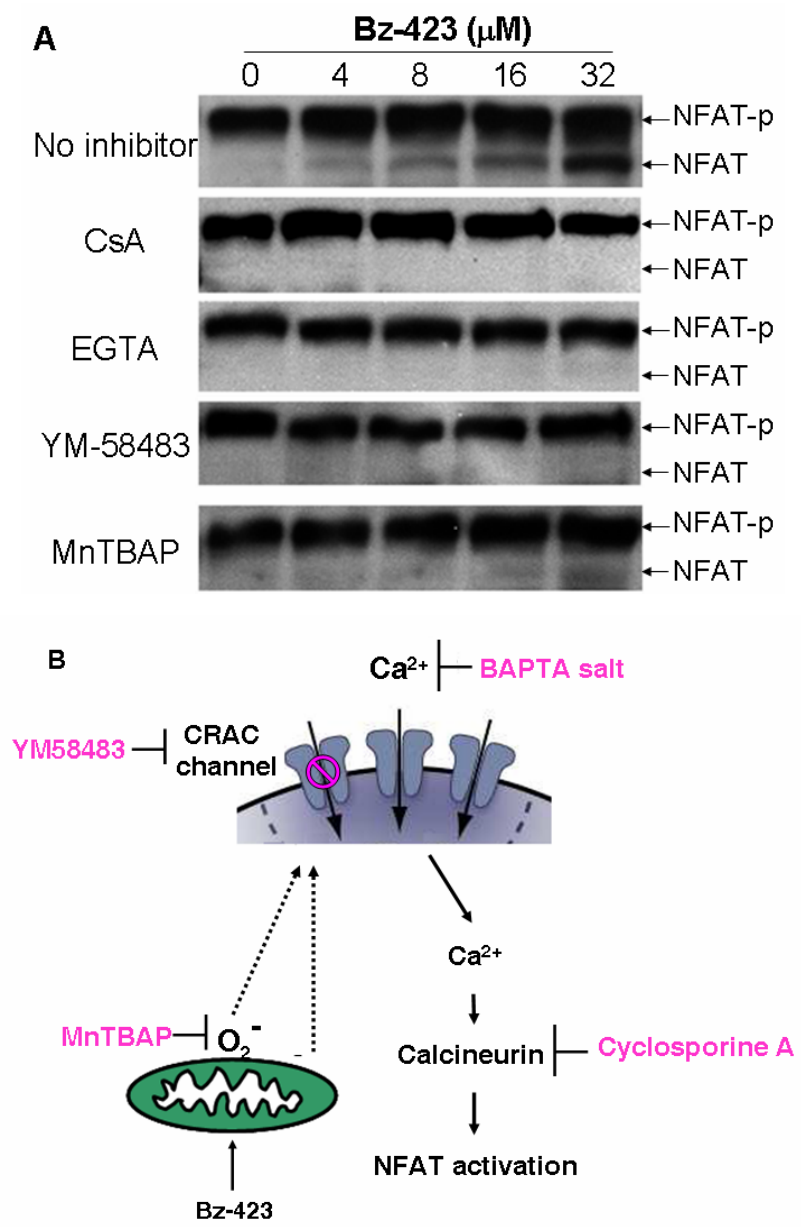

Figure 3.17: Inhibitors on Bz-423 induced NFAT dephosphorylation in Ramos cells. (A) Ramos B cells in 10% FBS media was treated a dose response of Bz-423. 15 min later, cells was harvested and the lysate was made to detect the NFAT dephosphorylation. CsA (250 nM), EGTA (1 mM), CRAC channel inhibitorYM-58483 (0.5 μM), MnTBAP (100 μM) were pretreated with cells 30 min before treatment (B) The proposed mechanism of Bz-423 induced NFAT dephosphorylation is proposed. The pink No sign (⃠) are indicating the inhibitors used in panel A. The experiment from panel A is representative of two experiments.

confirming the involvement of Ca^{2+} influx and indicating the involvement of CRAC channel. The results that CsA, EGTA, and YM-58483 inhibit Bz-423-induced NFAT

dephosphorylation indicate Ca^{2+}-calcinuerin-NFAT signaling pathway is involved in Bz-423 induced NFAT dephosphorylation. As Bz-423 induces superoxide, whether superoxide may be involved in Bz-423 induced NFAT activation was investigated by exploring the effect of anti-oxidant MnTBAP on Bz-423 induced NFAT dephosphorylation. MnTBAP inhibited Bz-423 induced NFAT dephosphorylation (Figure 3.17A), suggesting the involvement of superoxide in activating NFAT. Whether it directly activates the CRAC channel or it indirectly signals the CRAC channel activation is not clear.

Based on the results of inhibitors experiment, a mechanism for Bz-423 induced NFAT dephosphorylation is proposed (Figure 3.17B). Bz-423 binds to the oligomycin sensitivity conferring protein (OSCP) and inhibits activity of mitochondrial F_0F_1-ATPase. This leads to mitochondrial hyperpolarization and superoxide production. The superoxide directly or indirectly activates CRAC channel, resulting in extracellular Ca^{2+} influx, intracellular Ca^{2+} increase, calcineurin activation, NFAT dephosphorylation and transcription of NFAT responsive gene *IRF4*.

Bz-423 induced NFAT dephosphorylation is unique: The finding that Bz-423 inhibits the mitochondrial F_0F_1-ATPase and eventually causes NFAT dephosphorylation, prompted us to investigate whether other F_0F_1-ATPase inhibitors induce NFAT dephosphorylation. To study this question, the mitochondrial F_0F_1-ATPase inhibitors 3,3'-diindolylmethane (DIM) [188], resveratrol [189] and PK11195 [190] were used to study their effects on NFAT dephosphorylation in Ramos B cells. All of these inhibitors inhibit mitochondrial F_0F_1-ATPase synthase activity at

micromolar concentrations: the IC_{50} values for DIM, resveratrol and PK11195 are 20 [188], 12-28 [189], and 33 μM [190], respectively. As shown in Figure 3.18, at 15 min, DIM, resveratrol, and PK1195 all induce NFAT dephosphorylation in a dose-dependent manner. DIM (50 μM) induced ~25% dephosphorylation of total NFAT; resveratrol (100 μM) induced ~10% dephosphorylation of total NFAT; and PK11195 (50 μM) induced ~20% dephosphorylation of total NFAT (Figure 3.18). However, no dephosphorylation was observed at 4 h (Figure 3.18). The results indicate these mitochondrial F_0F_1-ATPase inhibitors induce a transient NFAT dephosphorylation. In contrast, NFAT dephosphorylation was still observed 6 h after Bz-423 treatment, suggesting the different mode of NFAT dephosphorylation adapted by Bz-423. Since continuous NFAT dephosphorylation is required for transcription activation, the sustained activation by Bz-423 is particularly unique and interesting.

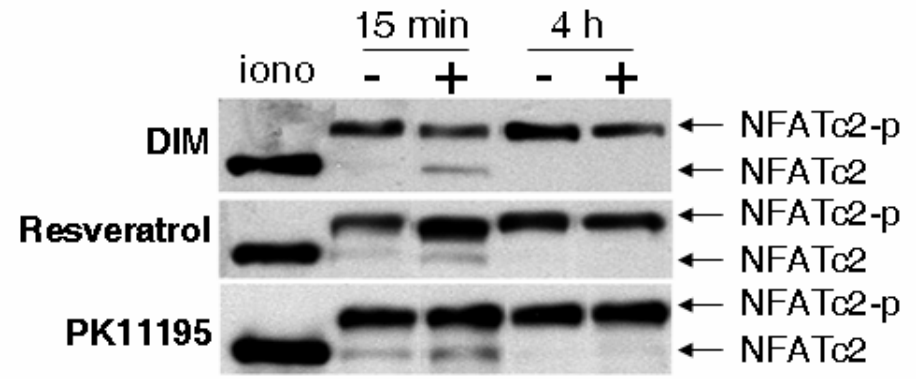

Figure 3.18: Other mitochondrial F_0F_1-ATPase inhibitors induce transient NFAT dephosphorylation. Ramos cells in 10% FBS media were treated with DIM (50 μM), resveratrol (100 μM), PK11195 (50 μM), using DMSO as a vehicle control. At indicated time, cells were harvested and cell lysates were obtained for NFAT dephosphorylation by western blot.

Bz-423 induces NFAT dephosphorylation in primary B cells: Before studying the functional consequences of Bz-423-induced NFAT activation, the question whether Bz-423 induced NFAT dephosphorylation in primary B cells was studied. In spleenic B cells, Bz-423 induces NFAT dephosphorylation in a dose-dependent manner (Figure 3.19). At 8 h, ~10 % NFAT was dephosphorylated by 8 μM Bz-423 and ~40% NFAT was dephosphorylated by 16 μM Bz-423 (Figure 3.19). Bz-423 also induces NFAT dephosphorylation in a time-dependent manner (Figure 3.19). At 16 μM, Bz-423 induced NFAT dephosphorylation at all the time points tested (Figure 3.19). The biphasic change of Bz-423 induced NFAT dephosphorylation observed in Ramos cells was not observed in spleen B cells (Figure 3.19), indicating it is only specific to Ramos B cells. These results demonstrate that Bz-423 induced NFAT dephosphorylation in primary B cells, supporting Ramos as an appropriate cell line to study NFAT.

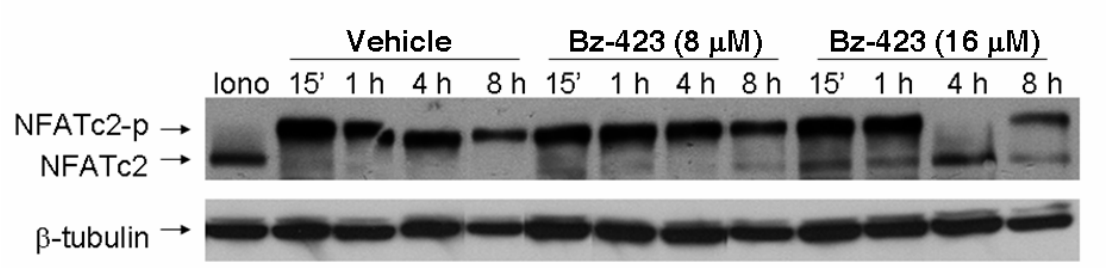

Figure 3.19: Bz-423 induces NFAT dephosphorylation in spleen B cells. Spleen B cells were isolated and positively selected from the spleen of Balb/c mice The cell lysates of ionomycin-treated (1 μg/mL for 20 min) or Bz-423-treated (8 or 16 μM for indicated time) spleen B cells were immunoblotted with specific antibodies for NFATc2 and β-tubulin. Before treatment, spleen B cells were recovering in DMEM containing 10% FBS for 1 h.

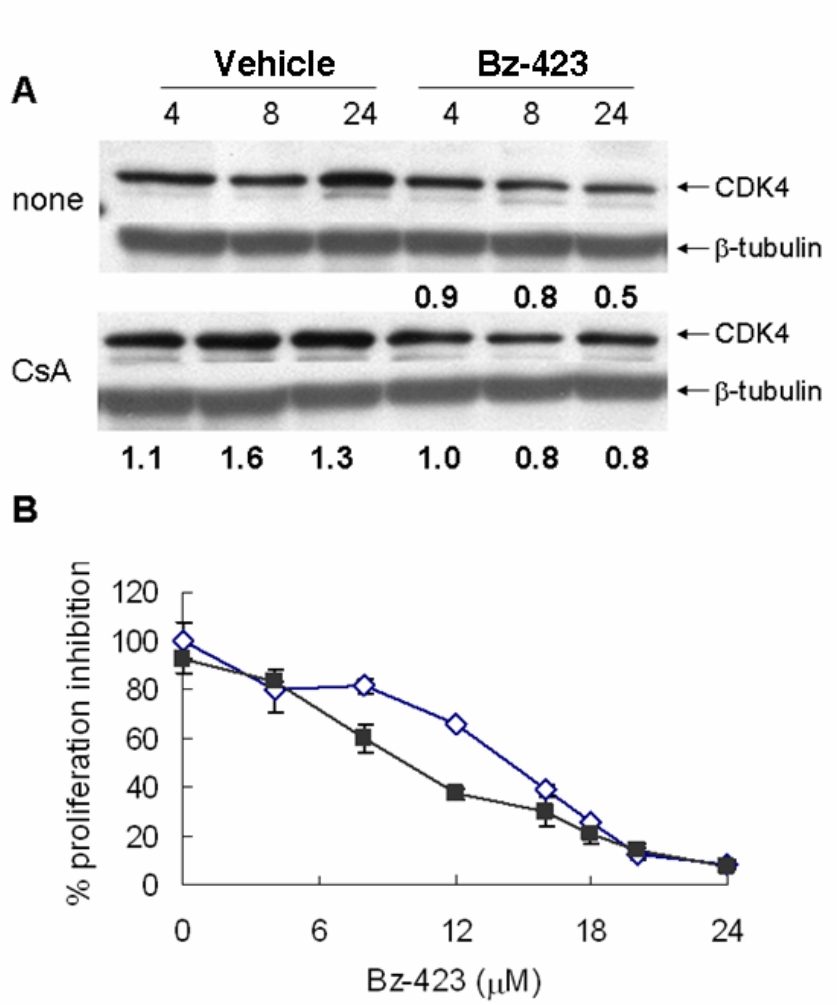

Figure 3.20: NFAT is not involved in Bz-423 induced growth arrest in Ramos B cells. (A) CsA on Bz-423 induced CDK4 decrease: Ramos B cells in 10% FBS were first incubated with CsA (100 nM) for 30 min before Bz-423 (16 μM) and vehicle. For western blot cells were harvested at the indicated times. And the cell lysate was obtained for western blots. The CDK4 expression level changes are indicated. (B) CsA on Bz-423 induced growth arrest by rhodmine assay. CsA (100 nM) was pre-incubated with Ramos before treatment. Bz-423 on the cell growth was monitored at 48 h. Bz-423 induced cell growth arrest in the presence (■) and absence (◇) of CsA was shown.

NFAT is not involved in growth arrest induced by Bz-423. The functional consequence of Bz-423 induced NFAT dephosphorylation was explored next. NFAT not only induces gene expression but also suppresses gene expression [58, 149]. Activated NFAT suppresses CDK4 expression [153], resulting in inhibiting cell

growth. Bz-423 inhibits B cell proliferation, during which CDK4 expression level is reduced [184]. It is thus hypothesized that Bz-423 decrease CDK4 through activating NFAT, which may be responsible for growth arrest. To test this hypothesis, the effect of CsA on Bz-423 induced CDK4 decrease was determined. CsA alone induced 50% increase in CDK4 expression level. However it did not inhibit Bz-423 induced CDK4 decrease, indicating that Bz-423 induced CDK4 decrease is not calcineurin dependent (Figure 3.20A). Moreover, pre-treatment of CsA does not inhibit Bz-423 induced cell growth arrest (Figure 3.20B). These results limit the possibility that Bz-423 inhibits proliferation through activating NFAT.

Possible involvement of NFAT in anergy

Bz-423 does not activate NFκB and JNK in Ramos cells. In response to cell receptor stimulation, different even controversial outcomes are observed, including activation, effector function, cell death, and growth arrest [92, 191]. The cell developmental stages and the presence of co-stimulatory molecules are important factors in determining the outcomes [92, 191]. They may affect the outcome by activating different signaling pathways, which results in activation of different transcriptional factors [92, 191]. On the transcriptional level, NFAT, nuclear factor κ-light-chain-enhancer of activated B cells (NFκB), and activator protein-1 (AP-1) are the three important transcriptional factors for various immune responses [73]. Activation of all these transcription factors results in proliferation and development of effector immune functions [73]. If none of them are activated, immune function is suppressed. Anergy occurs when NFAT is activated while AP-1 or NFκB is not [73].

Therefore, to test whether Bz-423 could induce anergy, the activation state of these three transcriptional factors was determined.

AP-1 activation was studied by JNK phosphorylation. Phosphorylated active JNK phosphorylates and activates c-Jun, which is a subunit for the transcription factor AP-1 [192]. 1,4-Benzoidiazepine-2,5-dione [193], a compound known to cause JNK phosphorylation was used as a positive control (personal communication with Joanne Cleary). At 16 μM, the concentration of Bz-423 that induces NFAT dephosphorylation, Bz-423 did not phosphorylate the two isoforms of JNK p54 and p46 (Figure 3.21A), indicating that Bz-423 does not activate AP-1. NFκB is sequestered in the cytosol by binding to the inhibitory protein IκB [194, 195]. In response to activation signals, IκB is phosphorylated and tagged for proteasomal degradation. The released NFκB translocates into the nucleus and activates transcription [194, 195]. Thus, IκB degradation can be used to study NFκB activation [194, 195]. PMA plus ionomycin co-treatment decrease IκB protein level [196], which were used as positive controls for IκB degradation. At 16 μM, the concentration of Bz-423 that induces NFAT dephosphorylation, decreases in IκB protein were not observed (Figure 3.21B). These data suggest that Bz-423 does not activate JNK and NFκB in the Ramos cells.

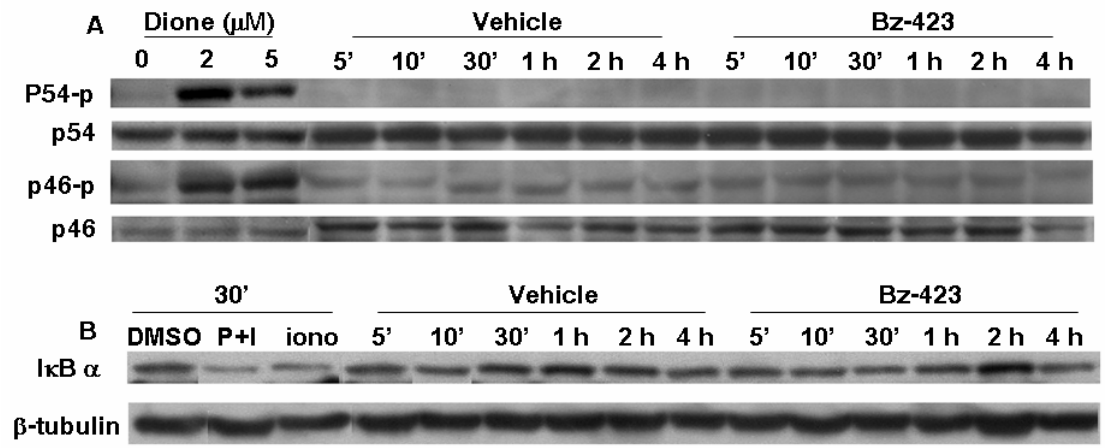

Figure 3.21: Bz-423 does not induce JNK phosphorylation (A) and IκB degradation (B). Ramos B cells in 10% FBS media were treated with Bz-423 (16 μM) or vehicle. At the indicated times, cells were harvested and cell lysate was obtained for western blot. As positive controls, Ramos in 5% FBS media was treated with indicated concentration of Dione for 1 h (A). PMA (50 ng/mL) and ionomycin (50 μg/mL) was used. P stands for PMA. Both I and Iono are short for ionomycin.

Because IκB degradation and JNK phosphorylation are one of many steps in AP-1 and NFκB activation [197-199], these results does not totally exclude the possibility that Bz-423 activates NFκB and AP-1. As an alternate, SEAP reporter plasmids for NFκB and AP-1 were used to monitor activations of NFκB and AP-1 [200, 201]. Consistent with the previous results, Bz-423 induced a NFAT-dependent SEAP expression in a dose response manner. In contrast, Bz-423 did not induce SEAP expression regulated by NFκB and AP-1 (Figure 3.22), further confirming that Bz-423 does not activate NFκB or AP-1.

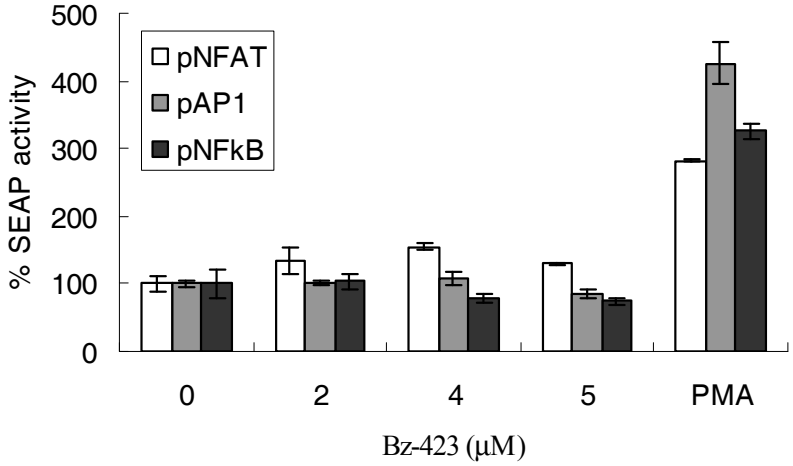

Figure 3.22: Bz-423 induces transcription by NFAT but not by AP-1 or NFκB. Ramos B cells was transiently transfected with pNFAT-SEAP (white bar), pAP-1-SEAP (gray bar), pNFκB-SEAP (black bar) through electroporation. 24 h later, cells were resuspended in 2% FBS, treated with a dose response of Bz-423 or PMA (50 ng/mL). 8 h later, the media was collected for SEAP assay. The % SEAP activity by Bz-423 treatment was shown.

Bz-423 pretreatment of Ramos B cells induces cells with anergic characteristics: As NFAT activation alone is a molecular characteristic of anergy, the observation that Bz-423 selectively activates NFAT but not NFκB and JNK suggests Bz-423 may induce anergy in Ramos B cells. Cell receptor down-regulation is one of the characteristics generally observed in anergic cells [8, 202]. Therefore, it was hypothesized that Bz-423 decreases IgM cell surface expression. Ionomycin was also included as it activates NFAT and overnight incubation was shown to induce anergy in T cell [63]. Ramos B cells were treated with Bz-423 (16 μM) or ionomycin for 16 h, and the IgM cell surface expression was monitored by FITC-IgM. Bz-423 shifted IgM expression to the left and decreased the Mean fluorescence intensity (MFI) by 50% (Figure 3.23), indicating that Bz-423 down-regulated the expression of IgM receptor. Ionomycindecreased the MFI of FITC-IgM by 20%(Figure 3.23A), suggesting

ionomycin is not as an effective as Bz-423.

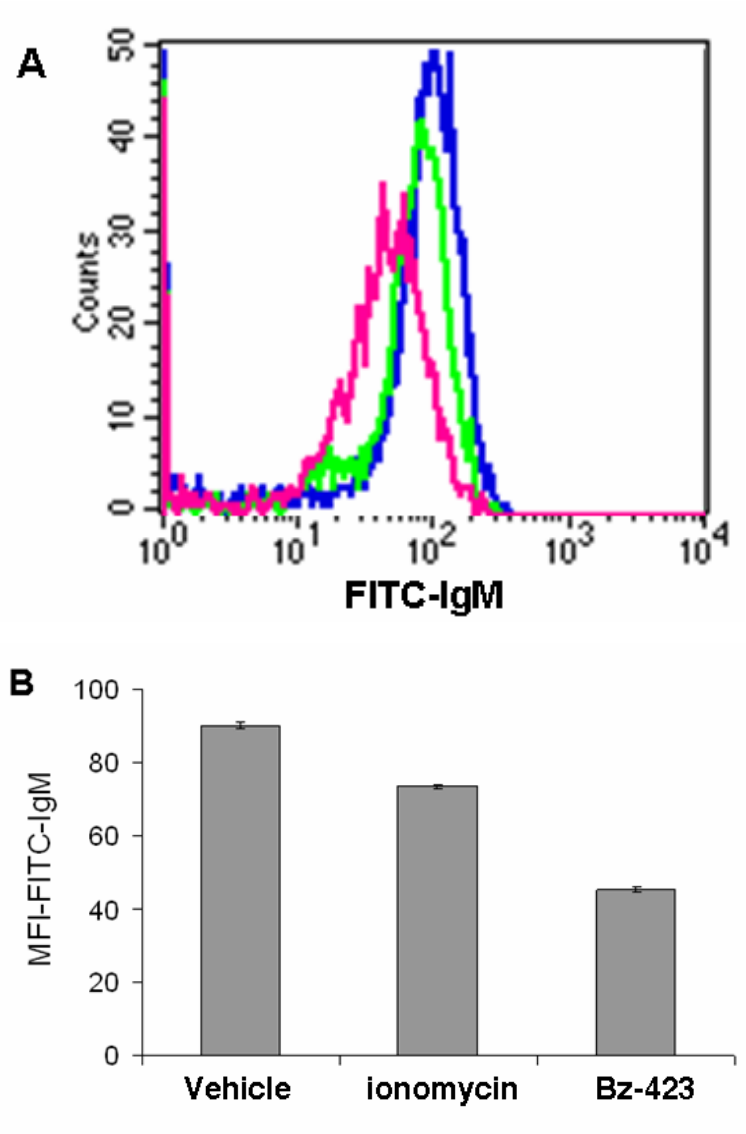

Figure 3.23: Overnight Bz-423 treatment decreases IgM receptor expression level. Ramos B cells in media containing 10% (v/v) FBS were treated with Bz-423 (16 µM) or ionomycin (1 µg/mL) or vehicle control DMSO for 16 h. The expression level of IgM receptor was detected by staining with FITC conjugated anti-human IgM. Only the live cells population was gated. (A) The histograms of IgM expression induced by vehicle (blue), ionomycin (green) and Bz-423 (pink) were shown. (B) The mean fluorescence intensity induced by ionomycin and Bz-423 treatment was plotted. This experiment is representative of three independent experiments.

IgM down-regulation can directly regulate cell tolerance [203]. It can also participate in anergy by dampening proximal BCR signaling, such as $[Ca^{2+}]_i$ increase [45]. To test whether IgM downregulation by Bz-423 treatment results in decreased

BCR-mediated calcium change, Ramos B cells were pre-treated with Bz-423 for 16 h, cells were then loaded with calcium indicator Fura-2 or Fluo-3. Anti-IgM induced $[Ca^{2+}]_i$ change was monitored using calcium indicator Fluo-3 in flow cytometry or using ratiometric calcium dye Fura-2 in the plate reader. Before anti-IgM treatment, Bz-423 was washed out to eliminate its interference with calcium indicators. Flow cytometry is a single cell analysis while plate reader can perform multiple samples at the same times. Bz-423 pre-treatment did not affect the mean fluorescence and distribution of Fluo-3 induced by anti-IgM stimulation (Figure 3.24A), indicating Bz-423 pre-incubation does not affect anti-IgM induced $[Ca^{2+}]_i$ change. This observation was also confirmed by studying the Fura-2-loaded Ramos cells using a plate-based assay, as Bz-423 did not affect anti-IgM induced $[Ca^{2+}]_i$ increase at either 8 μM or 16 μM (Figure 3.24B). Therefore, Bz-423 pre-incubation does not affect anti-IgM induced $[Ca^{2+}]$ change, although it downregulates IgM receptor. Since not all anergic cells with lowered IgM expression decreased anti-IgM induced $[Ca^{2+}]_i$ change [199], this experiment only rules out the possibility that Bz-423 induced anergy through decreasing BCR-mediated proximal signaling.

Bz-423 pre-treatment renders cells resistant to further activation: Another characteristic of anergic cells is the reduced response to activation signals such as antigen binding, PMA plus ionomycin, anti-CD3 and anti-CD28 [8, 204]. Therefore, the ability of Ramos cells to respond to activation signals such as anti-IgM and PMA plus ionomycin after Bz-423 pre-treatment was investigated.

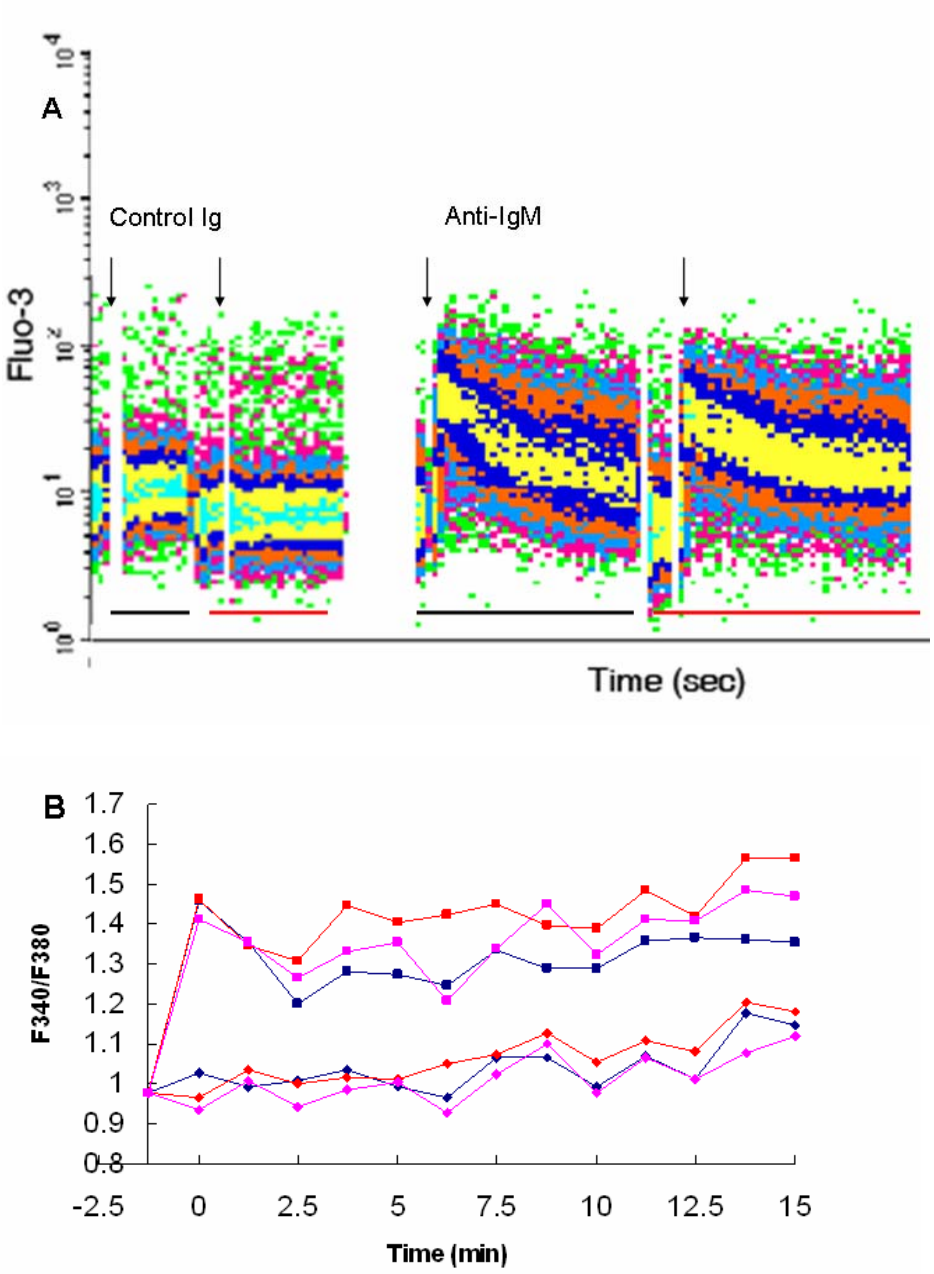

Figure 3.24: Bz-423 pre-treatment on anti-IgM-induced intracellular [Ca^{2+}] change. After Bz-423 (16 h) treatment, Ramos cells were loaded with Fluo-3-AM (3 µM, flow cytometry) or Fura-2 (3 µM, plate reader) for 30 min. The cells were washed and resuspended in buffer (PBS + 1mM $MgCl_2$ + 1 mM $CaCl_2$ + 2% (v/v) FBS) for anti-IgM (1 µg/mL) stimulation. (A) Bz-423 on anti-IgM induced Ca^{2+} increase by fluo-3 using flow cytometry. Arrow indicates treatment. The cells with black underline are vehicle-pretreated Ramos B cells and the cells with red underline are Bz-423 (16 µM) pre-treated Ramos B cells. Increase Fluo3 fluorescence indicates increased [Ca^{2+}]. (B) Intracellular Ca^{2+} change is monitored by Fura-2 using plate reader. The treatments used were control Ig (1 µg/mL,◆), anti-IgM (1 µg/mL, ■). vehicle (blue), Bz-423 (8 µM, pink; 16 µM, red). Increased F340/F380 indicates increased $[Ca^{2+}]_i$

Reduced proliferation is normally used to indicate the decreased response of anergic cells to activation signals [8, 204, 205]. Bz-423 itself inhibits cell growth, making it impossible to use proliferation as an endpoint for activation. CD69 is a early activation marker and was used for an endpoint of activation [206]. The effects of Bz-423 pre-incubation on CD69 expression in response to PKC activator PMA plus ionomycin were studied. Bz-423 pre-treatment increased CD69 expression by 15-20%. In response to PMA plus ionomycin stimulation, there was ~81-96% increase in CD69 expression, which was decreased by Bz-423 pre-treatment to 70% increase, irresponsive of whether Bz-423 is present during the stimulation (Figure 3.25B). This finding suggests that Bz-423 pre-treatment inhibits activation-induced CD69 expression. Moreover, the observation that Bz-423 presence is not required for inhibition of CD69 induction in response to stimulation suggests Bz-423 pre-treatment may render cells anergic, and Bz-423 is not needed when stimuli were applied.

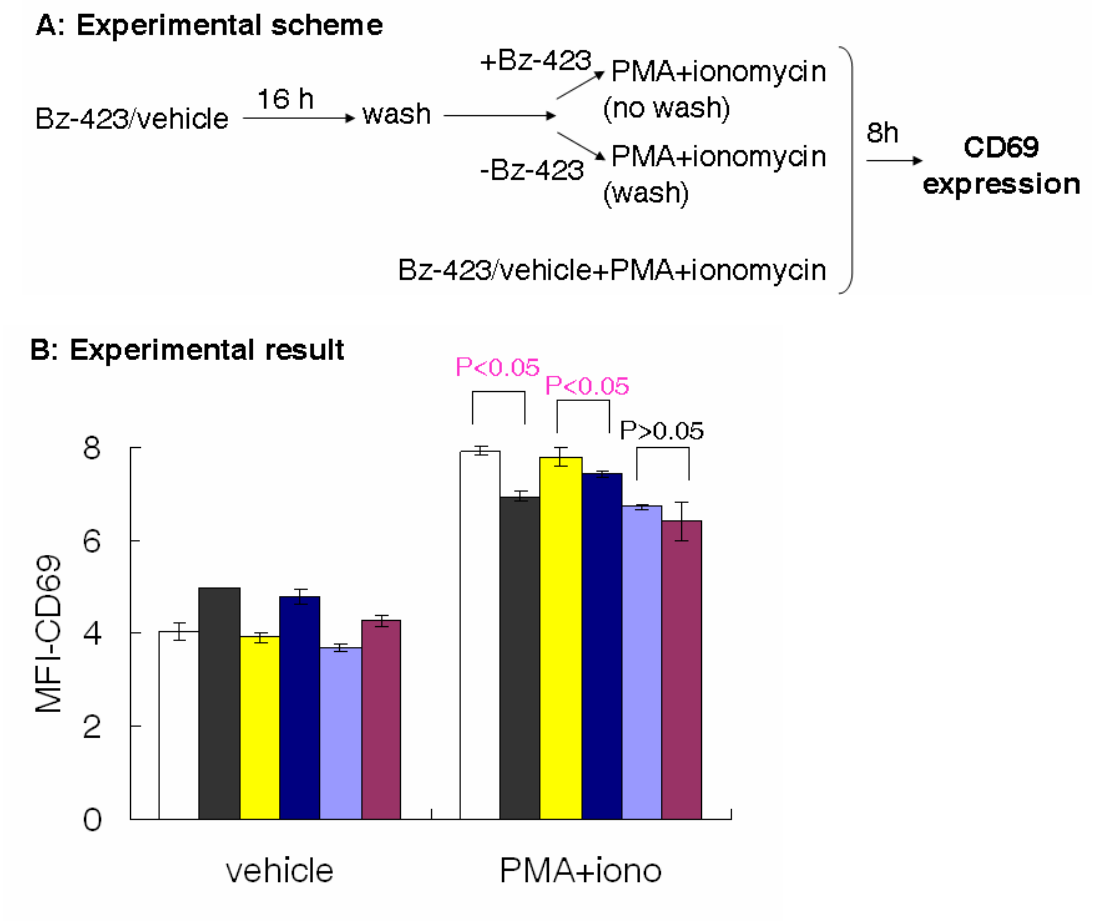

Figure 3.25: Bz-423 pre-treatment on CD69 expression in response to PMA (10 ng/mL) plus ionomycin (50 ng/mL). (A)Experimental scheme: Ramos cells were pre-treated with vehicle/Bz-423 (16 μM) for 16 h. Before stimulation, they were washed, resuspended in 10% FBS media with Bz-423 (no wash) or in 10% FBS media without Bz-423 (wash). At the same time, vehicle/Bz-423 (16 μM), PMA and ionomycin were also added. 8 h later, the expression of CD69 was studied by the flow cytometry. (B)Experimental result: The mean fluorescence (MFI) of CD69 expression was shown. The legends are vehicle_no wash (white bar), Bz-423_no wash (black bar), vehicle_wash (yellow bar), Bz-423_wash (blue bar), vehicle (light blue bar) and Bz-423 (plum bar). Both panel A and panel B are from one experiment of two.

As CD69 expression change in response to activation in Ramos is small, another endpoint for activation was used to confirm the previous observation. In response to activation, NFκB is activated. Thus IκBα degradation was used as another endpoint for activation [195]. Ramos B cells were pre-treated with Bz-423 for 16 h, then its effect on IκBα degradation induced by PMA plus ionomycin stimulation was

studied. In response to PMA plus ionomycin stimulation, there was ~40% reduction in IκBα expression level (Figure 3.26). Bz-423 pre-incubation prevented IκBα degradation induced by PMA plus ionomycin, as the expression level of IκBα is even higher than that in vehicle-treated Ramos cells (Figure 3.26), suggesting Bz-423 pre-treatment renders Ramos cells resistant to IκBα degradation in response to PMA plus ionomycin.

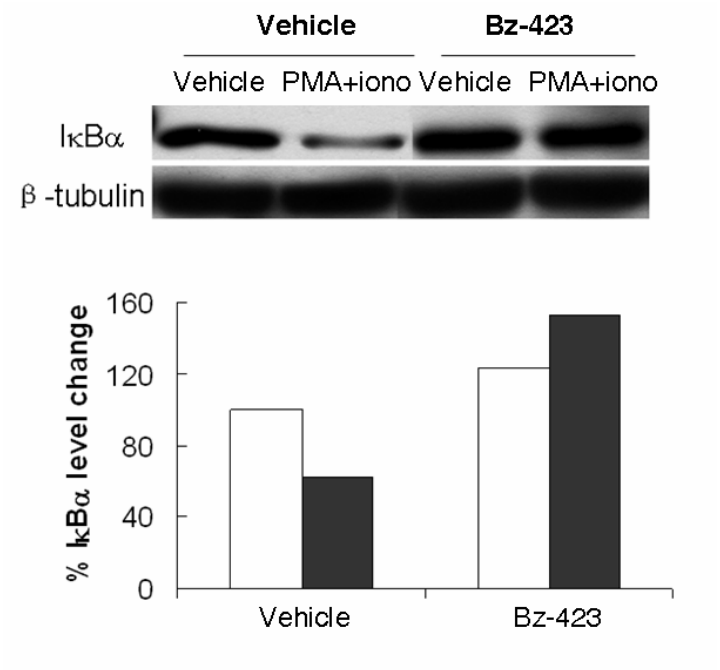

Figure 3.26: Bz-423 pre-treatment inhibit NFκB activation induced by PMA plus ionomycin in Ramos cells. Ramos B cells in 10% FBS were treated with Bz-423 (16 μM) for 16 h. The following days, these cells were treated with PMA (50 ng/mL) plus ionomycin (iono, 50 μg/mL) for 2 h. Then cells were harvested and lysates were obtained for western blot. The fold change in IκBα was indicated.

In summary, Bz-423 pretreatment renders Ramos B cells resistant to subsequent activation signals anti-IgM and PMA plus ionomycin. This conclusion is based on two observations: Bz-423 pretreatment inhibits CD69 increase in response to anti-IgM and PMA plus ionomycin. IκB degradation induced by PMA plus ionomycin was blocked by Bz-423 treatment.

Bz-423 induces NFAT activation in T cells and the functional consequence: Beside the critical role of NFAT in B cell function, it is essential for T cell development, differentiation and its immune function [139, 149, 150, 207]. NFAT activation in T cells induces a subset of anergy genes, including c-Cbl, DGKα [58, 208]. Once anergy is lost, autoreactive T cells either assist the abnormal activation of autoreactive B cells or itself directly cause self damage. Administration of Bz-423 to the lupus-prone MRL-*lpr* mice reduced the level of inflammatory cytokines IL-4, IL-10 and IFNγ [209]. As Bz-423 induced NFAT activation, NFAT-dependent transcription activation and possible anergy in Ramos B cells, it is interesting to study whether Bz-423 induced NFAT activation in T cells.

Bz-423 induces NFAT dephosphorylation in T cell lines: To study whether Bz-423 induced NFAT activation in T cells, Bz-423 induced NFAT dephosphorylation in several T cell lines was studied. Among the T cells accessible, Molt4 was eliminated because NFATc2 does not dephosphorylates in response to ionomycin treatment, and EL4 T cells were eliminated because of constitutive NFATc2 activation. Jurkat E6.1 and CCRF-CEM are the two T cell lines tested. In Jurkat T cells, only 3-5% NFAT was dephosphorylated by Bz-423 (Figure 3.27A). In CCRF-CEM cells, Bz-423 induces NFAT dephosphorylation in a dose-dependent manner. At 15 min, Bz-423 induced ~10% NFAT dephosphorylation at 16 μM, and ~20% at 32 μM (Figure 3.27B). Bz-423 also induces NFAT dephosphorylation in a time-dependent manner. At all times tested, 20-40% of total NFAT was induced by Bz-423 (Figure 3.27C). The NFATc2 resistance to dephosphorylation in Jurkat T cells may explain the

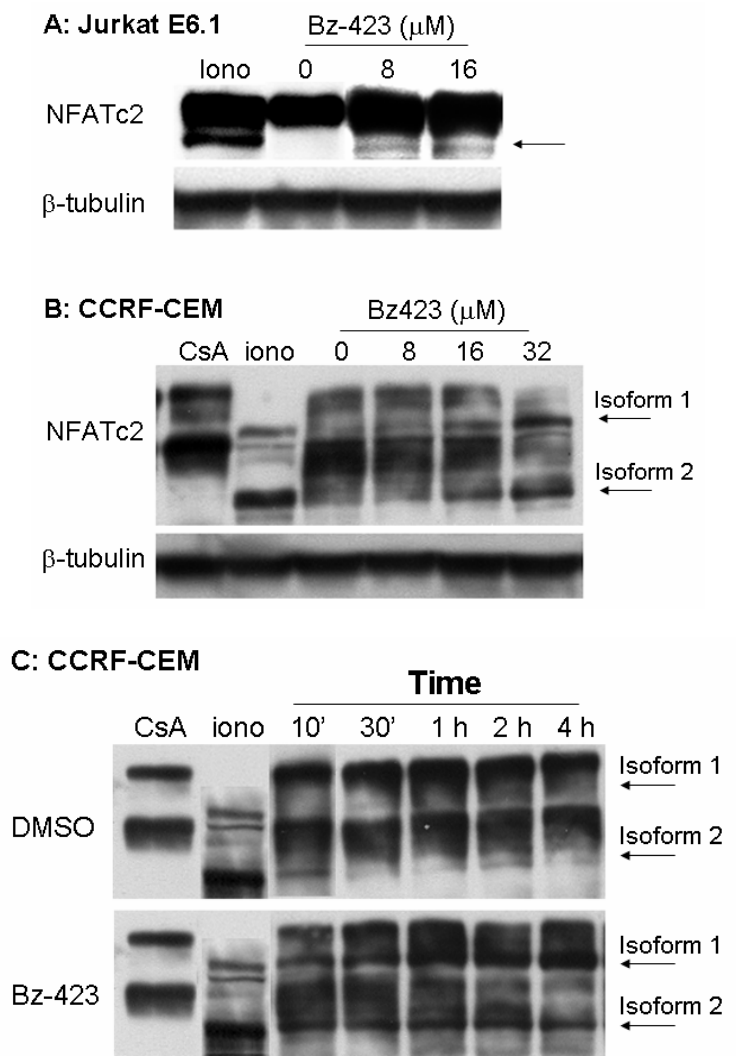

Figure 3.27: Bz-423 induces NFAT dephosphorylation in Jurkat E6.1 and CCRF-CEM cells. (A) Bz-423 induced NFAT dephosphorylation in Jurkat E6.1 cells. Cell lysates from Jurkat E6.1 treated with 10 minute ionomycin (1 μg/mL) and Bz-423 were immunoblotted by NFATc2 from BD pharmingen. The arrow indicated the dephosphorylated NFAT. (B) The dose response of Bz-423 induced NFAT dephosphorylation in CCRF-CEM cells at 10 min. Cell lysates from CCRF-CEM treated with CsA, ionomycin and Bz-423 were immunoblotted with anti-NFATc2. The arrow indicated the dephosphorylated NFAT. (C) The time course of Bz-423 induced NFAT dephosphorylation in CCRF-CEM. CCRF-CEM was treated with vehicle and Bz-423 (16 μM). At indicated times, cell lysates were obtained for immunoblotting with anti-NFATc2 Ab. CsA (250 nM) and ionomycin (1 μg/mL) were used as positive controls for dephosphorylated and phosphorylated NFATc2. The arrow indicated the dephosphorylated NFAT.

low NFAT dephosphorylation induced by Bz-423 as ionomycin only induced 30% dephosphorylation in Jurkat T cells but close to 100% in CCRF-CEM cells (Figure 3.27), which is consistent to the literature reports that different endogenous inhibitor for calcineurin or NFAT are present in the different cells [210]. Bz-423 induced NFAT dephosphorylation in T cell lines tested, suggesting that Bz-423 induced NFAT dephosphorylation in T cells.

Bz-423 does not induce NFAT dephosphorylation in spleen T cells. Whether Bz-423 induced NFAT dephosphorylation in primary T cells were studied next. Spleen T cells were negatively selected. About 50% of NFATc2 is dephosphorylated in the spleen T cells (Figure 3.28). Bz-423 treatment did not further induced NFAT dephosphorylation in these spleen T cells (Figure 3.28). In contrast, ionomycin induced dephosphorylation of all phosphorylated form of NFATc2 (Figure 3.28), indicating the phosphorylation form of NFATc2 can be dephosphorylated. Considering Bz-423 induces NFAT dephosphorylation in T cell lines, the observation in spleen T cells that Bz-423 may only activate NFAT in several T cell subsets, and spleen T cells is not responsive to Bz-423; or the kinetics of Bz-423 induced NFAT activation in spleen T cells is different from other primary cells and cell lines, and thus the timepoints chosen here are not appropriate.

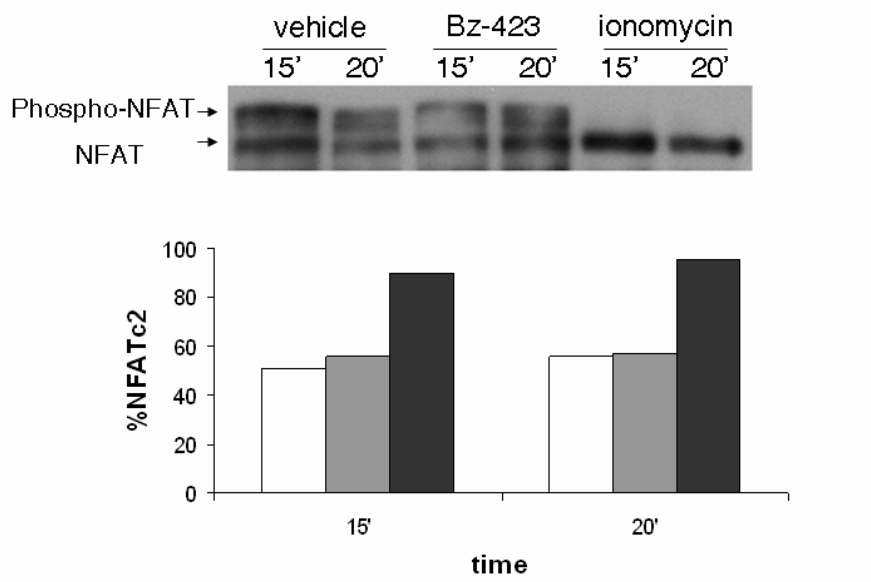

Figure 3.28: Bz-423 does not induce NFAT dephosphorylation in spleen T cells. Spleen T cells were negatively isolated from Balb/c mice. Before treatment, the spleen T cells were incubated in the pre-warmed DMEM media for 1 h. At indicated time, the whole cell lysates from cells treated with vehicle (white bar), Bz-423 (16 μM, gray bar), ionomycin (1 μg/mL, black bar) were immunoblotted with anti-NFATc2. % NFATc2 was calculated based on 100 x NFATc2/(NFATc2 + NFATc2-p).

Bz-423 induces NFAT dephosphorylation in human peripheral T cells and the functional consequence. Ionomycin (16 h) renders T cells resistant to activation through activating NFAT [49, 211]. Similar to ionomycin, Bz-423 incubation renders human blood peripheral T cells resistant to anti-CD3-induced T cell blast (Figure 3.29C; personal communication with Rod Morgan). It is therefore hypothesized that Bz-423 inhibited anti-CD3 induced T cell blast through activating NFAT.

To test this hypothesis, whether Bz-423 induced NFAT dephosphorylation in human blood peripheral T cell was studied by monitoring Bz-423 induced NFAT dephosphorylation in human blood peripheral T cells. At 10 min, Bz-423 induced 15% increase in NFAT dephosphorylation while it induced 32% increase at 2 h (Figure 3.29A), which indicates Bz-423 induces NFAT dephosphorylation. Anti-CD3

crosslinking induced 128% increase in NFAT dephosphorylation at 10 min and declined to 15% increase at 2 h (Figure 3.29A). Co-treatment of Bz-423 and anti-CD3 induced 96% increase in NFAT dephosphorylation at 10 min (Figure 3.29A), which indicates Bz-423 does not enhance anti-CD3 induced NFAT dephosphorylation. At 2 h, this co-treatment induced 69% increase in NFAT dephosphorylation (Figure 3.29A), indicating Bz-423 sustained anti-CD3 induced NFAT dephosphorylation.

Bz-423 on anti-CD3-induced T cell blast was monitored side by side with the NFAT dephosphorylation. Ionomycin was included as a positive control. As shown in Figure 3.29B, ionomycin inhibited anti-CD3-induced T cell blast from 22 % to 13 % while Bz-423 inhibited anti-CD3-induced T cell blast to 11 % (Figure 3.29C). This result suggests that Bz-423 as well as ionomycin inhibits T cell activation. As NFAT is shown to inhibit proliferation [153], Bz-423 inhibits anti-CD3 induced blast possibly by sustaining anti-CD3-induced NFATc2 dephophosphorylation.

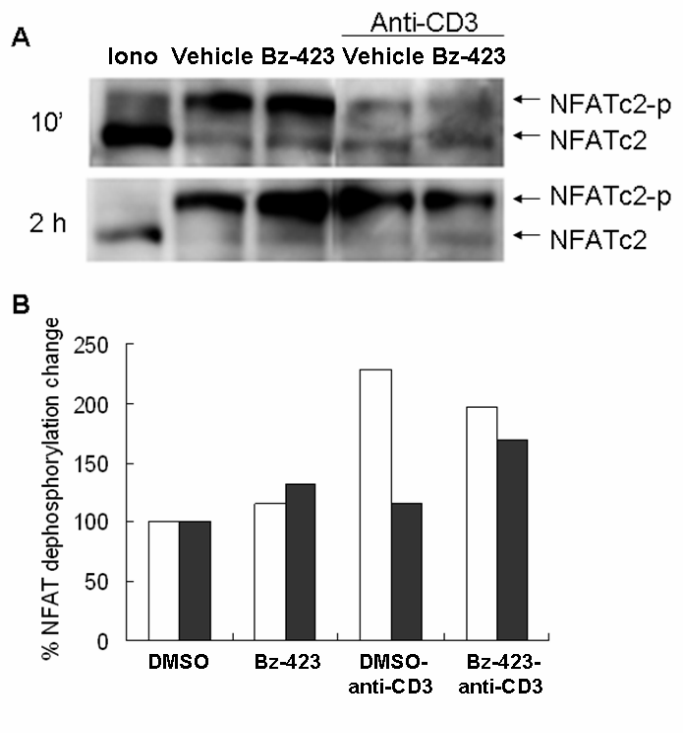

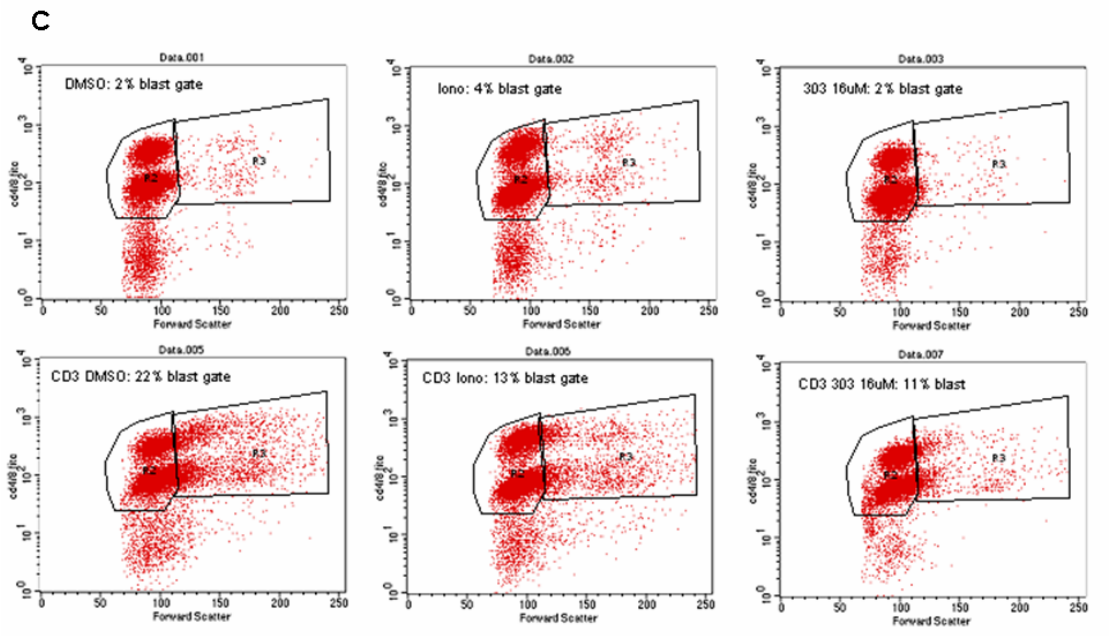

Figure 3.29: Bz-423 sustains anti-CD3-induced NFATc2 dephosphorylation and inhibits anti-CD3 induced T cell blast. (A, B) Bz-423 induced NFAT dephosphorylation and its effect on anti-CD3-induced NFAT dephosphorylation in human T cells. Human T cells were negatively selected from human blood. Cells were then incubated in pre-warmed DMEM + 10% FBS for 1 h to recover the stress. Cells were treated with ionomycin (1 µg/mL), Bz-423 (16 µM) in the presence or absence of plate-bounded anti-CD3 (1 µg/mL). Cell lysate were immunoblotted with NFATc2. (C) Bz-423 on anti-CD3 induced T cell blast: 72 h after treatment, the treated cells were stained with anti-CD4 and anti-CD8 and the size was analyzed based on the Forward Scatter. The R2 region indicates the blast T cells.

Discussion

Mechanism of Bz-423 induced NFAT activation: Bz-423 induces NFAT activation in a dose-dependent manner. 40-50% of NFAT is dephosphorylated by anti-IgM at 1 h and 2 h, which return to basal level at 4 and 6 h. In contrast, around 35% of the total NFAT is dephosphorylated 10 min after Bz-423 treatment. NFAT remains dephosphorylated at around 20% up to 6 h compared to anti-IgM alone. This result indicates that Bz-423 induces a low (< 40%) and sustained (> 2 h) NFAT activation. This NFAT dephosphorylation is significant as Bz-423 induces NFAT-dependent transcription activation.

Reactive oxygen species (ROS) mediates Bz-423 induced NFAT activation: Antioxidants MnTBAP and vitamin E both block Bz-423 induced NFAT dephosphorylation. This result shows that reactive oxygen species (ROS) is required for NFAT activation induced by Bz-423. There are several pieces of evidence that ROS can activate NFAT directly, although the mechanism is not clear. Exposure of lung cells to crystalline silica causes the generation of superoxide, which subsequently activates NFAT [212]. Similar results has been observed with nickel subsulfide [213], asbestos [214], doxorubicin [215], and vanadium [216]. Doxorubicin is a drug that induces production of mitochondrial superoxide by redox cycling. Doxorubicin-induced NFAT activation is inhibited by mitochondria-specific anti-oxidant mito-Q or intracellular calcium chelator [215], suggesting a link between mitochondrial ROS generation and intracellular calcium increase, which subsequently leads to NFAT activation. The calcium channel blocker nifedipine inhibits

ROS-mediated NFAT activation induced by vanadium [216], suggesting that ROS activates calcium influx to trigger NFAT activation. As the CRAC channel inhibitor YM-58483 inhibits ROS-mediated NFAT activation by Bz-423, suggesting Bz-423 induced ROS may trigger CRAC channel opening and subsequent calcium influx. It is not clear whether ROS induces calcium influx by directly triggering CRAC channel opening or by depleting endoplasmic reticulum (ER) calcium stores. Orai is the core of CRAC channel [217]. STIM proteins are sensors of ER luminal calcium changes and rapidly translocate into near plasma membrane junctions to trigger Orai to from CRAC channel [218]. Transient receptor potential C (TRPC) is a proposed subunit of a CRAC channel as it interacts with Orai and STIM [142, 219, 220]. To further support this, YM-58483, the specific CRAC channel inhibitor, inhibits calcium influx mediated by TRPC [145]. Moreover, ROS is shown to activate TRPC and to increase calcium influx [221]. Therefore, it is possible that TRPC senses ROS changes induced by Bz-423, which may trigger the opening of CRAC channel for calcium influx. However, the possibility that ROS induced by Bz-423 depletes ER calcium and subsequently activates CRAC channel can not be excluded.

In summary, Bz-423 inhibits the mitochondrial F_0F_1-ATPase, which increases superoxide production. This ROS increase can either be sensed by TRPC, which directly activate CRAC channel, or it may deplete ER calcium stores and subsequently trigger CRAC channel opening. Subsequent calcium influx through the CRAC channel increases intracellular calcium, which activates calcineurin and subsequent NFAT dephosphorylation (Figure 3.30).

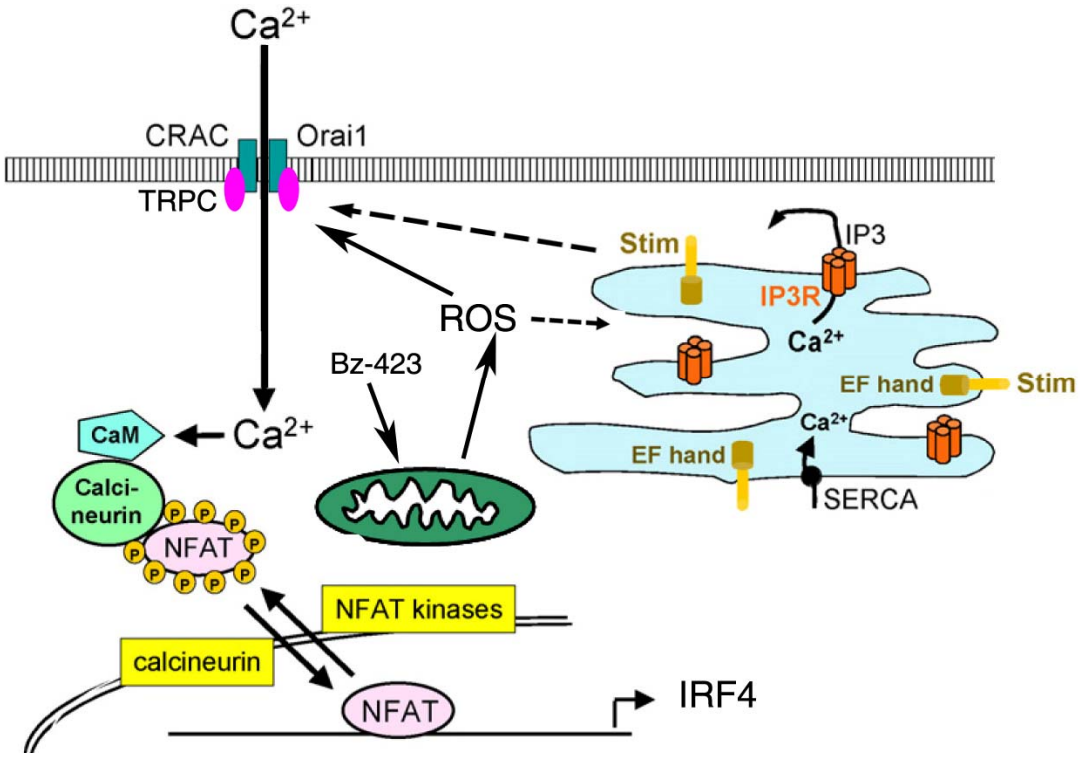

Figure 3.30: Proposed mechanism of Bz-423 induced NFAT activation: Bz-423 induces reactive oxygen species (ROS) by inhibiting mitochondrial F_0F_1-ATPase. ROS may trigger the opening of CRAC channel directly through modulating TRPC activity, or indirectly through depleting ER calcium. The calcium influx increases intracellular calcium, which activates calcineurin. Calcineurin then dephosphorylates NFAT, resulting in its nuclear translocation and transcription activation of targeted genes, such as *IRF4*.

Mitochondria are involved in sustained NFAT activation: Inhibition of ionomycin-induced calcium increase by BAPTA salt leads to a rapid translocation of NFATc1 from nucleus to cytosol [222], which suggests the a persistent calcium signaling is required to maintain NFAT activation. In this section, the ability of Bz-423 to sustain NFAT activation will be discussed. In response to an intracellular calcium increase, mitochondria can rapidly take up calcium and slowly release it later [223], which protects cells from calcium overload [224]. The increased intracellular calcium can binds to IP3 receptor (IP3R) and CRAC channel, inhibiting further calcium release from ER and calcium influx, respectively [225, 226]. Mitochondria calcium uptake release these inhibition, enhancing ER calcium depletion and

sustaining CRAC channel opening [227]. Tharpsigargin, an inhibitor of the sacro/endoplasmic reticulum calcium ATPase (SERCA), depletes ER calcium stores and triggers calcium influx through CRAC channel [228]. The uncoupler FCCP dissipates mitochondrial membrane potential ($\Delta\psi_m$), inhibits mitochondria calcium uptake, and blocks tharpsigargin-induced calcium influx [222]. Similar results are also observed with mitochondrial respiratory chain complex III inhibitor antimycin A plus mitochondrial F_0F_1-ATPase inhibitor oligomycin [229]. Mitochondrial membrane potential is the driving force for mitochondrial calcium uptake [230]. It is therefore speculated that chemicals to hyperpolarize $\Delta\psi_m$ will enhance mitochondrial calcium uptake and sustain calcium influx. In rat hearts, mitochondrial hyperpolarization is observed in isolated cardiomyocytes from right ventricular hypertrophy while normal $\Delta\psi_m$ is observed in isolated cardiomyocytes from right ventricle/ventricular [231]. Bz-423 inhibits mitochondrial F_0F_1-ATPase and induces mitochondrial membrane potential hyperpolarization [232]. Bz-423 will increase mitochondrial calcium uptake, which may prolong CRAC channel opening and calcium influx.

Bz-423 increases the expression of interferon regulatory factor 4 (IRF4) in a NFAT-dependent manner: Bz-423 increases *IRF4* mRNA levels in a time- and a dose-dependent manner. Pre-treatment with CsA blocks this *IRF4* increase, indicating the involvement of calcineurin. Chromatin immunoprecipitation (CHIP) analysis demonstrates increased binding of NFAT to *IRF4* promoter, which is blocked by CsA, indicating calcineurin-NFAT in *IRF4* transcription activation. IRF4 is known to be essential for the developments of B cells, T cells, macrophages and dendritic cells

[233], and increase expression of this factor could be responsible for Bz-423 efficacy against Lupus. Therefore, the possible consequences of Bz-423 induced *IRF4* increase will be discussed in this section.

Interferon regulatory factor 4 (IRF4, LSIRF, MUM1) is a transcription factor expressed in normal leukocytes and various malignant human hematopoietic cell lines [234]. IRF4 plays an essential role in B cell development from pre-B to plasma cells [233]. Although *IRF4*-deficient mice develop progressive lymphadenopathy, they fail to develop germinal centers (GCs) in B-cell follicles after immunization, which may explain the observed profound reduction in serum immunoglobulin concentration [235]. Conditional deletion of *IRF4* in GC B cells blocked further differentiation into plasma cells and memory B cells [236], indicating the critical role of IRF4 in plasma cell differentiation and class-switch recombination. This result is confirmed by IRF4 overexpression, as the overexpression of IRF4 in Daudi and Raji B cells promotes differentiation to plasma cells [237].

Receptor editing is a process through which self-reactive B cell receptors is replaced with a newly rearranged Ig chain to avoid self-reactivity [238]. IRF4 is also known to participate in receptor editing through promoting secondary rearrangement of immunoglobulin (Ig) genes and increasing recombination activating gene 1 (RAG1) [233]. Therefore, Bz-423 could reduce self-reactive lymphocytes through IRF4-mediated receptor editing. In HEL-transgenic mice, binding of self-antigen to the BCR rapidly increases IRF4 expression, which promotes secondary rearrangement of immunoglobulin (Ig) genes for receptor editing [239, 240]. This secondary Ig gene

rearrangement is impaired in *IRF4*-deficient mice [240]. In lupus-prone New Zealand Black (NZB) mice there is an increased portion of cells devoid of RAG1 expression [241]. Since RAG1 is an important enzyme involved in receptor editing [242], this observation indicates that lack of receptor editing may contribute to lupus development in NZB mice. Cells lacking RAG1 were also found to have low IRF-4 expression, suggesting that IRF4 may regulate RAG1 expression [241]. However, *rag1* induction in *IRF4*$^{-/-}$*IRF8*$^{-/-}$ pre-B cells reconstituted with IRF4 is only modest, indicating that IRF4 may be partially responsible for *rag1* transcription [243]. Reduced receptor editing is also observed in MRL/*lpr* mice, although the mechanism is still unknown [244]. Further studies are needed to determine if Bz-423 promotes receptor editing via IRF4. Transgenic mice such as HEL-transgenic mice could be used to study the effect of Bz-423 on receptor editing or RAG1 expression level. Also, the involvement of IRF4 or NFAT can be further studied by specific inhibitors of NFAT or IRF4-specific RNAi knockdown.

In addition to its critical role in B cell development and function, IRF4 also plays an important role in T cell differentiation. Th2 cell differentiation is compromised in *IRF4*-deficient CD4^{+} T cells challenged with the pathogen Leishmania [245, 246], indicating that IRF4 promotes Th2 differentiation. In response to stimulation, Jurkat cells overexpressing IRF4 display enhanced Th2-specific cytokine production [247]. On the other hand, selective deletion of *IRF4* in regulatory T cells (Treg) results in a exaggerated Th2 cytokine production such as IL-4 and IL-10, indicating IRF4 suppresses the Th2 response via Treg cells [247]. Previous

work showed that Bz-423 treatment of MRL-*lpr* mice significantly reduced Th2 cytokines IL-4 and IL-10 and increased Th1 cytokine IFNγ [209]. In light of the role of IRF4 in Th1 and Th2 differentiation, it is possible that Bz-423 could alter IRF4 expression in T cells in vivo and reduce Th2 cytokine production. This modulation of Th2 cytokine production may be mainly in the effector/memory $CD4^+$ T cells but not in naïve T cells. In response to T cell receptor (TCR) stimulation, *IRF4*-deficient naïve T cells produce higher Th2 cytokine than wild-type $CD4^+$ T cells while *IRF4*-deficient effector/memory $CD4^+$ T cells do not exhibit increased Th2 cytokine [248].

Exogenous oligonucleotides from bacteria bind to Toll-like receptor (TLR) and trigger TLR signaling, which leads to activation of NFκB and IFN family members for B cell activation [249]. MyD88 is an important adapter for TLR signaling as MyD88-deficient mice are profoundly unresponsive to ligand for TLR2, TLR4, TLR5, TLR7 and TLR9 [250, 251]. For example, recruitment of MyD88 to TLR activates IRF5, which induces transcriptions of pro-inflammatory cytokines [252]. In autoimmune disease, pathogenic endogenous oligonucleotides also bind to TLR and activate self-reactive cells, leading to the breakdown of self-tolerance [249]. Y-linked autoimmune accelerator (Yaa) has previously been shown to increase the severity of SLE in male mice [253]. Analysis of the *Yaa* locus demonstrated a duplication of the *TLR7* gene [253]. IRF4 decreases IRF5-meidated production of pro-inflammatory cytokines including IL-6 and TNF-α by competing with IRF5 in MyD88 binding [254]. This inhibitory role of IRF4 in TLR signaling was confirmed

by reducing or overexpressing IRF4 expression [255]. IRF4 downregulation by RNAi reduces the production of pro-inflammatory cytokines in response to TLR stimulation [255]. Conversely, IRF4 overexpression enhances the production of pro-inflammatory cytokines in response to TLR stimulation [255]. *IRF4*-deficient mice display a more potent and lethal inflammatory response to CpG oligonucleotide, which is consistent with the increased pro-inflammatory cytokine production observed *in vitro* [254, 255].

NFκB and NFAT are both involved in *IRF4* expression. Binding sites for both NFκB and NFAT have been identified in the *IRF4* promoter region [186, 256]. Human T cell leukemia virus-I infection increases binding of NFκB subunit p50, p65, and c-Rel as well as NFATc2 to *IRF4* promoter. The binding of these transcription factors to *IRF4* promoter is responsible for IRF4 induction as mutations in the binding sites of either NFκB or NFATc2 in *IRF4* promoter reduces the IRF4 increase [186]. Mitogen stimulation induces IRF4 expression in a NFκB-dependent manner, as IRF4 protein level are totally abolished in lymphocytes deficient in NFκB subunit c-Rel in response to mitogen stimulation including concanavalin A, PMA and lipopolysaccharide (LPS) [257]. In GC-like Ramos B cells, Bz-423 increases *IRF4* expression by activating NFAT alone, which is blocked by CsA. Consistent with this observation, IRF4 increase induced by PMA plus ionomycin is inhibited by CsA and by calcineurin B deficiency in the GC B cells from the mouse spleens [158]. Chromatin immunoprecipitation (CHIP) studies with NFATc2 indicate that Bz-423 increases binding of NFATc2 to the *IRF4* promoter, confirming Bz-423 increases *IRF4* mRNA by NFAT activation. Similarly, IRF4 is increased by ionomycin, a

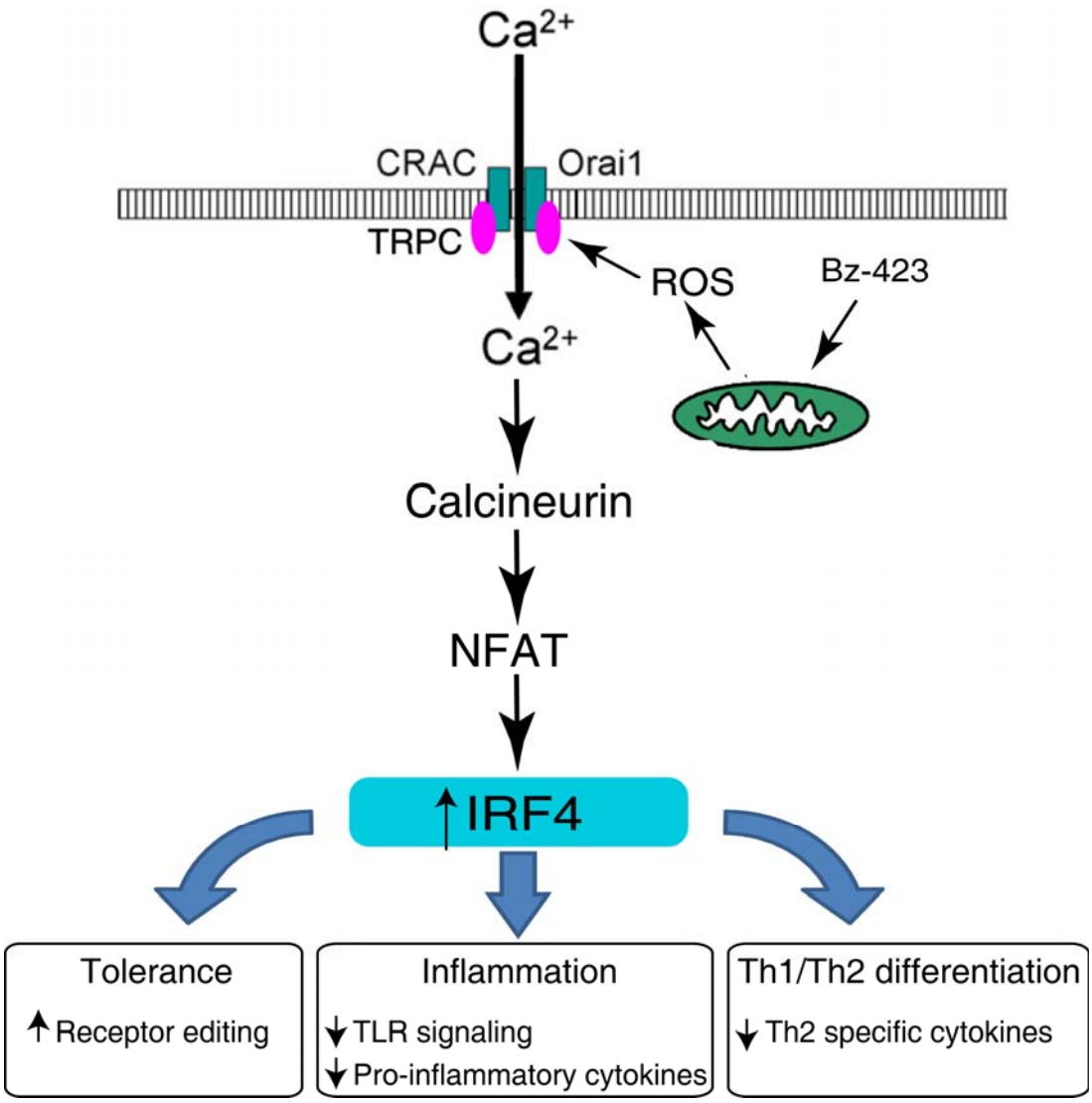

Figure 3.31: The proposed immunomodulatory effects by Bz-423 induced *IRF4* increase. Bz-423 increases *IRF4* expression via calcium-calcineurin-NFAT pathway. IRF4 can induce B cell tolerance by promoting receptor editing. It also can reduce inflammation by inhibiting TLR signaling and production of pro-inflammatory cytokines. It can affect Th1/Th2 differentiation by inhibiting Th2 specific cytokines.

well-known NFAT activator. *In vitro,* Bz-423 activates NFAT and increases *IRF4* mRNA levels in GC-like Ramos B cells, which may mimic the changes of Bz-423 in GC B cells. Bz-423 is therefore proposed to increase *IRF4* expression level in GC B cells, and this IRF4 increase may promote receptor editing to eliminate the self-reactive B cells (Figure 3.31). It may also inhibit TLR signaling induced by pathogenic oligonucleotides, which may reduce the inflammatory response observed

in the lupus-prone mice (Figure 3.31). Moreover, Bz-423 treatment to MRL-*lpr* mice suppresses Th2 response [209], which may possible through Bz-423 induced *IRF4* increase (Figure 3.31).

Bz-423 may induce anergy: Bz-423 was shown to activate NFAT and induce NFAT-dependent transcription activation. NFAT activation is known to promote tolerance through anergy, growth arrest, and cell death [151, 154, 208, 258]. The possible involvement of Bz-423 in anergy, growth arrest and cell death was explored by FK506 and CsA. FK506 and CsA do not inhibit Bz-423 induced apoptosis. Neither do they prevent Bz-423 mediated growth arrest and CDK4 downregulation. These results exclude the possibility that the calcineurin-NFAT pathway is responsible for Bz-423 induced apoptosis and cell growth in resting lymphocytes. However, the calcineurin-NFAT pathway is shown to be involved in apoptosis induced by anti-IgM and Bz-423 co-treatment, which provide the specificity of Bz-423 against autoimmune disease and has already been discussed in chapter 2 in detail.

Bz-423 activates NFAT but not AP-1 and NFκB: The molecular mechanisms for activation and tolerance has been studied by monitoring and comparing mRNA levels changes in activated B cells and anergic B cells [73]. NFAT, AP-1 and NFκB activation were observed in activated cells while only NFAT activation was observed in anergic cells, indicating NFAT activation leads to anergy while additional activation of AP-1 and NFκB results in activation [73]. The AP-1 subunit c-Jun is activated by JNK, and NFκB activation is mediated by degradation of

its repressor IκB [259, 260]. Therefore, JNK phosphorylation (activation) and IκB degradation can be used to monitor AP-1 and NFκB activation, respectively. Bz-423 does not induce JNK phosphorylation or IκB degradation, suggesting Bz-423 does not activate AP-1 or NFκB. Furthermore, reporter plasmids pNFκB-SEAP and pAP-1-SEAP are used to monitor NFκB- and AP-1-dependent gene transcription, respectively. Bz-423 does not increase SEAP expression, indicating that Bz-423 does not activate transcription by NFκB or AP-1. The observations that Bz-423 activates NFAT but not NFκB or AP-1 suggest Bz-423 may induce anergy. Ionomycin, which selectively activate NFAT, was therefore used for *in vitro* anergy induction in Jurkat T cells [63].

Bz-423 induces anergy-associated genes change: NFAT participates in anergy induction by regulating a series of anergy-associated genes [71, 77, 80]. Both upregulated and downregulated anergy-associated genes are found in anergic B cells, although the expression changes are subtle (1.5 fold – 6 fold) [71]. The upregulated genes include *SATB1, ApoE, CD83, cyclin D2, Cctg, MEF-2C, TGIF, Aeg-2, EGR-1, Lck, GFI-1, EGR-2, CD72, MacMARCKs, A1, NAB-2, neuorgranin* and *pcp-4*. And the downregulated genes include *SLAP, Ly6E.1, Vimentin, hIP-30, TRAP, Bmk, CD36, Evi-2* and *c-Fes* [71]. Among these genes, *EGR-2, NAB-2, CD72, MacMARCKs, A1, pcp-4* and *neuorgranin* are NFAT-dependent [71]. And *EGR-2, NAB-2,* and *neuorgranin* are upregulated in other anergic B cells [3]. The gene expression changes upon Bz-423 treatment were explored in previous work from our lab. Ramos cells were treated with Bz-423 (10 μM, 3 h) in 2% FBS media, then RNA was isolated and

mRNA expression levels were determined by affymetrix. Analysis of affymetrix data from the sample identified anergy associated genes: a 1.5-fold increase in *MEF2C*, a 3-fold increase in *Lck* and a 2-fold decreased in *EVI2*. These changes are consistent with anergy-associated genes reported in the literature. However, none of them are NFAT-dependent. Moreover, the exact roles of these genes in anergy are not known yet. In addition, several well-recognized anergy-associated genes such as *EGR-2, NAB-2, neuorgranin* and E3 ubiquitin ligases including *Cbl, Itch, Grail*, were unchanged in this experiment. Ramos B cell line might not be appropriate, considering that anergy-associated genes have typically been studied in primary anergic B cells, and little is known about their expression in transformed cell lines [71]. Moreover, the time and/or dose chosen here might not be appropriate for studying anergy. Significant changes in expression levels of anergy associated genes were typically observed by anergy-inducing stimuli at 6-16 h [63, 71]. Further studies demonstrate that Bz-423 also induces NFAT activation in mouse splenic B cells in a dose- and time-dependent manner. Therefore, primary splenic B lymphocytes could be used to study the effect of Bz-423 on the expression levels of anergy-associated genes. For the time and dose of Bz-423, 16 μM (10% FBS media) and 6 h would also be a good starting point.

***Bz-423 downregulates surface IgM expression*:** Various characteristics of anergic B cells have been described in different transgenic mouse models [8]. Among these, downregulation in surface Ig expression level is generally observed [8]. Bz-423 induces 2-fold decrease in IgM expression, which is similar to 2- to 5-fold

downregulation of surface Ig expression in V_H3H9 x Vκ8 mice [13]. This result suggests Bz-423 might render Ramos B cells anergic. In several anergy mouse models, such as MD4 x ML5, IgM downregulation is associated with the decreased calcium mobilization in response to BCR stimulation. However, Bz-423 pre-incubation does not inhibit anti-IgM induced calcium mobilization, which is consistent with normal calcium change in response to BCR stimulation in V_H3H9 x Vκ8 [13]. This discrepancy might be due to the degree of surface Ig downregulation. As in MD4 x ML5 mice, IgM expression is decreased by 20-100 fold decrease [37], as opposed to 2-5 fold decrease in V_H3H9 x Vκ8 mice.

In several tolerant B cells, impaired proximal BCR signaling, such as calcium mobilization, could explain the reduced response to stimulation (anergy). However, in other anergic B cells, normal proximal BCR signaling is observed, although IgM expression is still downregulated. In this case, the role of IgM downregulation in anergy induction is further studied by enforced BCR expression in self-reactive B cells from HKIR mice [203]. In the HKIR mice, an antibody H chain variable (V_H) region gene is inserted into the endogenous H chain locus to produce an autoreactive B cells against DNA [261]. The anergic B cells isolated from HKIR mice expressed IgM ~10-fold lower than those from wild type mice [261]. In response to anti-IgM stimulation, normal calcium mobilization is observed [261]. Enforced expression of IgM retarded B cell development and enhanced receptor editing [203]. This result indicates IgM downregulation acts a checkpoint for tolerance. Failure to decrease IgM expression level triggers receptor editing. Autoantigen-induced BCR

downregulation plays a pivotal role in the regulation of primary B cell tolerance [203]. This supports the possibility that Bz-423 may promote anergy by simply decreasing IgM surface expression.

As IgM surface expression can be regulated at the transcriptional, translational and post-translational levels. The relative contribution of each to IgM downregulation in tolerant B cells has been studied. In tolerant B cells, the absence of any decrease in mRNA encoding membrane type μ chains (IgM) indicates IgM reduction is not due to reduced transcription [262]. Therefore, IgM reduction occurs at translational or post-translational level [262]. Studies on the processing of newly synthesized IgM receptor demonstrated that IgM transport from the endoplasmic reticulum to the medial Golgi is blocked in tolerant B cells, leading to a rapid degradation [262]. Another mechanism of IgM downregulation is cell receptor endocytosis and subsequent degradation. E3 ubiquitin ligases play a critical role in this pathway [94]. E3 ubiquitin ligases are increased in anergic cells in a NFAT-dependent manner [263]. In response to self-antigen stimulation TCR downregulation is impaired in T cells deficient in Cbl-b, c-Cbl or both [263], indicating the role of E3 ubiquitin ligase in the decreased T cell receptor expression. Similar defects in IgM downregulation is observed in B cells lacking Cbl-b and c-Cbl [89]. It is therefore speculated that Bz-423 may increase the expression of E3 ubiquitin ligases, which may trigger IgM receptor endocytosis and result in IgM downregulation.

Bz-423 pre-treatment renders cells resistant to subsequent activation:

Anergic B cells are resistant to subsequent stimulation. In response to stimulation, anergic B cells display reduced upregulation of activation markers, including CD80(B7.1), CD86 (B7.2) and CD69 [7, 14, 17, 264, 265]. Moreover, elevated CD80 and CD86 are observed in activated B cells from lupus-prone mice NZB and NZB/NZW F1 mice, suggesting that tolerance breakdown leads to abnormal activation of self-reactive B cells [266, 267]. CD69, an activation marker for both T cells and B cells [268], was chosen to study the effect of Bz-423 pretreatment on subsequent activation. In response to stimulation induced by anti-IgM or PMA plus ionomycin, CD69 expression is moderately reduced in Bz-423-treated Ramos B cells, indicating Bz-423 pre-incubation renders cells resistant to subsequent activation. This reduction is not due to direct inhibition by Bz-423 since no reduction in CD69 was observed when cells were treated with Bz-423 and anti-IgM concurrently. In contrast, CD69 increase induced by self-antigen is totally abolished in anergic B cells [41]. As this anergic B cells also displayed impaired anti-IgM induced calcium signaling [41], it is possible CD69 increase is shut down more efficiently in these cells than Bz-423-treated cells. During activation, IκBα is degraded to activate NFκB for gene transcription for activation [260]. To confirm that Bz-423 pre-treatment inhibit subsequent activation, its effect on IκBα degradation induced by anti-IgM or PMA plus ionomycin were explored. Bz-423 pre-treatment inhibited IκBα degradation in response to activation, supporting Bz-423 suppresses further activation.

In summary, Bz-423 activates NFAT but not AP-1 and NFκB, suggesting Bz-423 might induce anergy. Bz-423 induces several anergy-associated gene changes,

downregulates IgM surface expression, and inhibits NFκB activation and CD69 upregulation in response to activation signals such as anti-IgM and PMA plus ionomycin, supporting that Bz-423 induces anergy. These findings suggest Bz-423 induces anergy in Ramos B cells. However, whether Bz-423 induces anergy *in vivo* should be further studied.

Materials and Methods

Materials: Chemicals were obtained from Sigma Aldrich unless indicated.

Cell culture: Human Burkitt's lymphoma cell line Ramos, human immature T cell line CCRF-CEM, human mature T cell line Jurkat E6.1, rat myoblastic cell line H_9C_2, and mouse immature B cell line WEHI-231 were purchased from American Type Culture Collection (ATCC). Ramos, CCRF-CEM, Jurkat E6.1 were maintained in RPMI 1640 (Mediatech) supplemented with 10% heat-inactivated fetal bovine serum (10% FBS, Mediatech), penicillin (100 U/mL), streptomycin (100 µg/mL) and L-glutamine (290 µg/mL) (1x PSG, Mediatech) in a humidified incubator (37^{o}C, 5% CO_2). H_9C_2 were cultured in ATCC-formulated Dulbecco's modified Eagle's medium (DMEM) supplemented with 10% FBS, and 1x PSG (Mediatech). And WHEI-231 cells were cultured in DMEM (ATCC) supplemented with 10% FBS, 1x PSG, non-essential amino acids (Mediatech) and 0.05 mM 2-mercaptoethanol (2-ME).

Isolation of primary lymphocytes from spleen: Spleens were first removed from C57BL/6 (B6) mice and placed in ice-cold complete DMEM containing 10% FBS. The Splenocytes were then squeezed by gentle grinding

between two frosted microscope slides. The resulting single cell suspension was filtered through a 40-μM nylon cell strainer (22363547, Fisher). Cells were collected and resuspended in red blood cells lysis buffer (R7757, Sigma) and incubated 10 min at room temperature (RT) to lysis red blood cells. After two washes with complete DMEM media, splenocytes were spun down and resuspended in 3.3 mL buffer 1 [PBS containing 0.1% (w/v) BSA, 2 mM EDTA] at a density of 10^8 cells /mL for isolation. Spleen B cells were positively selected using CD45R magnetic microbeads (114-41D, invitrogen) [269]. Briefly, 400 μL CD45R microbeads were added to 3.3 mL splenocytes and incubated for 20 min at 4^{o}C to label B cells. After washing with buffer 1, the cells were resuspended in 2 mL buffer 1 and loaded onto a pre-washed LS column (Miltenyi). The unlabelled cells pass through the column and the effluent included T cells and monocytes. B cells bind to the magnet of the column. The column was removed from the magnet and the magnetically labeled B cells were flushed out by firming pushing the plunger into the column. Both of the cell fractions were resuspended at a density of $5x10^6$ cells/mL in DMEM containing 10% FBS and rested for 1 h before treatment. The purity of T cells and B cells fraction were verified by flow cytometry using FITC-conjugated anti-CD19 (553785, BD Bioscience) and PE-conjugated anti-CD3 (555275, BD Bioscience). This procedure typically resulted in 94% pure B cells, and 70% of negatively selected splenocytes were T cells.

Isolation of resting T cells from human blood: Human PBMC were isolation by ficoll-paque plus density centrifugation according to the manufacture's instructions with minor modifications. Blood samples were diluted 1:1 with sterile

PBS and carefully layered onto ficoll-paque plus in a 50 mL conical tubes. The samples were spun at 2,200 rpm for 30 min. Four layers formed, consisting of plasma platelets, peripheral blood mononuclear cells (PBMCs), ficoll-paque plus, and granulocytes and erythrocyte from the top to bottom. The PBMCs layer was extracted and washed in ice-cold DMEM containing 10% FBS for three times. These lymphocytes were then resuspended in 14 mL PBS containing 0.5% (w/v) BSA at a density of 1.5 x 10^7 cells /mL and ready for negative T cell isolation. Briefly human PBMC was first labeled with biotinylated anti-CD19 (to remove B cells) and biotinylated anti-CD14 (to remove monocyte and macrophage) for 30 min at at 4^{o}C with gentle agitation. Then cells were washed with PBS containing 0.5% (w/v) BSA and resuspended in 14 mL PBS containing 0.5% (w/v) BSA. 1 mL pre-washed streptavidin Dynabeads was added and incubated for another 30 min at 4^{o}C. During the incubation, the biotinylated antibody-labeled cells bound to streptavidin Dynabeads. After washing, human PBMCs that bind to the beads were separated from the human PBMCs that do not bind to the beads through magnet. The cell suspension with beads-unbound human PBMCs was resuspended in 7 mL PBS containing 0.5% (w/v) BSA .Another 0.5 mL streptavidin Dynabeads was added and the above procedure was repeated to remove unwanted antibody-labeled B cells.. The beads-unbound PBMCs contained enriched human T cells. Therefore they were collected and suspended in pre-warmed DMEM media with 10% FBS. Before treatment, they were resting at 37^{o}C incubator for 1 h. The purity of T cells was increased from 65% before purification to 80% after purification based on the flow

cytometry analysis of cells stained with FITC-anti-CD3.

Treatment and inhibitor experiments: Ramos cells were pre-treated with inhibitors 30 min before Bz-423 treatment. Unless specific noted, cells were treated in media with 10% FBS to reduce the background of NFATc2 dephosphorylation induced by serum reduction. The effective concentration of inhibitors were listed below: 100 μM superoxide dismutase mimic MnTBAP, 100 μM anti-oxidant Vitamin E 500 μM extracellular Ca^{2+} chelator BAPTA salt, 0.5 μM Ca^{2+} release-activated Ca^{2+} (CRAC) channel inhibitor LY-58483, 100 nM FK506 and 100 nM Cyclosporin A.

Cell surface staining: CD69 and IgM surface expression in Ramos cells were detected using FITC-conjugated anti-human CD69 (cat# 555530, BD Bioscience) and FITC-conjugated anti-human IgM (cat#109-096-043, Jackson ImmunoResearch), respectively. At the indicated times, $0.5x10^6$ treated Ramos cells were resuspended in 100 μL staining buffer (PBS + 2% FBS + 0.02% (w/v) NaN_3) containing 2 μL of either FITC-conjugate anti-human CD69 or FITC-conjugate anti-human IgM, and incubated on ice for 30 min. After washing once with staining buffer, the FITC fluorescence was measured by FACSCalibur flow cytometry (BD Biosicence) in the FL1 channel. Data were collected and analyzed by the cellquest software. For each sample, 6000 events were recorded.

Cytosol and nuclear fractionation: At indicated times, $1x10^7$ Ramos cells were washed once with ice-cold PBS, resuspended in 200 μL ice-cold low-salt buffer (10 mM Hepes-KOH pH 7.9, 10 mM KCl, 0.2 mM EDTA, 1 mM DTT, 0.5 mM

PMSF plus protease inhibitor cocktail), and incubated on ice for 20 min. The homogenate was then centrifuged at 500x g for 10 min at 4^{o}C. The supernatant (cytosolic fraction) was removed, and the nuclear pellet was resuspended in 200 μL ice-cold high-salt buffer (20 mM Hepes-KOH pH 7.9, 400 mM NaCl, 0.2 mM EDTA, 1 mM DTT, 0.5 mM PMSF plus protease inhibitor cocktail). The nuclear fraction was vigorously vortexed for 5 min, followed by incubation on ice for another 5 min. This vortexing and ice-incubation steps were repeated for 5 times. This nuclear extract was spun down and the supernatant was saved as the nuclear fraction. The successful separation between cytosol and nuclear was confirmed by immunoblotting for cytosol-specific antibody β-tubulin and nucleus-specific antibody CREB.

Western Blot: 5x10^{6} treated cells were harvested and washed once in ice-cold PBS and lysed in 50 μL 1x WCE buffer with complete protease inhibitor cocktail. Following incubation on ice for 30 min, the supernatant was collected by centrifugation at full speed for 30 min. The protein concentration was quantified by Bradford protein assay, using BSA to make a standard curve. Equal amounts of the whole cell lysates were denatured in 30 μL total volume containing 5 μL of 6x SDS loading buffer (350 mM Tris-HCl pH 6.8, 10.28 % SDS, 36 % (v/v) glycerol, 0.6 M DTT, 0.012 % (w/v) bromophenol blue). The heated sample was loaded to Criterion^{TM} Pre-cast polyacrylamide gel from Bio-Rad. After transferring of gel to PVDF membrane (Bio-Rad), the PVDF membrane was blocked in 5% non-fat milk in Tween PBS [0.5% (v/v) tween 20 in PBS] at room temperature for 45 min. Primary antibody was incubated at 4^{o}C overnight in 1% non-fat milk Tween PBS. After 3 extensive 5

min washes in Tween PBS, secondary antibody (GE healthcare) was applied and incubated for 1 h at room temperature. The blots were detected using ECL^{TM} western blotting detection reagents (GE healthcare). The antibodies used were listed below: IκB-α (sc-847, Santa Cruz biotech), NFATc2 (4G6-G5, cat# sc-7296, Santa Cruz biotech), NFAT1 (cat# 610702, BD Bioscience), β-tubulin (Cat#T4026 Sigma-Aldrich,), GAPDH (cat# MAB374, Chemicon), For detecting NFAT dephosphorylation using anti-NFATc2 from Santa cruz biotech, to maximize the NFATc2 signaling and to minimize background, the membrane were blocked in 5% non-fat milk overnight followed by 2 h incubation with NFATc2 antibody (1:200 dilution in 1% non-fat milk Tween PBS) at room temperature.

Transient transfection and SEAP activity measurement: pNFAT-SEAP, pNFκB-SEAP, pAP1-SEAP are mammalian expression vectors (clontech) for reporting specific transcription activities, in which transcription of secreted alkaline phosphatase (SEAP) is driven by 3 copies of the NFAT response element, 4 copies of the NFκB consensus sequence or 4 copies of the AP1 enhancer respectively. $8x10^6$ cells were washed with ice-cold PBS, resuspended in 100 μL electroporation buffer T (Amaxa) containing 2 μg of the indicated reporter plasmids, and subjected to electroporation using amaxa nucleofector apparatus using program G-16. Electroporated cells were immediately transferred into media with 10% FBS and allowed to recover for 24 h. The following day, cells were resuspended in 2% FBS media for Bz-423 treatment. At the indicated time, the supernatant was harvested for the SEAP activity measurement, which was performed using the Great EscAPe SEAP

chemiluminescence kit (clontech) according to the manufacture protocol.

RNA isolation and Reverse Transcriptase-PCR (RT-PCR):`Total RNA was isolated from treated cells using the RNeasy Mini Kit (Qiagen). mRNA (2 μg) in reaction mix (100 μL) was converted to cDNA using general mRNA primer oligo $d(T)_{16}$ and the TaqMan Reverse Transcription kit (Applied Biosystems). The reverse transcription was run in a PTC100 Thermocycler (MJ Research Inc). The thermocycler program used is 25^{o}C for 10 min for the d(T)16 oligo annealing to mRNA, 48^{o}C for 30 min for extension and 95^{o}C for 5 min for inactivation. The cDNA level was measured by Applied Biosystems ABI 7700 using SYBR Green (dsDNA-specific fluorescent dye) PCR Master Mix (Applied Biosystems). The PCR was done using 40 cycles of 95^{o}C (60 s), 58 ^{o}C (30 s), 72 ^{o}C (30 s)**.** The primer information is listed in Table 3.5.

Genes	**Primer sequence**	**Product size (bp)**
IRF4	Forward: 5'-TTAATTCTCCAAGCGGATGC-3' Reverse: 5'-AAGGAATGAGGAAGCCGTTC-3'	289
ActB	Forward: 5'-GGACTTCGAGCAAGAGATGG-3' Reverse: 5'-AGCACTGTGTTGGCGTACAG-3'	234

Table 3.5: The list of Primers used for RT-PCR.

Chromatin Immunoprecipitation (ChIP) assay: Detection of binding of

NFATc2 to the *IRF4* promoter was performed by using a commercial CHIP assay kit (17-295, Millipore) following the manufacture's instructions. At indicated time, $5x10^7$ treated cells were fixed in 1% formaldehyde (37% stock) at room temperature to crosslink protein to DNA. 10 min later, the fixation was stopped by addition of 0.125 M glycerine followed by additional five min incubation at room temperature. Cells were lysed in 500 μL SDS nuclei lysis buffer on ice. 10 min later, chromatin was sheared by sonication (power 4, 20s for 3 times with 5 min interval on ice). The lysate was then collected after a brief centrifugation. It was then pre-cleared using 80 μL salmon-agarose A beads at 4^oC for 30 min. The pre-cleared lysate was immunoprecipitated using 10 μg mouse anti-NFATc2 (sc-7296x, Santa Cruz Biotech) overnight at 4^oC. After sequential one wash in low salt immune complex wash buffer, high salt immune complex wash buffer, LiCl immune complex wash buffer and two washes in TE buffer, the immune complex was eluted in 500 μL freshly-made elution buffer (1% SDS, 0.1M $NaHCO_3$). The crosslinks in the immune complex were reversed by overnight incubation at 65^oC in 0.2 M NaCl solution. Proteins were digested with 20 μg proteinase K at 45^oC for 1 h. The DNA was recovered after phenol/chloroform extraction and ethanol precipitation in the presence of 20 μg inert carrier glycogen. The DNA pellet was resuspended in 30 μL ddH_2O and was used for quantitative PCR. Input controls, representing the starting material before the immunoprecipitation, were also included. The binding of NFATc2 to *IRF4* promoter was then measured by Applied Biosystems ABI 7700 using SYBR Green (dsDNA-specific fluorescent dye) PCR Master Mix (Applied Biosystems). The PCR

cycles were 95°C (60 s), 58 °C (30 s), 72 °C (30 s) (45 cycles)**.** The primer information is listed in Table 3.6. The negative control primer was designed to flank a region of genomic DNA between the GAPDH gene and chromosome condensation-related SMC-associated protein (CNAP1) gene [187]. The PCR products were also visualized in 1.5% agarose gels.

name	sequence
IRF4 promoter primers set 1	Forward 5’ GGT TTC ACC GTG TTG GCC AGG CT-3’ Reverse: 5’-GGC TCC CTA AGG ATC CAA GTG CTT-3’
IRF4 promoter primers set 2	Forward: 5’-CCG CCC CCA TCT CTT TCA TGC TAA-3’ Reverse: 5’-CCG CGG TGT TTA GAG AAC ATC GCA-3’
IRF4 promoter primers set 3	Forward: 5’-GGC CAC ATC GCT GCA GTT TAG TGA-3’ Reverse: 5’-GGA CTT TGC AAG CCG AGA GCC T-3’
IRF4 promoter primers set 4	Forward: 5’-GCA ACC TCC ACC TCC AGT TCT CTT TG-3’ Reverse: 5’-GGG ACT GTC ACT GGG GCC GT -3’
IL-2 promoter primers set	Forward: 5’-CTT GCT CTT GTC CAC CAC AA-3’ Reverse: 5’-TGT GGC AGG AGT TGA GGT TA -3’
Negative control primers	Forward: 5′-ATGGTTGCCACTGGGGATCT-3′ Reverse: 5′-TGCCAAAGCCTAGGGGAAGA-3′
Act B primers	Forward: 5’-GGACTTCGAGCAAGAGATGG-3’ Reverse: 5’-AGCACTGTGTTGGCGTACAG-3’

Table 3.6: Primers sequence for CHIP assay.

Statement of collaboration: Dr. Jim Mobley helped to remove spleen from the mice. Lara Swanson helped in the experiment of NFAT dephosphorylation in spleen T cells and B cells. Rod Morgan helped to isolate T cells from human blood.

Bibliography

1. Goodnow, C.C. (1997). Glimpses into the balance between immunity and self-tolerance. Ciba Found Symp *204*, 190-202; discussion -7.

2. Wardemann, H., Yurasov, S., Schaefer, A., Young, J.W., Meffre, E., Nussenzweig, M.C. (2003). Predominant autoantibody production by early human B cell precursors. Science *301*, 1374-7.

3. Merrell, K.T., Benschop, R.J., Gauld, S.B., Aviszus, K., Decote-Ricardo, D., Wysocki, L.J., Cambier, J.C. (2006). Identification of anergic B cells within a wild-type repertoire. Immunity *25*, 953-62.

4. Goodnow, C.C. (1992). Transgenic mice and analysis of B-cell tolerance. Annu Rev Immunol *10*, 489-518.

5. Conrad, F.J., Rice, J.S., Cambier, J.C. (2007). Multiple paths to loss of anergy and gain of autoimmunity. Autoimmunity *40*, 418-24.

6. Hartley, S.B., Crosbie, J., Brink, R., Kantor, A.B., Basten, A., Goodnow, C.C. (1991). Elimination from peripheral lymphoid tissues of self-reactive B lymphocytes recognizing membrane-bound antigens. Nature *353*, 765-9.

7. Gauld, S.B., Benschop, R.J., Merrell, K.T., Cambier, J.C. (2005). Maintenance of B cell anergy requires constant antigen receptor occupancy and signaling. Nat Immunol *6*, 1160-7.

8. Cambier, J.C., Gauld, S.B., Merrell, K.T., Vilen, B.J. (2007). B-cell anergy: from transgenic models to naturally occurring anergic B cells? Nat Rev Immunol *7*, 633-43.

9. Barron, L., Knoechel, B., Lohr, J., Abbas, A.K. (2008). Cutting edge: contributions of apoptosis and anergy to systemic T cell tolerance. J Immunol *180*, 2762-6.

10. Goodnow, C.C., Crosbie, J., Adelstein, S., Lavoie, T.B., Smith-Gill, S.J., Brink, R.A., Pritchard-Briscoe, H., Wotherspoon, J.S., Loblay, R.H., Raphael, K., et al. (1988). Altered immunoglobulin expression and functional silencing of

self-reactive B lymphocytes in transgenic mice. Nature *334*, 676-82.

11. Erikson, J., Radic, M.Z., Camper, S.A., Hardy, R.R., Carmack, C., Weigert, M. (1991). Expression of anti-DNA immunoglobulin transgenes in non-autoimmune mice. Nature *349*, 331-4.

12. Roark, J.H., Bui, A., Nguyen, K.A., Mandik, L., Erikson, J. (1997). Persistence of functionally compromised anti-double-stranded DNA B cells in the periphery of non-autoimmune mice. Int Immunol *9*, 1615-26.

13. Nguyen, K.A., Mandik, L., Bui, A., Kavaler, J., Norvell, A., Monroe, J.G., Roark, J.H., Erikson, J. (1997). Characterization of anti-single-stranded DNA B cells in a non-autoimmune background. J Immunol *159*, 2633-44.

14. Benschop, R.J., Aviszus, K., Zhang, X., Manser, T., Cambier, J.C., Wysocki, L.J. (2001). Activation and anergy in bone marrow B cells of a novel immunoglobulin transgenic mouse that is both hapten specific and autoreactive. Immunity *14*, 33-43.

15. Culton, D.A., O'Conner, B.P., Conway, K.L., Diz, R., Rutan, J., Vilen, B.J., Clarke, S.H. (2006). Early preplasma cells define a tolerance checkpoint for autoreactive B cells. J Immunol *176*, 790-802.

16. Santulli-Marotto, S., Retter, M.W., Gee, R., Mamula, M.J., Clarke, S.H. (1998). Autoreactive B cell regulation: peripheral induction of developmental arrest by lupus-associated autoantigens. Immunity *8*, 209-19.

17. Borrero, M., Clarke, S.H. (2002). Low-affinity anti-Smith antigen B cells are regulated by anergy as opposed to developmental arrest or differentiation to B-1. J Immunol *168*, 13-21.

18. Rojas, M., Hulbert, C., Thomas, J.W. (2001). Anergy and not clonal ignorance determines the fate of B cells that recognize a physiological autoantigen. J Immunol *166*, 3194-200.

19. Ferry, H., Cornall, R.J. (2004). Analysis of B-cell immune tolerance induction using transgenic mice. Methods Mol Biol *271*, 239-60.

20. Fulcher, D.A., Basten, A. (1994). Reduced life span of anergic self-reactive B cells in a double-transgenic model. J Exp Med *179*, 125-34.

21. Spatz, L., Saenko, V., Iliev, A., Jones, L., Geskin, L., Diamond, B. (1997). Light chain usage in anti-double-stranded DNA B cell subsets: role in cell fate

determination. J Exp Med *185*, 1317-26.

22. Diz, R., McCray, S.K., Clarke, S.H. (2008). B cell receptor affinity and B cell subset identity integrate to define the effectiveness, affinity threshold, and mechanism of anergy. J Immunol *181*, 3834-40.

23. Henry, R.A., Acevedo-Suarez, C.A., Thomas, J.W. (2009). Functional silencing is initiated and maintained in immature anti-insulin B cells. J Immunol *182*, 3432-9.

24. Li, D.H., Winslow, M.M., Cao, T.M., Chen, A.H., Davis, C.R., Mellins, E.D., Utz, P.J., Crabtree, G.R., Parnes, J.R. (2008). Modulation of peripheral B cell tolerance by CD72 in a murine model. Arthritis Rheum *58*, 3192-204.

25. Reveille, J.D. (2004). Predictive value of autoantibodies for activity of systemic lupus erythematosus. Lupus *13*, 290-7.

26. Erikson, J., Mandik, L., Bui, A., Eaton, A., Noorchashm, H., Nguyen, K.A., Roark, J.H. (1998). Self-reactive B cells in nonautoimmune and autoimmune mice. Immunol Res *17*, 49-61.

27. Shlomchik, M.J., Aucoin, A.H., Pisetsky, D.S., Weigert, M.G. (1987). Structure and function of anti-DNA autoantibodies derived from a single autoimmune mouse. Proc Natl Acad Sci U S A *84*, 9150-4.

28. Mandik-Nayak, L., Seo, S.J., Sokol, C., Potts, K.M., Bui, A., Erikson, J. (1999). MRL-lpr/lpr mice exhibit a defect in maintaining developmental arrest and follicular exclusion of anti-double-stranded DNA B cells. J Exp Med *189*, 1799-814.

29. Healy, J.I., Dolmetsch, R.E., Timmerman, L.A., Cyster, J.G., Thomas, M.L., Crabtree, G.R., Lewis, R.S., Goodnow, C.C. (1997). Different nuclear signals are activated by the B cell receptor during positive versus negative signaling. Immunity *6*, 419-28.

30. Allman, D., Lindsley, R.C., DeMuth, W., Rudd, K., Shinton, S.A., Hardy, R.R. (2001). Resolution of three nonproliferative immature splenic B cell subsets reveals multiple selection points during peripheral B cell maturation. J Immunol *167*, 6834-40.

31. Gauld, S.B., Merrell, K.T., Cambier, J.C. (2006). Silencing of autoreactive B cells by anergy: a fresh perspective. Curr Opin Immunol *18*, 292-7.

32. Tough, D.F., Sprent, J. (1995). Lifespan of lymphocytes. Immunol Res *14*, 1-12.

33. Lesley, R., Xu, Y., Kalled, S.L., Hess, D.M., Schwab, S.R., Shu, H.B., Cyster, J.G. (2004). Reduced competitiveness of autoantigen-engaged B cells due to increased dependence on BAFF. Immunity *20*, 441-53.

34. Stohl, W., Xu, D., Kim, K.S., Koss, M.N., Jorgensen, T.N., Deocharan, B., Metzger, T.E., Bixler, S.A., Hong, Y.S., Ambrose, C.M., Mackay, F., Morel, L., Putterman, C., Kotzin, B.L., Kalled, S.L. (2005). BAFF overexpression and accelerated glomerular disease in mice with an incomplete genetic predisposition to systemic lupus erythematosus. Arthritis Rheum *52*, 2080-91.

35. Santulli-Marotto, S., Qian, Y., Ferguson, S., Clarke, S.H. (2001). Anti-Sm B cell differentiation in Ig transgenic MRL/Mp-lpr/lpr mice: altered differentiation and an accelerated response. J Immunol *166*, 5292-9.

36. Oliver, P.M., Vass, T., Kappler, J., Marrack, P. (2006). Loss of the proapoptotic protein, Bim, breaks B cell anergy. J Exp Med *203*, 731-41.

37. Brink, R., Goodnow, C.C., Crosbie, J., Adams, E., Eris, J., Mason, D.Y., Hartley, S.B., Basten, A. (1992). Immunoglobulin M and D antigen receptors are both capable of mediating B lymphocyte activation, deletion, or anergy after interaction with specific antigen. J Exp Med *176*, 991-1005.

38. Yamanashi, Y., Tamura, T., Kanamori, T., Yamane, H., Nariuchi, H., Yamamoto, T., Baltimore, D. (2000). Role of the rasGAP-associated docking protein p62(dok) in negative regulation of B cell receptor-mediated signaling. Genes Dev *14*, 11-6.

39. Healy, J.I., Goodnow, C.C. (1998). Positive versus negative signaling by lymphocyte antigen receptors. Annu Rev Immunol *16*, 645-70.

40. Cannons, J.L., Schwartzberg, P.L. (2004). Fine-tuning lymphocyte regulation: what's new with tyrosine kinases and phosphatases? Curr Opin Immunol *16*, 296-303.

41. Vilen, B.J., Burke, K.M., Sleater, M., Cambier, J.C. (2002). Transmodulation of BCR signaling by transduction-incompetent antigen receptors: implications for impaired signaling in anergic B cells. J Immunol *168*, 4344-51.

42. Hippen, K.L., Tze, L.E., Behrens, T.W. (2000). CD5 maintains tolerance in anergic B cells. J Exp Med *191*, 883-90.

43. Taylor, D.K., Ito, E., Thorn, M., Sundar, K., Tedder, T., Spatz, L.A. (2006). Loss of tolerance of anti-dsDNA B cells in mice overexpressing CD19. Mol Immunol *43*, 1776-90.

44. Melchers, F. (2006). Anergic B cells caught in the act. Immunity *25*, 864-7.

45. Duty, J.A., Szodoray, P., Zheng, N.Y., Koelsch, K.A., Zhang, Q., Swiatkowski, M., Mathias, M., Garman, L., Helms, C., Nakken, B., Smith, K., Farris, A.D., Wilson, P.C. (2009). Functional anergy in a subpopulation of naive B cells from healthy humans that express autoreactive immunoglobulin receptors. J Exp Med *206*, 139-51.

46. Tiller, T., Tsuiji, M., Yurasov, S., Velinzon, K., Nussenzweig, M.C., Wardemann, H. (2007). Autoreactivity in human IgG+ memory B cells. Immunity *26*, 205-13.

47. Macian, F., Im, S.H., Garcia-Cozar, F.J., Rao, A. (2004). T-cell anergy. Curr Opin Immunol *16*, 209-16.

48. Schwartz, R.H. (2003). T cell anergy. Annu Rev Immunol *21*, 305-34.

49. Hayashi, R.J., Loh, D.Y., Kanagawa, O., Wang, F. (1998). Differences between responses of naive and activated T cells to anergy induction. J Immunol *160*, 33-8.

50. Andris, F., Denanglaire, S., de Mattia, F., Urbain, J., Leo, O. (2004). Naive T cells are resistant to anergy induction by anti-CD3 antibodies. J Immunol *173*, 3201-8.

51. Davis, L.S., Lipsky, P.E. (1993). Tolerance induction of human CD4+ T cells: markedly enhanced sensitivity of memory versus naive T cells to peripheral anergy. Cell Immunol *146*, 351-61.

52. Nossal, G.J. (1993). Tolerance and ways to break it. Ann N Y Acad Sci *690*, 34-41.

53. Utting, O., Teh, S.J., Teh, H.S. (2000). A population of in vivo anergized T cells with a lower activation threshold for the induction of CD25 exhibit differential requirements in mobilization of intracellular calcium and mitogen-activated protein kinase activation. J Immunol *164*, 2881-9.

54. Tanchot, C., Guillaume, S., Delon, J., Bourgeois, C., Franzke, A., Sarukhan, A., Trautmann, A., Rocha, B. (1998). Modifications of CD8+ T cell function

during in vivo memory or tolerance induction. Immunity *8*, 581-90.

55. Gajewski, T.F., Qian, D., Fields, P., Fitch, F.W. (1994). Anergic T-lymphocyte clones have altered inositol phosphate, calcium, and tyrosine kinase signaling pathways. Proc Natl Acad Sci U S A *91*, 38-42.

56. Johnson, J.G., Jenkins, M.K. (1994). The role of anergy in peripheral T cell unresponsiveness. Life Sci *55*, 1767-80.

57. Pape, K.A., Merica, R., Mondino, A., Khoruts, A., Jenkins, M.K. (1998). Direct evidence that functionally impaired CD4+ T cells persist in vivo following induction of peripheral tolerance. J Immunol *160*, 4719-29.

58. Im, S.H., Rao, A. (2004). Activation and deactivation of gene expression by Ca2+/calcineurin-NFAT-mediated signaling. Mol Cells *18*, 1-9.

59. Brunswick, M., June, C.H., Mond, J.J. (1994). B lymphocyte immunoglobulin receptor desensitization is downstream of tyrosine kinase activation. Cell Immunol *156*, 240-4.

60. Cho, E.A., Riley, M.P., Sillman, A.L., Quill, H. (1993). Altered protein tyrosine phosphorylation in anergic Th1 cells. J Immunol *151*, 20-8.

61. Collins, S., Lutz, M.A., Zarek, P.E., Anders, R.A., Kersh, G.J., Powell, J.D. (2008). Opposing regulation of T cell function by Egr-1/NAB2 and Egr-2/Egr-3. Eur J Immunol *38*, 528-36.

62. Heissmeyer, V., Macian, F., Varma, R., Im, S.H., Garcia-Cozar, F., Horton, H.F., Byrne, M.C., Feske, S., Venuprasad, K., Gu, H., Liu, Y.C., Dustin, M.L., Rao, A. (2005). A molecular dissection of lymphocyte unresponsiveness induced by sustained calcium signalling. Novartis Found Symp *267*, 165-74; discussion 74-9.

63. Macian, F., Garcia-Cozar, F., Im, S.H., Horton, H.F., Byrne, M.C., Rao, A. (2002). Transcriptional mechanisms underlying lymphocyte tolerance. Cell *109*, 719-31.

64. Powell, J.D., Zheng, Y. (2006). Dissecting the mechanism of T-cell anergy with immunophilin ligands. Curr Opin Investig Drugs *7*, 1002-7.

65. Korb, L.C., Mirshahidi, S., Ramyar, K., Sadighi Akha, A.A., Sadegh-Nasseri, S. (1999). Induction of T cell anergy by low numbers of agonist ligands. J Immunol *162*, 6401-9.

66. Kimura, M., Yamashita, M., Kubo, M., Iwashima, M., Shimizu, C., Tokoyoda, K., Chiba, J., Taniguchi, M., Katsumata, M., Nakayama, T. (2000). Impaired Ca/calcineurin pathway in in vivo anergized CD4 T cells. Int Immunol *12*, 817-24.

67. Barrington, R.A., Borde, M., Rao, A., Carroll, M.C. (2006). Involvement of NFAT1 in B cell self-tolerance. J Immunol *177*, 1510-5.

68. Soto-Nieves, N., Puga, I., Abe, B.T., Bandyopadhyay, S., Baine, I., Rao, A., Macian, F. (2009). Transcriptional complexes formed by NFAT dimers regulate the induction of T cell tolerance. J Exp Med

69. Yuh, K., Siminovitch, K.A., Ochi, A. (1993). T cell anergy is programmed early after exposure to bacterial superantigen in vivo. Int Immunol *5*, 1375-82.

70. Schwartz, R.H. (1990). A cell culture model for T lymphocyte clonal anergy. Science *248*, 1349-56.

71. Glynne, R., Ghandour, G., Rayner, J., Mack, D.H., Goodnow, C.C. (2000). B-lymphocyte quiescence, tolerance and activation as viewed by global gene expression profiling on microarrays. Immunol Rev *176*, 216-46.

72. Bandyopadhyay, S., Soto-Nieves, N., Macian, F. (2007). Transcriptional regulation of T cell tolerance. Semin Immunol *19*, 180-7.

73. Glynne, R., Akkaraju, S., Healy, J.I., Rayner, J., Goodnow, C.C., Mack, D.H. (2000). How self-tolerance and the immunosuppressive drug FK506 prevent B-cell mitogenesis. Nature *403*, 672-6.

74. Zheng, Y., Zha, Y., Gajewski, T.F. (2008). Molecular regulation of T-cell anergy. EMBO Rep *9*, 50-5.

75. Lin, A.E., Mak, T.W. (2007). The role of E3 ligases in autoimmunity and the regulation of autoreactive T cells. Curr Opin Immunol *19*, 665-73.

76. Pickart, C.M. (2001). Mechanisms underlying ubiquitination. Annu Rev Biochem *70*, 503-33.

77. Heissmeyer, V., Macian, F., Im, S.H., Varma, R., Feske, S., Venuprasad, K., Gu, H., Liu, Y.C., Dustin, M.L., Rao, A. (2004). Calcineurin imposes T cell unresponsiveness through targeted proteolysis of signaling proteins. Nat Immunol *5*, 255-65.

78. Jeon, M.S., Atfield, A., Venuprasad, K., Krawczyk, C., Sarao, R., Elly, C., Yang, C., Arya, S., Bachmaier, K., Su, L., Bouchard, D., Jones, R., Gronski, M., Ohashi, P., Wada, T., Bloom, D., Fathman, C.G., Liu, Y.C., Penninger, J.M. (2004). Essential role of the E3 ubiquitin ligase Cbl-b in T cell anergy induction. Immunity *21*, 167-77.

79. Seroogy, C.M., Soares, L., Ranheim, E.A., Su, L., Holness, C., Bloom, D., Fathman, C.G. (2004). The gene related to anergy in lymphocytes, an E3 ubiquitin ligase, is necessary for anergy induction in CD4 T cells. J Immunol *173*, 79-85.

80. Anandasabapathy, N., Ford, G.S., Bloom, D., Holness, C., Paragas, V., Seroogy, C., Skrenta, H., Hollenhorst, M., Fathman, C.G., Soares, L. (2003). GRAIL: an E3 ubiquitin ligase that inhibits cytokine gene transcription is expressed in anergic CD4+ T cells. Immunity *18*, 535-47.

81. Thomas, R.M., Chunder, N., Chen, C., Umetsu, S.E., Winandy, S., Wells, A.D. (2007). Ikaros enforces the costimulatory requirement for IL2 gene expression and is required for anergy induction in CD4+ T lymphocytes. J Immunol *179*, 7305-15.

82. Bandyopadhyay, S., Dure, M., Paroder, M., Soto-Nieves, N., Puga, I., Macian, F. (2007). Interleukin 2 gene transcription is regulated by Ikaros-induced changes in histone acetylation in anergic T cells. Blood *109*, 2878-86.

83. Eberhard, D., Jimenez, G., Heavey, B., Busslinger, M. (2000). Transcriptional repression by Pax5 (BSAP) through interaction with corepressors of the Groucho family. Embo J *19*, 2292-303.

84. Olenchock, B.A., Guo, R., Carpenter, J.H., Jordan, M., Topham, M.K., Koretzky, G.A., Zhong, X.P. (2006). Disruption of diacylglycerol metabolism impairs the induction of T cell anergy. Nat Immunol *7*, 1174-81.

85. Zha, Y., Marks, R., Ho, A.W., Peterson, A.C., Janardhan, S., Brown, I., Praveen, K., Stang, S., Stone, J.C., Gajewski, T.F. (2006). T cell anergy is reversed by active Ras and is regulated by diacylglycerol kinase-alpha. Nat Immunol *7*, 1166-73.

86. Safford, M., Collins, S., Lutz, M.A., Allen, A., Huang, C.T., Kowalski, J., Blackford, A., Horton, M.R., Drake, C., Schwartz, R.H., Powell, J.D. (2005). Egr-2 and Egr-3 are negative regulators of T cell activation. Nat Immunol *6*, 472-80.

87. Harris, J.E., Bishop, K.D., Phillips, N.E., Mordes, J.P., Greiner, D.L., Rossini, A.A., Czech, M.P. (2004). Early growth response gene-2, a zinc-finger transcription factor, is required for full induction of clonal anergy in CD4+ T cells. J Immunol *173*, 7331-8.

88. Sela, U., Dayan, M., Hershkoviz, R., Lider, O., Mozes, E. (2008). A peptide that ameliorates lupus up-regulates the diminished expression of early growth response factors 2 and 3. J Immunol *180*, 1584-91.

89. Kitaura, Y., Jang, I.K., Wang, Y., Han, Y.C., Inazu, T., Cadera, E.J., Schlissel, M., Hardy, R.R., Gu, H. (2007). Control of the B cell-intrinsic tolerance programs by ubiquitin ligases Cbl and Cbl-b. Immunity *26*, 567-78.

90. Mueller, D.L. (2004). E3 ubiquitin ligases as T cell anergy factors. Nat Immunol *5*, 883-90.

91. Siegel, J.N., Egerton, M., Phillips, A.F., Samelson, L.E. (1991). Multiple signal transduction pathways activated through the T cell receptor for antigen. Semin Immunol *3*, 325-34.

92. Marsland, B.J., Kopf, M. (2008). T-cell fate and function: PKC-theta and beyond. Trends Immunol *29*, 179-85.

93. Marmor, M.D., Yarden, Y. (2004). Role of protein ubiquitylation in regulating endocytosis of receptor tyrosine kinases. Oncogene *23*, 2057-70.

94. Naramura, M., Jang, I.K., Kole, H., Huang, F., Haines, D., Gu, H. (2002). c-Cbl and Cbl-b regulate T cell responsiveness by promoting ligand-induced TCR down-modulation. Nat Immunol *3*, 1192-9.

95. Anderson, P.O., Manzo, B.A., Sundstedt, A., Minaee, S., Symonds, A., Khalid, S., Rodriguez-Cabezas, M.E., Nicolson, K., Li, S., Wraith, D.C., Wang, P. (2006). Persistent antigenic stimulation alters the transcription program in T cells, resulting in antigen-specific tolerance. Eur J Immunol *36*, 1374-85.

96. Akdis, C.A., Akdis, M. (2009). Mechanisms and treatment of allergic disease in the big picture of regulatory T cells. J Allergy Clin Immunol *123*, 735-46; quiz 47-8.

97. Mays, L.E., Chen, Y.H. (2007). Maintaining immunological tolerance with Foxp3. Cell Res *17*, 904-18.

98. Wu, Y., Borde, M., Heissmeyer, V., Feuerer, M., Lapan, A.D., Stroud, J.C.,

Bates, D.L., Guo, L., Han, A., Ziegler, S.F., Mathis, D., Benoist, C., Chen, L., Rao, A. (2006). FOXP3 controls regulatory T cell function through cooperation with NFAT. Cell *126*, 375-87.

99. Bopp, T., Palmetshofer, A., Serfling, E., Heib, V., Schmitt, S., Richter, C., Klein, M., Schild, H., Schmitt, E., Stassen, M. (2005). NFATc2 and NFATc3 transcription factors play a crucial role in suppression of CD4+ T lymphocytes by CD4+ CD25+ regulatory T cells. J Exp Med *201*, 181-7.

100. McCaffrey, P.G., Luo, C., Kerppola, T.K., Jain, J., Badalian, T.M., Ho, A.M., Burgeon, E., Lane, W.S., Lambert, J.N., Curran, T., et al. (1993). Isolation of the cyclosporin-sensitive T cell transcription factor NFATp. Science *262*, 750-4.

101. Masuda, E.S., Naito, Y., Tokumitsu, H., Campbell, D., Saito, F., Hannum, C., Arai, K., Arai, N. (1995). NFATx, a novel member of the nuclear factor of activated T cells family that is expressed predominantly in the thymus. Mol Cell Biol *15*, 2697-706.

102. Ho, S.N., Thomas, D.J., Timmerman, L.A., Li, X., Francke, U., Crabtree, G.R. (1995). NFATc3, a lymphoid-specific NFATc family member that is calcium-regulated and exhibits distinct DNA binding specificity. J Biol Chem *270*, 19898-907.

103. Northrop, J.P., Ho, S.N., Chen, L., Thomas, D.J., Timmerman, L.A., Nolan, G.P., Admon, A., Crabtree, G.R. (1994). NF-AT components define a family of transcription factors targeted in T-cell activation. Nature *369*, 497-502.

104. Hogan, P.G., Chen, L., Nardone, J., Rao, A. (2003). Transcriptional regulation by calcium, calcineurin, and NFAT. Genes Dev *17*, 2205-32.

105. Chuvpilo, S., Zimmer, M., Kerstan, A., Glockner, J., Avots, A., Escher, C., Fischer, C., Inashkina, I., Jankevics, E., Berberich-Siebelt, F., Schmitt, E., Serfling, E. (1999). Alternative polyadenylation events contribute to the induction of NF-ATc in effector T cells. Immunity *10*, 261-9.

106. Zhou, B., Cron, R.Q., Wu, B., Genin, A., Wang, Z., Liu, S., Robson, P., Baldwin, H.S. (2002). Regulation of the murine Nfatc1 gene by NFATc2. J Biol Chem *277*, 10704-11.

107. Amasaki, Y., Masuda, E.S., Imamura, R., Arai, K., Arai, N. (1998). Distinct NFAT family proteins are involved in the nuclear NFAT-DNA binding complexes from human thymocyte subsets. J Immunol *160*, 2324-33.

108. van Rooij, E., Doevendans, P.A., de Theije, C.C., Babiker, F.A., Molkentin, J.D., de Windt, L.J. (2002). Requirement of nuclear factor of activated T-cells in calcineurin-mediated cardiomyocyte hypertrophy. J Biol Chem *277*, 48617-26.

109. Lee, M., Park, J. (2006). Regulation of NFAT activation: a potential therapeutic target for immunosuppression. Mol Cells *22*, 1-7.

110. Gwack, Y., Feske, S., Srikanth, S., Hogan, P.G., Rao, A. (2007). Signalling to transcription: store-operated Ca2+ entry and NFAT activation in lymphocytes. Cell Calcium *42*, 145-56.

111. Okamura, H., Aramburu, J., Garcia-Rodriguez, C., Viola, J.P., Raghavan, A., Tahiliani, M., Zhang, X., Qin, J., Hogan, P.G., Rao, A. (2000). Concerted dephosphorylation of the transcription factor NFAT1 induces a conformational switch that regulates transcriptional activity. Mol Cell *6*, 539-50.

112. Macian, F., Lopez-Rodriguez, C., Rao, A. (2001). Partners in transcription: NFAT and AP-1. Oncogene *20*, 2476-89.

113. Zayzafoon, M. (2006). Calcium/calmodulin signaling controls osteoblast growth and differentiation. J Cell Biochem *97*, 56-70.

114. Rao, A., Luo, C., Hogan, P.G. (1997). Transcription factors of the NFAT family: regulation and function. Annu Rev Immunol *15*, 707-47.

115. Weiss, A., Littman, D.R. (1994). Signal transduction by lymphocyte antigen receptors. Cell *76*, 263-74.

116. Loh, C., Carew, J.A., Kim, J., Hogan, P.G., Rao, A. (1996). T-cell receptor stimulation elicits an early phase of activation and a later phase of deactivation of the transcription factor NFAT1. Mol Cell Biol *16*, 3945-54.

117. Loh, C., Shaw, K.T., Carew, J., Viola, J.P., Luo, C., Perrino, B.A., Rao, A. (1996). Calcineurin binds the transcription factor NFAT1 and reversibly regulates its activity. J Biol Chem *271*, 10884-91.

118. Shaw, K.T., Ho, A.M., Raghavan, A., Kim, J., Jain, J., Park, J., Sharma, S., Rao, A., Hogan, P.G. (1995). Immunosuppressive drugs prevent a rapid dephosphorylation of transcription factor NFAT1 in stimulated immune cells. Proc Natl Acad Sci U S A *92*, 11205-9.

119. Ruff, V.A., Leach, K.L. (1995). Direct demonstration of NFATp

dephosphorylation and nuclear localization in activated HT-2 cells using a specific NFATp polyclonal antibody. J Biol Chem *270*, 22602-7.

120. Okamura, H., Garcia-Rodriguez, C., Martinson, H., Qin, J., Virshup, D.M., Rao, A. (2004). A conserved docking motif for CK1 binding controls the nuclear localization of NFAT1. Mol Cell Biol *24*, 4184-95.

121. Gwack, Y., Sharma, S., Nardone, J., Tanasa, B., Iuga, A., Srikanth, S., Okamura, H., Bolton, D., Feske, S., Hogan, P.G., Rao, A. (2006). A genome-wide Drosophila RNAi screen identifies DYRK-family kinases as regulators of NFAT. Nature *441*, 646-50.

122. Hilioti, Z., Cunningham, K.W. (2003). The RCN family of calcineurin regulators. Biochem Biophys Res Commun *311*, 1089-93.

123. Lai, M.M., Burnett, P.E., Wolosker, H., Blackshaw, S., Snyder, S.H. (1998). Cain, a novel physiologic protein inhibitor of calcineurin. J Biol Chem *273*, 18325-31.

124. Coghlan, V.M., Perrino, B.A., Howard, M., Langeberg, L.K., Hicks, J.B., Gallatin, W.M., Scott, J.D. (1995). Association of protein kinase A and protein phosphatase 2B with a common anchoring protein. Science *267*, 108-11.

125. Lin, X., Sikkink, R.A., Rusnak, F., Barber, D.L. (1999). Inhibition of calcineurin phosphatase activity by a calcineurin B homologous protein. J Biol Chem *274*, 36125-31.

126. Fiedler, B., Wollert, K.C. (2004). Interference of antihypertrophic molecules and signaling pathways with the Ca2+-calcineurin-NFAT cascade in cardiac myocytes. Cardiovasc Res *63*, 450-7.

127. Sanna, B., Brandt, E.B., Kaiser, R.A., Pfluger, P., Witt, S.A., Kimball, T.R., van Rooij, E., De Windt, L.J., Rothenberg, M.E., Tschop, M.H., Benoit, S.C., Molkentin, J.D. (2006). Modulatory calcineurin-interacting proteins 1 and 2 function as calcineurin facilitators in vivo. Proc Natl Acad Sci U S A *103*, 7327-32.

128. Ryeom, S., Greenwald, R.J., Sharpe, A.H., McKeon, F. (2003). The threshold pattern of calcineurin-dependent gene expression is altered by loss of the endogenous inhibitor calcipressin. Nat Immunol *4*, 874-81.

129. Parekh, A.B. (2003). Store-operated Ca2+ entry: dynamic interplay between endoplasmic reticulum, mitochondria and plasma membrane. J Physiol *547*,

333-48.

130. Lewis, R.S. (2001). Calcium signaling mechanisms in T lymphocytes. Annu Rev Immunol *19*, 497-521.

131. Feske, S., Muller, J.M., Graf, D., Kroczek, R.A., Drager, R., Niemeyer, C., Baeuerle, P.A., Peter, H.H., Schlesier, M. (1996). Severe combined immunodeficiency due to defective binding of the nuclear factor of activated T cells in T lymphocytes of two male siblings. Eur J Immunol *26*, 2119-26.

132. Le Deist, F., Hivroz, C., Partiseti, M., Thomas, C., Buc, H.A., Oleastro, M., Belohradsky, B., Choquet, D., Fischer, A. (1995). A primary T-cell immunodeficiency associated with defective transmembrane calcium influx. Blood *85*, 1053-62.

133. Partiseti, M., Le Deist, F., Hivroz, C., Fischer, A., Korn, H., Choquet, D. (1994). The calcium current activated by T cell receptor and store depletion in human lymphocytes is absent in a primary immunodeficiency. J Biol Chem *269*, 32327-35.

134. Feske, S., Gwack, Y., Prakriya, M., Srikanth, S., Puppel, S.H., Tanasa, B., Hogan, P.G., Lewis, R.S., Daly, M., Rao, A. (2006). A mutation in Orai1 causes immune deficiency by abrogating CRAC channel function. Nature *441*, 179-85.

135. Vig, M., Peinelt, C., Beck, A., Koomoa, D.L., Rabah, D., Koblan-Huberson, M., Kraft, S., Turner, H., Fleig, A., Penner, R., Kinet, J.P. (2006). CRACM1 is a plasma membrane protein essential for store-operated Ca2+ entry. Science *312*, 1220-3.

136. Zhang, S.L., Yeromin, A.V., Zhang, X.H., Yu, Y., Safrina, O., Penna, A., Roos, J., Stauderman, K.A., Cahalan, M.D. (2006). Genome-wide RNAi screen of Ca(2+) influx identifies genes that regulate Ca(2+) release-activated Ca(2+) channel activity. Proc Natl Acad Sci U S A *103*, 9357-62.

137. Roos, J., DiGregorio, P.J., Yeromin, A.V., Ohlsen, K., Lioudyno, M., Zhang, S., Safrina, O., Kozak, J.A., Wagner, S.L., Cahalan, M.D., Velicelebi, G., Stauderman, K.A. (2005). STIM1, an essential and conserved component of store-operated Ca2+ channel function. J Cell Biol *169*, 435-45.

138. Liou, J., Kim, M.L., Heo, W.D., Jones, J.T., Myers, J.W., Ferrell, J.E., Jr., Meyer, T. (2005). STIM is a Ca2+ sensor essential for Ca2+-store-depletion-triggered Ca2+ influx. Curr Biol *15*, 1235-41.

139. Oh-hora, M., Rao, A. (2008). Calcium signaling in lymphocytes. Curr Opin Immunol *20*, 250-8.

140. Salido, G.M., Sage, S.O., Rosado, J.A. (2009). TRPC channels and store-operated Ca(2+) entry. Biochim Biophys Acta *1793*, 223-30.

141. Vig, M., Kinet, J.P. (2007). The long and arduous road to CRAC. Cell Calcium *42*, 157-62.

142. Ambudkar, I.S., Ong, H.L., Liu, X., Bandyopadhyay, B.C., Cheng, K.T. (2007). TRPC1: the link between functionally distinct store-operated calcium channels. Cell Calcium *42*, 213-23.

143. Ishikawa, J., Ohga, K., Yoshino, T., Takezawa, R., Ichikawa, A., Kubota, H., Yamada, T. (2003). A pyrazole derivative, YM-58483, potently inhibits store-operated sustained Ca2+ influx and IL-2 production in T lymphocytes. J Immunol *170*, 4441-9.

144. Zitt, C., Strauss, B., Schwarz, E.C., Spaeth, N., Rast, G., Hatzelmann, A., Hoth, M. (2004). Potent inhibition of Ca2+ release-activated Ca2+ channels and T-lymphocyte activation by the pyrazole derivative BTP2. J Biol Chem *279*, 12427-37.

145. He, L.P., Hewavitharana, T., Soboloff, J., Spassova, M.A., Gill, D.L. (2005). A functional link between store-operated and TRPC channels revealed by the 3,5-bis(trifluoromethyl)pyrazole derivative, BTP2. J Biol Chem *280*, 10997-1006.

146. Serfling, E., Avots, A., Neumann, M. (1995). The architecture of the interleukin-2 promoter: a reflection of T lymphocyte activation. Biochim Biophys Acta *1263*, 181-200.

147. Boise, L.H., Petryniak, B., Mao, X., June, C.H., Wang, C.Y., Lindsten, T., Bravo, R., Kovary, K., Leiden, J.M., Thompson, C.B. (1993). The NFAT-1 DNA binding complex in activated T cells contains Fra-1 and JunB. Mol Cell Biol *13*, 1911-9.

148. Macian, F., Garcia-Rodriguez, C., Rao, A. (2000). Gene expression elicited by NFAT in the presence or absence of cooperative recruitment of Fos and Jun. Embo J *19*, 4783-95.

149. Savignac, M., Mellstrom, B., Naranjo, J.R. (2007). Calcium-dependent transcription of cytokine genes in T lymphocytes. Pflugers Arch *454*, 523-33.

150. Macian, F. (2005). NFAT proteins: key regulators of T-cell development and function. Nat Rev Immunol *5*, 472-84.

151. Lipskaia, L., Lompre, A.M. (2004). Alteration in temporal kinetics of Ca2+ signaling and control of growth and proliferation. Biol Cell *96*, 55-68.

152. Kuklina, E.M., Shirshev, S.V. (2001). Role of transcription factor NFAT in the immune response. Biochemistry (Mosc) *66*, 467-75.

153. Baksh, S., Widlund, H.R., Frazer-Abel, A.A., Du, J., Fosmire, S., Fisher, D.E., DeCaprio, J.A., Modiano, J.F., Burakoff, S.J. (2002). NFATc2-mediated repression of cyclin-dependent kinase 4 expression. Mol Cell *10*, 1071-81.

154. Viola, J.P., Carvalho, L.D., Fonseca, B.P., Teixeira, L.K. (2005). NFAT transcription factors: from cell cycle to tumor development. Braz J Med Biol Res *38*, 335-44.

155. Baumann, G., Zenke, G., Wenger, R., Hiestand, P., Quesniaux, V., Andersen, E., Schreier, M.H. (1992). Molecular mechanisms of immunosuppression. J Autoimmun *5 Suppl A*, 67-72.

156. Zhang, B.W., Zimmer, G., Chen, J., Ladd, D., Li, E., Alt, F.W., Wiederrecht, G., Cryan, J., O'Neill, E.A., Seidman, C.E., Abbas, A.K., Seidman, J.G. (1996). T cell responses in calcineurin A alpha-deficient mice. J Exp Med *183*, 413-20.

157. Bueno, O.F., Brandt, E.B., Rothenberg, M.E., Molkentin, J.D. (2002). Defective T cell development and function in calcineurin A beta -deficient mice. Proc Natl Acad Sci U S A *99*, 9398-403.

158. Winslow, M.M., Gallo, E.M., Neilson, J.R., Crabtree, G.R. (2006). The calcineurin phosphatase complex modulates immunogenic B cell responses. Immunity *24*, 141-52.

159. de la Pompa, J.L., Timmerman, L.A., Takimoto, H., Yoshida, H., Elia, A.J., Samper, E., Potter, J., Wakeham, A., Marengere, L., Langille, B.L., Crabtree, G.R., Mak, T.W. (1998). Role of the NF-ATc transcription factor in morphogenesis of cardiac valves and septum. Nature *392*, 182-6.

160. Yoshida, H., Nishina, H., Takimoto, H., Marengere, L.E., Wakeham, A.C., Bouchard, D., Kong, Y.Y., Ohteki, T., Shahinian, A., Bachmann, M., Ohashi, P.S., Penninger, J.M., Crabtree, G.R., Mak, T.W. (1998). The transcription factor NF-ATc1 regulates lymphocyte proliferation and Th2 cytokine production. Immunity *8*, 115-24.

161. Xanthoudakis, S., Viola, J.P., Shaw, K.T., Luo, C., Wallace, J.D., Bozza, P.T., Luk, D.C., Curran, T., Rao, A. (1996). An enhanced immune response in mice lacking the transcription factor NFAT1. Science *272*, 892-5.

162. Hodge, M.R., Ranger, A.M., Charles de la Brousse, F., Hoey, T., Grusby, M.J., Glimcher, L.H. (1996). Hyperproliferation and dysregulation of IL-4 expression in NF-ATp-deficient mice. Immunity *4*, 397-405.

163. Oukka, M., Ho, I.C., de la Brousse, F.C., Hoey, T., Grusby, M.J., Glimcher, L.H. (1998). The transcription factor NFAT4 is involved in the generation and survival of T cells. Immunity *9*, 295-304.

164. Graef, I.A., Chen, F., Chen, L., Kuo, A., Crabtree, G.R. (2001). Signals transduced by Ca(2+)/calcineurin and NFATc3/c4 pattern the developing vasculature. Cell *105*, 863-75.

165. Ranger, A.M., Oukka, M., Rengarajan, J., Glimcher, L.H. (1998). Inhibitory function of two NFAT family members in lymphoid homeostasis and Th2 development. Immunity *9*, 627-35.

166. Peng, S.L., Gerth, A.J., Ranger, A.M., Glimcher, L.H. (2001). NFATc1 and NFATc2 together control both T and B cell activation and differentiation. Immunity *14*, 13-20.

167. Ranger, A.M., Hodge, M.R., Gravallese, E.M., Oukka, M., Davidson, L., Alt, F.W., de la Brousse, F.C., Hoey, T., Grusby, M., Glimcher, L.H. (1998). Delayed lymphoid repopulation with defects in IL-4-driven responses produced by inactivation of NF-ATc. Immunity *8*, 125-34.

168. Jiang, H., Xiong, F., Kong, S., Ogawa, T., Kobayashi, M., Liu, J.O. (1997). Distinct tissue and cellular distribution of two major isoforms of calcineurin. Mol Immunol *34*, 663-9.

169. Chuvpilo, S., Jankevics, E., Tyrsin, D., Akimzhanov, A., Moroz, D., Jha, M.K., Schulze-Luehrmann, J., Santner-Nanan, B., Feoktistova, E., Konig, T., Avots, A., Schmitt, E., Berberich-Siebelt, F., Schimpl, A., Serfling, E. (2002). Autoregulation of NFATc1/A expression facilitates effector T cells to escape from rapid apoptosis. Immunity *16*, 881-95.

170. Samanta, D.N., Palmetshofer, A., Marinkovic, D., Wirth, T., Serfling, E., Nitschke, L. (2005). B cell hyperresponsiveness and expansion of mature follicular B cells but not of marginal zone B cells in NFATc2/c3 double-deficient mice. J Immunol *174*, 4797-802.

171. Boitano, A., Ellman, J.A., Glick, G.D., Opipari, A.W., Jr. (2003). The proapoptotic benzodiazepine Bz-423 affects the growth and survival of malignant B cells. Cancer Res *63*, 6870-6.

172. Mishra, S., Mishra, J.P., Gee, K., McManus, D.C., LaCasse, E.C., Kumar, A. (2005). Distinct role of calmodulin and calmodulin-dependent protein kinase-II in lipopolysaccharide and tumor necrosis factor-alpha-mediated suppression of apoptosis and antiapoptotic c-IAP2 gene expression in human monocytic cells. J Biol Chem *280*, 37536-46.

173. Marafioti, T., Pozzobon, M., Hansmann, M.L., Ventura, R., Pileri, S.A., Roberton, H., Gesk, S., Gaulard, P., Barth, T.F., Du, M.Q., Leoncini, L., Moller, P., Natkunam, Y., Siebert, R., Mason, D.Y. (2005). The NFATc1 transcription factor is widely expressed in white cells and translocates from the cytoplasm to the nucleus in a subset of human lymphomas. Br J Haematol *128*, 333-42.

174. Gomez del Arco, P., Martinez-Martinez, S., Maldonado, J.L., Ortega-Perez, I., Redondo, J.M. (2000). A role for the p38 MAP kinase pathway in the nuclear shuttling of NFATp. J Biol Chem *275*, 13872-8.

175. Yang, T. 1994. In *Clontechniques IX*, pp. 1-5

176. Cullen, B.R., Malim, M.H. (1992). Secreted placental alkaline phosphatase as a eukaryotic reporter gene. Methods Enzymol *216*, 362-8.

177. Noguchi, H., Matsushita, M., Okitsu, T., Moriwaki, A., Tomizawa, K., Kang, S., Li, S.T., Kobayashi, N., Matsumoto, S., Tanaka, K., Tanaka, N., Matsui, H. (2004). A new cell-permeable peptide allows successful allogeneic islet transplantation in mice. Nat Med *10*, 305-9.

178. Truneh, A., Albert, F., Golstein, P., Schmitt-Verhulst, A.M. (1985). Early steps of lymphocyte activation bypassed by synergy between calcium ionophores and phorbol ester. Nature *313*, 318-20.

179. Fiering, S., Northrop, J.P., Nolan, G.P., Mattila, P.S., Crabtree, G.R., Herzenberg, L.A. (1990). Single cell assay of a transcription factor reveals a threshold in transcription activated by signals emanating from the T-cell antigen receptor. Genes Dev *4*, 1823-34.

180. Aramburu, J., Yaffe, M.B., Lopez-Rodriguez, C., Cantley, L.C., Hogan, P.G., Rao, A. (1999). Affinity-driven peptide selection of an NFAT inhibitor more selective than cyclosporin A. Science *285*, 2129-33.

181. Westwick, J.K., Weitzel, C., Minden, A., Karin, M., Brenner, D.A. (1994). Tumor necrosis factor alpha stimulates AP-1 activity through prolonged activation of the c-Jun kinase. J Biol Chem *269*, 26396-401.

182. Shin, Y., Yoon, S.H., Choe, E.Y., Cho, S.H., Woo, C.H., Rho, J.Y., Kim, J.H. (2007). PMA-induced up-regulation of MMP-9 is regulated by a PKCalpha-NF-kappaB cascade in human lung epithelial cells. Exp Mol Med *39*, 97-105.

183. Serafini, A.T., Lewis, R.S., Clipstone, N.A., Bram, R.J., Fanger, C., Fiering, S., Herzenberg, L.A., Crabtree, G.R. (1995). Isolation of mutant T lymphocytes with defects in capacitative calcium entry. Immunity *3*, 239-50.

184. Sundberg, T.B., Ney, G.M., Subramanian, C., Opipari, A.W., Jr., Glick, G.D. (2006). The immunomodulatory benzodiazepine Bz-423 inhibits B-cell proliferation by targeting c-myc protein for rapid and specific degradation. Cancer Res *66*, 1775-82.

185. Biosystems, A. 2008. The comparative C_T method. In Guide to Performing Relative Quantitation of Gene Expression Using Real-Time Quantative PCR. pp. 52-9

186. Sharma, S., Grandvaux, N., Mamane, Y., Genin, P., Azimi, N., Waldmann, T., Hiscott, J. (2002). Regulation of IFN regulatory factor 4 expression in human T cell leukemia virus-I-transformed T cells. J Immunol *169*, 3120-30.

187. Harvey, E.J., Li, N., Ramji, D.P. (2007). Critical role for casein kinase 2 and phosphoinositide-3-kinase in the interferon-gamma-induced expression of monocyte chemoattractant protein-1 and other key genes implicated in atherosclerosis. Arterioscler Thromb Vasc Biol *27*, 806-12.

188. Gong, Y., Sohn, H., Xue, L., Firestone, G.L., Bjeldanes, L.F. (2006). 3,3'-Diindolylmethane is a novel mitochondrial H(+)-ATP synthase inhibitor that can induce p21(Cip1/Waf1) expression by induction of oxidative stress in human breast cancer cells. Cancer Res *66*, 4880-7.

189. Zheng, J., Ramirez, V.D. (2000). Inhibition of mitochondrial proton F0F1-ATPase/ATP synthase by polyphenolic phytochemicals. Br J Pharmacol *130*, 1115-23.

190. Cleary, J., Johnson, K.M., Opipari, A.W., Jr., Glick, G.D. (2007). Inhibition of the mitochondrial F1F0-ATPase by ligands of the peripheral benzodiazepine receptor. Bioorg Med Chem Lett *17*, 1667-70.

191. Brezski, R.J., Monroe, J.G. (2008). B-cell receptor. Adv Exp Med Biol *640*, 12-21.

192. Fields, P., Fitch, F.W., Gajewski, T.F. (1996). Control of T lymphocyte signal transduction through clonal anergy. J Mol Med *74*, 673-83.

193. Francis, T.M., Sundberg, T.B., Cleary, J., Groendyke, T., Opipari, A.W., Jr., Glick, G.D. (2006). Identification of cytotoxic, T-cell-selective 1,4-benzodiazepine-2,5-diones. Bioorg Med Chem Lett *16*, 2423-7.

194. Sasaki, Y., Schmidt-Supprian, M., Derudder, E., Rajewsky, K. (2007). Role of NFkappaB signaling in normal and malignant B cell development. Adv Exp Med Biol *596*, 149-54.

195. Li, Z.W., Omori, S.A., Labuda, T., Karin, M., Rickert, R.C. (2003). IKK beta is required for peripheral B cell survival and proliferation. J Immunol *170*, 4630-7.

196. Shambharkar, P.B., Blonska, M., Pappu, B.P., Li, H., You, Y., Sakurai, H., Darnay, B.G., Hara, H., Penninger, J., Lin, X. (2007). Phosphorylation and ubiquitination of the IkappaB kinase complex by two distinct signaling pathways. Embo J *26*, 1794-805.

197. Li, X., Stark, G.R. (2002). NFkappaB-dependent signaling pathways. Exp Hematol *30*, 285-96.

198. Davis, R.J. (1999). Signal transduction by the c-Jun N-terminal kinase. Biochem Soc Symp *64*, 1-12.

199. Kumar, K.R., Mohan, C. (2008). Understanding B-cell tolerance through the use of immunoglobulin transgenic models. Immunol Res *40*, 208-23.

200. Moon, K.Y., Hahn, B.S., Lee, J., Kim, Y.S. (2001). A cell-based assay system for monitoring NF-kappaB activity in human HaCat transfectant cells. Anal Biochem *292*, 17-21.

201. Migita, K., Miyashita, T., Maeda, Y., Aoyagi, T., Kawabe, Y., Nakamura, M., Yatsuhashi, H., Ishibashi, H., Eguchi, K. (2005). FK506 suppresses the stimulation of matrix metalloproteinase 13 synthesis by interleukin-1beta in rheumatoid synovial fibroblasts. Immunol Lett *98*, 194-9.

202. Goodnow, C.C., Crosbie, J., Jorgensen, H., Brink, R.A., Basten, A. (1989). Induction of self-tolerance in mature peripheral B lymphocytes. Nature *342*,

385-91.

203. Liu, X., Shen, S., Manser, T. (2009). Influence of B cell antigen receptor expression level on pathways of B cell tolerance induction. J Immunol *182*, 398-407.

204. Howe, C.J., LaHair, M.M., Robinson, P.J., Rodriguez-Mora, O., McCubrey, J.A., Franklin, R.A. (2003). Models of anergy in the human Jurkat T cell line. Assay Drug Dev Technol *1*, 537-44.

205. Eroukhmanoff, L., Oderup, C., Ivars, F. (2009). T-cell tolerance induced by repeated antigen stimulation: selective loss of Foxp3- conventional CD4 T cells and induction of CD4 T-cell anergy. Eur J Immunol *39*, 1078-87.

206. Kitamura, H., Ohta, A., Sekimoto, M., Sato, M., Iwakabe, K., Nakui, M., Yahata, T., Meng, H., Koda, T., Nishimura, S., Kawano, T., Taniguchi, M., Nishimura, T. (2000). alpha-galactosylceramide induces early B-cell activation through IL-4 production by NKT cells. Cell Immunol *199*, 37-42.

207. Serfling, E., Berberich-Siebelt, F., Avots, A. (2007). NFAT in lymphocytes: a factor for all events? Sci STKE *2007*, pe42.

208. Serfling, E., Klein-Hessling, S., Palmetshofer, A., Bopp, T., Stassen, M., Schmitt, E. (2006). NFAT transcription factors in control of peripheral T cell tolerance. Eur J Immunol *36*, 2837-43.

209. Bednarski, J.J., Warner, R.E., Rao, T., Leonetti, F., Yung, R., Richardson, B.C., Johnson, K.J., Ellman, J.A., Opipari, A.W., Jr., Glick, G.D. (2003). Attenuation of autoimmune disease in Fas-deficient mice by treatment with a cytotoxic benzodiazepine. Arthritis Rheum *48*, 757-66.

210. Martinez-Martinez, S., Redondo, J.M. (2004). Inhibitors of the calcineurin/NFAT pathway. Curr Med Chem *11*, 997-1007.

211. Lineberry, N., Fathman, C.G. (2006). T cell anergy: where it's LAT. Immunity *24*, 501-3.

212. Ke, Q., Li, J., Ding, J., Ding, M., Wang, L., Liu, B., Costa, M., Huang, C. (2006). Essential role of ROS-mediated NFAT activation in TNF-alpha induction by crystalline silica exposure. Am J Physiol Lung Cell Mol Physiol *291*, L257-64.

213. Huang, C., Li, J., Costa, M., Zhang, Z., Leonard, S.S., Castranova, V.,

Vallyathan, V., Ju, G., Shi, X. (2001). Hydrogen peroxide mediates activation of nuclear factor of activated T cells (NFAT) by nickel subsulfide. Cancer Res *61*, 8051-7.

214. Li, J., Huang, B., Shi, X., Castranova, V., Vallyathan, V., Huang, C. (2002). Involvement of hydrogen peroxide in asbestos-induced NFAT activation. Mol Cell Biochem *234-235*, 161-8.

215. Kalivendi, S.V., Konorev, E.A., Cunningham, S., Vanamala, S.K., Kaji, E.H., Joseph, J., Kalyanaraman, B. (2005). Doxorubicin activates nuclear factor of activated T-lymphocytes and Fas ligand transcription: role of mitochondrial reactive oxygen species and calcium. Biochem J *389*, 527-39.

216. Huang, C., Ding, M., Li, J., Leonard, S.S., Rojanasakul, Y., Castranova, V., Vallyathan, V., Ju, G., Shi, X. (2001). Vanadium-induced nuclear factor of activated T cells activation through hydrogen peroxide. J Biol Chem *276*, 22397-403.

217. Penna, A., Demuro, A., Yeromin, A.V., Zhang, S.L., Safrina, O., Parker, I., Cahalan, M.D. (2008). The CRAC channel consists of a tetramer formed by Stim-induced dimerization of Orai dimers. Nature *456*, 116-20.

218. Wang, Y., Deng, X., Hewavitharana, T., Soboloff, J., Gill, D.L. (2008). Stim, ORAI and TRPC channels in the control of calcium entry signals in smooth muscle. Clin Exp Pharmacol Physiol *35*, 1127-33.

219. Liao, Y., Plummer, N.W., George, M.D., Abramowitz, J., Zhu, M.X., Birnbaumer, L. (2009). A role for Orai in TRPC-mediated Ca2+ entry suggests that a TRPC:Orai complex may mediate store and receptor operated Ca2+ entry. Proc Natl Acad Sci U S A *106*, 3202-6.

220. Liao, Y., Erxleben, C., Abramowitz, J., Flockerzi, V., Zhu, M.X., Armstrong, D.L., Birnbaumer, L. (2008). Functional interactions among Orai1, TRPCs, and STIM1 suggest a STIM-regulated heteromeric Orai/TRPC model for SOCE/Icrac channels. Proc Natl Acad Sci U S A *105*, 2895-900.

221. Hara, Y., Wakamori, M., Ishii, M., Maeno, E., Nishida, M., Yoshida, T., Yamada, H., Shimizu, S., Mori, E., Kudoh, J., Shimizu, N., Kurose, H., Okada, Y., Imoto, K., Mori, Y. (2002). LTRPC2 Ca2+-permeable channel activated by changes in redox status confers susceptibility to cell death. Mol Cell *9*, 163-73.

222. Hoth, M., Button, D.C., Lewis, R.S. (2000). Mitochondrial control of

calcium-channel gating: a mechanism for sustained signaling and transcriptional activation in T lymphocytes. Proc Natl Acad Sci U S A *97*, 10607-12.

223. Walsh, C., Barrow, S., Voronina, S., Chvanov, M., Petersen, O.H., Tepikin, A. (2009). Modulation of calcium signalling by mitochondria. Biochim Biophys Acta

224. Duchen, M.R. (2000). Mitochondria and calcium: from cell signalling to cell death. J Physiol *529 Pt 1*, 57-68.

225. Finch, E.A., Turner, T.J., Goldin, S.M. (1991). Calcium as a coagonist of inositol 1,4,5-trisphosphate-induced calcium release. Science *252*, 443-6.

226. Zweifach, A., Lewis, R.S. (1995). Rapid inactivation of depletion-activated calcium current (ICRAC) due to local calcium feedback. J Gen Physiol *105*, 209-26.

227. Parekh, A.B. (2008). Mitochondrial regulation of store-operated CRAC channels. Cell Calcium *44*, 6-13.

228. Inesi, G., Hua, S., Xu, C., Ma, H., Seth, M., Prasad, A.M., Sumbilla, C. (2005). Studies of Ca2+ ATPase (SERCA) inhibition. J Bioenerg Biomembr *37*, 365-8.

229. Hoth, M., Fanger, C.M., Lewis, R.S. (1997). Mitochondrial regulation of store-operated calcium signaling in T lymphocytes. J Cell Biol *137*, 633-48.

230. Graier, W.F., Frieden, M., Malli, R. (2007). Mitochondria and Ca(2+) signaling: old guests, new functions. Pflugers Arch *455*, 375-96.

231. Nagendran, J., Gurtu, V., Fu, D.Z., Dyck, J.R., Haromy, A., Ross, D.B., Rebeyka, I.M., Michelakis, E.D. (2008). A dynamic and chamber-specific mitochondrial remodeling in right ventricular hypertrophy can be therapeutically targeted. J Thorac Cardiovasc Surg *136*, 168-78, 78 e1-3.

232. Johnson, K.M., Chen, X., Boitano, A., Swenson, L., Opipari, A.W., Jr., Glick, G.D. (2005). Identification and validation of the mitochondrial F1F0-ATPase as the molecular target of the immunomodulatory benzodiazepine Bz-423. Chem Biol *12*, 485-96.

233. Lu, R. (2008). Interferon regulatory factor 4 and 8 in B-cell development. Trends Immunol *29*, 487-92.

234. Yamada, M., Asanuma, K., Kobayashi, D., Moriai, R., Yajima, T., Yagihashi, A., Yamamori, S., Watanabe, N. (2001). Quantitation of multiple myeloma oncogene 1/interferon-regulatory factor 4 gene expression in malignant B-cell proliferations and normal leukocytes. Anticancer Res *21*, 633-8.

235. Mittrucker, H.W., Matsuyama, T., Grossman, A., Kundig, T.M., Potter, J., Shahinian, A., Wakeham, A., Patterson, B., Ohashi, P.S., Mak, T.W. (1997). Requirement for the transcription factor LSIRF/IRF4 for mature B and T lymphocyte function. Science *275*, 540-3.

236. Klein, U., Casola, S., Cattoretti, G., Shen, Q., Lia, M., Mo, T., Ludwig, T., Rajewsky, K., Dalla-Favera, R. (2006). Transcription factor IRF4 controls plasma cell differentiation and class-switch recombination. Nat Immunol *7*, 773-82.

237. Teng, Y., Takahashi, Y., Yamada, M., Kurosu, T., Koyama, T., Miura, O., Miki, T. (2007). IRF4 negatively regulates proliferation of germinal center B cell-derived Burkitt's lymphoma cell lines and induces differentiation toward plasma cells. Eur J Cell Biol *86*, 581-9.

238. Schlissel, M.S. (2007). The regulation of receptor editing. Adv Exp Med Biol *596*, 173-9.

239. Nemazee, D. (2006). Receptor editing in lymphocyte development and central tolerance. Nat Rev Immunol *6*, 728-40.

240. Pathak, S., Ma, S., Trinh, L., Lu, R. (2008). A role for interferon regulatory factor 4 in receptor editing. Mol Cell Biol *28*, 2815-24.

241. Toda, T., Kitabatake, M., Igarashi, H., Sakaguchi, N. (2009). The immature B-cell subpopulation with low RAG1 expression is increased in the autoimmune New Zealand Black mouse. Eur J Immunol *39*, 600-11.

242. Jankovic, M., Casellas, R., Yannoutsos, N., Wardemann, H., Nussenzweig, M.C. (2004). RAGs and regulation of autoantibodies. Annu Rev Immunol *22*, 485-501.

243. Johnson, K., Hashimshony, T., Sawai, C.M., Pongubala, J.M., Skok, J.A., Aifantis, I., Singh, H. (2008). Regulation of immunoglobulin light-chain recombination by the transcription factor IRF-4 and the attenuation of interleukin-7 signaling. Immunity *28*, 335-45.

244. Lamoureux, J.L., Watson, L.C., Cherrier, M., Skog, P., Nemazee, D., Feeney,

A.J. (2007). Reduced receptor editing in lupus-prone MRL/lpr mice. J Exp Med *204*, 2853-64.

245. Lohoff, M., Mittrucker, H.W., Prechtl, S., Bischof, S., Sommer, F., Kock, S., Ferrick, D.A., Duncan, G.S., Gessner, A., Mak, T.W. (2002). Dysregulated T helper cell differentiation in the absence of interferon regulatory factor 4. Proc Natl Acad Sci U S A *99*, 11808-12.

246. Tominaga, N., Ohkusu-Tsukada, K., Udono, H., Abe, R., Matsuyama, T., Yui, K. (2003). Development of Th1 and not Th2 immune responses in mice lacking IFN-regulatory factor-4. Int Immunol *15*, 1-10.

247. Zheng, Y., Chaudhry, A., Kas, A., deRoos, P., Kim, J.M., Chu, T.T., Corcoran, L., Treuting, P., Klein, U., Rudensky, A.Y. (2009). Regulatory T-cell suppressor program co-opts transcription factor IRF4 to control T(H)2 responses. Nature *458*, 351-6.

248. Honma, K., Kimura, D., Tominaga, N., Miyakoda, M., Matsuyama, T., Yui, K. (2008). Interferon regulatory factor 4 differentially regulates the production of Th2 cytokines in naive vs. effector/memory CD4+ T cells. Proc Natl Acad Sci U S A *105*, 15890-5.

249. Meyer-Bahlburg, A., Rawlings, D.J. (2008). B cell autonomous TLR signaling and autoimmunity. Autoimmun Rev *7*, 313-6.

250. Kawai, T., Adachi, O., Ogawa, T., Takeda, K., Akira, S. (1999). Unresponsiveness of MyD88-deficient mice to endotoxin. Immunity *11*, 115-22.

251. Takeuchi, O., Takeda, K., Hoshino, K., Adachi, O., Ogawa, T., Akira, S. (2000). Cellular responses to bacterial cell wall components are mediated through MyD88-dependent signaling cascades. Int Immunol *12*, 113-7.

252. Takaoka, A., Yanai, H., Kondo, S., Duncan, G., Negishi, H., Mizutani, T., Kano, S., Honda, K., Ohba, Y., Mak, T.W., Taniguchi, T. (2005). Integral role of IRF-5 in the gene induction programme activated by Toll-like receptors. Nature *434*, 243-9.

253. Pisitkun, P., Deane, J.A., Difilippantonio, M.J., Tarasenko, T., Satterthwaite, A.B., Bolland, S. (2006). Autoreactive B cell responses to RNA-related antigens due to TLR7 gene duplication. Science *312*, 1669-72.

254. Negishi, H., Ohba, Y., Yanai, H., Takaoka, A., Honma, K., Yui, K., Matsuyama,

T., Taniguchi, T., Honda, K. (2005). Negative regulation of Toll-like-receptor signaling by IRF-4. Proc Natl Acad Sci U S A *102*, 15989-94.

255. Honma, K., Udono, H., Kohno, T., Yamamoto, K., Ogawa, A., Takemori, T., Kumatori, A., Suzuki, S., Matsuyama, T., Yui, K. (2005). Interferon regulatory factor 4 negatively regulates the production of proinflammatory cytokines by macrophages in response to LPS. Proc Natl Acad Sci U S A *102*, 16001-6.

256. Pan, M., Winslow, M.M., Chen, L., Kuo, A., Felsher, D., Crabtree, G.R. (2007). Enhanced NFATc1 nuclear occupancy causes T cell activation independent of CD28 costimulation. J Immunol *178*, 4315-21.

257. Grumont, R.J., Gerondakis, S. (2000). Rel induces interferon regulatory factor 4 (IRF-4) expression in lymphocytes: modulation of interferon-regulated gene expression by rel/nuclear factor kappaB. J Exp Med *191*, 1281-92.

258. Serfling, E., Berberich-Siebelt, F., Avots, A., Chuvpilo, S., Klein-Hessling, S., Jha, M.K., Kondo, E., Pagel, P., Schulze-Luehrmann, J., Palmetshofer, A. (2004). NFAT and NF-kappaB factors-the distant relatives. Int J Biochem Cell Biol *36*, 1166-70.

259. Kutuk, O., Basaga, H. (2007). Apoptosis signalling by 4-hydroxynonenal: a role for JNK-c-Jun/AP-1 pathway. Redox Rep *12*, 30-4.

260. Cortes Sempere, M., Rodriguez Fanjul, V., Sanchez Perez, I., Perona, R. (2008). The role of the NFkappaB signalling pathway in cancer. Clin Transl Oncol *10*, 143-7.

261. Notidis, E., Heltemes, L., Manser, T. (2002). Dominant, hierarchical induction of peripheral tolerance during foreign antigen-driven B cell development. Immunity *17*, 317-27.

262. Bell, S.E., Goodnow, C.C. (1994). A selective defect in IgM antigen receptor synthesis and transport causes loss of cell surface IgM expression on tolerant B lymphocytes. Embo J *13*, 816-26.

263. Huang, F., Gu, H. (2008). Negative regulation of lymphocyte development and function by the Cbl family of proteins. Immunol Rev *224*, 229-38.

264. Lenschow, D.J., Sperling, A.I., Cooke, M.P., Freeman, G., Rhee, L., Decker, D.C., Gray, G., Nadler, L.M., Goodnow, C.C., Bluestone, J.A. (1994). Differential up-regulation of the B7-1 and B7-2 costimulatory molecules after Ig receptor engagement by antigen. J Immunol *153*, 1990-7.

265. Wong, S.C., Chew, W.K., Tan, J.E., Melendez, A.J., Francis, F., Lam, K.P. (2002). Peritoneal CD5+ B-1 cells have signaling properties similar to tolerant B cells. J Biol Chem *277*, 30707-15.

266. Wither, J.E., Paterson, A.D., Vukusic, B. (2000). Genetic dissection of B cell traits in New Zealand black mice. The expanded population of B cells expressing up-regulated costimulatory molecules shows linkage to Nba2. Eur J Immunol *30*, 356-65.

267. Wither, J.E., Roy, V., Brennan, L.A. (2000). Activated B cells express increased levels of costimulatory molecules in young autoimmune NZB and (NZB x NZW)F(1) mice. Clin Immunol *94*, 51-63.

268. Sancho, D., Gomez, M., Sanchez-Madrid, F. (2005). CD69 is an immunoregulatory molecule induced following activation. Trends Immunol *26*, 136-40.

269. Thornton, A. (2003). Fractionation of T and B cells using magnetic beads. Current protocols in Immunology, Unit 3.5A.